Microbes, contaminants, and molecular biomonitoring: Structural and functional sediment community responses to multiple stressors

Author:
Birrer, Simone

Publication Date:
2017

DOI:
https://doi.org/10.26190/unsworks/19564

Microbes, contaminants, and molecular biomonitoring: Structural and functional sediment community responses to multiple stressors

By
Simone C. Birrer

A thesis submitted in fulfilment
of the requirement for the degree of
Doctor of Philosophy

School of Biological, Earth and Environmental Sciences
Faculty of Science

UNSW AUSTRALIA

Supervisors:
Prof. Emma L. Johnston and Dr. Katherine A. Dafforn

April, 2017

Abstract

The development of coastal areas often results in the introduction of a suite of contaminants to these highly productive systems. Contaminants accumulate in soft sedimentary environments where they may affect resident microorganisms responsible for driving major biogeochemical cycles and providing a range of ecosystem services. The cumulative effects of multiple contaminants can impact both the structure and function of microbial communities. These cumulative effects are not yet well understood, however they have potential repercussions at local, regional and global scales. Microbes are inherently difficult to study as the majority cannot be cultured in the laboratory. Modern molecular techniques enable the study of microbes at a genetic level. Targeted gene sequencing and meta-omics provide snapshots of community structure and function. However, their application as biomonitoring tools is still in its infancy. In this thesis, I investigate targeted sequencing for ecosystem health assessment and assess metatranscriptomics as a new biomonitoring tool. I use experiments and surveys to test the value of molecular techniques in informing ecosystem-wide consequences of structural and functional changes. Targeted sequencing revealed that bacterial communities are more sensitive to multiple disturbances than eukaryotes (traditionally used for biomonitoring) and are potentially better indicators of ecosystem change. Metatranscriptomics proved to be a sensitive, reliable and replicable tool, which provided rapid, ecologically relevant, information. Sediment communities exposed to metals and organic enrichment had significantly altered gene expression profiles that may reflect accumulation of toxic compounds and increased production of greenhouse gases. Surveys revealed that sediment communities impacted by legacy contaminants had reduced primary productivity and greater potential for community fracturing, which itself may lead to lower productivity and lower remediation capacity. Molecular approaches generated information that could revolutionise biomonitoring approaches. However, the lack of extensive genetic reference libraries and complex data processing requirements continue to pose challenges to the routine adoption of these techniques. My research highlights the power of molecular approaches for assessing ecosystem health and the consequences of urban contaminants on community structure and function.

Acknowledgements

Over the last few years I have been blessed to be surrounded by many great people. First of all, I would like to thank my supervisors, Emma Johnston and Katherine Dafforn. Emma, I am forever grateful for the great opportunities that you have provided me with and for leading me on this unexpected bacterial path. Through your great network I have made a lot of new friends and had the pleasure to meet many great scientists. Your enthusiasm for everything ecological will always be a great inspiration. Katie, you have supported me through all the ups and downs of my PhD, taught me and helped me with an immense amount of things over these last few years. I really admire your dedication to every student you supervise and every project you work on. You are not only an awesome supervisor and mentor, but also an amazing friend and yoga buddy.

I would also like to thank Melanie Sun for introducing me to the omics world and teaching me basically everything I know about molecular ecology. Your patience and friendship got me through my first horrifying moments in the sequencing world, thank you. A special thank you to Rohan Williams for sharing all your knowledge on omics data analysis and for great chats during my stays in Singapore. I also want to thank Jaimie Potts for countless meetings and your endless patience in introducing me to the world of biogeochemistry. Through our many great chats I lost my fear of biogeochemical pathways and you even managed to turn this fear into a fascination. Krithika Amurugam, thank you for all your help with the bioinformatics and for always being available to answer questions. I am also grateful to my collaborators Stuart Simpson, Brendan Kelaher, Peter Scanes, Staffan Kjelleberg, Sanjay Swarup, and Peter Steinberg for their support with the projects, and to Richard Carney, always willing to help.

An enormous thanks goes to the AMEE Lab. It was a pleasure to be part of this lab and I am grateful for having so many great friends. In particular, I would like to thank Sally Bracewell, Hannah Sheppard Brennand and Aria Lee for their encouragement and support over the years. Many great chats, turmeric teas and culinary experiences have helped heal the little wounds of a PhD. Vivian Sim, Michael Sutherland, and Tyson Haddad, thanks for your help with countless days in the field. Your company made it all much easier and enjoyable. Also, a big thanks to Damon Bolton for being a great support with the writing up. It was great to have a 'brother in arms' to share stories with.

A very special thank you to my family, who has supported me from close and far. Thanks for the many hours on skype, numerous yummy parcels full of Swiss goodies that kept me going, your enjoyable visits to Australia and for rooting for me always. Finally, I would like to thank Dominic for all his love and support over the years. Thank you for coming to Sydney so I could follow my dreams, for always believing in me and showing me that the impossible is possible. Our countless 'sanity retreats' and adventurous trips have kept me sane and motivated over these years. Without you this would not have been possible.

What an epic journey.

Contents

List of Figures

List of Tables

1 Introduction

Unprecedented rates of urbanisation (Cohen, 2003) are exposing numerous ecosystems to increasing anthropogenic pressure (Vitousek et al., 1997). Coastal regions in particular, have been subject to disproportionately increasing human populations (Small and Nicholls, 2003). In addition to biological and physical disturbances, coastal ecosystems are confronted with complex chemical contaminants, which rarely occur individually. Contaminants bind to particles and settle into the sediments, where they are stored and accumulate (Burton and Johnston, 2010). The combined effects of multiple stressors on affected ecosystems is not yet well understood (Griffen et al., 2016). Multiple contaminants have the potential to affect community structure due to different tolerance levels of organisms (Vinebrooke et al., 2004), and structural changes often result in functional dissimilarities within the community (Strickland et al., 2009). However, direct functional effects from contaminants may outweigh indirect effects through structure (Srivastava and Vellend, 2005). Community functioning, especially on a microbial level, is critical on local, regional and global scales (Falkowski et al., 2008). A comprehensive assessment of community functioning in combination with community structure would therefore significantly advance our understanding of the consequences from contaminant exposure and may substantially improve coastal ecosystem management.

Modern molecular techniques involving next-generation sequencing have enabled rapid structural and functional assessments through the investigation of genetic material. Molecular approaches have been shown to perform equally well as morphological approaches to detect environmental impacts (Lejzerowicz et al., 2015), and because they enable taxonomic information with higher certainty and higher resolution, molecular techniques can provide clearer responses to environmental stressors (Hajibabaei et al., 2011; Dafforn et al., 2014). Molecular approaches could thus revolutionise modern biomonitoring and the depth of information gained from genetic resources may allow for molecular biomonitoring tools to be used for diagnostic purposes (Baird and Hajibabaei, 2012). The rapid production of 'big data' from sequencing ensures that these modern techniques provide up-to-date data and may therefore be

highly relevant to inform timely management decisions. However, the application of many molecular techniques as biomonitoring tools is yet to be investigated. In order to address the use of molecular tools for biomonitoring, this thesis contributes experimental and survey studies using amplicon sequencing and metatranscriptomics to assess the impact of common multiple stressors on the structure and function of estuarine soft sediment communities.

Multiple stressors affect community structure and functions

Human activities have modified almost all of Earth's ecosystems (Vitousek et al., 1997). We have changed most of the terrestrial systems, are using the majority of surface freshwaters and have an impact on even the most remote marine ecosystems (Vitousek et al., 1997; Halpern et al., 2008). Furthermore, humans have introduced complex physical, chemical and biological stressors to all ecosystems (Vitousek et al., 1997). Anthropogenic stressors rarely occur individually and their interactive effects are not always additive, but can also be synergistic (more than expected based on individual effects) or antagonistic (less than expected based on individual effects) (Folt et al., 1999). Hence, single-stressor studies cannot be easily extrapolated to predict the impact of multiple stressors. Multiple stressor studies often result in 'ecological surprises' (Christensen et al., 2006), which lead to less predictable consequences for affected communities (Vye et al., 2015). Therefore, we need a better understanding of direct and indirect effects of multiple stressors on affected ecosystems.

Individual species within a community can exhibit different levels of tolerance towards different stressors (Vinebrooke et al., 2004). Through these variations in sensitivity, stressors can affect the biodiversity of a community, where co-tolerant species are more likely to survive (Vinebrooke et al., 2004). When exposed to stressors, structural changes are likely to lead to functionally dissimilar communities (Strickland et al., 2009) because the surviving organisms protect themselves through the activation of stress-related responses and shift their energetic resources from growth to survival mechanisms (Schimel et al., 2007). The diversity of a community is tightly linked to primary productivity, energy flow and a wide variety of ecological processes. Therefore, this shift of resources can significantly affect the energy and nutrient flows in an ecosystem (Schimel et al., 2007). More diverse systems exhibit improved tolerance to stressors, as more diversity provides a higher assembly of functions and emerging niches can be filled quickly from the pool of species already

existing in the community (Finlay et al. 1997). However, the direct impact of stressors on community function is likely to be more substantial than the indirect effects through structural changes (Srivastava and Vellend, 2005). Only if a community is not resistant, resilient or functionally redundant, we find a community with altered structure and function (Allison and Martiny, 2008). We need to include the measurement of impact of multiple stressors on community process rates in order to assess the functional consequences of such stressors.

Ecosystem functions, and therefore process rates, are driven mainly by microorganisms (Falkowski et al., 2008), which play a crucial role in the primary productivity of our ecosystems (Azam, 1998). Microbes are highly sensitive to environmental changes (Sun et al., 2012); their community compositions and functions are affected by contamination (Louati et al., 2013; Ager et al., 2010; Scott et al., 2014; Kandeler et al., 1996). Moreover, the connectivity of the community is important for the functional performance, as it can have an impact on the cohesiveness (Horvath and Dong, 2008) and stability of communities (Proulx et al., 2005). Microorganisms adjust their functional activities based on their responses to the environment (Westerhoff et al., 2014) and other organisms in the same community (Ross-Gillespie and Kümmerli, 2014). A fracturing of communities exposed to contaminants (e.g. Lawes et al., 2016b) could potentially lead to the disruption of functional processes and lower the potential for functional redundancy. These changes in microbial communities are likely to have knock-on effects on associated macrofauna (e.g. Lawes et al., 2016a) and can therefore change entire ecosystems, as well as globally relevant processes (Nogales et al., 2011; Johnson et al., 2015; Wang et al., 2015; Halstead et al., 2014). Due to microbial contributions to ecosystem processes, the assessment of microbial communities can provide an accurate snapshot of the health of ecosystems (Graham et al., 2016).

Molecular biomonitoring

Microbial process rates are commonly assessed using biogeochemical flux measurements from water, sediment and soil (Poissant and Casimir, 1998; Davidson et al., 2002; Eyre and Ferguson, 2005; Kelaher et al., 2013). These measurements rely on the incubation of the substrate of interest in light and dark conditions to analyse primary productivity, and nutrient and gas production during day and night scenarios. Such incubations are time-consuming and sampling is very sensitive and error-prone. Using next-generation sequencing of communities, we can now detect potential changes to biogeochemical fluxes

at the gene level and uncover the mechanisms behind such changes. This has been made possible by metatranscriptomics, which facilitates the measurement of all functional genes of an entire community (Urich et al., 2008; Moran, 2009). These approaches can identify the nature of the response of specific communities to specific stressors (Allison and Martiny, 2008) and may therefore be highly valuable tools for biomonitoring.

Biomonitoring tools have been a critical component of ecosystem health assessments when trying to understand the impacts of anthropogenic contaminants on the environment (Rainbow, 2002). Results from such assessments are used to inform ecosystem managers on the best strategies for mitigation and remediation (Barbour and Paul, 2010; Hering et al., 2010). To date, biomonitoring has mainly focused on taxonomic information provided by the sampling of macroinvertebrates, such as insects, fish and worms (Bonada et al., 2006; Magurran et al., 2010), and algal abundances (Reavie et al., 2010). The accumulation of toxic compounds, such as metals, in the tissues of macroinvertebrates has also been widely used to indicate contaminant loads within the ecosystems of interest (Rainbow, 2002). In recent years, the importance of community function for ecosystem health assessments has been recognised and the use of functional traits for biomonitoring is gaining momentum (Baird et al., 2011; Van den Brink et al., 2013; de Juan et al., 2014; van der Linden et al., 2016). However, most structural or trait-based techniques are time-consuming and require a high degree of expert knowledge on species-traits relationships and taxonomic identification. Moreover, the relevance of the data to ecological processes is unclear due to the limited variety of organism groups assessed (Bourlat et al., 2013).

Metatransctiptomics provides holistic information on the gene expression of an entire community, which yields ecologically relevant data through the inclusion of all organisms. Gene activity at the community level has been shown to directly impact ecosystem process rates (Morales et al., 2010; Philippot et al., 2011; Harter et al., 2014), however, the prediction of biogeochemical flux rates from gene expression measures remains problematic (Bowen et al., 2014). Systems approaches that include temporal and spatial parameters are required to better link community structure to function, and function to process rates (Bissett et al., 2013). Nevertheless, these extremely powerful molecular approaches permit a new depth of insight into microbial processes and have the potential to revolutionise ecosystem health assessments. Metatranscriptomics is yet to be validated as a biomonitoring tool and the sheer amount of data that it produces is intimidating. Nevertheless, metatranscriptomics may play a crucial role in the advancement of microbial ecotoxicology and the improve-

ment of ecosystem management, through the provision of rapid information on immediate community responses to stressors that leads to faster, up-to-date and ecologically relevant management decisions.

Contaminants in coastal soft sedimentary environments

Coastal areas in particular, have been subject to rapidly increasing urbanisation (Small and Nicholls, 2003). This urbanisation introduced extensive areas of impervious surface, which lead to large amounts of urban run-off after rainfall events (Arnold and Gibbons, 1996). On its way to the drainage systems, this run-off collects a complex mix of contaminants (Göbel et al., 2007; Laetz et al., 2015), from metals and polycyclic aromatic hydrocarbons (PAHs), to pesticides and nutrients (Göbel et al., 2007). In addition, industry and agricultural practices have long been major sources of metals and metalloids (e.g. Birch and Taylor, 1999; Nicholson et al., 2003), petroleum based toxicants (Santschi et al 2001), organic compounds (Birch et al., 1999), fertilisers, pesticides and herbicides (Arias-Estévez et al., 2008; Puckett, 1995). Industrial waste was historically directly discharged into adjacent waterways (Birch and Taylor, 1999; Birch et al., 2016), and nowadays often simple, non-effective run-off treatment techniques are applied (Davis and Birch, 2009). Urbanised waterways are therefore exposed to an array of stressors from a variety of sources (Kennish, 2002).

The sources of this cocktail of contaminants determine the timing and rate of exposure (Bender et al., 1984). Press exposures occur when contaminants are continuously introduced into the system and/or are trapped in legacy environments such as sediments. Pulse contaminant exposures occur from point source emissions; they are temporally variable, and often involve very high concentrations. The most common contaminants in coastal waterways are metals and organic enrichment (Jiang et al., 2001). While metals act as toxicants (Babich and Stotzky, 1985), organic enrichment can promote activity and growth (del Giorgio and Scarborough, 1995) at low levels. However, at high levels, organic enrichment can have toxic effects on aquatic organisms, due to the creation of anaerobic conditions and the increased production of toxic compounds (Meyer-Reil and Köster, 2000; Gray et al., 2002).

In waterways, contaminants tend to bind to particles in the water column and settle into the soft sediments (Burton and Johnston, 2010). In these sediments, the often anoxic conditions favour adsorption of contaminants onto sediment particles (Calmano et al., 1993). Hence, contaminants are accumulated in sediments, which act as contaminant sinks. However, through

changes in chemical properties of the sediment, contaminants can lose their binding affinity and be released into the water column (Eggleton and Thomas, 2004; Zoumis et al., 2001; Van Ryssen et al., 1999; Gibson et al., 2015; Latimer et al., 1999). Physical disturbances that lead to these chemical changes can be of biological nature, e.g. bioturbation (Davis, 1993), tidal movement and storms (e.g. Bogdan et al., 2002), or due to anthropogenic activities, such as dredging (Hedge et al 2009), boating, and fishing (Eggleton and Thomas, 2004). Sediment can therefore also act as a contaminant source and resuspension has been shown to have extensive ecological effects in marine systems (Roberts, 2012). The management of contaminants in sediments is not only critical for sediment organisms, but also for the overlying water column and thus the entire urbanised ecosystem.

Thesis outline

In this thesis, I use experiments and surveys to measure the impact of multiple anthropogenic stressors on estuarine sediment community structure and function. I simultaneously investigate the potential for next-generation sequencing approaches to become the next generation of ecosystem health monitoring tools.

Chapter 2 - Bacterial and eukaryotic community shifts upon experimental press and pulse exposure to common contaminants

In this chapter, I address targeted gene sequencing and its use for large biomonitoring projects involving multiple stressors applied at different rates (press and pulse disturbances). Nowadays, most biomonitoring approaches that utilise targeted gene sequencing use DNA as template and analyse eukaryotic genes. In this chapter I ask the following questions:

- Which genetic template (DNA or RNA) provides more detailed information on multiple stressors?
- Which community (eukaryotes or bacteria) is a better indicator for anthropogenic contamination?
- And is targeted gene sequencing applicable in scenarios with multiple stressors applied at different rates?

Chapter 3 - Functional biomonitoring: Using metatranscriptomics for ecosystem health assessment

In this chapter, I investigate the applicability of metatranscriptomics for biomonitoring and explore the different depths of analysis that are enabled by this modern sequencing technique. I assess metatranscriptomics as a biomonitoring tool based on the following criteria: Biomonitoring tools need to

1. Be sensitive to the stressor of interest and provide ecologically relevant results;

2. Show reliability of measures and repeatability across systems and contaminants;

3. Be cost- and time-effective and easy to use across disciplines.

Experimentally *in situ* manipulated sediments are used for this assessment of metatranscriptomics.

Chapter 4 - Transcriptional changes in greenhouse gas production pathways in experimentally contaminated coastal sediments

This chapter provides an example of a very detailed analysis that can be done using metatranscriptomics. Here, I investigate the responses of microbial sediment communities to metals and organic enrichment with a focus on climate-relevant pathways using metatatranscriptomics. This chapter reveals that common contaminants can affect the microbial mechanisms behind the production of greenhouse gases and therefore have potential global implications.

Chapter 5 - Altered microbial communication, productivity and nutrient cycling in contaminated sediments of an urbanised estuary

After establishing that metatranscriptomics can be used to assess the functional health of sediment microbes in an experimental set-up (Chapters 3 and 4), in this chapter, I apply metatranscriptomics to a real-world scenario in a survey. I measure the impact of legacy contaminants from industry and urban run-off on sediment communities in poorly flushed embayments of Sydney Harbour, Australia. Specifically, I analyse the pathways related to energy production, nutrient cycling and signalling activities. I discuss the consequences of altered gene expression for the affected ecosystem and the potential repercussions on a global scale.

Chapter 6 - Summary

In this last chapter, I discuss the collective results from this thesis and provide suggestions for future research. Will big data be the future of ecosystem health assessments? Here, I emphasise the contribution of this thesis towards solving ecological problems of urbanisation and assisting the improvement of biomonitoring.

This thesis is structured as a series of stand-alone manuscripts. Therefore, some repetition between the chapters, especially in the methods sections, is unavoidable.

2 Bacterial and eukaryotic community shifts upon experimental press and pulse exposure to common contaminants

Abstract

Coastal waterways are increasingly exposed to press and pulse disturbances from a range of contaminants. The ability to differentiate ecological impacts associated with multiple stressors that vary spatio-temporally is critical to guide the efficient and targeted reduction of ecosystem threats. Modern molecular techniques are tools that can be used to increase the relevance and sensitivity of biomonitoring by providing greater taxonomic resolution and a more holistic characterisation of biological communities. We investigated microbial community development in sediments as they responded to both press and pulse exposures to 'metals' (sediment contaminated with multiple metal(loid)s) and organic matter (organic enrichment). Our press exposures were represented by *in situ* mesocosm sediments containing four exposure levels for metals and three for organic enrichment, while the pulse exposure was simulated by a once-off increase in organic enrichment. All treatments and exposure concentrations were crossed in a factorial field experiment. We used amplicon sequencing of the 16S and 18S rRNA genes to compare the sensitivity of 1) different microbial communities and 2) total (DNA) and active (RNA) communities to contaminant exposures. Microbial communities of bacteria (16S) and eukaryotes (18S) shifted significantly with exposure to press and pulse disturbances, with the bacterial community showing higher response. Pulse exposures caused less change while press exposures created substantially altered communities. The metal and enrichment effects interacted such that the influence of metals were less obvious when the sediment also had organic enrichment. Taxa-level analyses revealed that press enrichment resulted in a lower relative abundance of active macromolecule degrading, as well as nitrite-oxidising and nitrous oxide reducing bacteria. Furthermore, enrichment generally reduced the abundance of active eukaryotes in the sediment. As well as demonstrating interactive impacts of metals and organic enrichment, this study highlights the valueof next-generation sequencing to ecosystem biomonitoring of a wide range of interacting stressors.

Introduction

Stressors in urban ecosystems are manifold. In addition to varying by mechanism of impact, stressors have different sources, determining the timing and rate of exposure (press and pulse, Bender et al., 1984). Press disturbances, for example, include legacy contaminants from historical contamination or stressors to which the system is continuously exposed (Knott et al., 2009). In contrast, pulse disturbances may originate from point sources, are temporally variable and can results in exposure to high contaminant concentrations (Johnston and Keough, 2002). Press disturbances are known to select for more tolerant communities (Piotrowska-Seget et al., 2005) and can thus lead to permanent structural and functional changes, while pulse disturbances can have deleterious effects on the resident communities in the short term, but may allow for full recovery to the pre-stressed state (Bender et al., 1984). The ability to differentiate ecological impacts associated with both the type and timing of multiple disturbances is therefore of crucial importance for the development of appropriate monitoring tools that can guide the management of highly stressed systems.

Coasts support some of the most diverse and productive ecosystems in the world (Nixon et al., 1986). However, the number and types of stressors in coastal ecosystems has increased with the concentration of industry, trade and urban activity in this region (Kennish, 2002; Johnston et al., 2015a). Chemical stress results from contaminants introduced by industrial and urban run-off, as well as shipping and leisure activities (Kennish, 2002). Contaminants enter waterways, bind to particles in the water column and eventually settle into the sediment (Burton and Johnston, 2010), where a substantial part of globally relevant biogeochemical pathways are performed (Devol, 2015). Contaminants have the ability to change the structure and function of communities in affected ecosystems (Kandeler et al., 1996; Ager et al., 2010; Louati et al., 2013; Scott et al., 2014), which can have repercussions for entire ecosystems (Nogales et al., 2011; Halstead et al., 2014; Johnson et al., 2015; Wang et al., 2015). Sediment microbial communities are thus ideal models to study the impact of press and pulse disturbances from multiple stressors.

Urbanised estuarine sediment communities are exposed to multiple stressors, most commonly metal(loid)s and organic chemical contaminants, and enrichment of organic matter and nutrients (Jiang et al., 2001). Both metals (hereon including metalloids) and organic enrichment (hereon including nutrient enrichment) have been shown to separately affect benthic communities (Meyer-Reil and Köster, 2000; Sun et al., 2012; Azarbad et al., 2013; Lawes

et al., 2016a). Many metals are known to have toxic effects on marine organisms (Babich and Stotzky, 1985; Dong et al., 2016). Organic enrichment can facilitate additional productivity (del Giorgio and Scarborough, 1995), however high levels of organic matter breakdown lead to increased hypoxia and a build-up of potentially toxic compounds such as dissolved ammonia and sulphide (Meyer-Reil and Köster, 2000; Gray et al., 2002). As two classes of common contaminants, elevated concentrations of metals and organic enrichment administered simultaneously, may act synergistically, additively or antagonistically (Crain et al., 2008). However, the combined effects of metals and organic enrichment on estuarine sediment communities have yet to be investigated.

Biomonitoring is an important tool to assess the impact of human activities on ecosystems in order to inform management actions. Although eukaryotes have previously dominated the attention of biomonitoring, community-wide monitoring has opened up the possibility of using microbial assemblages (Zimmerman et al., 2014; Ininbergs et al., 2015). Bacteria are highly sensitive to sediment stressors (Sun et al., 2012) and have very short generation times. In addition, they have the ability to break down a variety of chemical substances (Wiatrowski and Barkay, 2005; Antizar-Ladislao, 2010; Das and Chandran, 2011; Mason et al., 2014). This makes them ideal for biomonitoring as their response to chemical stressors should be rapid and stressor-specific. As such, the inclusion of bacterial analyses in biomonitoring could increase the potential for early detection of community change. This would provide ecosystem managers with necessary information for an early intervention and potentially decrease the costs of remediation.

Modern sequencing techniques have the potential to revolutionise conventional biomonitoring and extend our capacity for ecosystem health diagnoses (Baird and Hajibabaei, 2012). For these techniques, an entire community can be analysed based on its total DNA or RNA. DNA is most commonly used in monitoring and represents the total community, including dormant and recently dead organisms. Next-generation sequencing of DNA has already been widely applied to investigate microbial communities; in surveys, it was used to describe bacterial diversity associated with mangroves (Basak et al., 2016) and changes in soil microbial compositions due to urban stress (Reese et al., 2016); It was also used to experimentally determine the impact of environmental change on freshwater bacterioplankton communities (Ren et al., 2016). DNA provides information on the structure and potential function in a system (e.g. Díez et al., 2016), but does not clarify changes in activity of organisms upon exposure to a stressor. RNA, on the other hand, represents

the active organisms/genes in the community and could thus potentially better outline the impact of different stressors. For instance, in a study of forest soils, RNA data showed substantial differences of microbial activity between seasons, whereas changes in DNA suggested only moderate seasonal variation (Žifčáková et al., 2016). As RNA analyses are usually more labour-intensive and costly, a comparison of these different genetic materials and their applicability to biomonitoring would be invaluable to designing cost-effective monitoring programs.

Here, we manipulated press and pulse stressors *in situ* using field mesocosms and explored the associated structural and potential functional changes through next-generation sequencing. Specifically, we manipulated metal concentrations and organic enrichment of sediments and simulated an enrichment pulse. We sequenced the 16S and 18S genes from DNA and RNA to measure changes in community structure and simultaneously compare bacterial and eukaryotic, as well as total and active community changes. We highlight the general shifts in bacteria and eukaryotes, and discuss specific changes in the most highly affected taxa. We hypothesised that bacterial communities are more sensitive to metal contamination and organic enrichment than eukaryotes, potentially providing a better tool for future biomonitoring. Furthermore, we predicted that organic enrichment would counteract, or dampen, the impact of metal contamination and that highly organically enriched sediments support a more tolerant community to a pulsed stress through selection of tolerant organisms. Based on our results, we discuss the potential implications of metal contaminants, press organic enrichment and pulsed organic enrichment on ecosystem health, i.e. the condition of an area in relation to its productivity, resilience and biodiversity. Our work can inform future ecosystem management and highlights relevant indicator communities and molecular tools for estuarine health monitoring.

Methods

Press disturbance

Sediment was collected using a Van Veen grab from 5 m depth at unvegetated sites. Relatively clean sediment was collected in Botany Bay (BB) and metal contaminated sediment was collected in Port Kembla (PK) (Dafforn et al., 2012; Edge et al., 2015). The two sites were similar with respect to sediment characteristics, including grain size and total organic carbon (TOC, Dafforn et al., 2012). The sediment from both locations was mixed to create a gradient

of metal contamination: Control (100% BB), Moderate (75% BB, 25% PK), High (50% BB, 50% PK) and Very High (25% BB, 75% PK). In addition, the sediment was spiked with Yates Dynamic Lifter Turf Lifter (MOP) to obtain a range of organic enrichment treatments: Control (no added fertiliser), Moderate (10% Dry weight fertiliser) and High (20% Dry weight fertiliser) in a fully crossed design.

These prepared sediment mixtures were distributed into benthic recruitment containers (BRCs) consisting of transparent acrylic cylinders (15 cm diameter, 40 cm height) within PVC piping (15 cm diameter, 15 cm height) (Dafforn et al., 2013). The bottom of each container was lined with 1 kg of sand for drainage and contained 2 kg of sediment above the sand. Three replicates of every sediment mixture were prepared. They were frozen at -20°C for at least three months in order to defaunate the sediment. BRCs were deployed in Chowder Bay, Sydney, Australia (33°50'22"S, 151°15'17"E), while frozen and attached to aluminium frames (Dafforn et al., 2013) in a random manner where they thawed *in situ*. BRCs in the field were situated deep in the euphotic zone. Chowder Bay is close to the mouth of Sydney Harbour and is a well-flushed site.

Pulse disturbance

After three months we simulated a nutrient pulse on half of the samples from every treatment. For this we created an 'organic enrichment slurry' by mixing 10% dry weight fertiliser (Yates Dynamic Lifter Turf Lifter, MOP) with seawater from the site. While diving, we slowly emptied a syringe of 50 ml of this 'organic enrichment slurry' into the top of the BRCs and attached a 63 μm mesh net over the BRCs for 24 h to ensure settlement of the 'organic enrichment slurry' onto the sediments. The other half of the samples (controls) were dosed with a 50 ml syringe of local sea water and also covered with a 63 μm mesh net for 24 h to control for procedural effects. The metals, and press and pulse organic enrichment treatments were applied in a fully crossed design, resulting in the following treatments shown in Table 2.1.

Sampling

BRCs were capped and collected after another 5 weeks. Sediment samples from the surface (top 2 cm) were collected and homogenised for microbial analyses. The remaining sediment in the BRCs (depth ~5 cm) was homogenised and samples were taken for analyses of metals (Cd, Co, Cr, Cu, Fe, Mn, Ni, Pb, Zn; Table 2.3) and nutrients (TOC, TN, TP; Table 2.2). Bulk sediments

Table 2.1: Treatment names. Treatments were applied in a fully crossed design resulting in 24 different treatments with three replicates each. Treatment names consist of the first letters for metal, press enrichment and pulse enrichment treatments, separated by a '/'. For metals, C stands for control, M for moderate, H for high, and VH for very high. For press enrichment, C stands for control, M for moderate and H for high. For the enrichment pulse, C stands for control and D stands for dosed.

Metals	Press enrichment	Pulse enrichment	Treatment name
Control	Control	Control	C/C/C
Moderate	Control	Control	M/C/C
High	Control	Control	H/C/C
Very high	Control	Control	VH/C/C
Control	Moderate	Control	C/M/C
Moderate	Moderate	Control	M/M/C
High	Moderate	Control	H/M/C
Very high	Moderate	Control	VH/M/C
Control	High	Control	C/H/C
Moderate	High	Control	M/H/C
High	High	Control	H/H/C
Very high	High	Control	VH/H/C
Control	Control	Dosed	C/C/D
Moderate	Control	Dosed	M/C/D
High	Control	Dosed	H/C/D
Very high	Control	Dosed	VH/C/D
Control	Moderate	Dosed	C/M/D
Moderate	Moderate	Dosed	M/M/D
High	Moderate	Dosed	H/M/D
Very high	Moderate	Dosed	VH/M/D
Control	High	Dosed	C/H/D
Moderate	High	Dosed	M/H/D
High	High	Dosed	H/H/D
Very high	High	Dosed	VH/H/D

were used to include total concentrations of metals and nutrients that the surface sediments were potentially exposed to through leaching. Metals and nutrients were also analysed from sediment samples at the beginning of the experiment. Dilute-acid extractable metals analyses (1 M HCl, 60 min) were made according to Simpson and Spadaro (2011). Nutrients were measured according to standard methods (APHA 5310B, APHA 4500-Norg B and 4500-NH3C distillation/titration and USEPA 6010C/6020A ICP). Cu, Pb and Zn concentrations exceeded sediment quality guideline values (SQGVs, Simpson and Batley, 2016) in several treatments (Table 2.3). Copper concentrations were below SQGV in Control metal treatment, however exceeded the SQGV in Moderate and High metal treatments, and the SQG-High value in Very High

metal treatment. Pb and Zn exceeded the SQGV in Control and Moderate metal treatments, and exceeded the SQG-High value in High and Very High metal treatments. TOC increased by a factor of 1.3 and 1.6 in Moderate and High organic enrichment, respectively. TN and TP values were approximately doubled in Moderate enrichment and tripled in High organic enrichment treatments. At the time of sampling, TOC had decreased by about 20%, TN by 50% and TP by 30% over the 17 weeks of the experiment. Samples that had received an organic enrichment pulse had slightly decreased TN values (by 10%) and slightly increased TOC values (by 10%) at the time of sampling, while TP values remained the same as in the non-dosed samples. Average nutrient concentrations per treatment can be found in Table 2.2.

Amplicon sequencing

RNA and DNA were extracted from 1 g of sediment for microbial analyses on the same day using the PowerSoil™ Total RNA Isolation and PowerSoil™ DNA Elution Accessory Kit (Mo Bio Laboratories, Carlsbad, CA, USA). RNA was further processed and cleaned with TURBO DNA-free™ Kit (Lifetechnologies, Carlsbad, CA, USA) and Agencourt® RNAClean® XP (Beckman Coulter Inc.) according to manufacturer's instructions. DNA was cleaned with Agencourt® AMPure® XP (Beckman Coulter Inc.). RNA samples were stored at -80°C until reverse transcription with SuperScript® VILO™ cDNA Synthesis Kit (Invitrogen). DNA and cDNA samples were stored at -20°C until sequencing. Overall (DNA) and active (cDNA) bacterial community composition was determined using Illumina MiSeq 2x300 bp paired-end v2 sequencing runs at the Ramaciotti Centre (UNSW, Sydney, Australia) with the 27f/519r primer set for the V1-V3 region of the 16S rRNA gene. Eukaryotic composition was determined using Illumina MiSeq 2x150 bp paired-end v3 sequencing runs and the 1391f/EukBr primer set for the V9 region of the 18S rRNA gene. Primers were chosen based on the Biomes of Australian Soil Environments project, which has successfully tested the above primers for soil ecosystems. Furthermore, the chosen 16S primers are a good indicator for general bacterial communities (which are the focus of this thesis), whereas the chosen 18S primers are known to be good general indicators for eukaryotes (however not fungi). Amplification regimes, which were followed throughout this project can be found on the Earth Microbiome Project website (http://www.earthmicrobiome.org/emp-standard-protocols/18s). For details on primer sequences, see Table 2.4, and for sequence and OTU numbers per sample see Tables A.1 and A.2.

Table 2.2: Nutrient values in the different treatments at the beginning (T0) and end (T1) of the experiment. Nutrients were measured in mg/kg. The first letter of the treatment shows the metal treatment, the second (between the '/'s) shows the press enrichment treatment, and the last one shows the enrichment pulse. For metals, C stands for control, M for moderate, H for high, and VH for very high. For press enrichment, C stands for control, M for moderate and H for high. For the enrichment pulse, C stands for control and D stands for dosed.

	T0			T1		
Treatment	TP	TN	TOC	TP	TN	TOC
C/C/C	385	1100	14000	290	1005	14000
C/C/D				275	650	13000
C/M/C	995	2000	16500	590	1055	15000
C/M/D				660	875	16500
C/H/C	1365	3000	21000	920	1450	16500
C/H/D				840	1300	18500
M/C/C	455	1150	15000	315	870	15000
M/C/D				365	835	18500
M/M/C	1090	2150	20500	720	1085	16000
M/M/D				635	1050	18500
M/H/C	2115	4100	31500	765	1450	18500
M/H/D				775	965	22500
H/C/C	560	1150	18500	445	1250	17000
H/C/D				425	1400	23500
H/M/C	1180	2550	26000	740	1050	21500
H/M/D				815	1300	23000
H/H/C	1690	3350	31500	925	1700	26500
H/H/D				810	1550	20000
VH/C/C	620	1150	28500	610	890	22500
VH/C/D				735	845	27000
VH/M/C	1210	2550	35500	720	1000	20500
VH/M/D				995	995	28500
VH/H/C	1475	3650	38500	1065	1400	24500
VH/H/D				635	1400	27000

Data analysis

DNA and RNA sequences of bacterial and eukaryotic communities, respectively, were combined and processed together following the MiSeq SOP (accessed on the 16th of March 2016, Kozich et al., 2013) for Mothur (Schloss et al., 2009). In the 18S dataset, many of the forward sequences had sequenced into the reverse primer and vice versa. Therefore, the sequences were cut down to 90 bp length to enable merging of R1 and R2. Sequences were merged using the *make.contigs* command. Then, sequences with ambiguous contigs (maxambig=0) and a length exceeding 625 bp (maxlength=625) for

Table 2.3: Metal values in the different treatments at the beginning (T0) and end (T1) of the experiment. Acid-extractable metals were measured in mg/kg. Only sediment without an enrichment pulse were analysed for metals at the end of the experiment. Letters before '/' show the metal treatment and after show the press enrichment treatment. For metals, C stands for control, M for moderate, H for high and VH for very high. For enrichment, C stands for control, M for moderate and H for high.

	Treatment	Al	As	Ba	Cd	Co	Cr	Cu	Fe	Mn	Ni	Pb	S	Sn	V	Zn
T0	C/C	2650	5.9	2.5	< 1	4.2	10.5	14.3	10000	140.0	4.4	58.9	2150	< 2	19.3	183.1
	C/M	2700	7.7	6.5	< 1	5.0	11.6	21.9	10000	174.1	4.8	60.5	3050	< 2	19.6	208.8
	C/H	2550	5.9	7.2	< 1	4.3	11.2	21.3	10250	184.2	4.8	56.8	3100	< 2	19.5	212.5
	M/C	3700	9.8	7.0	< 1	5.4	19.7	101.8	13000	177.4	5.7	169.3	2700	23.1	27.8	345.7
	M/M	2900	9.5	8.2	< 1	3.7	15.9	90.5	9950	165.8	5.0	134.2	3050	13.9	22.1	298.4
	M/H	2900	9.5	12.8	< 1	3.9	17.0	95.9	9666.7	195.5	5.0	142.1	3133.3	13.8	21.6	333.7
	H/C	4225	14.6	10.8	< 1	5.0	28.1	270.2	13500	175.7	6.4	349.3	2375	53.3	34.0	559.9
	H/M	3700	11.8	13.2	< 1	5.2	24.1	209.2	11333.3	171.4	5.4	264.6	2566.7	41.3	27.9	479.3
	H/H	3125	12.4	12.5	< 1	4.1	22.3	188.1	11000	175.8	5.6	270.4	1375	37.1	26.9	491.7
	VH/C	4900	16.5	15.2	0.6	3.9	39.2	418.5	13500	179.3	7.1	507.6	1150	93.7	40.8	779.2
	VH/M	4900	17.4	19.3	< 1	4.6	39.6	399.3	13666.7	210.6	7.2	483.4	1366.7	89.3	40.3	808.9
	VH/H	4500	17.4	19.2	0.6	3.8	36.8	375.7	12500	210.1	6.7	458.3	1450	78.6	36.8	764.7
T1	C/C	2000	5.4	6.7	0.1	3.6	10.0	30.6	7750	94.6	4.1	71.7	1350	2.6	17.5	159.4
	C/M	2750	5.3	7.3	0.4	3.1	14.3	40.4	13000	90.3	5.6	93.7	1900	2.8	27.9	231.6
	C/H	3700	6.6	11.8	0.3	5.5	19.6	62.2	19150	124.4	8.1	122.9	3050	3.9	40.3	355.1

continued on next page

Table 2.3 – continued from previous page

Treatment	Al	As	Ba	Cd	Co	Cr	Cu	Fe	Mn	Ni	Pb	S	Sn	V	Zn
M/C	2700	7.0	8.1	0.4	3.8	16.6	86.3	9400	108.3	5.3	135.4	1500	15.3	23.3	264.9
M/M	2750	7.7	9.1	0.6	2.7	17.7	95.1	11800	89.1	5.4	156.2	1850	21.6	29.6	319.3
M/H	3000	4.7	9.7	0.3	5.2	18.6	74.9	15050	106.0	5.9	146.7	2050	19.0	33.5	331.8
H/C	3300	10.9	11.4	0.5	3.7	23.2	211.8	11050	130.6	6.2	289.0	1450	43.0	30.4	460.8
H/M	3600	11.4	12.8	0.5	5.3	25.4	176.6	13600	134.2	6.4	266.7	1600	53.4	35.0	477.3
H/H	3400	9.1	13.7	0.4	3.9	25.9	148.5	17050	125.4	6.7	288.3	2250	49.3	40.8	511.4
VH/C	3150	14.5	19.2	0.4	4.4	33.9	344.8	12100	166.2	6.6	414.7	1450	81.3	37.7	648.0
VH/M	4250	13.5	17.5	0.4	4.1	35.9	255.0	14850	139.8	6.7	391.5	1800	94.0	44.0	672.8
VH/H	4200	12.4	17.9	0.5	3.8	37.0	222.5	17800	153.3	7	383.9	2150	91.9	48	699.2

Table 2.4: Primer sequences used for 16S and 18S sequencing.

Primer	Sequence (5'-3')	Target region	Target group	Reference
27f	AGAGTTTGATCMTGGCTCAG	V1-V3	Bacteria	Lane (1991)
519r	GWATTACCGCGGCKGCTG			Turner et al. (1999)
1391f	GTACACACCGCCCGTC	V9	Eukarya	Amaral-Zettler et al. (2009)
EukBr	TGATCCTTCTGCAGGTTCACCTAC			

16S and 151 bp (maxlength=151) for 18S, respectively, were removed from the dataset (*screen.seqs*). Sequences that were not unique were removed from the dataset using *unique.seqs*. Subsequently, sequences were aligned to the SILVA (version 123) database (*align.seqs*). For both 16S and 18S, a maximum of 8 consecutive identical bases (maxhomop=8) was allowed (*screen.seqs* of the aligned datasets), and overhangs of sequences, as well as gap characters (i.e. '-') were removed using the *filter.seqs* command. To make the datasets smaller and, therefore, shorten the necessary run time for Mothur, all sequences that only occurred once were removed from both 16S and 18S datasets prior to *pre.cluster*. This was done using *split.abund* with a cut-off value of 1. Sequences were then clustered into operational taxonomic units (OTUs) using a similarity level of 99% for both bacteria and eukaryotes and the *pre.cluster* command. After removal of chimeric sequences (*chimera.uchime* and *remove.seqs*), taxonomies of OTUs were determined using the *classify.seqs* command with a Mothur formatted version of the RDP training set (version 9) and the SILVA database (version 123) for 16S and 18S sequences, respectively. Irrelevant classifications (16S: all except bacteria, 18S: all except eukaryotes) were removed with *remove.lineage* before clustering of the sequences using *cluster.split*. In the *cluster.split* command a cutoff value of 0.15 was used for both datasets, and a taxlevel of 4 and 12 for 16S and 18S, respectively. Data outputs with counts per sample for each OTU and taxonomic information were achieved using the *make.shared* and *classify.otu* commands. The Mothur output was analysed using R version 3.2.3 (R Core Team, 2015) and packages *vegan* (Oksanen et al., 2016) and *DESeq* (Anders and Huber, 2010). Plots were generated using the *ggplot2* (Wickham, 2009) package. For information on sequence and OTU numbers per sample, see Tables A.1 and A.2.

Operational taxonomic unit level analyses

Raw Operational Taxonomic Unit (OTU) counts were variance stabilised using the getVarianceStabilizedData function of the *DESeq* package. Community changes between treatments were calculated at OTU (operational taxonomic unit) level using the *adonis* function (package *vegan*), which performs a permutational multivariate analysis of variance (PERMANOVA). Community composition was visualised with non-metric multidimensional scaling (NMDS) plots. Taxa driving the changes in composition (class level for 16S and class/-phylum level for 18S datasets) were identified using the *envfit* function (package *vegan*) at a significance level of $\alpha \leq 0.001$. Planned comparisons were performed using the *adonis* function to detect differences between metal treatments within organic enrichment treatments, as we expect the potentially toxic

effects of metals to be masked in the presence of organic enrichment.

A comparison of the degree of community shifts between bacterial (16S) and eukaryotic (18S), and total (DNA) and active (RNA) communities, respectively, was performed using the *mantel* function (package *vegan*) for a Mantel's test. Furthermore, OTUs were classified as abundant if they contributed at least 1% to the total counts of a specific sample. All OTUs with <1% contribution were classified as rare. The contribution of all abundant OTUs per sample (sum of counts of all abundant OTUs divided by total counts) were determined and the number of abundant OTUs was noted. Using an analysis of variance (ANOVA), we determined if the contribution of abundant OTUs changed between treatments.

Taxonomic analyses

Taxonomic data was analysed on the class level for bacteria and on the class or phylum level for eukaryotes. This taxonomic level was chosen based on the number of classified OTUs per level, in order to maximise diversity and taxonomic information at the same time. In addition, the focus here is on substantial shifts in community composition, which should be represented at higher taxonomic levels. Unclassified taxa, 36% and 69% of OTUs in the 16S and 18S datasets, respectively, were excluded from the analyses. Also, only taxa comprised of at least 5 OTUs across all samples were included, in order to create a smaller and more manageable dataset for analysis. In the eukaryotic dataset many classes would have been excluded due to low read levels, therefore we grouped these highly diverse classes together on the phylum level. Class/phylum data were overlaid onto the NMDS plot using the *envfit* function (package *vegan*) in R. Taxa with a significance value of $p \leq 0.0001$ and a correlation of $r > 0.5$ for the environmental fit were determined as those with the highest contribution to the structural changes of the community and used for further univariate analyses (ANOVAs) for the specific dataset (16S or 18S, DNA or RNA). Tukey's honest significant difference tests (TukeyHSD) were used to determine what treatment levels were significantly different from each other on the taxa level.

Results and Discussion

Organic enrichment vs metal contamination

The organic enrichment resulted in a significant shift in structure of both bacterial and eukaryotic communities identified from DNA and RNA, here-

after referred to as 'total' and 'active' community, respectively (all communities: $p<0.001$, Table A.3). The shift in community structure was especially pronounced between Control and Moderate organic enrichment treatments, whereas only a relatively minor shift occurred between the Moderate and High organic enrichment treatments (Figures 2.1 to 2.4, Table 2.5). This suggests that organic enrichment affects the sediment communities at relatively modest levels, a result also observed in marine biofilms by Lawes et al. (2016b). This altering of eutrophied communities can affect primary productivity and influence the production of greenhouse gases (Smith et al., 1999).

Press metal contamination affected both active and total bacterial, and total eukaryotic communities (Table A.3). The active part of the eukaryotic community was not affected by metal contamination (Table A.3), suggesting some resilience of eukaryotic fauna to metal stress. The clustering of metal affected communities is not well represented in the NMDS plots because within our study, enrichment effects were stronger and dominated the clustering of samples along both axes.

To test our hypothesis that organic enrichment interacts and potentially ameliorates the toxicity of metals, planned comparisons of metal effects within organic enrichment levels were conducted (Table 2.6). Within the samples with no organic enrichment (i.e. press or pulse organic enrichment Controls, Table 2.1), metals affected the community composition of total and active bacterial communities in High and Very High metal treatments, but not in the Moderate metal treatment. The total eukaryotic community was only affected at Very High metal treatments within Control organic enrichment. Within Moderate organic enrichment treatments, the active bacterial and total eukaryotic communities were both affected by High and Very High metal treatments, while the total bacterial community was only affected by Very High metal treatment. For the High organic enrichment, only the Very High metal treatment had an effect on any community, in this case the total bacterial community. The effect of metal contaminants on both bacterial and eukaryotic communities decreased with the increasing organic enrichment resulting in masking of metal toxicity. This may be partly explained by the fact that dissolved and particulate organic matter lower the bioavailability and toxicity of metals such as copper in sediments due to formation of non-labile complexes (Strom et al., 2011; Hook et al., 2014; Campana et al., 2015).

Bacteria vs eukaryotes

The comparison of bacteria and eukaryotes has to be treated with caution, as the efficiency of DNA and RNA extractions and the gene amplification could

Table 2.5: Euclidean distances between the centroids of all levels of significant treatments (according to *adonis* results) in all four datasets. Larger distances of centroids represent less similarity between the two tested groups.

dataset	treatment	levels	distance of centroids
16S DNA	nutrients	control – moderate	0.1299
		control – high	0.1493
		moderate – high	0.0194
	metals	control – moderate	0.0154
		control – high	0.0250
		control – very high	0.0586
		moderate – high	0.0134
		moderate – very high	0.0481
		high – very high	0.0348
16S RNA	nutrients	control – moderate	0.2712
		control – high	0.3014
		moderate – high	0.0410
	metals	control – moderate	0.0190
		control – high	0.0183
		control – very high	0.0651
		moderate – high	0.n0246
		moderate – very high	0.0706
		high – very high	0.0478
18S DNA	nutrients	control – moderate	0.1482
		control – high	0.1675
		moderate – high	0.0296
	metals	control – moderate	0.0403
		control – high	0.0452
		control – very high	0.0041
		moderate – high	0.0257
		moderate – very high	0.0196
		high – very high	0.0435
18S RNA	nutrients	control – moderate	0.1795
		control – high	0.2213
		moderate – high	0.0439

be different for bacteria and eukaryotes. DNA/RNA of different molecular weights have different optimal extraction procedures, e.g. homogenisation time and speed (Miller et al., 1999). Furthermore, the concept of diversity is very different between bacteria and eukaryotes (Grattepanche et al., 2014). Methods developed for bacterial diversity analysis cannot necessarily be used for eukaryotic diversity analysis. For example, bacterial OTUs are usually determined based on a 97% similarity, whereas for eukaryotes it has been shown that different species can share more than 98% of their genes (Caron,

Table 2.6: Planned comparison ANOVA results. For every dataset, each metal level was compared to the control metal level within the different enrichment levels. Significant *p*-values (at a level of α=0.05) are highlighted in bold.

enrichment	metals	16S DNA *p*-value	16S RNA *p*-value	18S DNA *p*-value	18S RNA *p*-value
control	moderate	0.28	0.27	0.3	0.5
	high	**0.002**	**0.011**	0.07	0.57
	very high	**0.001**	**0.001**	**0.04**	0.21
moderate	moderate	0.82	0.49	0.92	0.87
	high	0.08	**0.003**	**0.03**	0.4
	very high	**0.002**	**0.006**	**0.04**	0.57
high	moderate	0.31	0.31	0.6	0.61
	high	0.07	0.16	0.47	0.42
	very high	**0.036**	0.09	0.14	0.39

2009), while still being separate. The fact that we used a 99% similarity for our OTUs minimises the loss of eukaryotic diversity in our dataset. However, we cannot control for the potential imbalances at the extraction and amplification steps. Imbalances in efficiency of DNA extraction and amplification between bacterial and eukaryotic can lead to an underestimation of diversity of the group with lower efficiency.

From our study it becomes apparent that bacterial communities are more sensitive indicators of historical metal contamination than eukaryotes. The active eukaryotic community was not affected by metal contamination. The active component of the bacterial community, however, was significantly impacted by metals, indicating that bacteria are more sensitive (Table A.3). In addition, bacterial communities were affected at lower metal concentrations than eukaryotes under non-enriched conditions, and only bacterial communities responded to metal contamination at high enrichment levels. This result may be predicted by ecotoxicological research that showed extensive detoxification mechanisms in more complex organisms, such as benthic invertebrates (Rainbow, 2002; Campana et al., 2015), while other studies found an underrepresentation of detoxification systems in marine bacteria (Bengtsson-Palme et al., 2014). The higher susceptibility of smaller and simpler organisms to metal toxicants makes them a good basis for the use as indicators of harmful levels of pollutants (Sun et al., 2012).

While the bacterial communities were more sensitive and produced more statistically significant effects, the responses of total and active bacterial and eukaryotic communities were highly correlated and similar in degree and direction (Table 2.7). The ability of bacterial communities to simultaneously

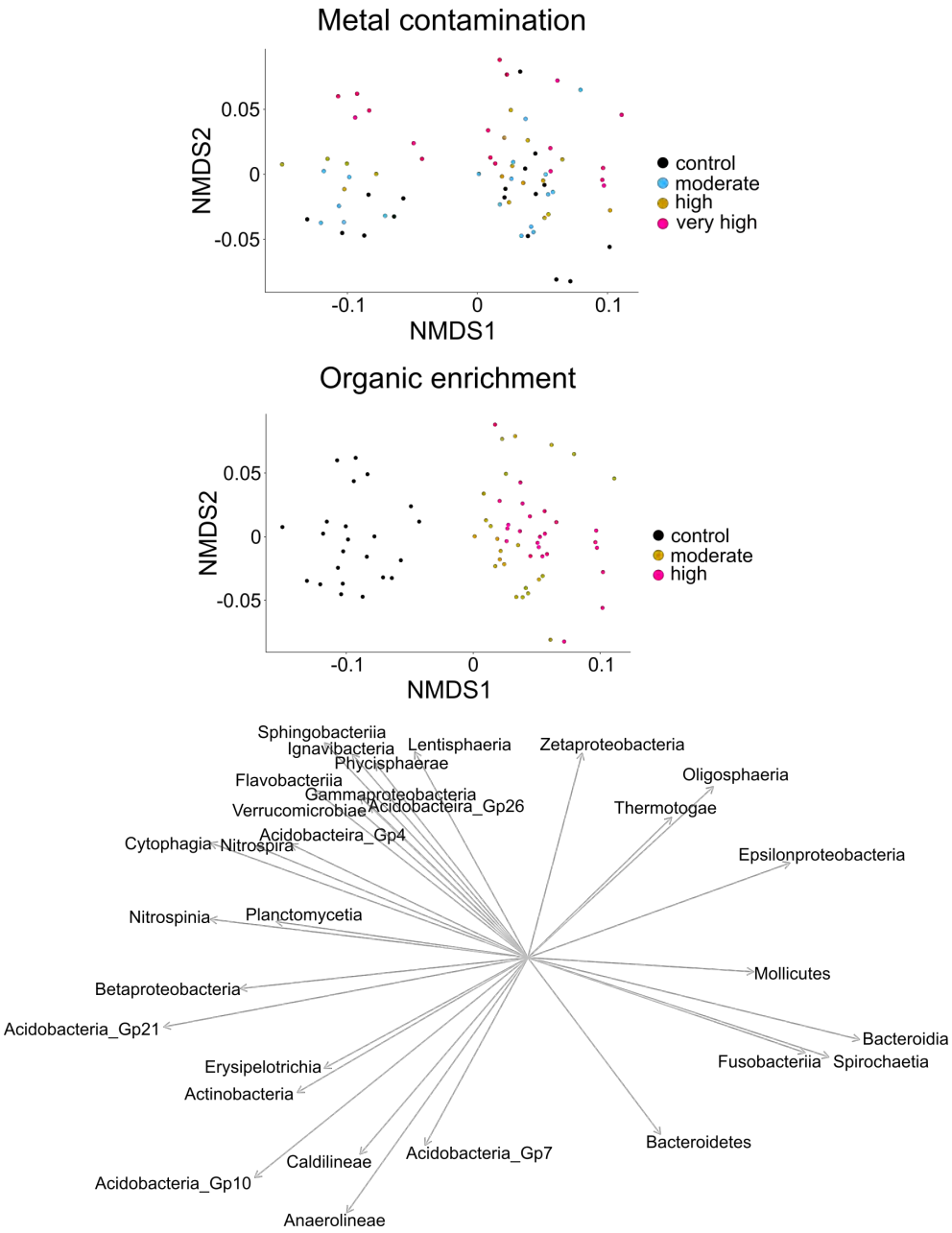

Figure 2.1: Non-metric multidimensional scaling (NMDS) plots for the **16S DNA** dataset and all treatments that significantly impacted the community compositions according to the *adonis* results. The colours of the samples in the plots represent the treatment levels. The bottom plot shows the taxa (class level) which were found to most significantly drive the community changes (i.e. significance level of $p \leq 0.0001$ and a correlation of $r > 0.5$).

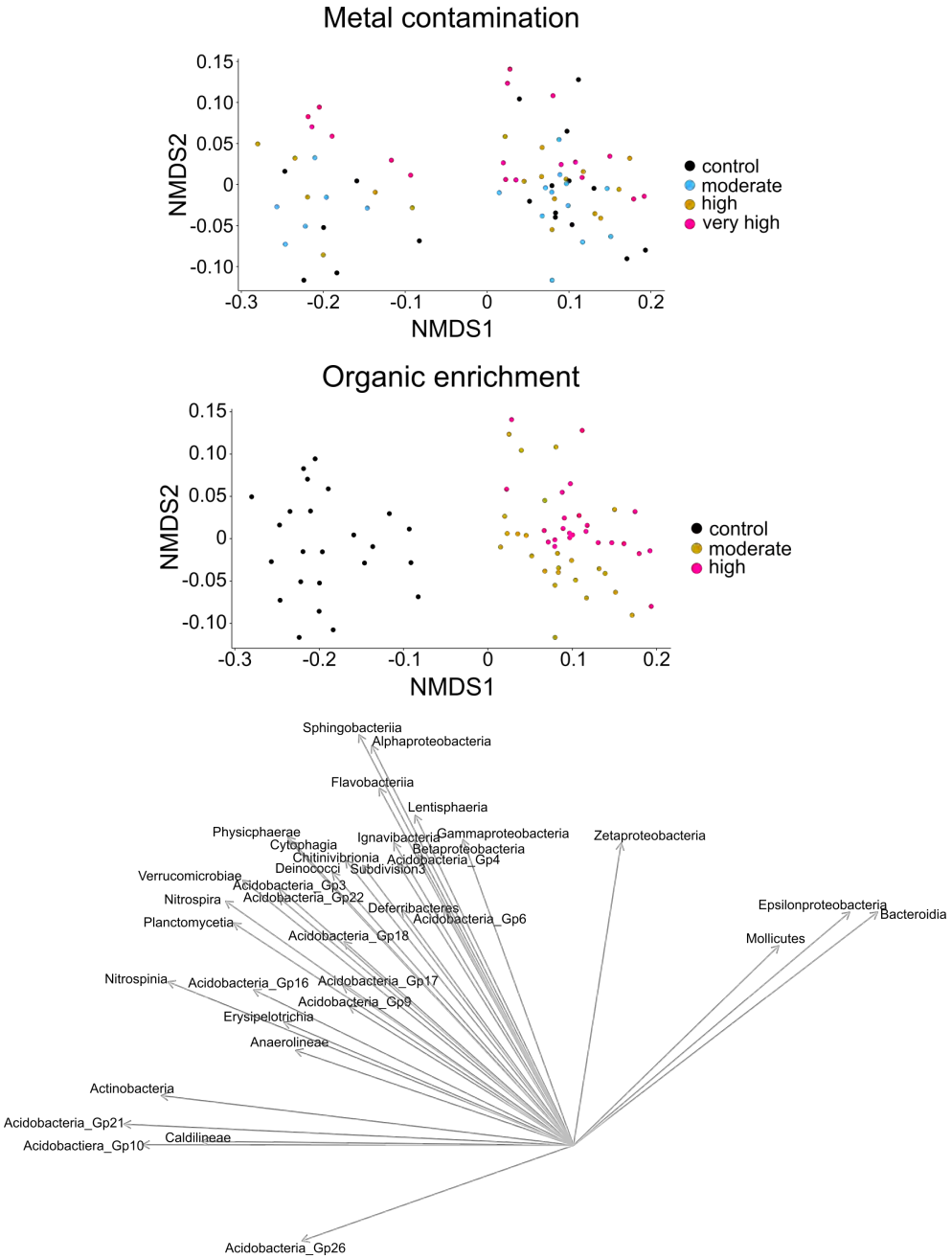

Figure 2.2: Non-metric multidimensional scaling (NMDS) plots for the **16S RNA** dataset and all treatments that significantly impacted the community compositions according to the *adonis* results. The colours of the samples in the plots represent the treatment levels. The bottom plot shows the taxa (class level) which were found to most significantly drive the community changes (i.e. significance level of $p \leq 0.0001$ and a correlation of $r > 0.5$).

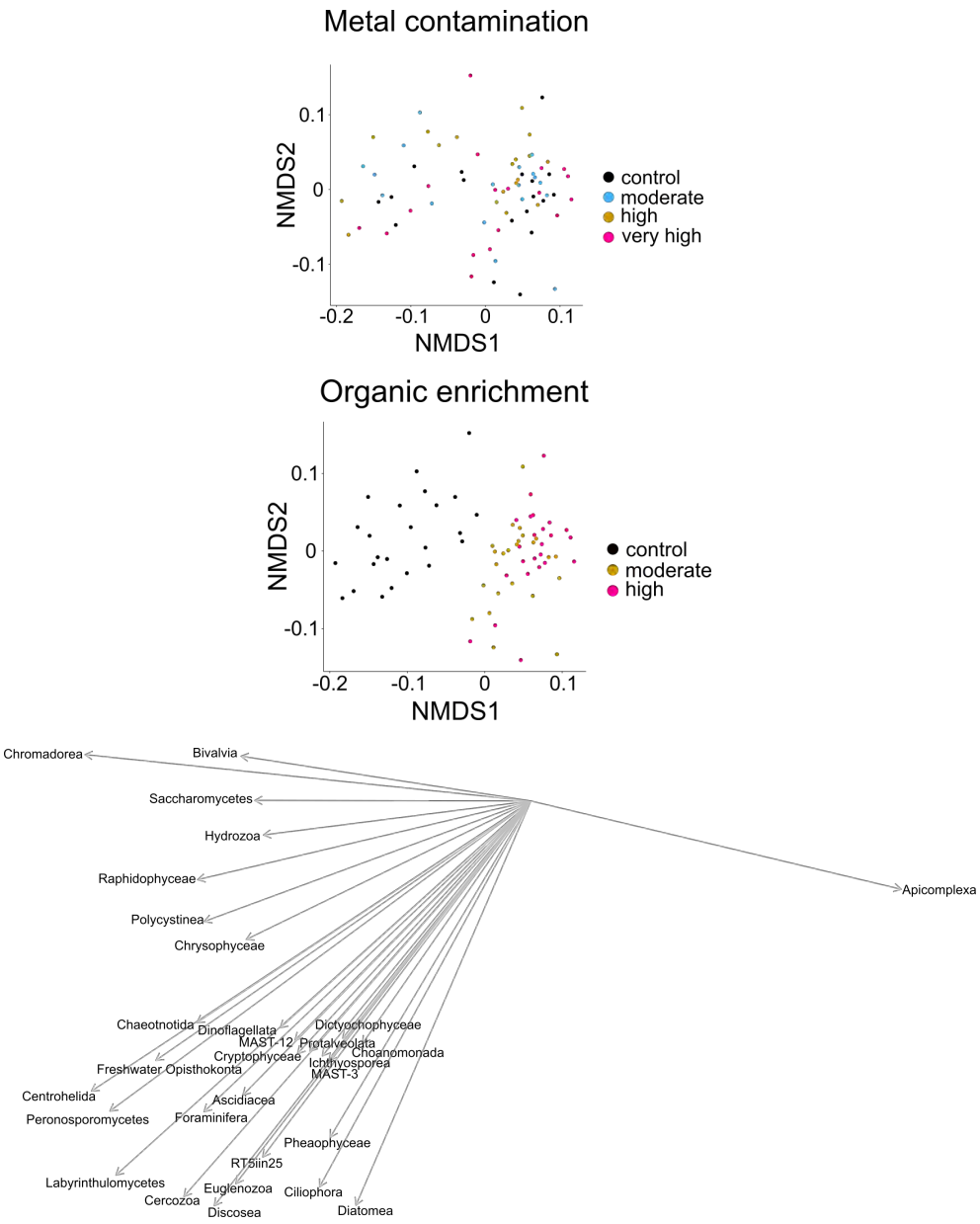

Figure 2.3: Non-metric multidimensional scaling (NMDS) plots 18S DNA dataset and all treatments that significantly impacted the community compositions according to the *adonis* results. The colours of the samples in the plots represent the treatment levels. The bottom plot shows the taxa (class/phylum level) which were found to most significantly drive the community changes (i.e. significance level of $p \leq 0.0001$ and a correlation of $r > 0.5$).

present bacterial responses and represent the shift in the eukaryotic community makes them a useful focus for biomonitoring. Organic enrichment induced changes in marine biofilm communities have recently been shown to affect the associated macrofauna (Lawes et al., 2016a). Therefore, this similarity in shift is likely due to direct effects between organisms from different domains in the

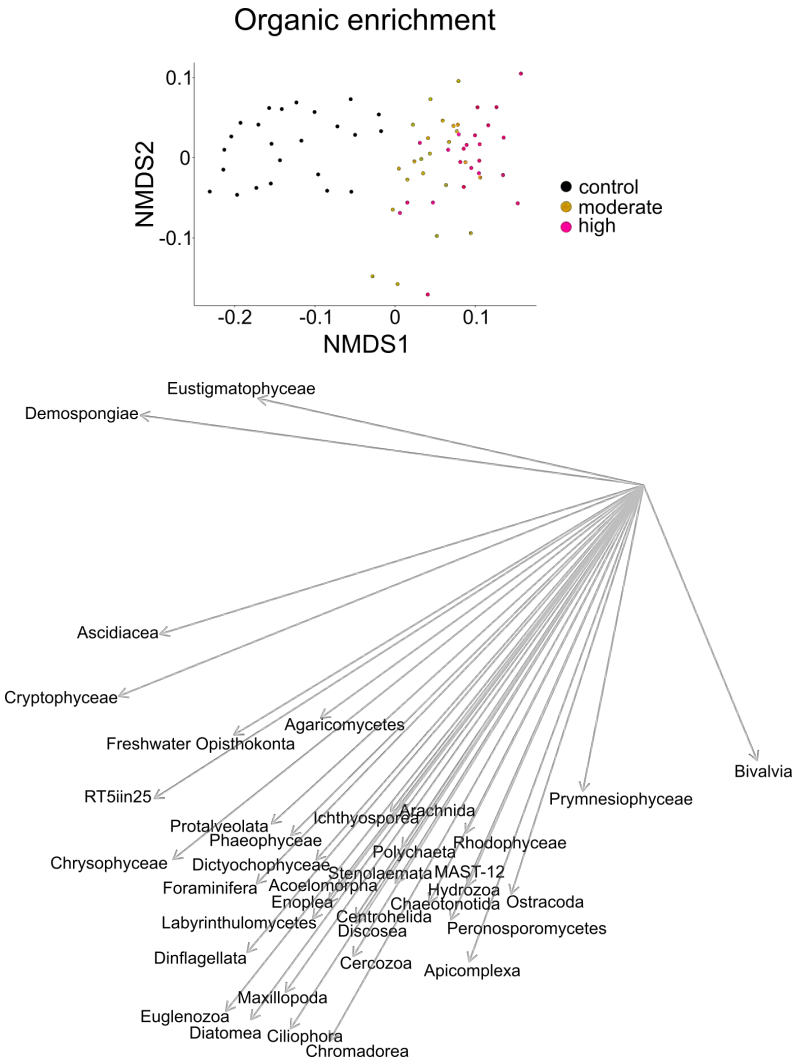

Figure 2.4: Non-metric multidimensional scaling (NMDS) plots for the **18S RNA** dataset and all treatments that significantly impacted the community compositions according to the *adonis* results. The colours of the samples in the plots represent the treatment levels. The bottom plot shows the taxa (class/phylum level) which were found to most significantly drive the community changes (i.e. significance level of $p \leq 0.0001$ and a correlation of $r > 0.5$).

Table 2.7: R output from the Mantel's tests. Community shifts are compared within communities (16S and 18S) and within genetic material (DNA and RNA). Significant *p*-values (at a level of α=0.05) are highlighted in bold.

				Upper quantiles of permutations			
comparison	Mantel statistic r	*p*-value	# permutations	90%	95%	97.5%	99%
16S – DNA vs RNA	0.923	**0.001**	999	0.0613	0.077	0.0913	0.1086
18S – DNA vs RNA	0.7735	**0.001**	999	0.0628	0.0835	0.1026	0.1299
DNA – 16S vs 18S	0.8269	**0.001**	999	0.0671	0.0851	0.1111	0.1279
RNA – 16S vs 18S	0.7955	**0.001**	999	0.0548	0.0718	0.0889	0.108

same habitat.

The press organic enrichment in our experiment led to bacterial and eukaryotic community structures with higher dominance. Operational Taxonomic Units (OTUs) that account for >1% of the total counts are commonly regarded as the abundant OTUs in a community (Logares et al., 2014). In bacterial and eukaryotic communities, the contribution of abundant OTUs to the total community increased with increasing levels of organic enrichment (Figure 2.5), shifting communities to a state of higher dominance and lower community evenness. Bacterial community evenness already decreased in Moderate organic enrichment treatments, while the eukaryotic community evenness was only altered in High organic enrichment treatments. Contaminants have commonly been shown to reduce diversity by increasing the dominance of certain eukaryotic species (Johnston and Roberts, 2009) and by shifting microbial resources to survival mode, e.g. dormancy (Schimel et al., 2007). Lower community evenness can affect the resistance and resilience of a community (Lyons and Schwartz, 2001; Allison, 2004), as well as alter species interactions and ecosystem processes (Schimel et al., 2007; Hillebrand et al., 2008). Thus, communities exposed to repeated and multiple stressors may reach a tipping point, at which the community and ecosystem functions are permanently altered or completely collapse (Dai et al., 2012).

Community response to a pulse disturbance

The organic enrichment pulse did not significantly affect the structure of any of the communities in the long term. A potential initial effect on the structure of either bacterial or eukaryotic communities, would have been detectable in the DNA dataset, as extracellular DNA (from dead organisms) can persist for several weeks (i.e. longer than time from dosing to sampling) in sediment (Nielsen et al., 2007). Therefore, we conclude that bacterial and eukaryotic sediment communities are generally resistant to organic enrichment pulses, as the one simulated in this experiment. This does not, however, exclude effects on specific taxa and abundant OTUs (discussed further down). Also, it does not exclude the possibility of functional changes straight after the dosing occurred. Most likely, the microbial sediment community would be able to cycle the excess organic matter and nutrients out of the sediment and thus prevent a lasting effect of the pulse on the sediment community in general. This would have required an initial functional shift of the sediment community, which would not be reflected in our structural data largely showing resistance to the organic enrichment pulse. However, in the abundant OTUs of the total bacterial communities, we detected a significant interaction between

press organic enrichment and pulse organic enrichment (Figure 2.5), where the evenness-enhancing effect of the pulse organic enrichment increases with increasing press organic enrichment, and thus with increasing dominance. This suggests that abundant organisms might be more sensitive to pulse stressors, leading to a decrease in their counts. Alternatively, the organic enrichment pulse could negatively affect all species/OTUs in the community and thus push the abundant OTU numbers below 1% of the total counts, thus increasing the evenness of the community.

DNA vs RNA

Metal contamination affected the active part of the bacterial community, whereas it affected both the total bacterial and total eukaryotic communities. The total part of the communities include what is living, dead, eaten and recently moved through the sediments, because DNA can persist in sediments for up to two months before degrading (Nielsen et al., 2007). DNA is therefore a more time-integrated measure (Figure 2.6) and suggests that metal contamination was toxic to both bacteria and eukaryotes at the beginning of the experiment. Using RNA, this early effect of metals on the community would not be detectable. Furthermore, the Mantel's test showed that the DNA and RNA communities were highly correlated in both datasets and the general community structures (Figures 2.1 to 2.4) were significantly similar in degree and direction (Table 2.7). In general, this suggests that either DNA or RNA can be used to measure community shifts in contaminated sediments. The handling of DNA and the extraction kits are significantly cheaper to RNA kits (personal observation) and we thus suggest that DNA is the more cost-effective option for large biomonitoring studies. Furthermore, for the bacterial community, the shifts of the total and active communities were more similar than the ones in the eukaryotic community (Table 2.7). This means that when using DNA as the genetic material of choice for ecosystem assessments, the bacterial community would be the preferable option, as the total community shifts also closely represent the shifts of the active community.

Bacterial taxa analysis

We used the *envfit* function (R package *vegan*) to determine which taxa were the ones significantly driving the community shifts upon disturbance. Using *envfit* results we chose ($p \geq 0.0001$ and $r > 0.5$) the following bacterial taxa for further analysis of the total community: *Acidobacteria Gp10*, *Acidobacteria Gp21*, *Cytophagia*, and *Bacteroidia*. For the active community, these were:

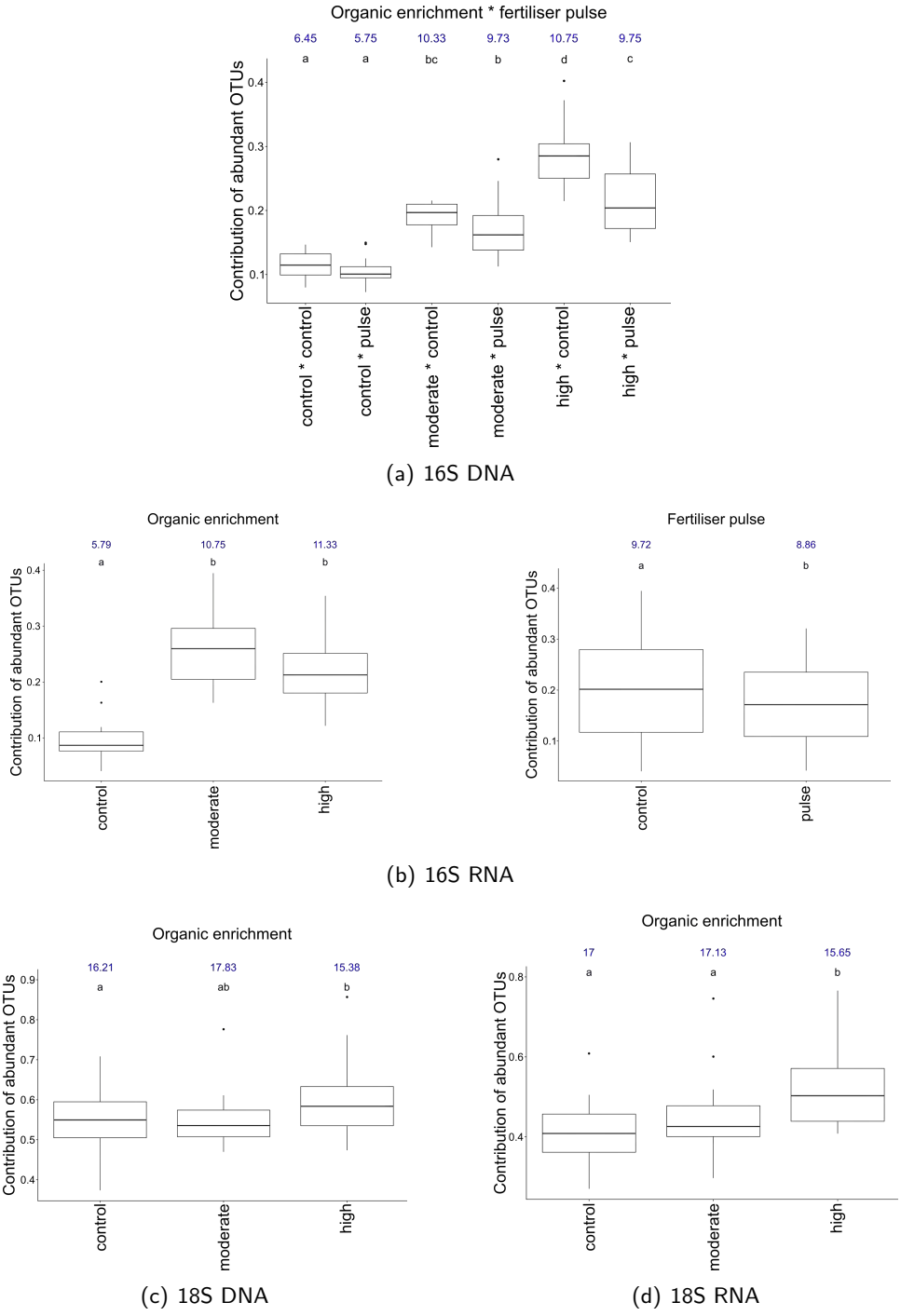

(a) 16S DNA

(b) 16S RNA

(c) 18S DNA

(d) 18S RNA

Figure 2.5: Contribution of abundant OTUs in each dataset: (a) 16S DNA, (b) 16S RNA, (c) 18S DNA, (d) 18S RNA. Blue numbers indicate the mean number of OTUs that were abundant (>1% of total counts). Only treatments with significant differences of contribution of abundant OTUs are shown. The letters (a-d) above the boxplots show the significance groups. For example, a and b are significantly different, while a and ab are not.

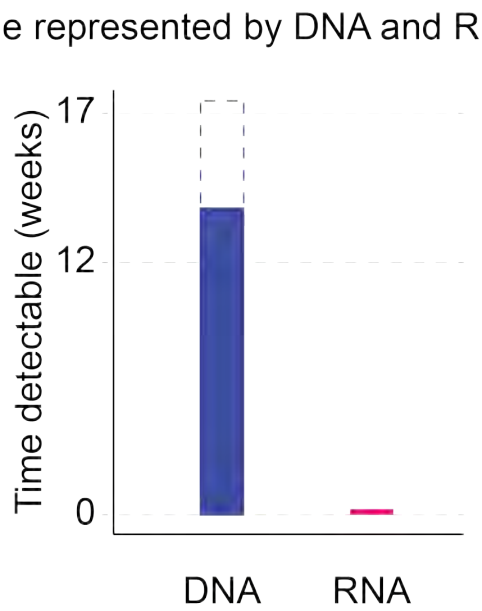

Figure 2.6: Time represented by DNA and RNA datasets in sediments. DNA can persist in marine sediments for weeks and is therefore a more time-integrated measure, while RNA is rapidly degraded within minutes and therefore represents the momentary status of a community. Therefore, the DNA informs on structural changes that happened due to the organic enrichment pulse (five weeks before sampling), and potentially even since the beginning of the experiment (17 weeks). RNA, on the other hand, reflects only very recent (within hours) structural changes.

Acidobacteria Gp10, *Acidobacteria Gp21*, *Alphaproteobacteria*, *Nitrospinia*, *Nitrospira*, *Sphingobacteriia*, and *Verrucomicrobiae*. Total and active counts of *Acidobacteria* (*Gp10* and *Gp21*, respectively) were impacted by metal contamination. *Acidobacteria* are a very diverse acidophilic phylum, which is abundant in soil ecosystems world-wide (Jones et al., 2009). While total *Gp10* counts were significantly lower in very high metal treatments than in high metal treatments, active *Gp21* counts decreased significantly from moderate to high metal levels (Figure 2.7). Furthermore, both total and active *Gp10* and *Gp21* decreased significantly with organic enrichment. This suggests that *Acidobacteria* down-regulate their proliferation (low DNA combined with low RNA) when exposed to organic enrichment.

The organic enrichment further led to a decrease in total levels of *Cytophagia*. *Cytophagia* have the ability to degrade macromolecules, such as proteins, starch and cellulose (Reichenbach, 2006) and thus a decrease might lead to a lower potential of degradation of organic matter at the sediment-water interface. *Bacteroidia*, on the other hand, increased in the total community when press organic enrichment was present. The class *Bacteroidia* is abundant in the gastrointestinal system of animals, in soils, sediments and sea water and in-

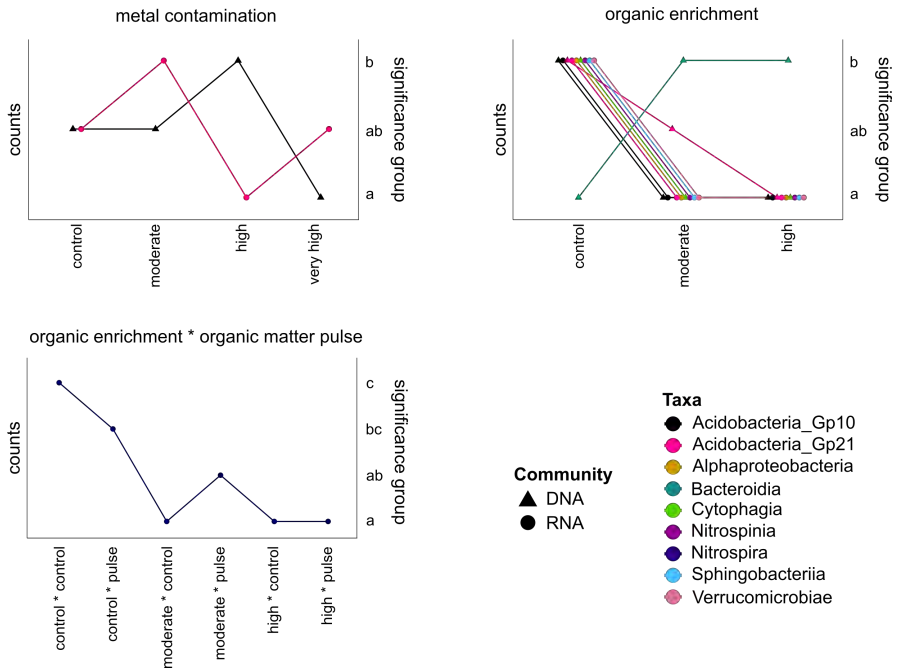

Figure 2.7: Summary of boxplots for taxa specific analyses of **16S dataset**. Taxa were analysed on the class level and selected based on a *p*-value of $p<0.0001$ and a correlation of $r>0.5$ in the *envfit* analysis. This means that the taxa analysed in detail here are the ones that most significantly drove the community changes (see NMDS plots, Figures 2.1 to 2.4) between the treatments. Only significant treatments and taxa are shown. The left y axis indicates total counts of sequences assigned to the different taxa, the right y axis shows the significance group. For example, a and b are significantly different, while a and ab are not.

cludes many opportunistic pathogens (Thomas et al., 2011). *Bacteroidia* have been shown to be involved in the degradation of organic matter in marine ecosystems (Fernández-Gómez et al., 2013). The increase in DNA, without an increase or decrease in activity (RNA), suggests that *Bacteroidia* must have increased temporarily with organic enrichment. Nonetheless, the *Bacteroidia* DNA was most likely introduced through the fertiliser used to simulate enrichment, as its main component is chicken faecal matter.

Active levels of *Alphaproteobacteria*, *Nitrospinia*, *Sphingobacteriia* and *Verrucomicrobiae* all significantly decreased with organic enrichment (Figure 2.7). In addition, active levels of *Nitrospira* were impacted by an interaction of press and pulse organic enrichment, where the impact of a pulse seems to be dampened by pre-existing organic enrichment. While the organic enrichment pulse significantly decreased the active counts of *Nitrospira* if the sediment was not exposed to previous press organic enrichment, it did not have an effect in Moderate or High press organic enrichment treatments. *Nitrospinia* and *Nitrospira* are important players in the nitrogen metabolism as they are both

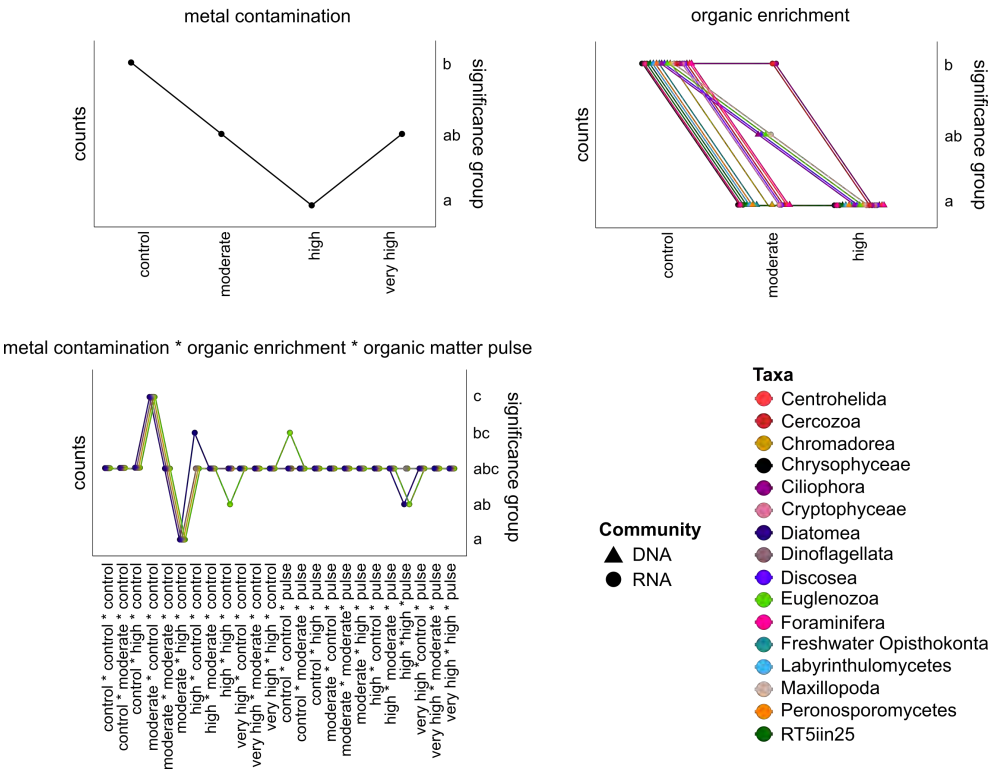

Figure 2.8: Summary of boxplots for taxa specific analyses of **18S dataset**. Taxa were analysed on the class/phylum level (mostly classes, but phyla were used where more appropriate) and selected based on a *p*-value of $p<0.0001$ and a correlation of $r>0.5$ in the *envfit* analysis. This means that the taxa analysed in detail here are the ones that most significantly drove the community changes (see NMDS plots, Figures 2.1 to 2.4) between the treatments. Only significant treatments and taxa are shown. The left y axis indicates total counts of taxa, the right y axis shows the significance group. For example, a and b are significantly different, while a and ab are not.

nitrite (NO_2^-) oxidisers (Altmann et al., 2003; Lücker et al., 2013). These bacteria convert NO_2^- into nitrate (NO_3^-), which is an important step in nitrification, and are therefore crucial for the cycling of N through the system. A lack of NO_2^- oxidation can result in an accumulation of toxic ammonia and NO_2^- in the system (Ruiz et al., 2003). Hence, *Nitrospinia* and *Nitrospira* are crucial for detoxification of the sediments and the cycling of N through the system. Metatranscriptomics data on a part of the samples from the same experiment showed that increased organic enrichment led to higher ammonification levels in the sediments (see Chapter 3 of this thesis). In such sediments, the role of nitrification-related organisms becomes even more crucial. Furthermore, the class *Alphaproteobacteria*, which was negatively affected by enrichment, includes important denitrifying bacteria, which express the gene (*nosZ*) involved in nitrous oxide (N_2O) reduction to nitrogen gas (N_2). This reduction of N_2O is essential, due to its involvement in ozone depletion and

therefore climate change (Ravishankara et al., 2009). *Alphaproteobacteria* in general and the gene expression of *nosZ* are both known to decrease in enriched sediments (e.g. Kearns et al., 2015, Chapter 3 of this thesis). The downregulation of *Nitrospinia* and *Nitrospira* activities, and possibly some bacteria from the class *Alphaproteobacteria*, in organically enriched sediments can lead to an incomplete removal of nitrogen from the system, increasing the toxicity of the sediments, and a potential increase in production of a greenhouse gas. However, the class *Alphaproteobacteria* is very diverse and it is therefore not possible to know the consequences of a decrease without further information.

Sphingobacteriia are ubiquitous in sediments and have been shown to degrade complex organic macromolecules (Luo et al., 2008; Qu et al., 2015); thus, their decreasing activity with increasing enrichment suggests, as for Cytophagia, a loss of organic matter degradation capacity of the sediment community. *Verrucomicrobiae* are often associated with eukaryotic hosts (Wagner and Horn, 2006) and are also frequently found in sediments, but they have not been well studied and their ecological relevance is not clear (Bergmann et al., 2011).

Eukaryotic taxa analysis

As for the bacterial community, we used the *envfit* function to determine the taxa most strongly driving the eukaryotic community shift upon disturbance. From the *envfit* results, classes and in some cases phyla that were chosen ($p \geq 0.0001$ and $r > 0.5$) for univariate analyses for the total eukaryotic community were: *Centrohelida*, *Cercozoa*, *Chromadorea*, *Ciliophora*, *Diatomea*, *Discosea*, *Euglenozoa*, *Foraminifera*, Freshwater *Opisthokonta*, *Laburynthulomycetes*, *Peronosporomycetes*, and *RT5iin25*. And for the active community, these were: *Cercozoa*, *Chromadorea*, *Chrysophyceae*, *Ciliophora*, *Cryptophyceae*, *Diatomea*, *Dinoflagellata*, *Discosea*, *Euglenozoa*, *Foraminifera*, *Maxillopoda*, and *RT5iin25*. Many of these eukaryotes have previously been shown to be impacted in highly modified estuaries (Dafforn et al., 2014).

Total levels of all classes/phyla, except *Diatomea*, significantly decreased with organic enrichment (Figure 2.8), corroborating that organic enrichment can be toxic to many eukaryotic organisms (Pearson and Rosenberg, 1978). Furthermore, organic enrichment decreased activity of *Cercozoa*, *Chrysophyceae*, *Ciliophora*, *Cryptophyceae*, *Discosea*, *Foraminifera*, *Maxillopoda*, and *RT5iin25* in the sediments (Figure 2.8). Chrysophyceae were also negatively impacted by High metal treatments. In combination with the DNA results this shows that organic enrichment is toxic to *Cercozoa*, *Ciliophora*, *Discosea*, *Foraminifera* and *RT5iin25*, whereas *Cryptophyceae*, *Chrysophyceae* and *Max-*

illopoda downregulate their activity with increasing press contamination.

We further found a significant interaction of metal contamination, press and pulse organic enrichment for *Chromadorea*, *Diatomea*, *Dinoflagellata* and *Euglenozoa*. In all four taxa, the biggest impact was that of High organic enrichment at Moderate metal treatments without an organic enrichment pulse, which decreased the activity of these taxa. Our results suggest that moderate metal contamination levels together with high enrichment might have pushed these organisms over the edge. *Diatomea* and *Dinoflagellata* are well known for their blooms (Smayda, 1997) and are thus important for the carbon cycling of coastal ecosystems by providing large amounts of biological material to fuel ecosystem processes after algal blooms.

Our taxa specific results show that press organic enrichment is the main factor affecting the eukaryotic community. All responses to elevated organic enrichment involved lower numbers and activity of the affected taxa, which suggests a toxicity of press organic enrichments towards eukaryotic organisms.

Conclusions

Rapid urbanisation of the coasts is driving increased exposure of local ecosystems to multiple press and pulse stressors. Legacy metal contamination in sediments is a common press stressor to resident communities, while organic enrichment can be delivered as a press (e.g. continuous inputs of sewage effluent) or as a pulse stressor (e.g. after large rainfall events). Although metals and organic enrichment co-occur on estuarine sediments throughout the world, their interactive effects on ecological communities are not yet well understood (Lawes et al., 2016a). Using a field manipulative experiment *in situ*, we revealed that both bacteria and eukaryotes are impacted by metals and organic enrichment. In addition, we found that organic enrichment had the ability to mask the toxic effects of metal contamination. This supports the idea of using organic enrichment to counteract metal contamination in urbanised systems, as suggested by Taylor et al. (2016) in copper contaminated freshwater systems.

The ability to test hypotheses about entire communities using molecular tools is invaluable for the advancement of biomonitoring tools. However, a few questions prevail:

- What kind of communities should be targeted (bacteria vs eukaryotes)?
- What kind of genetic material provides the most detailed information (DNA vs RNA)?

- Are these techniques applicable to different types of disturbances?

We have addressed these questions in an experiment that simulated common press (metals and organic enrichment) and pulse (organic enrichment pulse) disturbances in coastal sediments. Our experiment allowed us to rigorously differentiate the effects of metals and organic enrichment as press stressors, and a pulse of organic enrichment as pulse stressor on the structure and activity of estuarine sediment communities, accounting for organisms across all domains through next-generation sequencing. In general, we found that microbial communities respond more strongly to organic enrichment, regardless of toxic metal concentrations, and that press organic enrichment can dampen the impact of elevated metal concentrations in sediment communities. We further showed that bacterial and eukaryotic communities shift to a similar degree upon contamination. However, we found that bacteria are more sensitive to moderate levels of press and pulse contaminants, with longer lasting structural changes. Furthermore, total bacterial communities showed more evidence of contamination than the active part of the community. In addition to DNA extractions being more economical than RNA extractions, the handling of DNA samples is much easier due to higher stability. We therefore suggest that total bacterial community analysis is ideal for future studies with the aim to investigate structural changes of entire sediment communities. Also, we found that communities are largely structurally resistant to pulse stressors. As molecular techniques are becoming more available and are increasingly being used for biomonitoring, our results are crucial to improve the balance between information yield and costs for extensive biomonitoring studies.

3 Functional biomonitoring: Using metatranscriptomics for ecosystem health assessment

Abstract

Human activities are increasingly exposing natural ecosystems to a variety of biological, chemical and physical stressors, and have the potential to impact the structure and function of the affected ecosystems. However, monitoring and management approaches have primarily focused on structural changes. The relevance of structural data to ecosystem function is largely unclear and therefore our understanding of functional change in response to stressors remains limited. Metatranscriptomics is a modern molecular technique that has enabled the holistic measurement of the structure and function of an entire community. This approach has the potential to revolutionise biomonitoring. We manipulated metal concentrations and organic enrichment of marine sediments in field-based mesocosms to assess metatranscriptomics as a tool for ecosystem health assessment. We discuss the applicability of this technique based on three criteria: 1) sensitivity to stressor and ecological relevance of data; 2) repeatability of measures and reproducibility across systems; and 3) ease of use for managers. We found that measures of functional change were more sensitive to multiple stressors (metals and organic enrichment) than measures of structural change, which only responded to enrichment. Furthermore, most affected genes were down-regulated in metals or enriched sediments, which could potentially lead to lower primary productivity, lower nutrient cycling and also potentially lower remediation potential of the microbial community. We demonstrate that this next-generation sequencing technique not only measures the sensitivity of a community to a stressor, but also provides information on the mechanisms behind observable changes. Metatranscriptomics generates repeatable data with high ecological relevance. This will further improve as metatranscriptomics becomes more standardised and streamlined, and reference databases improve.

Introduction

Natural and human-induced stressors can affect both the structure and function of a natural community. Although the changes to structure can have a direct impact on important ecosystem functions (Strickland et al., 2009; Reed and Martiny, 2012; Allison et al., 2013), this is not always the case (Van Der Zaan et al., 2010; Johnston et al., 2015b). Structurally dissimilar communities have been found to perform the same functions at similar rates if their constituent species occupy similar niches (Burke et al., 2011). Moreover, following stressor-induced structural changes, some communities have exhibited stable functioning due to functional redundancy (Bissett et al., 2007; Allison and Martiny, 2008). Community function is affected by both biotic and abiotic factors, as well as interactions and feedbacks within the community, which makes predicting function from structural information very challenging (Bissett et al., 2013). However, functions ultimately underpin ecosystem processes (Falkowski et al., 2008), and so a number of recent studies have called for more integration of functional measurements into monitoring (Baird et al., 2011; Van den Brink et al., 2013; de Juan et al., 2014; Johnston et al., 2015b; van der Linden et al., 2016) in order to fully understand the ecological impacts of stressors on an ecosystem.

Meta-omics provides the opportunity to measure the entirety of both structural and functional genes at a certain point in time (Urich et al., 2008; Moran, 2009). Metagenomics approaches use DNA as a template, which includes inactive genes and genes from deceased, extinct and dormant organisms (e.g. Thomsen and Willerslev, 2015; Bengtsson-Palme et al., 2014; Hemme et al., 2015; Eloe-Fadrosh et al., 2016) (for a review, see Thomsen and Willerslev, 2015). Thus, metagenomics offers a measure of the functional potential of an entire community, but may misrepresent the present state of the community and their response to the immediate stressor of interest. Metatranscriptomics uses RNA as a template and provides a comprehensive snapshot of the active structure and functions of the community at the point of sampling (Helbling et al., 2012). Metatranscriptomic responses are considered highly sensitive to environmental conditions (Moran et al., 2013) and have the potential to illuminate the underlying gene expressions that drive functional change. While metatranscriptomics has been used as a tool for biodiversity discovery and the assessment of ecological processes (e.g. Stewart et al., 2012; Turner et al., 2013; Thureborn et al., 2016)(for a methods paper, see Creer et al., 2016), its enormous potential for biomonitoring and ecosystem management is yet to be investigated.

The development of more sensitive biomonitoring tools has been increasingly linked to the development of molecular sampling and sequencing techniques (Baird and Hajibabaei, 2012; Bourlat et al., 2013; Aylagas et al., 2014). Such techniques not only illuminate individual organism activity through gene expression (e.g. Hill et al., 2005), they enable the inclusion of bacterial communities in ecosystem health assessment (e.g. Sims et al., 2013). They do this by removing the restrictions of previous methods that could only observe culturable organisms (Hall, 2007). They also produce reliable information on macroinvertebrates (Aylagas et al., 2016) and sampling that reflects the presence of larger organisms, from arthropods to birds (Ji et al., 2013). The incorporation of microbes into modern-day biomonitoring is particularly important, because microbes are some of the most productive organisms in the world and drive the Earth's major biogeochemical cycles (Falkowski et al., 2008). They are so abundant and ubiquitous (Finlay and Clarke, 1999) that their response to stressors is relevant at every scale, from the micro- to the ecosystem and indeed the globe (Nogales et al., 2011; Halstead et al., 2014; Johnson et al., 2015; Wang et al., 2015).

New molecular biomonitoring tools have, to date, been constrained by the requirement for *a priori* predictions of stressor mechanism and consequence. Quantitative PCR (qPCR), microarray and amplicon sequencing (16S/18S) approaches (Tan et al., 2015) enable the investigation of the structure and activity of specific genes of a microbial community. However, they require a pre-selection of genes of interest through the selection of primers. As such, the importance of particular genes needs to be anticipated (Moran, 2009); this is a technical challenge when working with novel microbial communities and novel environmental stressors (e.g. emerging contaminants and climate related stressors). Hence, even though the techniques have proved sensitive to a variety of investigated stressors, and are repeatable and relatively easy to use, they may be missing ecologically relevant information.

To date, biomonitoring tools consist mainly of taxonomic identification of macroinvertebrate communities (Bonada et al., 2006; Magurran et al., 2010; Reavie et al., 2010), in addition to fish (Shedd et al., 2001; Hitt and Angermeier, 2006) and diatoms (Winter and Duthie, 2000; Stevenson et al., 2008). In water, soils and sediments, invertebrates such as insects and worms are sensitive indicators of anthropogenic stressors and are thus most commonly used for the detection of contamination (Rainbow, 2002; Bonada et al., 2006). Taxonomic identification, however, requires detailed expertise and can be time-consuming (Rainbow, 1995; Pik et al., 1999; Hopkins and Freckleton, 2002; Terlizzi et al., 2003), and due to different types of indicators in each system

is not easily reproducible across systems. Moreover, as these tools focus on a small group of organisms and do not incorporate functional measures, the relevance of the generated data to other groups of organisms and ecological processes is often unclear (Bourlat et al., 2013).

In order to adequately inform ecosystem management and improve our understanding of the need for mitigation and remediation practices, biomonitoring tools need to fulfil a number of objectives (Rainbow, 1995). Firstly, biomonitoring tools need to be sensitive to the stressor of interest and need to provide ecologically relevant information. This requires detailed knowledge on traits associated with the investigated stressors (van der Linden et al., 2016). In order to be ecologically relevant, information from such studies should enable predictions of the consequences on an ecosystem scale and the 'potential to assess ecological functions' (Bonada et al., 2006). For example, reductions in community diversity and evenness are likely to impact the resilience of communities to additional stressors (Tobor-Kaplon et al., 2005; Johnston and Roberts, 2009), and sediment ecotoxicity bioassays have been shown to accurately predict the ecological status of surface waters (Roig et al., 2015). Secondly, biomonitoring tools need to produce repeatable information (i.e. low variability in the results from different replicates of the same treatment) and be reproducible in other systems with different contaminant concentrations. For instance, the choice of indicator organism might rely on the rate of contaminant accumulation (Rainbow and Phillips, 1993; Fialkowski and Rainbow, 2006). Thus, biomonitoring tools that include a variety of measures might be more reliable across contaminant types (Borja et al., 2009). Finally, biomonitoring tools should be easy to use to facilitate the application across disciplines and professions. In order to provide ecosystem managers with information for up-to-date implementation of necessary actions, biomonitoring tools ideally result in real-time information (Borja and Elliott, 2013) and such tools should be transferable from the scientific sector to monitoring programs for easy and cost-effective application (Bourlat et al., 2013).

The urbanisation of coastal regions is exposing these ecosystems to increasing numbers of stressors (Kennish, 2002; Johnston et al., 2015a). These stressors have significant impacts on a suite of organisms and have the potential to affect general ecosystem functioning (Barbier et al., 2011). Since coastal areas are highly productive (Nixon et al., 1986) and provide an array of ecosystem services (Barbier et al., 2011), mitigation of these impacts is crucial for both nature and society. In order to develop appropriate mitigation or remediation strategies, we need to understand the various responses of affected ecosystems to anthropogenic stressors. New biomonitoring tools

that simultaneously provide information on altered ecosystem structure and function are therefore essential to improved ecosystem health assessment.

Here, we investigate metatranscriptomics as a tool to measure ecosystem health. We use experimentally manipulated coastal sediments to mimic common metal contamination and organic enrichment in urbanised systems. We compare several analyses that are possible using this technique and assess the application of this approach as a biomonitoring tool based on the following criteria:

1. Sensitivity to stressor of interest and ecological relevance;
2. Repeatability of measures and reproducibility across systems;
3. Ease of use across disciplines and professions.

We highlight the advantages and disadvantages of this new technique and the potential consequences for our understanding of anthropogenic impacts on microbial communities.

Methods

Sediment collection and experimental set-up

'Clean' sediments (with background metal concentrations) were collected from Botany Bay (Geroges River, NSW, Australia) and combined with 'contaminated' sediments (metal concentrations above upper sediment quality guideline values (SQGVs, Simpson and Batley, 2016)) from Port Kembla (Wollongong, NSW, Australia) to produce Control (100% Botany Bay) and Metal (50% Botany Bay, 50% Port Kembla) sediment mixtures. Half of each sediment metal mixture was then enriched by spiking with slow-release organic fertiliser (Yates Dynamic Lifter) at 10% dry weight. Metal and enrichment treatments were applied in a fully crossed design: background metals/no enrichment (subsequently called control), metals (no enrichment), enriched (background metals), and metals/enriched. Sediment mixtures were distributed into benthic recruitment containers (BRCs, for details see Chapter 2) and frozen to defaunate the sediment. BRCs were then deployed in Chowder Bay in the outer part of Sydney Harbour, Australia.

Sample processing and analysis

BRCs were capped and collected after 17 weeks. Sediment samples from the surface (top 1 cm) were collected and homogenised for microbial analyses.

The remaining sediment in the BRCs was homogenised and analysed for metals (Cd, Co, Cr, Cu, Fe, Mn, Ni, Pb, Zn) and nutrients (TOC, TN, TP). RNA was extracted from 1 g of sediment on the collection day using PowerSoil^{TM} Total RNA Isolation Kit (MoBio Laboratories, Carlsbad, CA, USA). For details on cleaning steps and RNA storage until sequencing, see Chapter 2. The quality of extracted RNA was determined using a Bioanalyzer (Agilent Technologies, Santa Clara, CA, USA). The mean RNA integrity number (RIN) for all samples was 7.9, where a RIN of 10 represents no RNA degradation. RNA libraries (n=12) with fragment lengths of ∼200 nt were prepared using the Illumina standard protocols. Prior to library preparation, the quality of the total RNA samples was assessed on a Bioanalyzer 2100, using an RNA 6000 Nano Chip (Agilent). Sample quantitation was carried out using Invitrogen's Ribogreen assay. Library preparation was then performed according to Illumina's TruSeq Stranded mRNA protocol with the following modifications: The oligo-dT mRNA purification step was omitted and instead, 200 ng of total RNA were directly added to the Elution2-Frag-Prime step. The PCR amplification step, which selectively enriches for library fragments that have adapters ligated on both ends, was performed according to the manufacturer's recommendations but the number of amplification cycles was reduced to 12. Each library was uniquely tagged with one of Illumina's TruSeq LT RNA barcodes to allow libraries to be pooled for sequencing. The finished libraries were quantitated using Invitrogen's Picogreen assay and the average library size was determined on a Bioanalyzer 2100, using a DNA 7500 chip (Agilent). Library concentrations were then normalised to 2 nM and validated by qPCR on a ViiA-7 real-time thermocycler (Applied Biosystems), using qPCR primers recommended in Illumina's qPCR protocol, and Illumina's PhiX control library as standard. The libraries were then pooled at equimolar concentrations and sequenced across two lanes on an Illumina HiSeq2500 sequencer in rapid mode at a read-length of 100 bp paired-end. Sequencing was performed at the Singapore Centre for Environmental Life Sciences Engineering (SCELSE).

Metal concentrations and organic enrichment measures in sediment treatments

The metal concentrations and organic enrichment measures in the four treatments were characterized at the beginning and end of the experiment as described in Chapter 2, and full details are provided in Table 3.1. In control treatments, the metal concentrations were below all of the recommended sediment quality guideline values for Australian Estuaries (SQGVs, Simpson and Batley, 2016) and in the high metals treatments the concentrations of toxic

metals (e.g. Cu, Pb and Zn) exceeded the upper SQGVs. These values represent concentrations that may be expected to have an ecological effect (Simpson et al., 2013). At the beginning of the experiment, total phosphorous (TP) and total nitrogen (TN) values were approximately doubled in enriched sediments, while total organic carbon (TOC) was increased by about 30%. At the end of the experiment, TP, TN and TOC had dropped by approximately 40%, 50% and 20% in enriched sediments, respectively, while the values in control samples remained similar.

General sequencing numbers

Total RNA sequencing generated a mean of 40.4 million bases (reads) per sample (for more details see Table B.1). Standard QC was performed using Cutadapt (Martin, 2011) with a quality cut-off value of 20. After rRNA read removal through classification using SortMeRNA (Kopylova et al., 2012) and the SILVA database, an average of two million mRNA reads (5% of total reads) remained. rRNA reads were analysed and assigned to ribotags and taxonomies using RiboTagger as described in Jeffries et al. (2015). With the remaining mRNA reads we performed a homology search using RapSearch2 (Zhao et al., 2012) against the NCBI NR (non-redundant protein) database (Pruitt, 2004). The reads were then assigned to a known KEGG (Kyoto Encyclopedia of Genes and Genomes) orthologous gene (KO) using the lowest common ancestor (LCA) algorithm in MEGAN4 (Huson et al., 2011). Total read counts of each KO per sample were calculated and normalized using the variance stabilization function (*getVarianceStabilizedData*) in the *DESeq* package (Anders and Huber, 2010) in R. A total number of 7,861 unique KOs were detected in our samples. One of the metals/enriched replicates (sample ME2) was identified as an outlier based on generally higher read counts (the mean value of normalised reads of ME2 was 80% above the mean value of normalised reads across all samples) than any other sample (Figure B.1). This was possibly due to degradation of the RNA (RIN of 5.9) and the sample was excluded from analyses. Furthermore, we only used the unique KOs which were detected in all samples of at least one treatment (3,687 unique KOs, 47% of all detected). This was to ensure that we analysed genes that were consistently detected, and at the same time included genes which might be turned off in some of the treatments or expressed at levels below the detection limit implied by sequencing depth. The read counts for every KO were used as a proxy for gene transcription rates, and therefore used as a measure for the activity of the gene.

Table 3.1: Average of total measured metals and nutrients per treatment at the beginning (T0) and end (T1) of the field experiment. Metals and nutrients were measured in mg/kg sediment dry weight. TP stands for Total Phosphorous, TN for Total Nitrogen and TOC for Total Organic Carbon. C stands for control treatment, E stands for organically enriched, M for high metal contamination and ME for high metal contamination with organic enrichment.

		T0				T1			
		C	E	M	ME	C	E	M	ME
Metals	Al	2650	2600	4200	3700	2000	2750	3300	3600
	As	5.9	7.1	14.8	11.8	5.4	5.3	10.9	11.4
	Ba	2.5	6.6	10.4	13.2	6.7	7.3	11.4	12.8
	Cd	<1	<1	<1	<1	0.1	0.4	0.5	0.5
	Co	4.2	4.8	4.9	5.2	3.6	3.1	3.7	5.3
	Cr	10.5	11.3	28.0	24.1	10.0	14.3	23.2	25.4
	Cu	14.3	22.2	273.3	209.2	30.6	40.4	211.8	176.6
	Fe	10 000	9750	13 666.7	11 333.3	7750	13 000	11 050	13 600
	Mn	140.0	177.1	177.6	171.4	94.6	90.3	130.6	134.1
	Ni	4.4	4.7	6.5	5.4	4.1	5.6	6.2	6.4
	Pb	58.9	58.7	355.8	264.6	71.7	93.7	289.0	266.7
	S	2150	3100	2366.7	2566.7	1350	1900	1450	1600
	Sn	<2	<2	52.0	41.3	2.6	2.8	43.0	53.4
	V	19.3	19.2	34.1	27.9	17.5	27.9	30.4	35.0
	Zn	183.1	209.6	565.3	479.3	159.4	231.6	460.8	477.3
Nutrients	TP	385	995	560	1180	290	590	445	740
	TN	1100	2000	1150	2550	1005	1055	1250	1050
	TOC	14 000	16 500	18 500	26 000	14 000	15 000	17 000	21 500

Analysis of metatranscriptome data – structure

Using the ribotag counts in the rRNA dataset, we performed a permutational multivariate analysis of variance (function *adonis* of package *vegan* in R). To visualise the community shifts in our treatments, we used non-metric multidimensional scaling (NMDS) plots and the *envfit* function (package *vegan*) to determine which taxa (on order level) were mostly driving the observed structural changes ($p \geq 0.001$). Furthermore, we calculated the Shannon diversity index and Pielou's measure of species evenness for all our samples.

Analysis of metatranscriptome data – function

First, we conducted a permutational multivariate analysis of variance (*adonis*) on the entire mRNA dataset and visualised the data using NMDS plots. Then, we performed univariate analyses on the gene level. To test for differential expression of the functional genes, we performed gene-wise ANOVAs on the mRNA dataset and subsequently applied False Discovery Rate (FDR) corrections using the Benjamini-Hochberg method to all p-values in our final dataset to correct for multiple testing. In order to determine if metatranscriptomics results are repeatable, we calculated the maximum fold change between biological replicates for every gene in each treatment, excluding the genes that were not detected at all in that treatment. We then calculated the percentiles of these maximum fold changes for easy visualisation of the variability of gene expression within biological replicates. In addition, we calculated the correlations between each replicate pair.

Subsequently, we analysed the data on a pathway level, according to the assignment of genes into pathways by KEGG (as of January 2014). We determined which pathways were most strongly affected by the experimental treatments through a Fisher's exact test with subsequent Benjamini-Hochberg correction for multiple testing. That is, we identified the pathways with a significantly higher proportion of differentially expressed genes than expected by chance given the proportion of differential expression in the gene level analysis. We were also interested in the most highly expressed pathways, therefore we identified the pathways that contained the 50 genes with overall highest expression across all samples. In order to narrow down the pathways that we could confidently interpret, given the sequencing depth of our samples, we examined pathways that were well represented in our dataset, i.e. of which we had detected $\geq 80\%$ of the associated genes. We then extracted the differentially expressed genes that were found to only occur in one pathway. This was done to enable a more transparent interpretation of what the differential

expression of a gene entails and why this differential expression may have been brought about by our experimental treatments.

A significance level of α=0.05 was applied for all statistical tests and multiple test corrections. All data were analysed in R (version 3.0.2, R Core Team 2015) with packages *DESeq* (Anders and Huber, 2010) and *vegan* (Oksanen et al., 2016). All plots were generated using the *ggplot2* package (Wickham, 2009).

Results

Structure and function of the sediment microbial community shifted significantly in response to organic enrichment and community function was also altered by metal contamination. The most highly expressed genes across all samples were genes involved in energy production, signalling and biodegradation. These three pathways were also the most impacted by our treatments. Differentially expressed genes with known annotation were generally expressed in lower numbers in contaminated (metals and/or organic enrichment) sediments compared to control samples.

Gene level analysis

Functional gene expression of the sediment microbial community responded to metals and organic enrichment, while the community structure shifted in response to organic enrichment but not to metals (Table 3.2 and Figure 3.1). Analysis of structural changes classified at the order level identified Methanosarcinales, Desulfitobacterales, Spirochaetales, Syntrophobacterales and B10 (order of Creanarchaeota) as bacterial taxa that were relatively more abundant in enriched treatments. These taxa explained most of the variation between control and enriched sediment communities. Furthermore, organic enrichment significantly decreased the overall diversity and evenness of the microbial community (Table 3.3 and Figure 3.2).

In regards to the repeatability of gene counts across replicates, we found that 55% of the maximum fold change within biological replicates were equal to or below two (Figure 3.3), which reveals that the majority of gene counts were relatively stable within treatments. Furthermore, the variability of replicates seems to have decreased within metal contaminated and enriched sediments. In enriched sediments, both with and without metals, 75% of all genes exhibited a fold change of around two or below within replicates. In addition, the gene expressions of all replicate pairs were highly correlated (r^2 >0.89, Figures B.2 to B.5).

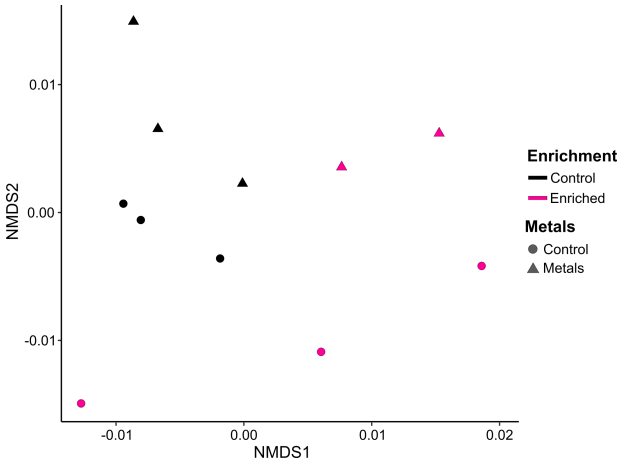

(a) NMDS based on mRNA

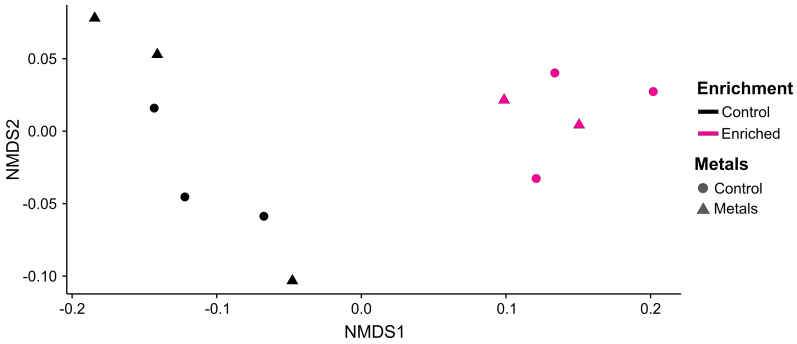

(b) NMDS based on rRNA

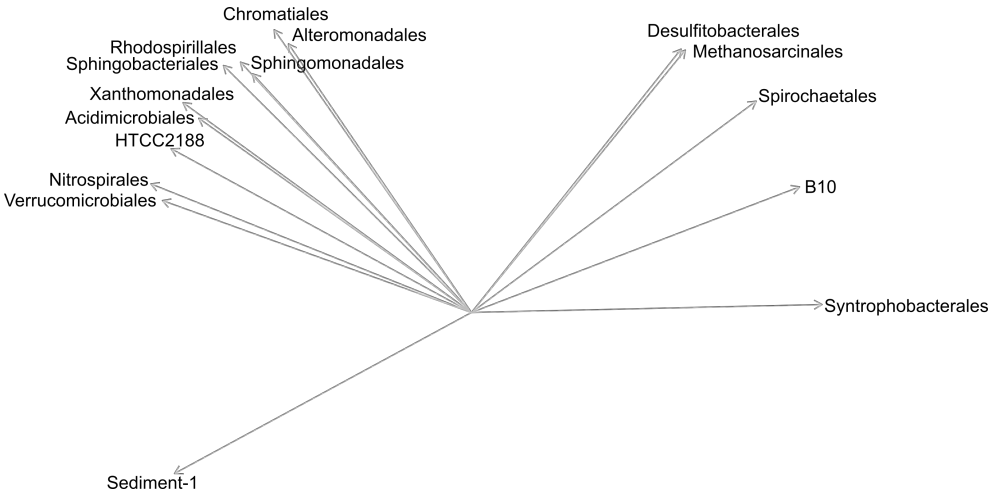

(c) rRNA envfit on order level

Figure 3.1: Non-metric multidimensional scaling (NMDS) plots of both (a) mRNA and (b) rRNA datasets. The shape of the points symbolise the metal treatments (circles for control and triangles for high metal treatment), and the colour stands for the enrichment treatment (black for control and pink for enriched). An *envfit* plot (c) of the taxa driving the community shift in the rRNA data is also shown.

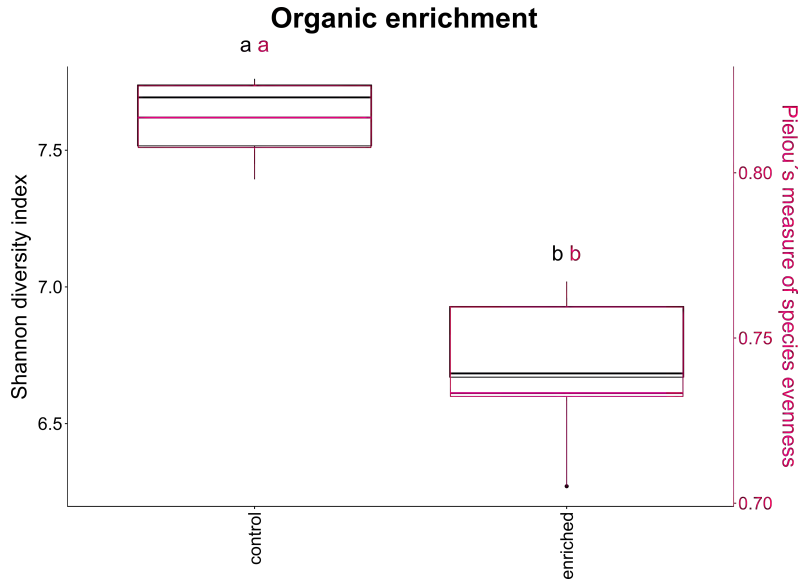

Figure 3.2: Shannon diversity index (black) and Pielou's measure of species evenness (pink) for control and enriched sediments. The letters above the boxplots show the significance groups. a and b are significantly different from each other.

Table 3.2: R output of the permutational multivariate analysis of variance (*adonis* function of the *vegan* package) for the gene counts within the rRNA and mRNA datasets. Significant *p*-values (at a level of α=0.05) are highlighted in bold.

		Df	SumsOfSqs	MeanSqs	F.Model	R2	Pr(>F)
rRNA	metals	1	0.0135	0.0135	0.9890	0.0220	0.3494
	nutrients	1	0.4909	0.4909	35.8650	0.7971	**0.0011**
	metals*nutrients	1	0.0156	0.0156	1.1410	0.0254	0.3072
	Residuals	7	0.0958	0.0137	0.1556		
	Total	10	0.6159	1			
mRNA	metals	1	0.0135	0.0135	1.6242	0.1341	**0.0163**
	nutrients	1	0.0179	0.0179	2.1501	0.1775	**0.0001**
	metals*nutrients	1	0.0111	0.0111	1.3379	0.1105	0.0699
	Residuals	7	0.0582	0.0083	0.5779		
	Total	10	0.1006	1			

Table 3.3: R output of the ANOVAs for the Shannon index and Pielou's evenness for the rRNA structural data. Significant *p*-values (at a level of α=0.05) are highlighted in bold.

		Df	Sum Sq	Mean Sq	F value	Pr(>F)
Shannon Index	metals	1	0.0878	0.0878	1.6550	0.2392
	nutrients	1	2.3016	2.3016	43.3930	**0.0003**
	metals:nutrients	1	0.0118	0.0118	0.2230	0.6514
	Residuals	7	0.3713	0.0530		
Pielou's evenness	metals	1	0.0005	0.0005	1.0280	0.3443
	nutrients	1	0.0155	0.0155	35.3100	**0.0006**
	metals:nutrients	1	0.0001	0.0001	0.1450	0.7143
	Residuals	7	0.0031	0.0004		

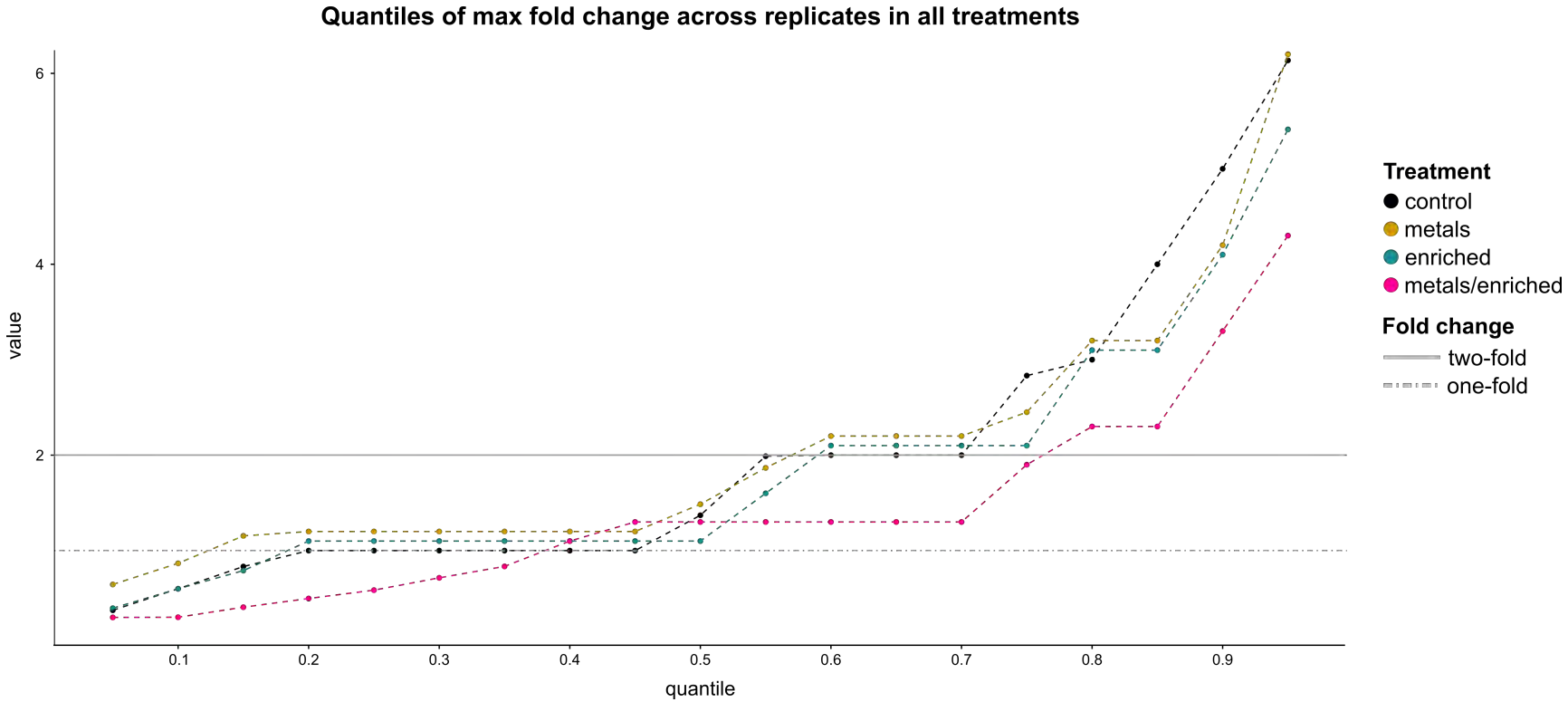

Figure 3.3: Maximum fold changes between replicates within the four different treatments. The quantiles of max fold changes are shown on the x-axis to give an idea of what percentage of genes were how variable. The colours of the dots and lines stand for the different treatments (black = control, yellow = metals, blue = enriched, pink = metals/enriched). The dotted grey line highlights a fold change of one, and the solid grey line is a reference for a two-fold change.

Gene-wise ANOVAs yielded 271 genes that were differentially expressed in response to metals (7.35% of total number of detected genes, Figure 3.4), 447 genes that were differentially expressed in response to organic enrichment (12.12% of total detected, Figure 3.5), and 229 genes that were differentially expressed when metals and organic enrichment were present in the sediments (6.21% of total detected, Figures 3.6). A subsequent conservative false discovery rate (FDR) correction yielded 13 differentially expressed genes for metals, 31 for enrichment and twelve that were significantly affected by metals in combination with enrichment. Looking at the expression levels for these differentially expressed genes we found that ten out of the 13 significant genes for metals (77%) were down-regulated in response to metals, and 21 out of 31 significant genes for organic enrichment (68%) were down-regulated in enriched systems. Of the significant interactions, five were only measured in control sediments (42%), whereas another six were only measured in metals/enriched sediments (50%). One gene was only measured in control and metals/enriched treatments, whereas the expression in metals/enriched was up-regulated.

Pathway level analysis

The detected genes belonged to 205 different biogeochemical pathways in total. Pathways here are defined as cycles in which substances are turned over or transformed into other substances, which are subsequently transformed again in other pathways. Each pathway consists of multiple genes involved in the different steps of substance turnover/transformation. To determine the most highly expressed pathways in our sediments, we examined pathways including the 50 genes with the overall highest expression rates. The largest number of highly expressed genes belonged to the following categories of pathways: energy metabolism (20 genes), carbohydrate metabolism (nine genes), amino acid metabolism (six genes), nucleotide metabolism (six genes), signal transduction (four genes), xenobiotics biodegradation and metabolism (four genes), and folding, sorting and degradation (three genes). For gene names and a comprehensive list of pathways and pathway categories, see Table B.2.

Of all the detected pathways, 63% (129 pathways) had at least one gene affected by metal treatment, 65% (134 pathways) were affected by organic enrichment and 52% (107 pathways) included genes that were affected by combined metals and enrichment (prior to conservative false discovery rate correction). The Fisher's exact test (Table B.3) revealed that eight pathways included more differentially expressed genes than expected by chance (given the number of differentially expressed genes in the entire dataset) and were thus most affected by our treatments: Citrate cycle, C5-branched dibasic acid

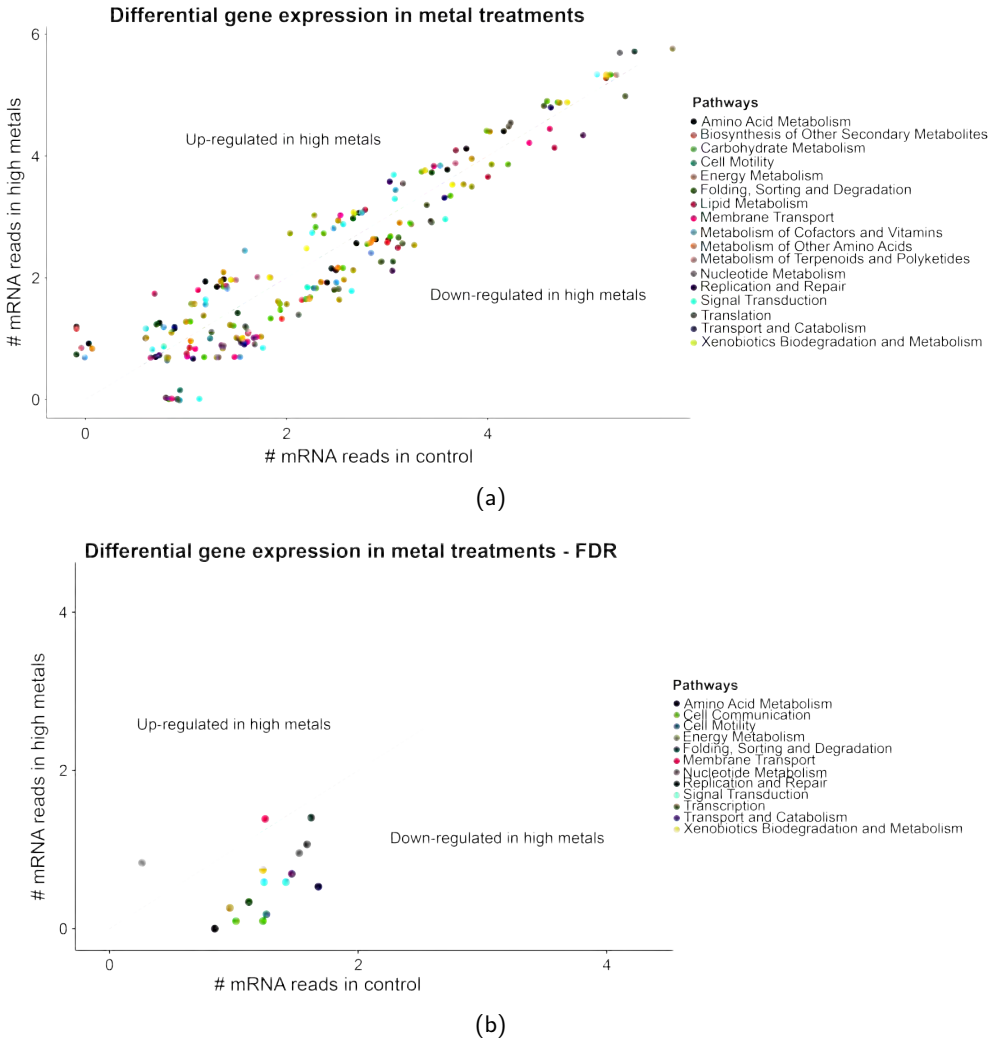

Figure 3.4: The up- and down-regulation of all differentially expressed genes ((a) pre and (b) post false discovery rate correction (FDR)) for **metal treatments**. The colour of the dots stands for the different pathways that these genes belong to. For some genes there are multiple dots because they are part of several pathways. All genes above the 1:1 line are up-regulated in metals/enriched, whereas the genes below the line are down-regulated in the treatments in comparison to the control. C stands for control, E for enriched, M for metals, and ME for metals/enriched.

metabolism, Carbon fixation pathways in prokaryotes, Methane metabolism, Phenylpropanoid biosynthesis, Nitrotoluene degradation, MAPK signalling pathway and Endocytosis (Figure 3.7). After conservative correction for multiple testing using Benjamini-Hochberg correction, only the Nitrotoluene degradation pathway remained significantly different from the expected differential expression values. In this pathway, two genes were differentially expressed in elevated metals (both were down-regulated) and twelve genes were differentially expressed in organically enriched sediments (75% up-regulated in

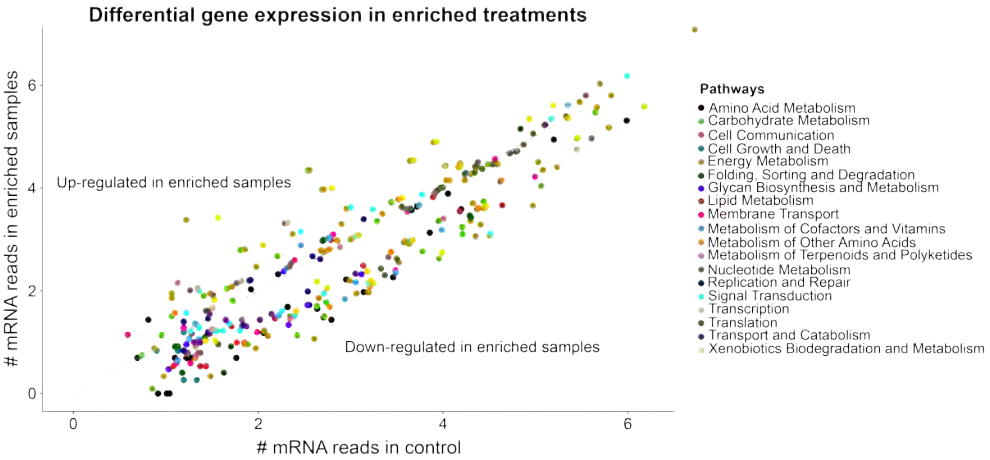

(a)

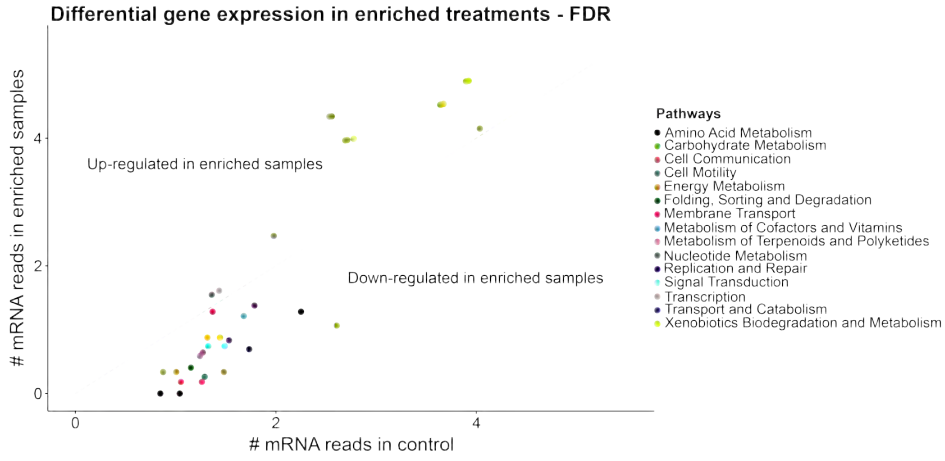

(b)

Figure 3.5: The up- and down-regulation of all differentially expressed genes ((a) pre and (b) post false discovery rate correction (FDR)) for **enriched treatments**. The colour of the dots stands for the different pathways that these genes belong to. For some genes there are multiple dots because they are part of several pathways. All genes above the 1:1 line are up-regulated in metals/enriched, whereas the genes below the line are down-regulated in the treatments in comparison to the control.

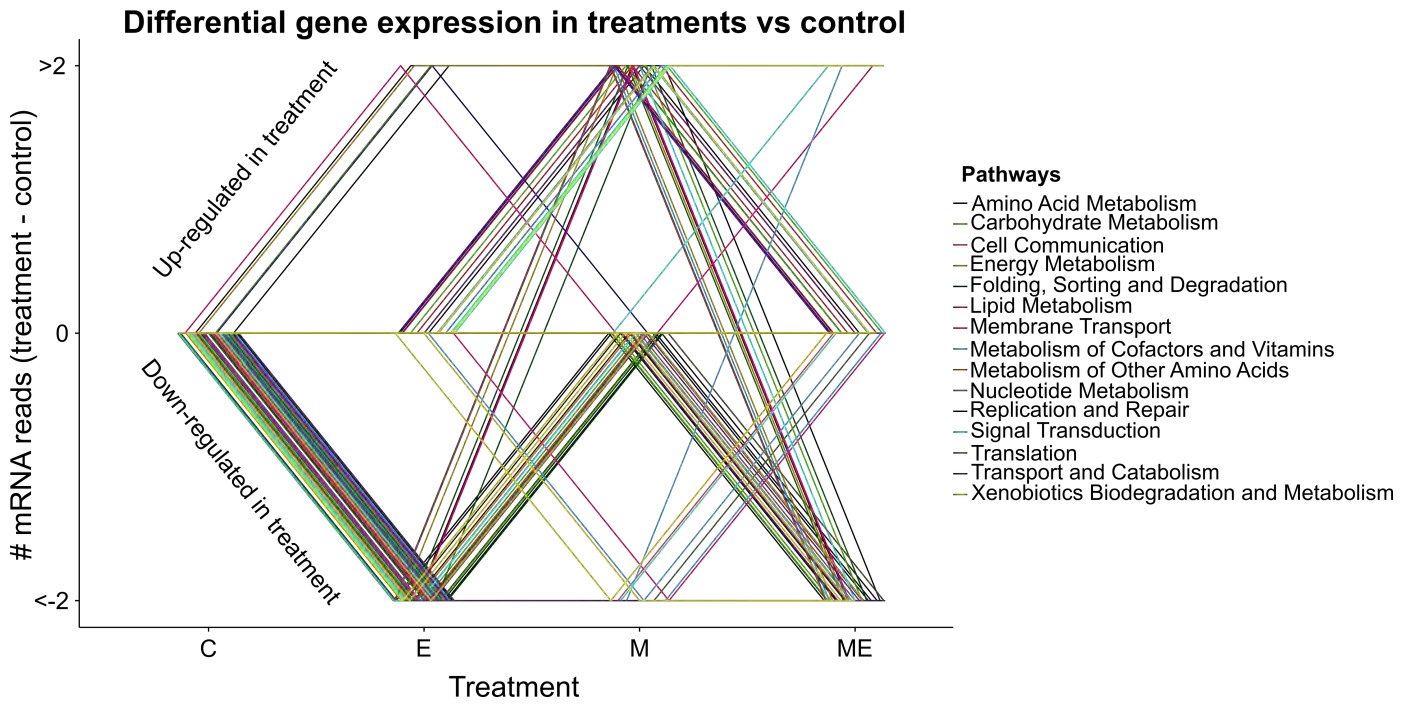

Figure 3.6: The up- and down-regulation of all differentially expressed genes pre false discovery rate (FDR) correction for the **interaction of metals and enriched treatments** (metals*enriched). The colour of the lines stands for the different pathways that these genes belong to. For some genes there are multiple lines because they are part of several pathways. All the lines above zero are up-regulated and all below zero are down-regulated in the respective treatments (x-axis) in comparison to control samples. Differences in expression of ≤ 2 are shown as up- or down-regulated. Treatment abbreviations are as follows: C for control, E for enriched, M for metals and ME for metals/enriched.

enriched). For proportions of up-regulated differentially expressed genes in all pathways with a significant Fisher's test, see Table 3.4.

We identified 50 pathways in which there was detectable expression of at least 80% of the associated genes. Of these, 17 pathways included at least one gene that was differentially expressed in at least one treatment (metals, enriched, or metals/enriched) after FDR correction. Eleven of these differentially expressed genes were found to only be part of one pathway (Tables 3.5 and 3.6). These genes were from the following 8 pathways: Cysteine and methionine metabolism, Geraniol degradation, Glutathione metabolism, Glycine, Serine and Threonine metabolism, Glyoxylate and dicarboxylate metabolism, Nitrogen metabolism, Sulfur metabolism and Proteasome. Ten out of these eleven genes were found to be differentially expressed due to organic enrichment, one of these ten was also differentially expressed due to metal treatment and the remaining gene displayed a significant response to exposure to both metals and organic enrichment.

Discussion

We identified structural (rRNA gene expression) and functional (mRNA gene expression) changes in sediment microbial communities using total RNA sequencing of experimentally contaminated sediments. We assessed data generated from metatranscriptomics at the functional pathway and pathway category level. Functional changes revealed contaminant effects on critical ecological processes such as carbon fixation (pathway) and energy production (pathway category). Sediment microbial community functions were sensitive to both metal contamination and organic enrichment, while community structure only responded to enrichment. Metatranscriptomics provided sensitive information on the immediate whole-community functional responses to stressors. By exposing the genetic mechanisms underpinning functional changes, metatranscriptomics can enhance our understanding of the ecological consequences of anthropogenic stressors.

Sensitivity to stressors and ecological relevance

Functional gene expression was sensitive to both organic enrichment and metal contamination, while structural responses were only detected under enrichment conditions (Table 3.2 and Figure 3.1). Ren et al. (2016) also recently found that functional measures were more sensitive to environmental changes, while structural measures were dominated by stochastic processes. Our gene-level analysis revealed that >7% of detected functional genes were altered by

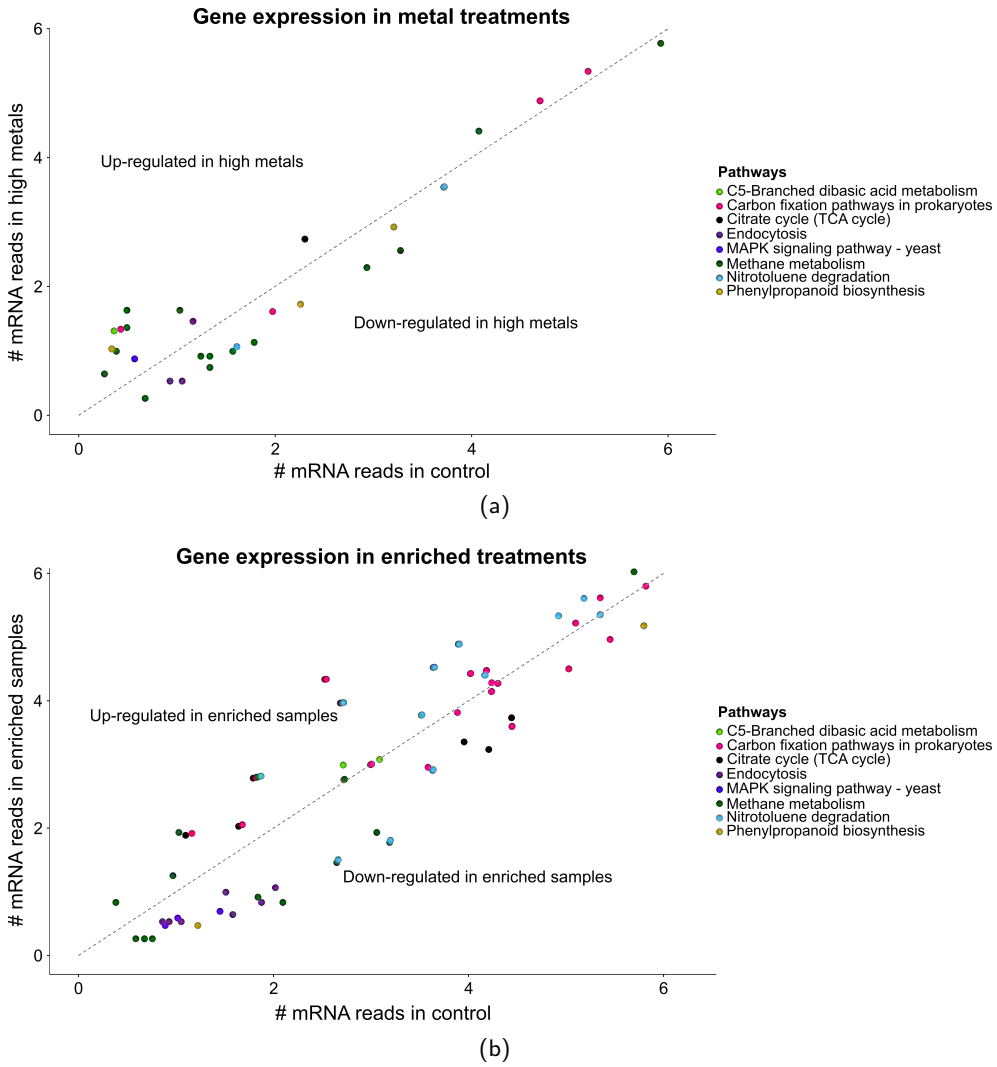

Figure 3.7: The up- and down-regulation in (a) metal and (b) enriched treatments of all genes involved in the eight pathways that had a significant result from the Fisher's exact test. These pathways contain more differentially expressed genes than expected by chance, given the total number of differentially expressed genes in the entire dataset. The colour of the dots/lines stand for the different pathways that these genes belong to. All genes above the 1:1 line are up-regulated in metals/enriched, whereas the genes below the line are down-regulated in the treatments in comparison to the control.

experimental treatments. Both metal contamination and organic enrichment led to a general down-regulation of affected genes. Many geochemical cycles have been shown to be disrupted or minimised in contaminated microbial communities (Hemme et al., 2015). This could potentially lead to lower primary productivity, lower nutrient cycling, and also lower remediation potential of the microbial community. Moreover, contaminated communities can show higher susceptibility to additional stressors (Hemme et al., 2015). Our use of gene expression responses to reveal stressor sensitivity builds on the understanding

Table 3.4: Number of differentially expressed genes for the different treatments ($p \leq 0.05$) and the number of genes that were up-regulated within those significant genes for all pathways that included more differential expression than expected by chance, given the number of differentially expressed genes in the total dataset (Fisher's test). Treatment abbreviations are as follows: E for enriched, M for metals and ME for metals/enriched.

		$p \geq 0.05$			# up-regulated	
pathway KO ID	pathway name	E	M	ME	E	M
path:ko00020	Citrate cycle (TCA cycle)	18	2	0	10	2
path:ko00633	Nitrotoluene degradation	12	2	0	9	0
path:ko00660	C5-Branched dibasic acid metabolism	4	1	0	1	1
path:ko00680	Methane metabolism	22	16	4	11	6
path:ko00720	Carbon fixation pathways in prokaryotes	22	4	1	13	3
path:ko00940	Phenylpropanoid biosynthesis	2	3	0	0	0
path:ko04011	MAPK signalling pathway – yeast	3	1	3	0	1
path:ko04144	Endocytosis	7	3	3	0	0

Table 3.5: The table shows the eleven differentially expressed genes that are part of one of the pathways of which we detected at least 80% of all associated genes, and at the same time only belong to one pathway. Gene and pathway information are shown.

gene KO ID	gene name	pathway KO ID	pathway name	pathway category
K03030	PSMD14	path:ko03050	Proteasome	Folding, Sorting and Degradation
K04014	nrfC	path:ko00910	Nitrogen metabolism	Energy Metabolism
K01251	ahcY	path:ko00270	Cysteine and methionine metabolism	Amino Acid Metabolism
K01637	aceA	path:ko00630	Glyoxylate and dicarboxylate metabolism	Carbohydrate Metabolism
K00376	nosZ	path:ko00910	Nitrogen metabolism	Energy Metabolism
K11180	dsrA	path:ko00633	Nitrotoluene degradation	Xenobiotics Biodegradation and Metabolism
K00302	soxA	path:ko00260	Glycine, serine and threonine metabolism	Amino Acid Metabolism
K10946	amoC	path:ko00910	Nitrogen metabolism	Energy Metabolism
K13778	atuC	path:ko00281	Geraniol degradation	Metabolism of Terpenoids and Polyketides
K01917	E6.3.1.8	path:ko00480	Glutathione metabolism	Metabolism of Other Amino Acids
K00872	thrB1	path:ko00260	Glycine, serine and threonine metabolism	Amino Acid Metabolism

Table 3.6: The table shows the eleven differentially expressed genes that are part of one of the pathways of which we detected at least 80% of all associated genes, and at the same time only belong to one pathway. Raw read counts in the different samples (except for the outlier ME2) are shown. Sample names are as follows: C for control, E for enriched, M for metals, and ME for metals/enriched.

gene KO ID	C1	C2	C3	E1	E2	E3	M1	M2	M3	ME1	ME3
K03030	4	3	5	2	5	3	4	2	2	NA	NA
K04014	7	5	9	9	7	11	7	2	5	13	12
K01251	213	183	303	136	125	116	275	171	258	148	155
K01637	135	81	186	38	60	47	281	115	145	65	67
K00376	184	114	125	30	26	37	245	83	106	45	48
K11180	135	144	195	208	155	134	118	56	168	287	244
K00302	7	5	12	3	4	4	12	8	7	1	1
K10946	21	5	13	NA	NA	NA	10	20	4	1	2
K13778	1	2	2	NA	NA	NA	1	3	1	NA	NA
K01917	1	NA	1	3	2	2	1	NA	NA	4	3
K00872	1	1	3	NA	NA	NA	NA	NA	NA	3	3

that changes in gene expression is the most immediate response to stressors (Moran, 2009). Our evidence, provided by the metatranscriptomic sequencing of metal and organically enriched sediments, suggests that functional gene responses might be more sensitive to stressors than taxonomically conserved gene responses. Thus, our results corroborate the findings of studies that used more conventional approaches and found that while microbial biomass and structure did not change upon contamination with heavy metals, enzymatic activity was highly impacted in both soils (Kandeler et al., 1996) and marine sediments (Dell'Anno et al., 2003). Further, Srivastava and Vellend (2005) have suggested that functional responses of communities to stressors are possibly more relevant to ecosystem conservation than structural changes. Community function is therefore a critical measure for both the early detection and broad understanding of community change upon contamination.

Providing a link between differential gene expression and altered ecosystem processes (e.g. fluxes of matter from a system) is important to ensure that metatranscriptomics can be recognised as an ecologically relevant tool. While proteins are the cellular components ultimately responsible for the rate of biogeochemical processes, the abundance of mRNA molecules accurately predicts the number of proteins in a population (Taniguchi et al., 2010). This means that gene expression can provide an accurate reflection of the biogeochemical process rates of a microbial community. Studies that measured greenhouse gas production in soil microbial communities and compared them to the activity of the associated genes, proved this relationship between gene activity and biogeochemical process rates to be accurate (Morales et al., 2010; Philippot et al., 2011; Harter et al., 2014). In a relatively recent article on metatranscriptomics, Moran et al. (2013) also conclude that mRNA reads are better indicators of instant change to stressors than proteins, due to slower response of the latter. The activity level of a gene can also be accurately predicted based on its transcript abundance, even for functions of organisms with low abundance in the community (Helbling et al., 2012). Hence, metatranscriptomics generates information that is of high ecological relevance and can be useful for biomonitoring.

For effective and targeted management, we need biomonitoring tools that are adaptable for general and specific questions about ecosystem change. We have demonstrated that metatranscriptomics provides required information for ecosystem managers. The analysis can be adjusted to the depth of information necessary to inform new mitigation or remediation strategies. mRNA reads can be analysed on a genetic level to provide information on all genes that change following a stressor (Moran, 2009). These gene expression datasets can

be filtered for specific genes of interest, but also provide information on additional, potentially unanticipated, community responses (Moran, 2009). This is a crucial difference compared to the molecular techniques already in use in biomonitoring, such as qPCR and amplicon sequencing (Tan et al., 2015), which require a pre-selection of genes of interest. Hence, metatranscriptomics provides important information, which would not be attainable using conventional techniques.

In addition to a gene-level analysis, the metatranscriptomics dataset can be divided up into pathways, using the gene to pathway information from KEGG. The microbial pathways with the highest overall expressions or those that are most highly affected by the stressor can thus be determined. Commonly, the most frequently expressed genes in marine ecosystems are related to transcription/translation, protein folding/export and DNA replication/repair (Moran, 2009). In our metal contaminated and enriched sediments, energy production, signalling and biodegradation seemed to become more important (Table B.2). Also, both metal contamination and organic enrichment led to a significant decrease in the activity of genes involved in cell motility, cell communication and signal transduction (Figures 3.4 and 3.5). Lower cell motility of diatoms has been suggested as a fast screening method of toxic sediments (Cohn and McGuire, 2000). Moreover, lower cell motility can affect microbial population growth potential (Lauffenburger et al., 1982) and can thus be detrimental to the affected community. Furthermore, cell communication is vital for the modulation of gene expression on a population level (Mitchell et al., 2011). Signal transduction enables communication not only between organisms of the same species, but also across kingdoms and may directly increase bacterial survival (Williams, 2007). Contaminants have been shown to act as 'information disruptors' at even very low levels (Lürling and Scheffer, 2007). Because signalling systems serve as detectors for subtle chemical cues from the environment, they are naturally built to be sensitive and are thus highly susceptible to contamination (Lürling and Scheffer, 2007). Surprisingly, we have an overall down-regulation of signalling genes, but at the same time some signalling genes that were among the most highly expressed in the entire dataset. The highly expressed genes, however, are all part of the two-component system. The two-component system enables cells to detect changes in their environment and to produce a cellular response, most often through differential expression of target genes (Mascher et al., 2006). Thus the expression of these two-component system genes reveals that the microbes were sensitive to the stressor.

In addition, the pathways which were mostly affected by our experimental

treatments are mainly involved in energy production, signalling and biodegradation (Figure 3.7). The differentially expressed genes in these eight pathways were mainly down-regulated in metal contaminated sediments treatments. In enriched sediments, especially the signalling genes were down-regulated. The numerous down-regulated signalling and cell communication genes from different pathways are likely to impede the delivery of information within the microbial community (Lürling and Scheffer, 2007). Like larger organisms, microbes adapt their behaviour and functions to the environment, in response to biological and chemical information (Westerhoff et al., 2014). Responses are made in dependence of the responses of other organisms in the same community (Ross-Gillespie and Kümmerli, 2014). Therefore, a down-regulation of signalling genes can impede the capacity to regulate gene expression on a population level (Mitchell et al., 2011) and even affect the bacterial survival capacity (Williams, 2007). As such, a disruption in cell communication could potentially lead to community fracturing, as has recently been shown in microbial biofilms (Lawes et al., 2016b). This could result in a decreased primary productivity and lower effectiveness of remediation and biogeochemical cycling.

We were also interested in the potential to investigate entire pathways in relation to a stressor and to make predictions on consequences for the entire ecosystem. We found that eight pathways were well-represented in our dataset and could be interpreted in regards to the differentially expressed genes within. Two of these eight pathways are the nitrogen and sulphur metabolisms, which are both commonly impacted by organic enrichment (Asami et al., 2005; Nizzoli et al., 2006). Both pathways include the production of highly potent greenhouse gases – nitrous oxide and hydrogen sulphide, respectively (Schreiber et al., 2012; Kump et al., 2005). Therefore, changes in gene expression in these pathways could not only lead to consequences for the ecosystem, but could have a global impact. Chapter 4 of this thesis investigates these two metabolisms from the same dataset in detail and discusses the consequences of altered gene expression on a local and global scale.

Repeatability of measures and reproducibility across systems

Apart from sensitivity and ecological relevance, metatranscriptomics needs to exhibit low variability of measures across biological replicates, in order to be a reliable tool for biomonitoring. The gene expression measures of our replicates proved to be highly correlated within treatments (Figures B.2 to B.5). When looking at the maximum fold-changes across replicates, we found that the majority of genes (70%) had a maximum fold-change of around two or

less within the same treatment (Figure 3.3). Although there are some studies that consider a two-fold change of a gene to be up-regulated (e.g. Zhang et al., 2013), many only consider genes with at least three- or four-fold change to be differentially expressed (e.g. Kohlmann et al., 2014; Nakamura et al., 2016). Ishii et al. (2013) even define a fold change of five or above to be 'moderately' up-regulated, and only consider a ten-fold change or higher to be 'highly' up-regulated. In our data, some genes have a very high variability between replicates. The genes with highest variability between replicates belong to pathways from all different categories; there are no pathways that are substantially more variable than others. Therefore, this variability is likely not due to treatments (which could lead to higher variability in certain genes), but to random variability in the environment or to differences in amplification and sequencing efficiencies across samples. However, high variability of genes has previously been found in sediments (Bulow et al., 2008), which shows that the inclusion of variability across samples is extremely important, despite potential biases in sample processing. It enables the detection of differentially expressed genes between treatments despite intra-treatment variability and enables meaningful interpretation of the data and accurate comparison of samples from different conditions (Prosser, 2010; Zhou et al., 2015).

A further issue that needs to be considered before applying metatranscriptomic techniques is the trade-off between sequencing depth and replication. With limited funds, replication usually comes at the cost of lower sequencing depth. Lower sequencing depth can impact the technical precision of sequencing on a gene level (Sims et al., 2014) and also impact the detection of differentially expressed genes (Tarazona et al., 2011). However, mRNA reads across samples were reproducible and highly correlated in various systems and across several molecular techniques (Frias-Lopez et al., 2008; Caporaso et al., 2012; Turner et al., 2013; Tsementzi et al., 2014). The high correlations (Figures B.2 to B.5) and predominantly low fold changes between our biological replicates reveal that, in general, the variability of gene expression within our treatments is modest and thus validate metatranscriptomics as a highly reliable tool.

Metatranscriptomics has been successfully applied across highly diverse systems. Studies have used this technique to look at the functional activity of specific organisms or genes in freshwater (Penn et al., 2014), oceans (Gifford et al., 2011; Hilton et al., 2015) and permafrost (Hultman et al., 2015), and to describe functions of previously unexplored habitats (Urich et al., 2014; Thureborn et al., 2016). Microbiomes of plants (Turner et al., 2013; Franzosa et al., 2014) have also been characterised using the rRNA component of a metatranscriptomics dataset and using RNA/DNA ratios to explore under- or

over-expressed functional genes. However, to the best of our knowledge, thus far metatranscriptomics has not been used to holistically investigate differentially expressed functions between impacted and unimpacted samples on a gene and/or pathway level. In this study, we have demonstrated the breadth of its potential to characterise community function and identify functional changes.

Ease of use across disciplines

Metatranscriptomics poses a suite of challenges from sampling to data analysis. Firstly, the sampling of RNA must be done in a very cautious manner, due to its instability. RNA has a half-life of seconds to minutes (Carvalhais et al., 2012; Moran et al., 2013), and samples must therefore be instantly preserved or extracted. In addition, rRNA typically comprises about 95% of the total RNA extracted in a single cell, thus heavily dominating the presence of mRNA (McGrath et al., 2008). If only the functional part of the community is of interest, the rRNA needs to be removed to improve sequencing depth of the mRNA. In eukaryotes, mRNA can be isolated with a simple poly-dT pull-down; however, bacterial and archaeal mRNA does not have the necessary poly-A tail for this method (Moran, 2009). Some prokaryotic mRNA isolation kits exist (Carvalhais et al., 2012), however many sequencing facilities do not yet use these techniques (personal observation). Moreover, there is a substantial advantage to including rRNA in the analysis and thus using total RNA as input for sequencing. rRNA and mRNA sequences can be separated post-sequencing and the rRNA component can be used to gain insight into community structure changes occurring alongside the functional changes (mRNA) from the same sample (Urich et al., 2008).

A further very significant challenge is the lack of annotation of environmental genes in reference libraries. This results in most of the sequences without annotation to any known gene and thus these genes are usually excluded from the analysis (except for simple community shift analyses). Genes without annotation can also function as a marker for environmental status, however, without annotation its function is unknown and interpretations are therefore challenging. Even if the gene has been annotated, a 100% confidence of the assignment to a function is still not possible (Moran, 2009). Most genetic databases are biased towards annotation of medically relevant genes, which can lead to confusion with the interpretation of environmental samples (personal observation). However, as more and more research is being done using these modern molecular techniques, the reference libraries are growing and enabling the annotation of more and more environmentally relevant genes.

This is crucial for the viability of molecular techniques (Aylagas et al., 2014). Once the samples have been extracted, sequenced and taxonomies (rRNA) or gene names (mRNA) assigned to the reads, the investigator is faced with the challenge of making sense out of a tremendous amount of data. Therefore, it is important to know the depth of information that is needed beforehand, so that the analysis can be scaled to those needs. Also, the increasing amount of data generated poses serious challenges for efficient computation (Muir et al., 2016). As we are still in the advent of metatranscriptomics as a widely used tool, we are confident that computation technologies will advance and analyses will get more streamlined, making the technique more accessible across disciplines and professions.

Conclusions

Modern molecular techniques have created the opportunity to 'eavesdrop on microbial communities' (Moran, 2009). By doing so, we not only identify the changes that altered conditions provoke in microbial communities, but also explore the mechanisms behind these changes. With the ever-increasing anthropogenic pressure on ecosystems, the necessity for immediate, reproducible biomonitoring tools is increasing. We have assessed the use of metatranscriptomics as a biomonitoring tool, using experimentally manipulated sediment microbial communities in the field. Metatranscriptomics is a highly sensitive tool for detecting community response to common stressors and provides a vast amount of ecologically relevant information. This technique can be used to simultaneously report structural and functional changes of an entire community. In this study, gene expression measures exhibited low variability across biological replicates, suggesting a high utility for biomonitoring purposes. Metatranscriptomics generates rapid information about the living community and thus allows for an immediate and highly relevant investigation of stressor response. There are still a number of challenges associated with the stream-lined use of this modern molecular technique; however, we are confident that a significantly growing application of meta-omics to environmental studies will contribute to higher accessibility of this approach across disciplines. In conclusion, metatranscriptomics is a very powerful modern technique and highly scalable to the needs of the investigator. The large amount of data generated can be used for multiple assessments targeting different aspects of a community simultaneously and has immense potential to inform the integrative management of urbanised ecosystems.

4 Transcriptional changes in greenhouse gas production pathways in experimentally contaminated coastal sediments

Abstract

Microbially mediated biogeochemical processes are crucial for climate regulation and may be disrupted by anthropogenic contaminants. To better manage contaminants we need tools that identify causal links between stressors and altered microbial functions and can predict the consequences for ecosystem services such as climate regulation. In a field experiment, we used for the first time metatranscriptomics coupled with common biogeochemical measurements to investigate the impact of metal contamination and excess organic enrichment on the gene expression of nitrogen and sulphur metabolisms in coastal sediments. We show that excess organic enrichment could result in 1) accumulation of toxic products, and 2) increased greenhouse gas production. Furthermore, metal contamination altered nitrogen metabolism when in combination with organic enrichment. Our findings suggest that the presence of metal contamination may compound the toxic effects of excess organic matter. We reveal the genetic mechanisms that may lead to altered productivity and greenhouse gas production in coastal sediments due to anthropogenic contaminants.

Introduction

Biogeochemical cycles encompass the production and degradation of organic nutrients, and are therefore essential to the regulation of the Earth's climate (Ducklow, 2008). Specialised microorganisms mediate these cycles and control the production of associated end-products, including greenhouse gases. Microbial communities are widely distributed across all biomes and their functioning is essential for maintaining balanced biogeochemical cycling and ecosystem services. However, stress from human activities can modify the structure and/or function of microbial communities (Johnston and Roberts, 2009; Berga et al., 2012). These modifications can result in incomplete biogeochemical cycles and, subsequently, an accumulation of intermediate metabolic products or altered rates of gas production (Schimel and Gulledge, 1998). Such biogeochemical

changes are likely to have direct repercussions for entire ecosystems (Chapin et al., 2000). In order to build accurate climate models (Singh et al., 2010) and improve ecosystem management, we need to understand the impacts of anthropogenic perturbations on microbial function. Despite the significant contribution of microbial communities to biogeochemical cycles, we have little understanding of the link between microbial communities, anthropogenic activities, and greenhouse gases.

Human activities are increasingly impacting the composition and health of our aquatic ecosystems. Coastal marine ecosystems are some of the most productive in the world (Nixon et al., 1986). The microbial communities that inhabit the coastal soft sediments regulate numerous biogeochemical cycles and impact biogeochemical cycling on a global scale. However, the intensification of human activities in and around coastal areas exposes these systems to multiple environmental stressors (Kennish, 2002). Contaminants, such as metals and excess organic matter, enter coastal waterways and bind to particles in the water column, eventually settling and accumulating in the soft sediments (Burton and Johnston, 2010). This accumulation may alter general microbial function in the sediments over large scales (Nogales et al., 2011) and result in modifications to ecosystem processes and functions (Barbier et al., 2011).

Two of the most prevalent types of contaminants in coastal waterways are elevated metals and excess organic matter (Jiang et al., 2001). Metals are known to have toxic effects on sediment communities (Babich and Stotzky, 1985) and excess organic matter causes high respiration rates, low oxygen concentrations and a build-up of sulphides and ammonia (Meyer-Reil and Köster, 2000; Gray et al., 2002). The provision of excess substrate can thus change the rate of community functions, and activate positive feedback loops (Howarth et al., 2011) which may lead to accumulation of toxic end-products. Individually, these two common contaminant types are known to alter the overall microbial activity of soft sedimentary environments, however the combined effect of metals and organic enrichment is yet to be understood.

Until recently, we lacked the ability to directly link single and multiple stressor effects to the specific activities of microbes. The link between contaminants and altered microbial functions are yet largely unknown. Modern molecular tools enable us to measure the structure and function of entire communities at the gene level (Urich et al., 2008; Moran, 2009). Such 'omics' approaches provide an economical and powerful means to rapidly gather substantial and specific information on microbial communities and their functions. These methods enable the quantification of gene expressions, which

represent potential rates of microbially driven processes. They represent a promising technique that allows a unique perspective on whole community analysis. Therefore, molecular tools, can be very effective for understanding the genetic mechanisms of impact on biogeochemical processes; the endpoint of such impacts being commonly measured as functional rates (e.g. gas or nutrient fluxes) (Kelaher et al., 2013).

Here, we investigate the biogeochemical response of a coastal sediment microbial community to different concentrations of metals and organic enrichment in a field experiment. Specifically, we measure altered gene expression of metabolic pathways that involve the production and consumption of two greenhouse gases: nitrous oxide (N_2O) and hydrogen sulphide (H_2S). We show that anthropogenic contaminants can lead to an accumulation of toxic compounds and an increased production of N_2O and H_2S in affected sediments. We discuss the potential implications for ecosystem productivity and the global climate. To our knowledge, this is the first study of its kind to employ metatranscriptomics to investigate the indirect impact of anthropogenic contaminants on the climate.

Methods

Sediment collection and experimental set-up

Sediments (grain size: >95% fines (<63 μm), total organic carbon content: 4-5%) were collected using a Van Veen grab from 5 m depth at unvegetated sites in NSW, Australia (Dafforn et al., 2012). Metal concentrations in collected sediments were either at background concentrations and below Australian Sediment Quality Guideline Values (SQGVs, Simpson and Batley, 2016) (Botany Bay, Georges River, NSW, Australia), or above high SQGVs (Port Kembla, Wollongong, NSW, Australia). Port Kembla has a legacy of metal contamination from industrial practices (He and Morrison, 2001). Metal treatments comprised volume-based mixtures of these two sediments and had two levels - Control (100% Botany Bay), which had Cu, Pb and Zn concentrations below SQGVs, and High (50% Botany Bay, 50% Port Kembla), which had Cu, Pb and Zn concentrations approximately representing high SQGVs (±25%, Table C.3). Half of each sediment mixture was then spiked with a commonly used organic fertiliser (10% dry weight, Yates Dynamic Lifter). Treatments were applied in a fully crossed and replicated experimental design representing background metals/no enrichment (subsequently called control), high metals (no enrichment), enriched (background metals plus enrichment), and high met-

als/enriched.

The prepared sediment mixtures were distributed into benthic recruitment containers consisting of transparent acrylic cylinders (15 cm diameter, 40 cm height) fixed within grey PVC piping (15 cm diameter, 15 cm height). The base of each container was lined with 1 kg of sand for drainage, aeration and to minimise compaction and contained 2 kg of sediment mixture above the sand. Triplicates of every sediment mixture were prepared and frozen at -20°C for three months to kill the fauna in the sediment. Benthic recruitment containers were deployed on the sediment surface at 3 to 4 m depth while frozen and attached to aluminium frames (Dafforn et al., 2013) where they thawed *in situ*. The experiment was carried out in the euphotic zone of the well flushed Chowder Bay near the mouth of Sydney Harbour, Australia (33°50'22"S, 151°15'17"E).

Metal and nutrient concentrations in sediment treatments

The metals and nutrient concentrations in the four treatments were characterised at the beginning and end of the experiment by analyses of dilute-acid extractable metals, total organic carbon (TOC), total Kjehldahl nitrogen (TN) and total phosphorous (TP). Dilute-acid extractable metals analyses (1 M HCl, 60 min) were made, with appropriate QA/QC, as described previously (Simpson and Spadaro, 2011). Organic contents (TOC, TN and TP) were measured according to the following standard methods for the examination of water and wastewater: APHA 5310B, APHA 4500-Norg B and 4500-NH3C distillation/titration and USEPA 6010C/6020A ICP. Metal and nutrient concentrations in the four treatments are provided in Table C.3. In high metals treatments the concentrations of commonly monitored metals (e.g. Cu, Pb and Zn) were elevated substantially from the concentrations in the control samples both at the beginning and at the end of the experiment. At the same time, the exceedance of SQGVs and high SQGVs in every sample was maintained over the duration of the experiment. At the start of the experiment, C:N ratios of samples with no enrichment were around 14:1 (by atoms), while C:N ratios for enriched samples were around 9:1. At the end of the experiment, samples without enrichment and samples with background metals and enrichment had C:N ratios of around 14:1 and sediments with metal contamination and enrichment had a C:N ratio of 20:1. The added fertiliser led to medium-range organic enrichment, however the added nutrients and organics are very labile, which can be utilised quickly. Thus this medium-range enrichment leads to high metabolism and would mainly have an intense short term effect.

Sample processing

Benthic recruitment containers were retrieved and destructively sampled 17 weeks after deployment. The time point was chosen to allow the sediments to equilibrate and capture recruitment responses to the different treatments. Furthermore, treatment effects were assessed after multiple weeks in the field to investigate if the impact of contaminants on community function is sustained over longer time periods relative to natural temporal change in RNA, which is known to happen within minutes (Carvalhais et al., 2012; Moran et al., 2013). Sediment samples from the surface (top 2 cm) were collected, homogenised and carried to the laboratory adjacent to the experimental site for immediate RNA and DNA extraction for microbial function analysis. Total RNA and DNA were extracted from the same 1 g of sediment using a PowerSoil™ Total RNA Isolation Kit and a PowerSoil™ DNA Elution Accessory Kit (MoBio Laboratories, Carlsbad, CA, USA), respectively. RNA samples were cleaned with TURBO DNA-free™ Kit (Lifetechnologies, Carlsbad, CA, USA) and Agencourt® RNAClean® XP (Beckman Coulter Inc.), and DNA samples were cleaned with Agencourt® AMPure® XP (Beckman Coulter Inc.) according to manufacturer's instructions. Cleaned RNA and DNA were stored at -80°C until sequencing. The quality of extracted RNA was determined using a Bioanalyzer (Agilent Technologies, Santa Clara, CA, USA). The mean RNA integrity number (RIN) for all samples was 7.9 ± 1.196, where a RIN of 10 represents no RNA degradation. RNA libraries (n=12) with fragment lengths of approx. 200 nt were prepared using the Illumina standard protocols. Prior to library preparation, the quality of the total RNA samples was assessed on a Bioanalyzer 2100, using an RNA 6000 Nano Chip (Agilent). Sample quantitation was carried out using Invitrogen's Ribogreen assay. Library preparation was then performed according to Illumina's TruSeq Stranded mRNA protocol with the following modifications: The oligo-dT mRNA purification step was omitted and instead, 200 ng of total RNA were directly added to the Elution2-Frag-Prime step. The PCR amplification step, which selectively enriches for library fragments that have adapters ligated on both ends, was performed according to the manufacturer's recommendations but the number of amplification cycles was reduced to 12. Each library was uniquely tagged with one of Illumina's TruSeq LT RNA barcodes to allow libraries to be pooled for sequencing. The finished libraries were quantitated using Invitrogen's Picogreen assay and the average library size was determined on a Bioanalyzer 2100, using a DNA 7500 chip (Agilent). Library concentrations were then normalised to 2 nM and validated by qPCR on a ViiA-7 real-time thermocycler (Applied Biosystems), using qPCR primers recommended in Illumina's qPCR protocol, and

Illumina's PhiX control library as standard. The libraries were then pooled at equimolar concentrations and sequenced across two lanes on an Illumina HiSeq2500 sequencer in rapid mode at a read-length of 100 bp paired-end. Sequencing was performed at the Singapore Centre for Environmental Life Sciences Engineering (SCELSE).

Mass balance measurements

To do mass balance calculations to estimate the potential amount of N gas produced in the different treatments, sub-cores were taken from all benthic recruitment containers for measurements of dissolved oxygen and dissolved inorganic nitrogen (NO_3^-, NO_2^- and NH_3/NH_4^+) fluxes, as seen in Sutherland et al. (2016). These fluxes were measured from water sampled after cores were incubated in dark and light conditions and analysed according to (Kelaher et al., 2013). All fluxes were determined as μmol/m^2/hr. O_2 fluxes in light conditions represent net primary productivity (NPP) while O_2 fluxes in the dark represent the benthic community respiration (BCR) rate. Gross primary productivity (GPP) of the sediment community was calculated as NPP - BCR. Net ecosystem metabolism (NEM) and net N sediment-water fluxes, which represent average net productivity of the sediment over a daily period, were calculated by averaging light and dark fluxes. Mass balance calculations can be found in Table C.2.

General sequencing numbers

Total RNA and DNA sequencing generated a mean of 40.4 million bases (reads) and 29.7 million bases per sample, respectively (for more details see Table B.1). Standard QC was performed using Cutadapt (Martin, 2011) with a quality cut-off value of 20. After rRNA read removal through classification using SortMeRNA 2.0 (Kopylova et al., 2012) and the SILVA database, an average of two million mRNA reads (5% of total reads) remained. With the remaining mRNA and the DNA reads we performed a homology search using RapSearch2 (Zhao et al., 2012) against the NCBI NR (non-redundant protein) database (Pruitt, 2004) and only sequences with homology to annotated genes were used downstream. The reads were then assigned to a known KEGG (Kyoto Encyclopedia of Genes and Genomes) orthologous gene (KO) using the lowest common ancestor (LCA) algorithm in MEGAN4 (Huson et al., 2011). Total read counts of each KO per sample were calculated and normalised using the variance stabilization function (*getVarianceStabilizedData*) in the *DESeq* package (Anders and Huber, 2010) in R. The following steps were only performed

for the RNA dataset. A total number of 7,861 unique KOs were detected in at least one of the samples. One of the high metals/enriched replicates (sample ME2) was identified as an outlier based on generally higher read counts than in the other two samples of the same treatment (Figure B.1). This was possibly due to degradation of the RNA (RIN of 5.9) and the sample was excluded from analyses. Furthermore, we only used the unique KOs which were detected in all samples of at least one treatment (3,687 unique KOs, 46.9% of all detected). This was to ensure that we analysed genes that were consistently detected and at the same time included genes, which might be turned off in some of the treatments or expressed at levels below the detection limit implied by sequencing depth. The read counts for every KO were used as a proxy for gene transcription rates and therefore used as a measure for the activity of the gene.

Analysis of metatranscriptome data

Firstly, all analysis was conducted using the RNA dataset. Based on RNA results, a subset of genes in the DNA dataset were analysed. We identified genes of metabolic pathways involved in greenhouse gas production: nitrogen (KEGG pathway map00910), sulphur (KEGG pathway map00920), methane (KEGG pathway map00680) and carbon (KEGG pathway map01200) metabolisms. Of these metabolisms only the core parts which are directly involved with the production of gases were investigated for simplification. In addition, non-core parts of the pathways were only detected in low read counts. Genes from the methane and carbon metabolisms did not show clear patterns of up- or down-regulation. Therefore, the results of these two metabolisms are not included here, but can be found in Figures C.1 and C.2, and Table C.1. To test for differential expression, we performed gene-wise ANOVAs and subsequently applied False Discovery Rate (FDR) corrections using the Benjamini-Hochberg method to all p-values in our final dataset to correct for multiple testing. All differentially expressed genes according to the ANOVAs are discussed to make sure that no important patterns are missed due to conservative treatment of p-values. FDR significances of discussed genes are shown in brackets throughout this manuscript. Differentially expressed genes from the RNA dataset were subsequently analysed in the DNA dataset to determine if a functional change was a direct consequence of altered structure (abundance of gene in community) or if it was due to transcriptional changes. All data analysis was conducted using R (version 3.0.2; R Core Team, 2013) with packages *DESeq* (Anders and Huber, 2010) and *vegan* (Oksanen et al., 2016). Plots were generated using the R package *ggplot2* (Wickham, 2009).

Results

Figures 4.1 and 4.2 show the gene expression profiles of the nitrogen and sulphur metabolisms in our treatments. Detailed gene expression can be found in Figures 4.3 and 4.4. Changes in gene abundance (DNA) can be found in Figure 4.5.

Nitrogen metabolism

Enrichment significantly altered the expression of nitrogen metabolism genes, whereas metals had a weaker effect, i.e. not significant post false discovery rate (FDR) correction. The potential for increased nitrogen fixation rates (transformation of dinitrogen gas (N_2) to ammonia/ammonium (NH_3/NH_4^+)) was detected in enriched samples (*nifD*: $p = 0.02$, $p_{adj} = 0.069$, DNA: increase). Nitrification (oxidation of NH_4^+ to nitrite (NO_2^-) and then nitrate (NO_3^-)) was affected differentially by enrichment and metals at multiple steps in the pathway. Firstly, genes involved in the conversion of NH_3/NH_4^+ to hydroxylamine, decreased significantly with enrichment (*pmoB-amoB*: $p = 0.034$, *padj* $= 0.1$, DNA: no change; *pmoC-amoC*: $p < 0.001$, $p_{adj} = 0.006$, DNA: no change; *hcp*: $p = 0.007$, $p_{adj} = 0.041$, DNA: decrease), whereas one gene increased and one slightly decreased in metal contaminated sediments (*pmoB-amoB*: $p = 0.02$, $p_{adj} = 0.334$, DNA: no change; *pmoC-amoC*: $p = 0.04$, $p_{adj} = 0.334$, DNA: no change). The gene involved in conversion of NH_3/NH_4^+ to carbamoyl-P also decreased with metal contamination (*CPS1*: $p = 0.02$, $p_{adj} = 0.334$, DNA: increase). Secondly, increased transformation of NO_2^- to NH_3/NH_4^+ was detected in enriched treatments (*nrfC*: $p < 0.001$, $p_{adj} = 0.004$, DNA: not detected) and transformation of nitroalkanes into NO_2^- was increased in all treatments (*ncd2*: metals, $p = 0.03$, $p_{adj} = 0.334$, DNA: no change; enrichment, $p = 0.03$, $p_{adj} = 0.084$, DNA: no change). Additionally, *narG* (transformation of NO_2^- to NO_3^- and vice versa) decreased in all enriched samples ($p = 0.018$, $p_{adj} = 0.069$, DNA: decrease). The remaining nitrification genes did not significantly differ between treatments (see Figure 4.3). Denitrification (transformation of NO_3^- to ultimately N_2) was affected in two different genes: nitrite reductase (*nirK*) and nitrous oxide reductase (*nosZ*). *nirK* was only detected at low levels in the high metals/enriched treatment, whereas metal contamination alone had an increasing effect and purely enrichment significantly decreased expression of this gene (enrichment: $p = 0.003$, $p_{adj} = 0.02$, DNA: decrease; metals*enrichment: $p = 0.025$, $p_{adj} = 0.879$, DNA: significant interaction). *nosZ*, which is responsible for the last step of denitrification and therefore for reduction of nitrous oxide (N_2O) to N_2, was significantly decreased in all enriched

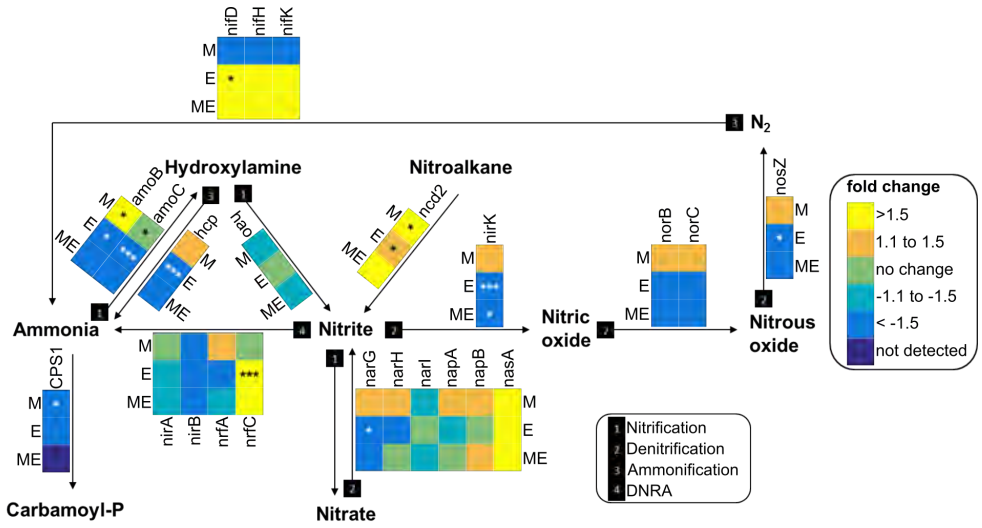

Figure 4.1: This diagram shows a summary of the results for the **nitrogen metabolism**. All genes that were measured in our samples are depicted in the figure next to the arrows representing the process that these genes facilitate. The heatmaps depict gene expression fold changes in different treatments compared to control (C). M stands for high metal treatments, E for organically enriched treatments and ME for treatments with high metals and organic enrichment. For M and E, fold changes were calculated as expression of M+ME in relation to C+E and expression of E+ME in relation to C+M, respectively. For ME, fold changes were calculated in relation to control samples. A fold change of 1 means there was no change at all (green boxes). Genes that were up-regulated in different treatments are shown in shades of yellow, while down-regulated genes are shown in shades of blue. Genes that were not detected in treatment samples, but were present in control samples, are shown as not detected. Also, statistical significances are shown within the heatmaps. * represents statistical significance before false discovery rate (FDR) correction for multiple testing and *** represents significance even after FDR correction. A significance level of α=0.05 was applied to all tests. White numbers in black boxes at the beginning of arrows show the specific process that these reactions belong to. Genes involved in anaerobic ammonia oxidation (anammox) are not shown here, because they were not detected in our dataset.

samples ($p < 0.001$, $p_{adj} = 0.009$, DNA: decrease). The nitrogen metabolism genes which were significantly different between enrichment treatments after FDR correction are *pmoC-amoC*, *hcp*, *nrfC*, *nirK* and *nosZ*. Overall, enrichment has the potential to increase NH_3/NH_4^+ and N_2O production. Detailed ANOVA results can be found in Table C.1.

Sulphur metabolism

Numerous sulphur metabolism genes were strongly affected by organic enrichment; two genes were affected by metal contamination. Sulphate (SO_4^{2-}) reduction to sulphite (SO_3^{2-}) was increased in enriched samples (*sat*: $p = 0.014$, $p_{adj} = 0.064$, DNA: increase; *aprA*: $p = 0.016$, $p_{adj} = 0.065$, DNA: increase; aprB: p = 0.026, $p_{adj} = 0.082$, DNA: increase). Sulphite dehydro-

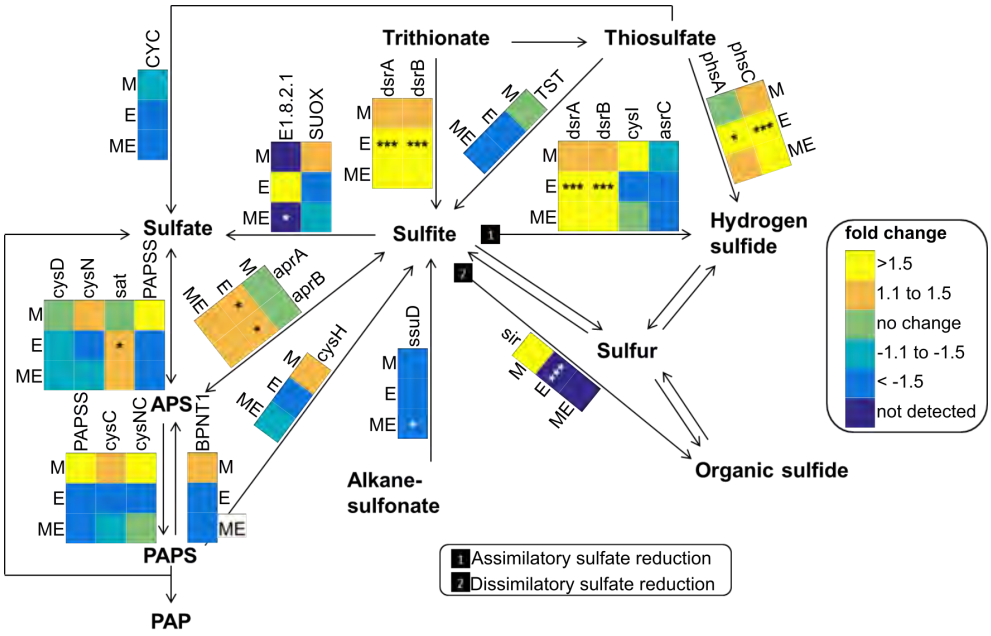

Figure 4.2: This diagram shows a summary of the results for the **sulphur metabolism**. All genes that were measured in our samples are depicted in the figure next to the arrows representing the process that these genes facilitate. The heatmaps depict gene expression fold changes in different treatments. M stands for high metal treatments, E for organically enriched treatments and ME for treatments with high metals and organic enrichment. For M and E, fold changes were calculated as expression of M+ME in relation to C+E and expression of E+ME in relation to C+M, respectively. For ME, fold changes were calculated in relation to control samples. A fold change of 1 means there was no change at all (green boxes). Genes that were up-regulated in different treatments are shown in shades of yellow, while down-regulated genes are shown in shades of blue. Genes that were not detected in treatment samples, but were present in control samples, are shown as not detected. Also, statistical significances are shown within the heatmaps. * represents statistical significance before false discovery rate (FDR) correction for multiple testing and *** represents significance even after FDR correction. A significance level of α=0.05 was applied to all tests. White numbers in black boxes at the beginning of arrows show the specific process that these reactions belong to.

genase (*E1.8.2.1*), which is responsible for the transformation of SO_3^{2-} back to SO_4^{2-}, was only expressed in purely enriched and in one control sample (metals*enrichment: $p = 0.018$, $p_{adj} = 0.879$, DNA: significant interaction). The detection limit for the sulphite reductase gene (*sir*) from the assimilatory sulphate reduction (ASR) pathway was generally low; however, *sir* was completely switched off in enriched samples ($p < 0.001$, $p_{adj} = 0.002$, DNA: decrease). In contrast, sulphite reductase genes, which are part of the dissimilatory sulphate reduction (DSR) and oxidation, were significantly increased with enrichment (*dsrA*: $p = 0.001$, $p_{adj} = 0.009$, DNA: increase; *dsrB*: $p = 0.003$, $p_{adj} = 0.02$, DNA: increase). The genes responsible for H_2S production from thiosulphates were found in significantly higher numbers in enriched

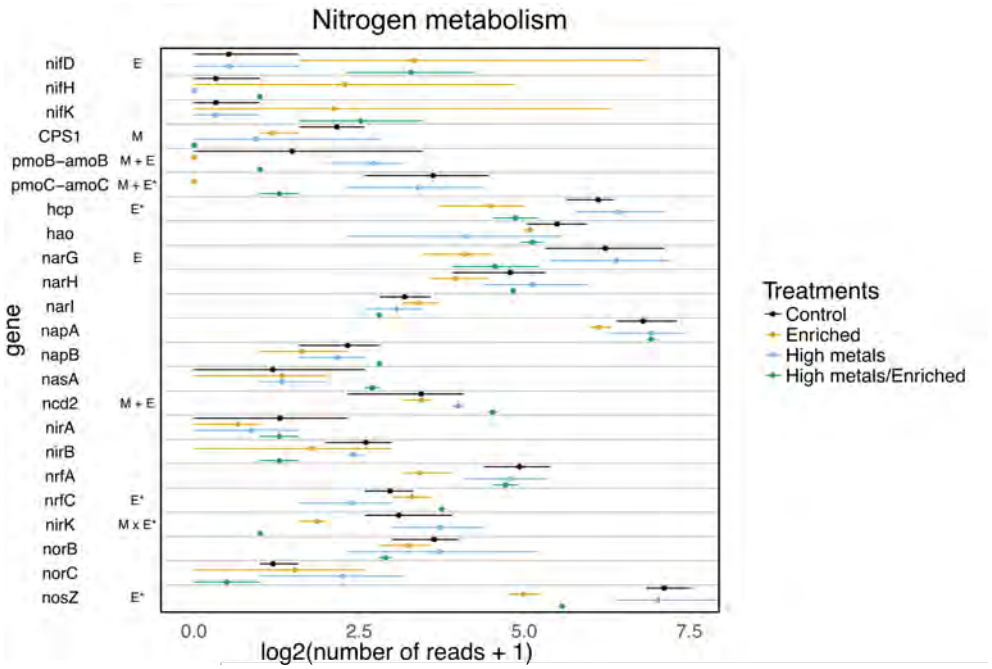

Figure 4.3: Gene expression levels of all **nitrogen metabolism** genes that were detected in our dataset. The letters next to the gene name indicate the treatment (M = High metals, E = Enrichment) that has significantly affected the expression of that gene, whereas M+E means that both metal contaminants and organic enrichment had a significant effect, and MxE indicates that there was a significant interaction between the treatments. An asterisk (*) next to the treatment letter indicates that the *p*-value was still significant (at an α level of 0.05) after false discovery rate (FDR) correction. The horizontal bars range from the lowest to the highest measured expression value and the dot symbolises the mean.

samples (*phsA*: $p = 0.019$, $p_{adj} = 0.069$, DNA: not detected; *phsC*: $p = 0.001$, $p_{adj} = 0.009$, DNA: not detected). In all but the control samples, SO_3^{2-} production from alkane-sulphonates (*ssuD*) was decreased, whereas the gene was not detected at all in purely enriched samples (metals*enrichment: $p = 0.039$, $p_{adj} = 0.879$, DNA: not detected). The sulphur metabolism genes significantly different between enrichment treatments after FDR correction are *sir*, *dsrA*, *dsrB* and *phsC*. Genes for only one reaction involved in the production of dimethylsulphoniopropionate (DMSP), which is a gas that is often discussed for its effect on climate change (Gabric et al., 2013), were detected in our dataset and were not found to be significantly affected by metal contamination or organic enrichment. Therefore, we excluded that part of the sulphur cycle from our analyses.

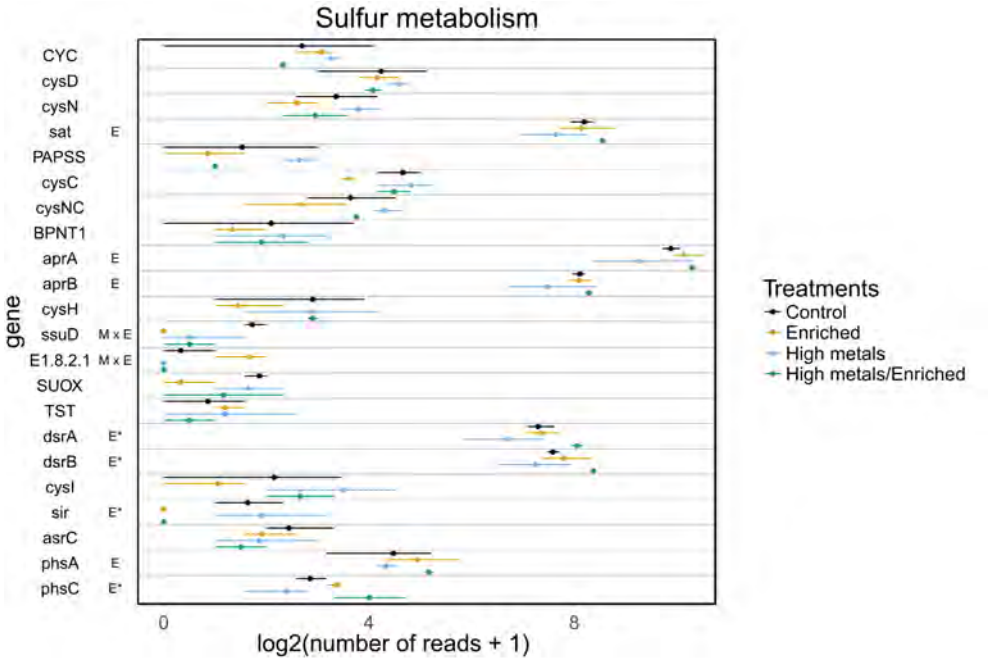

Figure 4.4: Gene expression levels of all **sulphur metabolism** genes that were detected in our dataset. The letters next to the gene name indicate the treatment (M = High metals, E = Enrichment) that has significantly affected the expression of that gene, whereas M+E means that both metal contaminants and organic enrichment had a significant effect, and MxE indicates that there was a significant interaction between the treatments. An asterisk (*) next to the treatment letter indicates that the *p*-value was still significant (at an α level of 0.05) after false discovery rate (FDR) correction. The horizontal bars range from the lowest to the highest measured expression value and the dot symbolises the mean.

Benthic metabolism and sediment-water N fluxes

There were no significant differences across treatments for benthic community respiration (BCR) with mean treatment rates ranging from -3250 to -1800 O_2 μmol/m^2/h. In contrast, significant differences between metal treatments were found for net primary productivity (NPP) (Figure 4.6(a)). Net daily sediment NH_3/NH_4^+ fluxes were directed out of the sediment to the water column (Table C.4) and did not significantly differ among treatments. In contrast, NO_x was mostly taken up by the sediments and this uptake increased significantly in enriched treatments with and without metals (Figure 4.6(b)). Exact fluxes and according *p*-values can be found in Tables C.4 and C.5.

Discussion

Human activity along coastal areas exposes these ecosystems to increasing numbers and concentrations of contaminants. How these contaminants affect crucial biogeochemical processes and the genetic regulators of these processes

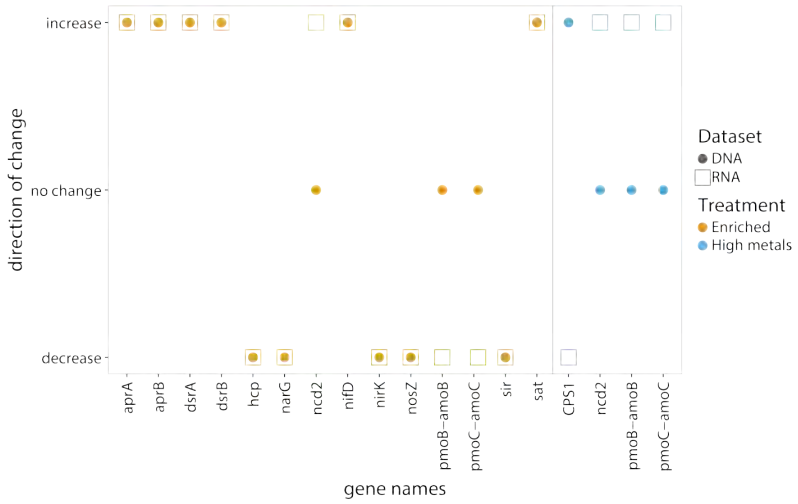

(a) Changes in gene abundance and expression due to enrichment and high metals

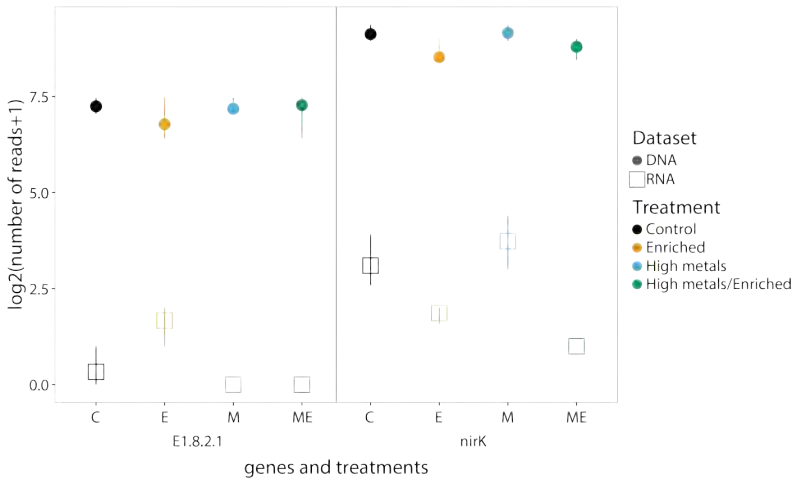

(b) Gene abundance and expression with significant interaction

Figure 4.5: (a) Gene abundance changes (DNA - circles) and gene expression changes (RNA - squares) compared to control due to enrichment or high metals of all the differentially expressed genes from the nitrogen and sulphur metabolisms. (b) The gene abundance and expression levels of differentially expressed nitrogen and sulphur metabolism genes with a significant interaction of enrichment and high metals. The vertical bars in (b) range from the lowest to the highest measured gene abundance value and the dot symbolises the mean. C stands for control, M for high metal treatments, E for organically enriched treatments, and ME for treatments with high metals and organic enrichment. Symbols are coloured according to treatment.

in coastal sediments is poorly understood (Nogales et al., 2011). Our study measures the metatranscriptomic response of an entire sediment microbial community to common multiple stressors - a combination of metal contamination and organic enrichment - in a robust field experiment. Specifically, we used metatranscriptomics to investigate the impact of these contaminants

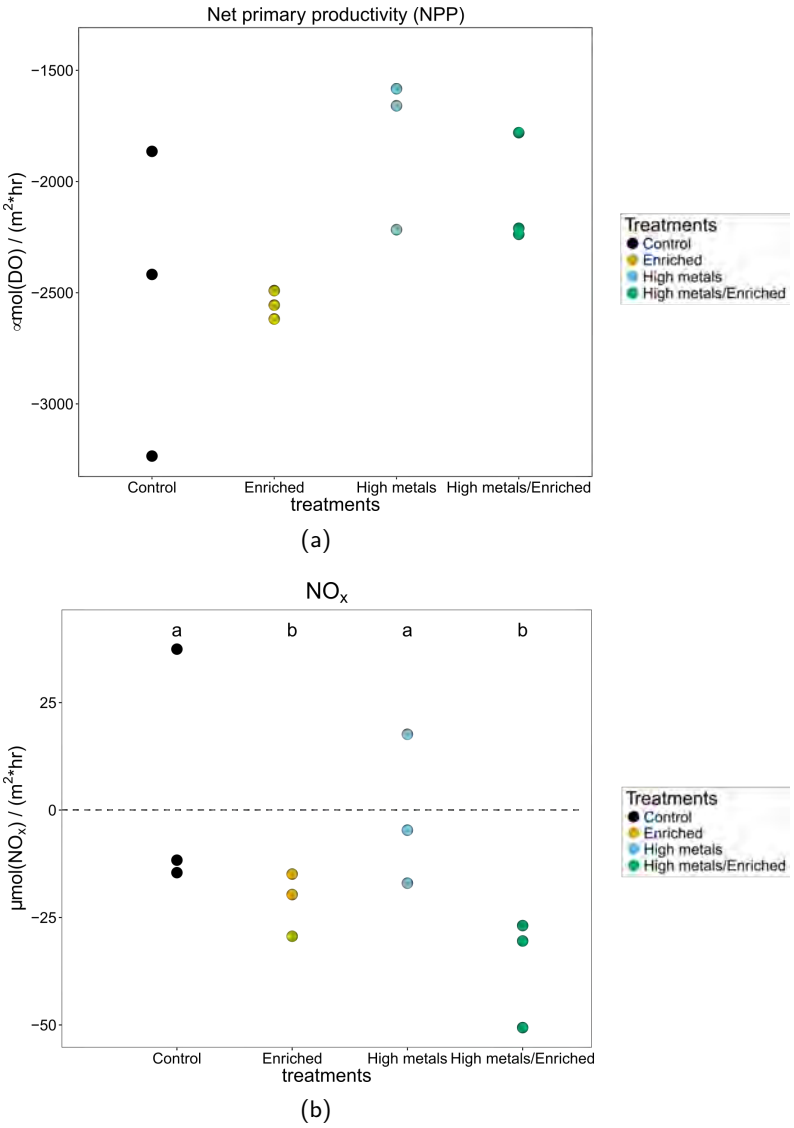

Figure 4.6: Fluxes from the sediment into the overlying water as measured through sediment core incubations. (a) shows net primary productivity (NPP, dissolved oxygen flux in light). All values are negative, showing that all sediments were heterotrophic by taking up oxygen from the overlying water. (b) shows net nitric oxide (NO_x – nitrite and nitrate) fluxes. Net fluxes were calculated as the average of dark and light fluxes. Negative values represent NO_x being taken up into the sediment from the overlying water.

on the activity of functional genes relevant to climate change - genes from the nitrogen and sulphur metabolisms. These metabolisms include the production and degradation of some of the most potent greenhouse gases - nitrous oxide (N_2O) and hydrogen sulphide (H_2S) - and can therefore directly affect climate change. The abundance of the genes associated with gas production have been directly linked to the measured production of gases in soil systems (Morales et al., 2010; Philippot et al., 2011; Harter et al., 2014), the activity of such

genes may be even more tightly linked. Consequently, investigating the genetic activity involved in greenhouse gas production is of major importance. Our findings highlight the potential impact of single and multiple anthropogenic contaminants on the global climate and elucidate the underlying genetic mechanisms of altered gas production.

Nitrogen metabolism

Nitrogen fixation genes were more active in enriched samples (with and without metals, p_{adj} >0.05). Nitrogen fixation is energetically costly and is therefore usually limited. However, in enriched samples the breakdown of organic matter produces a high amount of energy and can thereby facilitate higher rates of nitrogen fixation. An increase in nitrogen fixation activity is often termed 'internal eutrophication' (Smolders et al., 2006), and directly leads to increased concentrations of ammonia/ammonium (NH_3/NH_4^+) in the sediments (Gardner and McCarthy, 2009). In estuarine and marine sediments, NH_4^+ typically comprises >95% of the total ammonia-N (NH_3 + NH_4^+). NH_3 is far more toxic than NH_4^+, as the latter contributes less than 1% of the total toxicity of ammonia-N (Batley and Simpson, 2009). The effects of both NH_3 and NH_4^+ are being considered here. Accumulated NH_3/NH_4^+ is most commonly removed from the system through coupled nitrification/denitrification, diffusion into the overlying water column or uptake by algae at the sediment-water interface (benthic microalgae, BMA). However, our data suggest a disruption in these processes. Activity of genes associated with the degradation of NH_3/NH_4^+ to nitrite (NO_2^-), was decreased in enriched sediments (p_{adj} ≤0.05), which suggests ineffective nitrification. As nitrification requires oxygen to occur, the likely anoxic conditions of our sediments could be the reason for this down-regulation of nitrification and eventually a decoupling of the nitrification and denitrification processes. Also, our flux measurements (Table C.4) show that the accumulated NH_3/NH_4^+ did not diffuse into the water column, nor was it taken up by BMA, as the photosynthetic activity was low in all treatments.

Apart from NH_3/NH_4^++ removal through BMA or plants and coupled nitrification/denitrification, NH_3/NH_4^+ can be directly transformed into dinitrogen gas (N_2) through anaerobic ammonium oxidation (anammox). This process simultaneously removes NO_2^- from the system (Dalsgaard et al., 2005; Engström et al., 2005). Anammox can only occur in anoxic sediments and is performed by very specialised bacteria (Dalsgaard et al., 2005), however, it can constitute up to 50% of the fixed N turnover from marine systems (Devol, 2003). The anoxic nature of our sediments suggests a high potential for

this process, but high H_2S concentrations are known to inhibit the anammox process (Thamdrup and Dalsgaard, 2002). Unfortunately, we were not able to detect anammox genes in enough samples and in high enough read counts to determine if this process was up-regulated in any of our treatments. Mass balance calculations (Table C.2) suggest that in all treatments 25% of nitrogen (N) must be escaping the sediment system as a gas. Gene expression data show that in enriched samples regardless of metal content this N is most likely accumulated in the system as NH_3/NH_4^+ or lost through incomplete denitrification.

We also found evidence that NO_2^- concentrations increase in enriched sediments through transformation of nitroalkanes (p_{adj} >0.05), and nitric oxide (NO_x, nitrite and nitrate) uptake from the overlying water. NO_x can be used as a source of N by BMA living at the sediment-water interface. However, an overall efflux of NH_3/NH_4^+, which is BMA's preferred form of N (Sundbäck and Granéli, 1988), suggests that there is an excess of N available in all our samples and therefore BMA is unlikely to take up any NO_x. The influx of NO_x could suggest an increased rate of denitrification in the sediment. However, organic enrichment instead led to an up-regulation of the dissimilatory nitrate reduction to ammonium (DNRA, p_{adj} ≤0.05). DNRA is an alternative pathway to denitrification (Burgin and Hamilton, 2007) that produces highly bioavailable NH_3/NH_4^+, and can thereby lead to a further increase in NH_3/NH_4^+ concentrations in the sediment. DNRA is equally significant as denitrification for NO_3^- reduction in marine (Bernard et al., 2015) and freshwater (Burgin and Hamilton, 2008) sediments, and in soils (Yang et al., 2015). High concentrations of NH_4^+ favour toxic cyanobacteria and can lead to an overall suppression of growth (Glibert et al., 2016), while NH_3 is highly toxic, both resulting in a decrease of ecosystem productivity.

We also found decreased activity of the respiratory nitrate reduction in enriched sediments (p_{adj} >0.05). This is potentially due to the system being NO_x limited, as suggested by the influx of NO_x from the overlying water column. Influx of NO_x in combination with this low activity of nitrate reduction can lead to an accumulation of NO_3^- in the system, which is a highly potent fertiliser. However, NO_3^- is unlikely to remain in the sediment, as it is used as one of the preferred electron acceptors for the high concentrations of sulphate reduction (sulphide production) in our enriched treatments.

Metal contamination led to increased rates of nitrification (p_{adj} >0.05) and NO_2^- production from nitroalkanes (p_{adj} >0.05). In contrast, it led to a decrease in production of carbamoyl phosphate from NH_4^+ (p_{adj} >0.05), which is a precursor of arginine and pyrimidine (Lacroute et al., 1965), two

essential amino acids. This suggests that general metabolic activity involving these two amino acids decreased, while the production of toxic NO_2^- increased. Therefore, increased metal concentrations in the sediment have the potential to lead to internal eutrophication through accumulation of NO_2^-.

Organically enriched sediments with (p_{adj} >0.05) and without (p_{adj} ≤0.05) metals also showed a significant decrease in NO_2^- reduction to nitric oxide (NO). This *nirK* gene was only detected once in each sample with a combination of metal contamination and organic enrichment while it was still somewhat active in purely enriched samples. This suggests that while eutrophication can shut down denitrification, as has previously been shown (Gardner and McCarthy, 2009), contaminants such as metals can exacerbate the impact of organic enrichment, potentially by binding nutrients (Reuter and Perdue, 1977) and increasing their residence time in the sediment.

The activity of genes involved in N_2O reduction to N_2 was also significantly decreased in all enriched samples (p_{adj} >0.05), while the activity of the gene involved in N_2O production from NO remained unchanged. NO reduction is closely linked to NO_2^- reduction because of the highly toxic nature of NO radicals, while N_2O reduction can function as an autonomous respiratory process (Zumft, 1997). In addition, N_2O reduction yields the least amount of energy of all nitrogen metabolism steps (Zumft, 1997). Therefore, it is commonly one of the first genes to be down-regulated when there is enough substrate present for the microbes to perform more energetically beneficial reactions. Also, a high fraction of known denitrifiers are not able to reduce N further than to N_2O. Very few bacteria possess the necessary gene (*nosZ,* Jones et al., 2008). Therefore, some N_2O is always produced in denitrifying conditions (Philippot et al., 2011), even when N_2O reduction is not affected by environmental factors. In addition, a significant proportion of the produced N_2O results from nitrification under oxic conditions (Murray et al., 2015). Our enriched sediments were, however, likely mostly anoxic and we found nitrification genes to be down-regulated in these enriched sediments. The accumulation of N_2O does not induce any reaction in the benthic community because N_2O is non-toxic, and, being a gas, is fluxed out into the water column due to a concentration gradient. From there it is then potentially released to the atmosphere. Complex processes in the water column dictate how much gas ultimately reaches the atmosphere (Leifer and Patro, 2002), however, the activity of the *nosZ* gene directly affects the amount of N_2O gas released, e.g. from soil systems (Morales et al., 2010; Philippot et al., 2011; Harter et al., 2014). Oceans are also known to represent a source of atmospheric N_2O (Law and Owens, 1990). We have shown here that the potential for accumulation of N_2O in organically

enriched sediments increases, whereas the extent of N_2O production might well be exponential with increasing organic enrichment, as has been shown for agricultural soils (Shcherbak et al., 2014). N_2O is a highly potent greenhouse gas with a global warming potential of approximately 300 times that of a carbon dioxide (CO_2) molecule (Schreiber et al., 2012). Estuarine systems contribute at least 11% of the total N_2O emissions on a global scale (Seitzinger and Kroeze, 1998). Additionally, atmospheric N_2O concentrations have been increasing at a rate of 0.3% per year, which is thought to be related to anthropogenic N release (Forster et al., 2007). In line with this, our data suggest that eutrophication of waterways can indirectly exacerbate climate change via increased production of N_2O.

The majority of differentially expressed nitrogen metabolism genes due to enrichment or an interaction of enrichment and high metals, showed the same direction of significant change in gene abundance (Figure 4.5). For these genes, the functional change seems to be a direct consequence of an altered community structure. However, three differentially expressed genes, *nirK*, *pmoB-amoB*, and *pmoC-amoC*, did not show any changes in gene abundance. Thus the transformation of nitroalkanes into nitrite and the first step of nitrification seem to be transcriptionally regulated in a stressed community, instead of the activity being dictated by gene abundance. Furthermore, differentially expressed genes due to the presence of high metals in the sediment seem to all be transcriptionally regulated. Although high metals can lead to changes in gene abundance, as seen for gene *CPS1*, the expression of genes impacted by metal concentrations is regulated independently of community structure.

Sulphur metabolism

Breakdown of organic matter depletes the O_2 molecules in the sediment and produces an anoxic environment, which is known to favour sulphate (SO_4^{2-}) reduction. Interestingly, the end product of the sulphate reduction can vary at different levels of enrichment, and have distinct effects on the overall sediment microbial community. In our enriched treatments (with and without metals), SO_4^{2-} reduction to sulphide was significantly increased ($p_{adj} \leq 0.05$). In addition, we saw a shift from combined assimilatory and dissimilatory sulphate reduction (ASR and DSR) to purely DSR. This means that the SO_4^{2-} is no longer transformed into organic sulphide but rather into inorganic sulphide, i.e. H_2S. Measurements of acid volatile sulphides in a parallel run experiment with the same enrichment treatments (Sun, 2016) confirmed the production of sulphides, as did the strong smell of the sediment at the time of sampling. The inactivity of ASR ($p_{adj} \leq 0.05$) implies a lower rate of gen-

eral metabolic activity and growth that involves the production of sulphide-containing amino acids (Khan et al., 2010). H_2S produced through DSR is highly toxic and known to inhibit nitrifying bacteria (Joye and Hollibaugh, 1995). Also, H_2S promotes the activity of DNRA by favouring NO_3^- over NO_2^- production (Kraft et al., 2014), and by serving as an electron donor for DNRA organisms. Moreover, H_2S inhibits NO and N_2O reductases (Brunet and Garcia-Gil, 1996), and therefore denitrification in general (Aelion and Warttinger, 2010), and negatively affects anammox processes (Thamdrup and Dalsgaard, 2002). The increased concentrations of H_2S may, therefore, explain the increased NO_x influx and transformation of this NO_x to NH_4^+ in enriched sediments. Increased concentrations of H_2S are also likely the driving force behind the down-regulation of the *nosZ* gene. The production of H_2S is therefore likely to be the driver behind the observed changes in nitrogen metabolism, some of which further facilitate H_2S production, and the factor that increases the potential for greenhouse gas production in eutrophied sediments.

In addition to the toxicity of H_2S and its effects on the nitrogen metabolism, H_2S is considered a greenhouse gas due to its rapid reaction with singlet O atoms (Kump et al., 2005). Photosynthetic organisms efficiently oxidise H_2S during the day (Hansen et al., 1978) and can thus decrease the likelihood of the gas being released into the atmosphere. However, the heterotrophic nature of our samples suggests that photosynthetic organisms (such as BMA) were not highly active and we therefore hypothesise that this detoxifying effect is negligible with most of the produced H_2S being released into the water column, potentially reaching the atmosphere (Watts, 2000). Furthermore, H_2S is released into the atmosphere at night regardless of the level of photosynthetic activity during the day (Hansen et al., 1978).

Similarly to the nitrogen metabolism, differentially expressed sulphur metabolism genes due to enrichment seem to be regulated by changes in gene abundance rather than through transcriptional alterations (Figure 4.5(a)). However, gene *E1.8.2.1*, which is responsible for the transformation of sulphites to sulphates, showed different directions of change in gene abundance and expression. While the combination of enrichment with metals led to the elimination of the effects of enrichment in both datasets (Figure 4.5(b)), the direction of change due to enrichment was reversed, suggesting that this gene is transcriptionally regulated in a stressed community.

Conclusions

This study is the first to experimentally determine the effects of metals and organic matter on estuarine sediment community functioning using metatranscriptomics. To date, most ecosystem monitoring techniques are based on macroinvertebrates (Magurran et al., 2010), algae (Reavie et al., 2010) and total microbial biomass (Dequiedt et al., 2011). Microbial functions have largely been disregarded in such biomonitoring approaches, probably due to high diversity of microbial communities complicating the detection of patterns (Nogales et al., 2011), even though they have been shown to shift upon environmental change (Schimel et al., 2007; Dafforn et al., 2014; Chariton et al., 2016). With metatranscriptomics we were able to explore the genetic mechanisms driving functional change in contaminated sediments and therefore progress this tool for environmental monitoring.

Metal treatments affected few genes in the investigated metabolisms, without major consequences for the biogeochemical output of the system. Only in combination with organic enrichment did metals affect the nitrogen metabolism by exacerbating the effects of enrichment on the decoupling of nitrification and denitrification. In contrast, organic enrichment had extensive effects on both nitrogen and sulphur metabolisms. Organic matter can change the sediment profile of O_2 and thus favour the use of alternative electron acceptors such as NO_3^-, SO_4^{2-} and CO_2 (Middelburg and Levin, 2009). The loss of an upper oxic zone in the sediment decreases rates of nitrification and favours the activity of SO_4^{2-} reducers. The increased production of H_2S then significantly affects the nitrogen metabolism resulting in increased NH_3/NH_4^+, NO_3^- and N_2O concentrations. Higher NO_3^- concentrations in turn facilitate SO_4^{2-} reduction, which leads to higher concentrations of H_2S. These dynamic processes ultimately activate a positive feedback loop, in which the accumulation of toxic intermediate products (NH_3) and highly potent greenhouse gases (N_2O and H_2S) are significantly increased, while ecosystem productivity is likely decreased. We have therefore experimentally demonstrated that while organic enrichment can indirectly contribute to climate change, contaminants such as metals may exacerbate the impact of enrichment, potentially by binding nutrients and increasing their residence time in the sediment. Furthermore, our data revealed that the majority of functional changes were a result of altered community structure. This supports the idea of bioaugmentation, where specific microbes are added to a stressed system (Vidali, 2011), and suggests that this technique of bioremediation could be used to directly manipulate the production of toxic compounds and greenhouse gases in contaminated ecosys-

tems.

5 Altered microbial communication, productivity and nutrient cycling in contaminated sediments of an urbanised estuary

Abstract

Industry and agriculture have been major sources of toxic contaminants and organic matter for adjacent waterways. Due to increasing urbanisation of coastal areas, additional pollution of water bodies is occurring as stormwater transports a complex mixture of contaminants from gardens, grooves and roads. When contaminants reach estuarine waters, they generally bind to particles and concentrate on the sea floor thereby exposing sediment communities to high concentrations of toxicants. Sediment microbes are important for urban ecosystems through their provision of a variety of ecosystem functions. Exposure to legacy contaminants from industry, agriculture and stormwater run-off has the potential to affect the function of these critical communities. To prioritise ecosystem management actions, we need to understand the nature and extent of the impact of multiple legacy contaminants on sediment microbial communities. We investigated the differences in functioning of sediment communities adjacent to stormwater drains in poorly flushed embayments and at better flushed reference sites within the same embayment. We found that proximity to stormwater drains was associated with significantly lower activity of signalling genes, suggesting that communication within the contaminated communities might be fractured. Furthermore, we found lower metabolic rates and disrupted nutrient cycling close to stormwater drains, potentially leading to overall lower productivity but higher production of greenhouse gases. Our results suggest that contaminants can lead to lower productivity, higher impact on climate change, and potentially lower remediation capacity of sediment communities. This study emphasises the need for improved industrial waste and stormwater management in our increasingly urbanised coastal waterways.

Introduction

Ecological communities are increasingly exposed to a complex mix of multiple stressors from the industrialisation and urbanisation of natural systems. Chemical stressors include toxic contaminants such as metals and metalloids

(e.g. Nicholson et al., 2003) that have been linked to community shifts from the loss of sensitive species (Johnston and Roberts, 2009; Dong et al., 2016). Furthermore, application of enriching contaminants such as fertilisers has overloaded many systems with nutrients. While these are essential for growth and productivity, excess organic enrichment can cause mortality through hypoxia and a build-up of toxic compounds (Meyer-Reil and Köster, 2000; Gray et al., 2002). Much of our understanding of the impacts of multiple stressors has been restricted to what can be observed and quantified; that is, primarily changes to abundance and identity within communities (Dafforn et al., 2016). Advances in molecular techniques have created opportunities to study community functions by linking gene expression to biogeochemical pathways. To better predict and manage urban stressors requires an approach that can identify functional responses and improve our understanding of ecosystem consequences (Johnston et al., 2015b).

The maintenance of ecosystem functioning is reliant on interactions taking place within communities (Stachowicz, 2001; Falkowski et al., 2008), as organisms respond to environmental cues (Westerhoff et al., 2014) and signals from other organisms in the same community (Ross-Gillespie and Kümmerli, 2014). Pathways involved in signalling, energy, and nutrient cycling are particularly important for the maintenance of ecosystem services by microbial organisms. When communities are exposed to stress, the signalling pathways involved in the reception and production of chemical signals from the environment and to/from other cells in the community may be disrupted. This can potentially result in the loss of ecosystem services that require multiple steps, such as remediation. Further, primary production of marine ecosystems is one of the functions most affected by contamination (Johnston et al., 2015b), and as contaminants can change the chemical conditions of a system, they also impact nutrient cycles. For example, Scott et al. (2014) have shown that the degradation of polyaromatic hydrocarbons produces anoxic conditions in marine sediments, which favours denitrification over nitrification, and organic pollution affects the release rates of highly potent nutrients from sediments (Sanz-Lázaro et al., 2015). In order to fully understand the repercussions of contamination in the affected ecosystem, it is therefore crucial to understand the impacts of contaminants on these important functional pathways.

Contaminant inputs to coastal waterways have increased as physical modifications associated with urbanisation increased the amount of impervious surface within catchments. High proportions of impervious surface results in large and rapid surface flows during rainfall events (Arnold and Gibbons, 1996). To mitigate property damage and life threats in urban areas, these

large amounts of water are collected in drainage systems and transported into adjacent waterways via stormwater drains. Through this process, more than half of the rainwater may end up in adjacent waterways (Arnold and Gibbons, 1996). Moreover, stormwater picks up a complex mix of contaminants on its way to the drainage system (Göbel et al., 2007; Laetz et al., 2015). Metals leak into the water from the roofs of houses, and pesticides and organic matter are washed out from partly sealed surfaces such as urban gardens and animal rearing facilities (Göbel et al., 2007). Stormwater has therefore been considered a major source of contaminants to urbanised waterways, and the accumulation of stormwater contaminants over time represents a significant ecological risk (e.g. Birch and McCready, 2009; Birch et al., 2015; Lintern et al., 2015).

Upon entering a waterway, many contaminants such as dissolved metals and polycyclic aromatic hydrocarbons (PAHs) readily bind to sediments (Chapman et al., 1998), and organic matter. Such particulates settle in low flow environments, where they accumulate in bedded sediments (Burton and Johnston, 2010). Hence, even though point source waste management has generally improved in developed economies over the last century, high concentrations of legacy contaminants can still be measured, especially in the sediment of shallow, low flow environments of urbanised waterways that are poorly flushed (e.g. embayments, Irvine and Birch, 1998; Johnston et al., 2015a). Organisms living in these sediments are thus exposed to extraordinarily high concentrations of multiple contaminants, where changes to benthic infaunal assemblages (Birch et al., 2008; Dafforn et al., 2012), as well as altered bacterial community structures (Sun et al., 2012), have been observed. Microbes are some of the most productive organisms in the world and are responsible for crucial biogeochemical cycles (Falkowski et al., 2008). Their role in nutrient cycling (Arrigo, 2005) and ability to remediate contaminants (Wiatrowski and Barkay, 2005; Antizar-Ladislao, 2010; Das and Chandran, 2011; Mason et al., 2014) makes them indispensable constituents of coastal ecosystems.

Here, we investigate the impact of legacy contaminants from stormwater inputs on a sediment community in the highly urbanised estuary of Sydney Harbour (Mayer-Pinto et al., 2015). We measured gene expression in sediment communities at the ends of poorly flushed embayments with adjacent stormwater drains and at better flushed sites within the same embayment. We used modern metatranscriptomics techniques to elucidate the range of mechanisms of contaminant impact on sediment functioning and focused our analysis on genes involved in signalling, energy and nutrient pathways. Our findings show that sediments in very poorly flushed areas have a lower rate of productivity

and higher production of toxic compounds and greenhouse gases. Furthermore, heavily contaminated communities show signs of community fracturing, which can lead to poor remediation capacity and disrupted ecosystem services. This study highlights the importance of improved waste management and contaminant remediation in urbanised waterways.

Methods

Sampling design and collection

The two sampling locations were Hen and Chicken Bay (-33°86'08"S, 151°11'59"E) and Iron Cove (-33°87'18"S, 151°15'05"E) within Sydney Harbour, Australia. Both embayments have been shown to contain high concentrations of contaminants (Irvine and Birch, 1998). Two replicates of sediments were sampled in February and March 2014 (Austral summer) from contaminated sites adjacent to stormwater drains, and at reference sites 1 km away from the stormwater drains towards the embayment entrance. The ends of embayments were considered highly exposed to legacy contaminants (metals and organic enrichment) due to poor flushing and the proximity to stormwater input. The latter sites were considered reference sites as they had lower contamination in the sediments and less direct exposure to stormwater due to flushing. Sampling was done during dry conditions (<5 mm rainfall/day, Bureau of Meteorology) and therefore ongoing stormwater inputs into the estuary were minimal (<0.1 m^3/s) (Birch and Rochford, 2010) and unlikely to have influenced ecological or environmental patterns. Salinity and temperature of the two sites (adjacent to stormwater drain and reference) were similar (Table D.3). Sediments metals, isotopes and water quality variables were measured in order to confirm the appropriateness of sites. For details on water quality variables see (Sutherland et al., 2016). A replicate number of two was used for this survey, because the high costs of metatranscriptomic analyses significantly constrain the number of samples that can be analysed. Using two replicates we were able to assess variation between replicates, and observe statistically significant temporal and spatial differences (two time points and two embayments).

Sediment was collected using a Van Veen grab and 2 g of surficial sediment was transferred into a collection tube, immediately frozen in liquid nitrogen on the boat and stored at -80°C until total RNA extraction. The remaining sediment from the grab was then homogenised, transferred into 50 ml collection tubes and stored on ice for chemical analyses. Two replicates were sampled

for each site and time point.

Chemical analyses

In short, metal analyses followed (Dafforn et al., 2012) with sediments oven-dried (50°C) and homogenised to a fine powder with mortar and pestle before microwave digestion according to method 3051A (USEPA 2007). Following digestion metal concentrations were analysed using ICP-AES (Perkin Elmer, OptimaOptima7300DV, USA). Individual sediment contaminants were highly correlated with one another, so we derived a single measure of toxicity by calculating a mean sediment quality guideline quotient (mSQGQ). This quotient was obtained by scaling contaminant concentrations against their guideline values and upper guidelines (Simpson et al., 2013), then summing scaled concentrations at each site (Long et al., 2006). Ecological impairment of benthic communities has been observed with increasing mSQGVs (Long et al., 2006). Total organic carbon and total nitrogen were analysed at Isoenvironmental (South Africa) using 5-20 mg of dried, homogenised sample in a 20-20 IRMS linked to an ANCA SL element analyser (Europa Scientific). Details on mSQGQ, and carbon and nitrogen stable isotopes are shown in Table 5.1.

RNA extractions and sequencing

RNA was extracted from 1 g of sediment within one week of sampling using a PowerSoil™ Total RNA Isolation Kit (MoBio Laboratories, Carlsbad, CA, USA). RNA samples were further cleaned using the TURBO DNA-free™ Kit (Lifetechnologies, Carlsbad, CA, USA) and Agencourt® RNAClean® XP (Beckman Coulter Inc.) according to manufacturer's instructions. RNA was then stored at -80°C until sequencing. RNA integrity number (RIN) was measured for every sample to check for RNA degradation. The mean RIN for all samples was 7.72, where a RIN of 10 represents no degradation. RNA libraries (n=16) with fragment lengths of ∼200 nt were prepared. Prior to library preparation, the quality of the total RNA samples was assessed on a Bioanalyzer 2100, using an RNA 6000 Nano Chip (Agilent). Sample quantitation was carried out using Invitrogen's Ribogreen assay. Library preparation was then performed according to Illumina's TruSeq Stranded mRNA protocol with the following modifications: The oligo-dT mRNA purification step was omitted and instead, 200 ng of total RNA were directly added to the Elution2-Frag-Prime step. The PCR amplification step, which selectively enriches for library fragments that have adapters ligated on both ends, was performed according to the manufacturer's recommendations but the number of amplification

Table 5.1: Mean sediment quality guideline quotients (mSQGQ) of metals and stable isotopes per sampling site and time point.

Site	Location	Sampling time	mSQGQ (metals)	corrδ^{15}N	corrδ^{13}C
stormwater drain	Hen and Chicken Bay	Feb-14	12.6	4.9	-26.2
stormwater drain	Hen and Chicken Bay	Mar-14	4.1	5.4	-26.6
stormwater drain	Iron Cove	Feb-14	9.3	5.4	-25.6
stormwater drain	Iron Cove	Mar-14	18.0	6.1	-22.2
reference site	Hen and Chicken Bay	Feb-14	3.8	5.8	-21.3
reference site	Hen and Chicken Bay	Mar-14	1.9	6.9	-22.4
reference site	Iron Cove	Feb-14	2.3	5.8	-24.5
reference site	Iron Cove	Mar-14	2.3	7.9	-18.7

cycles was reduced to 12. Each library was uniquely tagged with one of Illumina's TruSeq LT RNA barcodes to allow libraries to be pooled for sequencing. The finished libraries were quantitated using Invitrogen's Picogreen assay and the average library size was determined on a Bioanalyzer 2100, using a DNA 7500 chip (Agilent). Library concentrations were then normalised to 2 nM and validated by qPCR on a ViiA-7 real-time thermocycler (Applied Biosystems), using qPCR primers recommended in Illumina's qPCR protocol, and Illumina's PhiX control library as standard. The libraries were then pooled at equimolar concentrations and sequenced across two lanes on an Illumina HiSeq2500 sequencer in rapid mode at a read-length of 100 bp paired-end. Sequencing was performed at the Singapore Centre for Environmental Life Sciences Engineering (SCELSE).

General sequencing numbers and data processing

Total RNA sequencing yielded a mean of 67.5 million bases (reads) per sample. Standard QC was conducted using Cutadapt 1.8.1 (Martin, 2011) with an overlap of 10, minimum read length of 30, and quality cut-off value of 20. Subsequently, rRNA reads were removed from the dataset using SortMeRNA 2.0 (Kopylova et al., 2012) and the SILVA database version 119. The remaining sequences were classified as mRNA reads (on average 2.5 million reads per sample, 3.7%) and used to perform a homology search using DIAMOND version 0.7.9.58 (Buchfink et al., 2015) against the NCBI NR (non-redundant protein) database (May 2015 version) (Pruitt, 2004). All mRNA reads were assigned to a KEGG (Kyoto Encyclopedia of Genes and Genomes) orthologous gene (KO) using the lowest common ancestor (LCA) algorithm in MEGAN5 (Huson et al., 2011). The total number of reads per KO ID was calculated, and the dataset was normalised using the variance stabilisation function (*getVarianceStabilizedData*) from the *DESEq* package (Anders and Huber, 2010) in R. Sample HC.R.TP1.2 was identified as an outlier due to the generally higher read numbers compared to the other samples (Figure D.1), probably due to degradation of RNA (RIN=5.9). Only genes that were present in at least all replicates of one location at one site and time point were included in the dataset used for statistical analyses.

Metatranscriptome data analysis

Differences in microbial community function (annotated mRNA genes) between contaminated sites (adjacent to stormwater drains) and reference sites (1 km away) was explored with permutational multivariate analyses of vari-

ance (*adonis* function in R package *vegan*), and shifts were visualised with non-metric multidimensional scaling (NMDS) plot. Linear models were performed for every functional gene using site (two levels: stormwater drain and reference), location (two levels: Hen and Chicken Bay and Iron Cove), and sampling time (two levels: February 2014 and March 2014) as fixed factors. Although we had no specific hypotheses about location or sampling time, these factors had only two levels and were therefore treated as fixed factors. To account for this in our analyses, we took the conservative approach of excluding all genes with a significant interaction from further pathway exploration. Genes which were differentially expressed between stormwater drain and reference (1 km away) sites were filtered out for pathway analysis. Pathways with at least five differentially expressed genes were identified and assigned to one of the following pathway groups: signalling, energy and nutrient pathways. Signalling pathways are all involved in the reception and production of chemical signals from the environment and to/from other cells in the community. Energy pathways include carbon fixation which is responsible for net primary production (Field et al., 1998), pathways providing the building blocks for proteins through the production of nucleotides and amino acids, and pathways involved in the production of energy. Pathways involved in nutrient cycling drive Earth's major biogeochemical cycles and remove excess nutrients from the system (Falkowski et al., 2008). Furthermore, nutrient cycles involve the production of greenhouse gases and are thus important on a global scale. From Chapter 4 we know that the nutrient pathways are highly impacted by organic enrichment and that the changes have potential effects on a global level. Therefore, the core parts of the nutrient cycles were analysed in more detail (as in Chapter 4). All data were analysed in R (version 3.2.3, R Core Team 2015) with packages *DESeq* (Anders and Huber, 2010) and *vegan* (Oksanen et al., 2016). All plots were generated using the *ggplot2* package (Wickham, 2009).

Results

Chemical analyses

Metal concentrations were consistently elevated at stormwater drains compared to reference sites 1 km away. Stable isotopes showed a larger input of terrestrial organic material adjacent to stormwater drains. For details see Table 5.1.

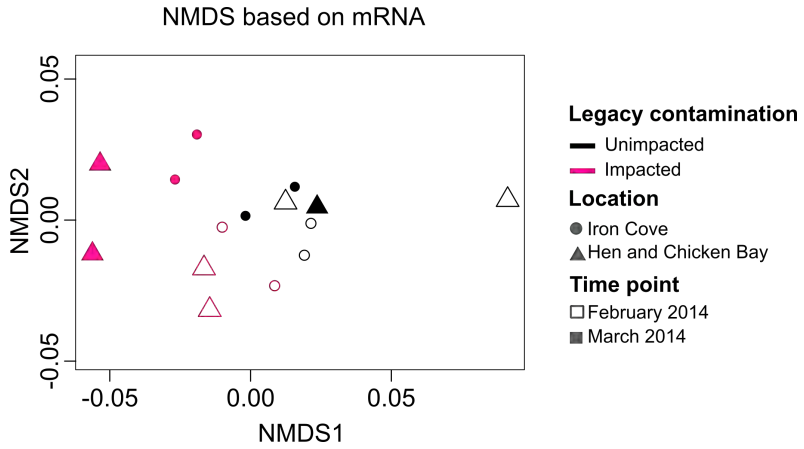

Figure 5.1: Non-metric multidimensional scaling plot for community function (mRNA). Unimpacted and impacted sites are represented in black and pink, respectively. Triangles represent samples from Hen and Chicken Bay, while circles represent samples from Iron Cove. The first and second sampling time points are represented as open and closed symbols, respectively.

Metatranscriptome data analysis

Microbial community function (mRNA) differed significantly between contaminated sites (adjacent to stormwater drains) and reference sites (1 km away). This pattern was spatially (between embayments) and temporally (between sampling times) variable (Table 5.2). The pattern of functional shift was visualised with non-metric multidimensional scaling (NMDS) (Figure 5.1). The first axis (NMDS1), which explains the largest amount of variation in the data, separates the samples along sites (adjacent to stormwater drain and reference 1 km away).

Genes which were differentially expressed between stormwater drain sites and reference sites were identified with gene-wise linear models. Over 6% of all measured genes (523 out of 8305) were significantly affected by proximity to stormwater drain (Table D.1). Plotting the estimates from all linear models (Figure 5.2) revealed that 75% of affected genes were down-regulated at stormwater drain sites (382 out of 523). Moreover, genes that were down-regulated (with an estimate <-1) or up-regulated (estimate >1) were identified (Table D.2). The four genes which were up-regulated at stormwater drains and had an estimate >1 belonged to the following pathways: Glycerolipid metabolism, glycerophospholipid metabolism, sulphur relay system, and ABC transporters. Genes that were down-regulated at stormwater drains and had an estimate <-1, belonged to 34 different pathways. Pathways with two or more genes with an estimate <-1 were: glycolysis/gluconeogenesis, chloroalkane and chloroalkene degradation, methane metabolism, nitrogen

Table 5.2: *Adonis* (permutational multivariate ANOVA) results for mRNA (function) dataset. Significant *p*-values are highlighted in bold.

		Df	Sums Of Sqs	Mean Sqs	F Model	R2	Pr(>F)
mRNA	location	1	0.0062	0.0062	1.5366	0.0756	**0.0325**
	time point	1	0.0089	0.0089	2.1983	0.1081	**0.0011**
	distance	1	0.0128	0.0128	3.1668	0.1558	**0.0001**
	location:time point	1	0.0059	0.0059	1.4528	0.0715	0.0512
	location:distance	1	0.0069	0.0069	1.7229	0.0848	**0.0114**
	time point:distance	1	0.0068	0.0068	1.6976	0.0835	**0.0147**
	location:time point:distance	1	0.0063	0.0063	1.5527	0.0764	**0.0314**
	Residuals	7	0.0282	0.0040	0.3444		

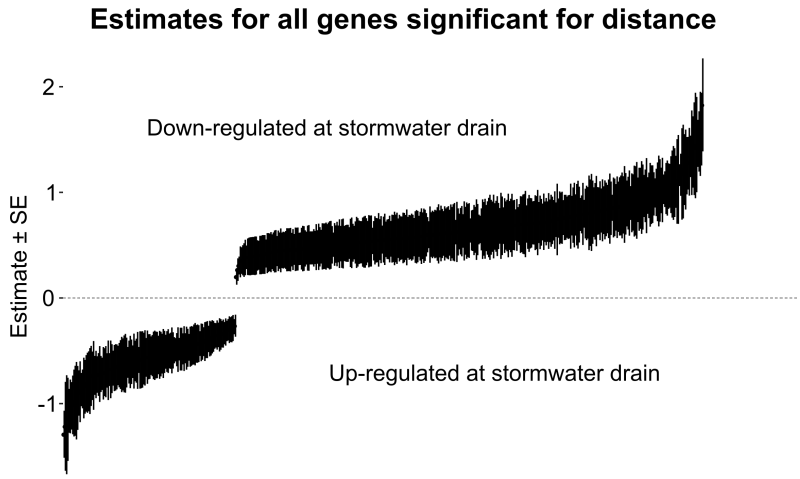

Figure 5.2: All estimates from the linear models of genes that were significantly affected by distance only (after exclusion of all interactions). This plot shows that the majority of genes were down-regulated adjacent to stormwater drains in contrast to reference sites. The estimate is the estimated slope in the linear models. Positive and negative estimates symbolise up- and down-regulation adjacent to stormwater drains, respectively.

metabolism, ribosome, mRNA surveillance pathway, calcium signalling pathway, focal adhesion and tight junction.

All pathways with five or more differentially expressed genes at stormwater drain sites, were sorted into three pathway categories: signalling (Figure 5.3), energy (Figure 5.4), and nutrient pathways (Figure 5.5). In all three pathway categories, the majority of genes were significantly down-regulated at stormwater drains compared to reference sites, with the exception of ribosome genes (Figure 5.4 part 1).

The genes from the nutrient pathways that belong to the core part of the metabolisms (see Figure 5.6) were analysed in more detail, because we knew from our earlier experimental study (Chapter 4) that these genes are significantly affected by organic enrichment. Expression patterns of the methyl genes (*mtaC* and *mcrB*) revealed that the transformation of methanol (CH_3OH) into methane was being down-regulated in sediments close to stormwater drains. For the sulphur metabolism, the genes involved in hydrogen sulphide (H_2S) production (*dsrA*, *dsrB* and *phsA*) were up-regulated, while genes involved in amino acid production from sulphides were down-regulated (*cysK* and *metB*) in these areas. Furthermore, genes involved in sulphate degradation (*PAPSS* and *cysD*) were also down-regulated close to stormwater drains. Proximity to stormwater drains affected three aspects of the nitrogen metabolism, down-regulating *napA* (associated with the transformation of nitrate (NO_3^-) to nitrite (NO_2^-)), as well as the first step of denitrification performed by the gene *nirS* (NO_2^- to nitric oxide (NO)) and the expression of *nosZ* (the degradation

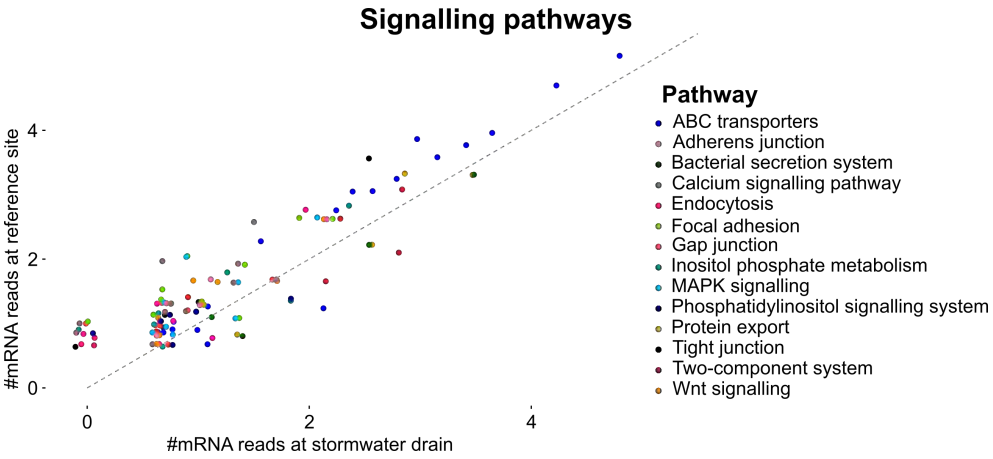

Figure 5.3: Gene expression of all **signalling pathway** genes that were significantly impacted by proximity to stormwater drains. All genes above and below the dotted line are up- and down-regulated adjacent to stormwater drains, respectively. Genes from the same pathway have the same colour, whereas every dot represents one gene.

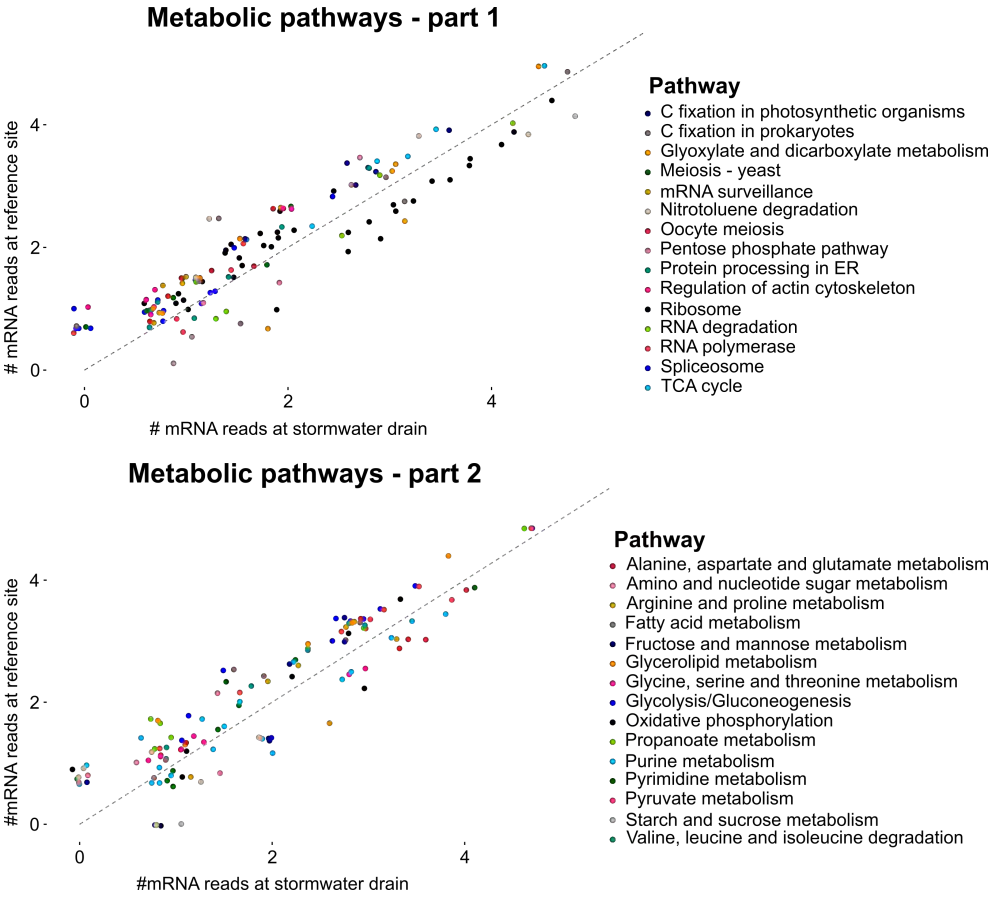

Figure 5.4: Gene expression of all **energy pathway** genes that were significantly impacted by proximity to stormwater drains. All genes above and below the dotted line are up- and down-regulated adjacent to stormwater drains, respectively. Genes from the same pathway have the same colour, whereas every dot represents one gene. Energy pathways were divided into two plots for clarity.

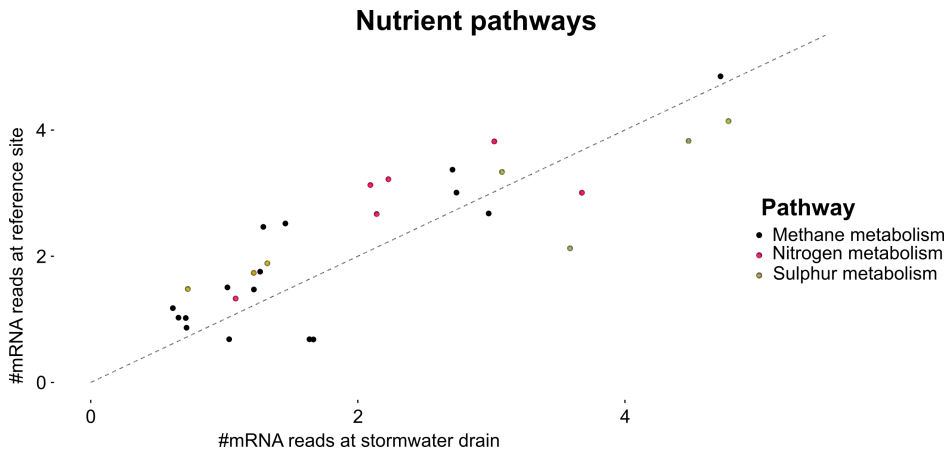

Figure 5.5: Gene expression of all **nutrient pathway**genes that were significantly impacted by proximity to stormwater drains. All genes above and below the dotted line are up- and down-regulated adjacent to stormwater drains, respectively. Genes from the same pathway have the same colour, whereas every dot represents one gene.

of nitrous oxide (N_2O) to dinitrogen gas (N_2)).

Discussion

Urbanised waterways have been historically exposed to multiple stressors. It has been estimated that between 79-87% of priority contaminants in aquatic systems originate from stormwater due to impervious surfaces (Davis and Birch, 2009). Our study is the first to investigate the impact of contaminants associated with stormwater drains on estuarine sediment communities using metatranscriptomics. Sediments adjacent to stormwater drains were more contaminated with metals, and there was some evidence of organic matter input from terrestrial sources (Table 5.1). We discovered that functional genes in sediment communities at stormwater drains had generally down-regulated genes in comparison to reference sites. The exceptions were genes related to hydrogen sulphide (H_2S) gas production that were significantly up-regulated. Moreover, the degradation of nitrous oxide (N_2O) was down-regulated, which could influence the global climate. Also, changes in pathways suggest that more toxic compounds are accumulating in the sediments adjacent to stormwater drains, such as methanol (CH_3OH), nitrate (NO_3^-) and nitrite (NO_2^-). These functional changes could be related to the significantly higher metal concentrations found at stormwater drain sites compared to reference sites and/or the organic enrichment evidence by isotope signals. Our findings highlight significant impacts from legacy stormwater associated contaminants including a decrease in signalling, which would likely result in a loss of community connec-

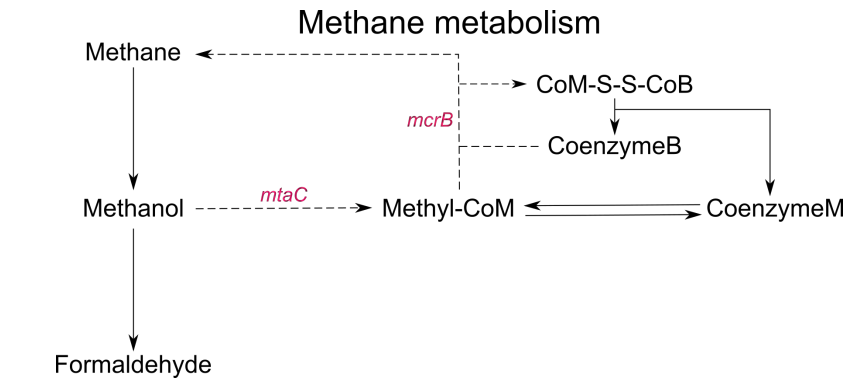

(a)

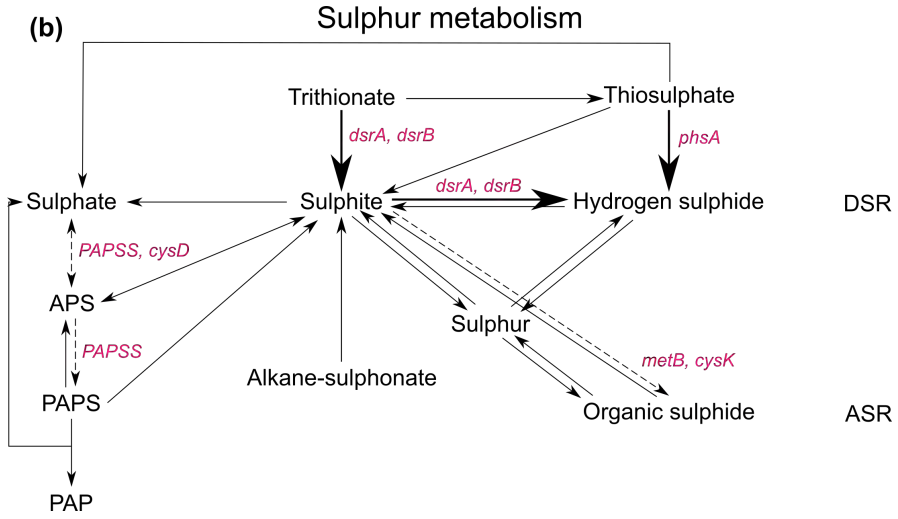

(b)

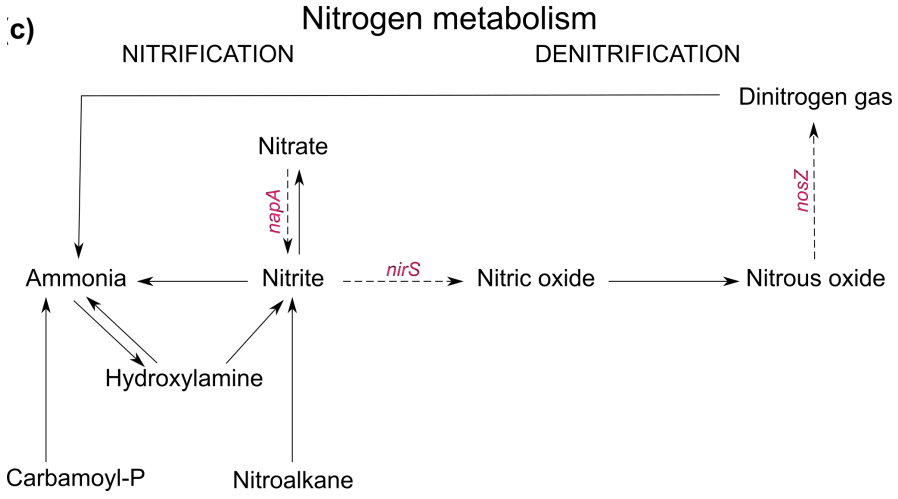

(c)

Figure 5.6: The core part of the three nutrient pathways (of which the gene expression is shown in Figure 5.5): (a) Methane metabolism, (b) Sulphur metabolism, and (c) Nitrogen metabolism. The effects of stormwater on the gene expression of these parts of the pathways are shown and the gene names of the significantly altered genes are shown in pink. Thicker and dotted arrows symbolise a up- and down-regulation of the gene adjacent to stormwater drains, respectively.

tivity which may decrease the remediation capacity and efficiency of ecosystem functions. In addition, lower energetic activity and nutrient metabolism may lead to a decrease in ecosystem productivity and nutrient cycling. This study emphasises the need to include functional responses in assessments of ecosystem change if we are to better understand and predict the consequences of multiple stressors.

Sediment communities adjacent to stormwater drains displayed a general down-regulation of genes involved in signalling pathways, possibly due to highly toxic metal concentrations. Microbes respond to biological and chemical information (Westerhoff et al., 2014), and the responses of other organisms in the same community (Ross-Gillespie and Kümmerli, 2014). We suggest that lower expression rates in signalling pathways is a signal of community fracturing, which has previously been observed in contaminant exposed biofilm communities (Lawes et al., 2016b). The fracturing of a community and the impairment of communication may lead to poor functioning for processes that include multiple sequential steps such as toxicant remediation. Microbial communities are well known for their potential to break down contaminants and remediate contaminated systems (Wiatrowski and Barkay, 2005; Antizar-Ladislao, 2010; Das and Chandran, 2011; Mason et al., 2014). However, it seems that sediment communities subject to high concentrations of contamination might suffer a reduced capacity for contaminant breakdown. This could potentially result in a further build-up of contaminants from stormwater drains over time. This has potentially serious consequences for the ecosystem itself and for the public health of those exposed to such sediments and waters (e.g. Zhang et al., 2010; Glibert et al., 2014). In addition, a breakdown in signalling and communication within this community can potentially result in lower metabolic rates and lower rates of biogeochemical cycling.

Energy pathways, such as primary production, are known to be negatively affected by contamination (Johnston et al., 2015b); whether this is through a breakdown in signalling or a direct effect of contamination is yet unknown. In our study, energy pathways were predominantly expressed at lower rates in heavily contaminated sediments than at the reference sites. The toxicity of the metals may explain the lower energy pathway rates. Spliceosomes are responsible for transforming the pre-mRNA into mRNA for protein transcription (Wahl et al., 2009). Spliceosome genes were invariably down-regulated at stormwater drains, which suggests a lower rate of protein synthesis and energetic activity. Furthermore, RNA degradation genes were mainly up-regulated at poorly flushed sites. RNA degradation does not only play a role in the recycling of nucleases from mRNA molecules no longer needed,

but is also known to play an important role in controlling gene expression (Condon, 2007). That is, up-regulated RNA degradation can prevent protein synthesis coded by mRNA molecules. These results suggest that in addition to a directly decreased general energetic activity of the sediment microbial community, the increased RNA degradation may further lead to an indirect decrease in general activity in proximity to stormwater drains. From the energy pathways, only the ribosome proteins were partially up-regulated. All but one up-regulated ribosomal protein are bacterial/archaeal, while all but one down-regulated ribosomal protein belong to eukaryotes. The activity of ribosomal proteins has been proposed as a measure of cellular growth rates (Gifford et al., 2013); hence, the up-regulation of ribosomal proteins suggests enhanced bacterial/archaeal growth rates.

Carbon fixation rates by both photosynthetic and prokaryotic organisms in heavily contaminated sediments were significantly decreased in comparison to reference sites. Stable isotope studies have revealed that some microbes, such as diatoms, decrease their carbon fixation rates when exposed to toxins (Torres et al., 2000). This was contrary to the hypothesis that algae increase their photosynthesis rate upon contamination in order to increase the energy for detoxification (Rachlin et al., 1982). More recently, aquifer microbial communities have shown low carbon fixation rates, despite a high prevalence of genes involved in carbon fixation (Kellermann et al., 2012). Lower carbon fixation rates result in lower uptake of inorganic carbon in the form of CO_2. This fixed carbon would then be transformed into organic carbon, which in turn is available to heterotrophic organisms (Hügler and Sievert, 2011). Reduced carbon fixation rates can therefore result in lower biomass and productivity, which can affect higher trophic levels and potentially lead to lower ecosystem service rates. Furthermore, microbial carbon fixation provides a biological sink of anthropogenic CO_2 (Zhao and Su, 2014). Hence lower carbon fixation due to contamination may have serious implications for the global climate.

Analyses of the core parts of the affected nutrient metabolisms revealed that the degradation of methanol (CH_3OH) to methane (CH_4) was reduced in poorly flushed sediments, along with a decrease in sulphate (SO_4^{2-}) reduction. Sediments with high organic matter input are often anoxic, which means that the sediment community will use an alternative electron acceptor to O_2. NO_3^- is highly prevalent in stormwater (Collins et al., 2010) and is the preferred electron acceptor to SO_4^{2-} and CH_4 under anoxic conditions (Capone and Kiene, 1988). Therefore, a down-regulation of SO_4^{2-} and CH_4 transformation genes could be due to the saturation of the system with NO_3^-. Moreover, in the sulphur metabolism the production of H_2S was enhanced in areas close to

stormwater drains, while the use of sulphides for amino acid production was decreased. This suggests a shift from assimilatory sulphate reduction (ASR) to dissimilatory sulphate reduction (DSR), which results in lower production of amino acids and the accumulation of H_2S in the sediments, as we have observed in experimentally enriched sediments (Chapter 3). H_2S is not only highly toxic, but also a potent greenhouse gas (Kump et al., 2005). Thus, our sulphur metabolism findings show that sediments with high concentrations of legacy contaminants have possibly lowered metabolic rates due to lower production of amino acids, and have the potential to contribute to climate change. Further, nitrogen metabolism was significantly affected in sediments adjacent to stormwater drains. Lower transformation of NO_3^- to NO_2^- suggests an accumulation of the highly toxic NO_3^- in the system. The first step of denitrification was down-regulated, potentially leading to an accumulation of NO_2^- in the system, which is also highly toxic and can in turn result in decreased community productivity. N_2O transformation to dinitrogen gas (N_2) was performed at lower rates in poorly flushed sites compared to reference sites. This last step of the nitrogen cycle is the one that yields the least amount of energy (Zumft, 1997), and has been shown to be down-regulated in organically enriched systems (see Chapter 3). Furthermore, H_2S inhibits this last step of the nitrogen cycle (Brunet and Garcia-Gil, 1996). This likely results in an accumulation of N_2O in the system, which is a gas and therefore may eventually escape into the water column and possibly to the atmosphere. N_2O is a highly potent greenhouse gas – about 300 times as potent as a CO_2 molecule (Schreiber et al., 2012).

Conclusions

Microbial community functioning was markedly different in close proximity to stormwater drains, where sediments were contaminated with metals and organically enriched. Sediment communities at stormwater drains had generally down-regulated genes in comparison to reference sites. This phenomenon has recently been observed in contaminated groundwater microbe communities, where biogeochemical cycling was minimised (Hemme et al., 2015). The lower energetic activity in contaminated sediments can potentially lead to lower productivity of the ecosystem as a whole. Furthermore, a lower signalling activity of the microbial cells suggests a fracturing of the sediment community that may result in lower remediation capacities. Changed expression patterns implied an increased production of toxic compounds and greenhouse gases htat would not only impact estuarine ecosystems, but also climate regulating processes.

We successfully applied metatranscriptomics, to provide a holistic understanding of all genes and all cycles in a community exposed to chemical stress. Direct measures of functional responses (e.g. chemical flux rates) would not have provided this amount of detail, as the mechanisms behind altered fluxes remain unknown. Here, we measured functional changes in dry conditions; the crucial next step will be to investigate the impact of a heavy rainfall event in these poorly flushed areas. In addition, analysing the rRNA data (which was removed for the functional analysis described here) could provide insight into the community structure changes due to stormwater impact. Information on structural changes would provide further understanding of the functional changes; e.g. are altered functions a direct consequence of structural shifts or do they result from shifts in gene transcription? Such an analysis was beyond the remit of this chapter but will be undertaken as an additional study. This study highlights the need to remediate heavily contaminated sediments and prevent additional contaminant inputs from stormwater in order to counteract negative ecological consequences. Ecosystems particularly at risk are those in shallow, low flow areas of urbanised estuaries where there is the potential for high retention of contaminants. Such locations should therefore be a priority for management and remediation activity.

6 Summary

In this thesis, I measured altered ecosystem process rates in an estuarine sediment community following exposure to multiple anthropogenic stressors, and simultaneously evaluated the application of next-generation sequencing methods for biomonitoring. Specifically, I investigated the structural and functional responses of microbial communities to two of the most common contaminants classes in urbanised systems: Metals and organic matter (Jiang et al., 2001). Sediment microbial communities responded to excess organic enrichment by altering gene expression rates in a number of key biogeochemical pathways. The impact of metals was more subtle, changing the expression of a smaller number of genes and community changes could be masked by the shifts driven by organic enrichment. The observed changes in gene expression might results in the increased production of toxic compounds and greenhouse gases in contaminated sediments. My results reveal that bacterial communities are more sensitive to anthropogenic stressors than eukaryotes and may therefore be a better indicator of impacted communities in biomonitoring approaches. Functional responses to stressors as measured by changes in mRNA gene expression were also more obvious than structural shifts as measured by rRNA gene expression. Metatranscriptomics, as a tool that can measure both structure and function, opens up opportunities for more holistic ecosystem biomonitoring. Metatranscriptomics measures were reliable across replicates, and this technique was successfully applied to experimental and survey settings. The use of 'big data' from modern molecular techniques relies on information from an increased number of receptors and is predictably more sensitive to changes following stressor exposures. However, to make the most of this information source, genetic reference libraries should be expanded to include more ecologically relevant gene annotations.

Sediment microbial community responses to multiple contaminants

One of the main foci of this thesis was to measure the impact of multiple contaminants on estuarine sediment microbial communities. In Chapter 2, I

manipulated the metal content and organic enrichment of sediments in field-based mesocosms to mimic common press stressors in urbanised estuaries. Using these field-based mesocosms, I tested the applicability of amplicon sequencing (16S and 18S) to investigate community shifts in response to multiple stressors. And I compared the responsiveness of bacterial and eukaryotic communities, as well as the active (RNA) and total (DNA) component of each community. Bacteria were generally more sensitive to the applied stressors than eukaryotes. The active part of the eukaryotic community did not shift in response to press metal contamination. However, the shift in the total community shows that the eukaryotes also responded to initial metal contamination, but were able to recover within the time frame of the experiment (17 weeks). I also found that press organic enrichment masked the impact of metals on the sediment communities. The potential for excess organic enrichment to mask the toxic effects of metals may be related to the binding capacity of metal ions to organic matter (e.g. Benedetti et al., 1996; McIntyre and Guéguen, 2013). The binding of metals to organic matter can increase the metal uptake in some species that are known to collect organic matter (Bundschuh and Mckie, 2015), however, this binding generally decreases the bioavailability of metals to most organisms (Aiken et al., 2011). From this phenomenon, suggestions have arisen to combat metal contamination with the addition of organic matter to the affected system (e.g. Taylor et al., 2016). My results will add to our ability to predict the impact of cumulative stressors (Halpern et al., 2008), however, I would hesitate to recommend remedial organic enrichment given the substantial direct impacts of organics that I observed.

In addition to press contamination (added at the beginning of the experiment), I exposed sediment communities to a pulse of organic matter to mimic what might be delivered through run-off after a major precipitation event (Göbel et al., 2007). Sediment communities were generally able to quickly recover from the pulsed enrichment. However, I found some evidence for a response of specific taxa and a decrease in abundant operational taxonomic units (OTUs). The five week interval between exposure and sampling appears to have allowed for sufficient recovery of the general community. A full recovery within a few weeks has been observed in river biofilm communities exposed to a toxic pulse (Proia et al., 2011), and marine serpulids were able to recover from copper pulses within a only few weeks (Johnston et al., 2002). In the real world, however, recovery will depend on the frequency of contaminant or enrichment pulses, and the frequency of intense rainfall events is predicted to increase with climate change (Trenberth, 1998). Occurring at high frequencies, pulse events may result in the same effect as press stressors resulting in a sig-

nificant impact on sediment communities (Johnston and Keough, 2002). The impact of regular pulse events can be seen in Chapter 5, which includes the sediment microbial responses to legacy contaminants from urban stormwater inputs. The regular input of stormwater is most likely one of the pulse stressors that occurs at high frequencies, thus resulting in the accumulation of stressors in the sediments, and therefore having a lasting effect on community structure and function.

In order to investigate the functional responses of sediment communities to metal contamination and press organic enrichment, I used a subsample of the sediments from the field-based experiment, and applied metatranscriptomic sequencing to these samples (Chapter 3). Again, the effect of organic enrichment was more pronounced than the effect of metal contamination. Generally, genes that were affected by combined metal contamination and enrichment were down-regulated, i.e. expressed in lower numbers, compared to the controls. Most of the affected genes were associated with signalling and energy pathways. Signalling is crucial for the communication between microbes which enables them to live as a community (Watnick and Kolter, 2000; Shank and Kolter, 2009) and respond to cues from their environment and other organisms living within it (Westerhoff et al., 2014; Ross-Gillespie and Kümmerli, 2014). Down-regulation in signalling genes is likely to disrupt communication and thus the connectivity within the sediment community. This could lead to community fracturing, as recently observed in marine biofilms (Lawes et al., 2016b), and could potentially decrease the remediation capacity of the affected community. Decreased remediation would result in accumulation of contaminants, which would increase the contaminant concentrations and thus exacerbate impacts on communities associated with the sediment. Chapter 3 also revealed that community functions are more sensitive to multiple stressors than community structure. Functional genes responded significantly to metals and enrichment, while community structure was only affected by enrichment. This provides another line of evidence that supports the integration of functional parameters in impact assessments (Baird et al., 2011; Van den Brink et al., 2013; de Juan et al., 2014; Johnston et al., 2015b; van der Linden et al., 2016).

To show the potential of metatranscriptomics as a means of providing detailed information on specific genes/pathways, I analysed the gene expression of climate relevant pathways (using the data from Chapter 3) in detail. Specifically, Chapter 4 was focused on the following pathways: nitrogen, sulphur, methane, and carbon metabolisms. The nitrogen and sulphur pathways were significantly impacted by organic enrichment. Metal contamination only

affected the gene expression when applied in combination with organic enrichment, where it exacerbated the enrichment effects. This suggests that the addition of organic matter to metal contaminated communities for mitigation purposes of toxic metal effects (Taylor et al., 2016) or stimulation of bioremediation of persistent organic pollutants (Xu et al., 2014), would have serious unforeseeable side-effects. This highlights the need for better understanding of the dynamics of multiple stressors to inform proper management decisions.

Changes in sulphur-associated gene expression resulted in a shift from the assimilatory sulphate reduction (ASR) to dissimilatory sulphate reduction (DSR), which results in the production of hydrogen sulphide (H_2S). H_2S is a highly toxic gas and also acts as a greenhouse gas through its capacity to deplete ozone (Kump et al., 2005). Further, changes in the nitrogen metabolism led to an accumulation of highly toxic ammonia/ammonium and of nitrous oxide (N_2O), one of the most potent greenhouse gases (Schreiber et al., 2012). This chapter highlights the importance of sediment functions on a global level, and the global consequences of localised contamination.

After having established the applicability of metatranscriptomics under controlled experimental conditions, I used this technique in a survey in Chapter 5 to investigate the impact of legacy contaminants on sediment communities at poorly flushed sites in Sydney Harbour, NSW, Australia. The contaminated sediments were located at the end of embayments adjacent to major stormwater drains and reference sediments were located 1km away, within the same embayment. Distance from the stormwater drain mainly drove the observable community changes, and was detectable over and above natural spatial and temporal variability. This shows that pulse stressors, such as stormwater input, can lead to an accumulation of contaminants when applied frequently and in poorly flushed systems. As in contaminated sediments explored in Chapter 3, the majority of differentially expressed genes were down-regulated in sediments adjacent to stormwater drains in comparison to reference sites. The affected pathways in the survey were similar to the affected pathways in the experiment. This result validates the relevance of my experimental manipulation to the real world, and also suggests the relevant contaminants impacting the sediment community in embayments are metals and organic matter. I observed similar changes to the nitrogen and sulphur metabolisms as in Chapter 4; I found the potential for accumulation of toxic compounds and greenhouse gases. Based on the experiment in Chapters 3 and 4 and the similarity of results, it is very likely that organic enrichment is the major driver of changes to energy metabolisms within contaminated sediments.

Molecular biomonitoring tools

In Chapter 2, I investigated the best application of amplicon sequencing (16S and 18S) as a biomonitoring tool. Contaminant effects were more distinct in the total communities (DNA) as opposed to the active component (RNA). This is likely due to the extremely short half-life of RNA of seconds to minutes (Carvalhais et al., 2012; Moran et al., 2013) and the persistence of DNA from dead organisms in sediments for up to two months (Nielsen et al., 2007). Due to the robustness of DNA, the handling of the samples is much easier. In addition, DNA extractions are less costly and much faster than RNA extractions (personal observation). Therefore, I recommend using bacterial (16S) DNA for large biomonitoring studies. However, the viability of extracellular DNA in sediments demands careful interpretation of the data. While extracellular DNA can be used to detect recent impacts of a contaminant on a sediment community, it can also originate from external sources, such as the contaminant itself or rainwater. In the experiment, I was able to exclude the possibility of the DNA coming from the sediment itself or from the added fertiliser, because I ran the experiment over 17 weeks, by which time the extracellular DNA from external sources would have degraded.

Amplicon sequencing, however, does not include any functional measures, which I showed to be more sensitive to multiple stressors (Chapters 3 and 5). To my knowledge, the study I presented in Chapter 3 is the first study to validate metatranscriptomics as a tool for ecosystem health assessment. I showed that metatranscriptomics is a sensitive tool for impact assessment and generates ecologically relevant data. I also demonstrated that metatranscriptomics is repeatable, with low variability across replicates, and generates reproducible results from experimental and survey studies. Although metatranscriptomics has not previously been discussed or validated as a tool for biomonitoring, it has been successfully used in a variety of systems (Penn et al., 2014; Gifford et al., 2011; Hilton et al., 2015; Hultman et al., 2015; Urich et al., 2014; Thureborn et al., 2016) and organisms (Turner et al., 2013; Franzosa et al., 2014), thus validating the applicability of this technique across ecosystems. Although this remains an expensive technique (∼AUD 1,000.- per sample), metatranscriptomics is likely to be more economic than common approaches if the amount of data and sensitivity are considered. With regards to time-effectiveness, the extractions and preparation for sequencing are a matter of days, and the sequencing itself usually takes less than a day (personal observations). Therefore, with good access to a sequencing facility, metatranscriptomics is likely orders of magnitude faster than conventional taxonomic

identification in generating data. As mechanisms for the rapid interpretation of data and access to bioinformatics support and high computing power increase, this is likely to become an increasingly desirable approach to biomonitoring.

Metatranscriptomics provides detailed information on gene expression, which is directly related to ecosystem process rates (Morales et al., 2010; Philippot et al., 2011; Harter et al., 2014). However, the translation of gene expression into actual gas fluxes is problematic (Bowen et al., 2014). In Chapter 4, I not only measured gene expression but also used incubation chambers to measure direct gas and nutrient fluxes out of the sediment. This flux data was very useful for the interpretation of the changes in gene expression. For example, the significantly increased NO_x influx into enriched sediments confirmed the source of all the nitrite/nitrate that is transformed into ammonia/ammonium through dissimilatory nitrate reduction to ammonium (DNRA). Together, these techniques simultaneously revealed the functional output of a system and the mechanisms behind these measurable changes.

Future directions

The analysis and interpretation of 'big data' poses a great many challenges. New multivariate statistics and statistical programs that can handle very large datasets will be crucial in the advancement of molecular techniques and the application of these to biomonitoring. Moreover, the improvement of reference libraries is critical to the correct annotation of sequences. Although there are numerous reference libraries available, they are far from complete. Many ecologically relevant genes are yet to be annotated. Environmental studies have found that over two thirds of the sequences did not have matches to annotated reference libraries (Moran, 2009). In addition, many genetic databases are biased towards results from medical research (personal observation). Hence it is not uncommon to find an annotation of a cancer-related gene in sediment samples, so the annotation of genes today has to be treated with caution. The improvement of the confidence of gene annotations will enable easier interpretation of large environmental datasets. Microbial culture-dependent research will likely be indispensable to the advancement of such reference libraries (Zimmerman et al., 2014). However, the growing body of culture-independent omics research will also contribute to the improvement of gene annotations.

In order to use next-generation sequencing approaches for biomonitoring purposes, our understanding of the relationships between community structure and function, and between gene expression and biogeochemical flux rates must improve. In both my experimental and survey approaches, I observed

that most differentially expressed genes were down-regulated in response to contaminants, and the majority of these genes were associated with signalling pathways. In addition, I observed sign of community fracturing which has recently been noted as a consequence of contamination in marine biofilms (Lawes et al., 2016b). Metatranscriptomic analyses may provide the mechanism behind this loss of connectivity in the form of reduced signalling activity. It may therefore be useful to combine the metatranscriptomics results in Chapter 5 with a community network analysis, as has been done in Lawes et al. (2016b) and Sun (2016, Chapter 2). I predict that within the next few years of metaomics research, we will witness the application of many new combinations of analyses and statistical tests to environmental datasets and this will help embed modern molecular techniques as a standard tool in ecological research.

Final remarks

This thesis advances our understanding of the impacts of multiple contaminants on sediment microbial communities using modern molecular techniques. The concurrence of results from a manipulative experiment and a field survey demonstrated that altered gene expression in contaminated sediments generally results in lower activity of the affected genes. Most of the down-regulated genes were associated with energy and signalling metabolisms. The impact on the signalling metabolism may lead to a loss of community connectivity and potentially lower remediation capacity, and the changes in energy metabolisms may lead to significant impacts on the climate through increased production of greenhouse gases. I was able to show that the functions of estuarine sediment communities are critical to the entire ecosystem and can have repercussions on a global level, as they involve ecosystem processes relevant to the climate. Furthermore, this thesis revealed that bacteria and functional measures are more sensitive to multiple stressors than eukaryotes and community composition, respectively. Bacterial functions may therefore be the more appropriate indicator of anthropogenic contamination. Using field experiment and survey data, I demonstrated the applicability of metatranscriptomics as a tool for biomonitoring. Despite many challenges posed by this modern technique, metatranscriptomics has the potential to revolutionise ecosystem health assessment by providing ecologically relevant data and unmasking the mechanisms behind changes to community function.

A

Appendix - Chapter 2

Table A.1: Sequencing information per sample. Sample names are according to Table 2.1. The numbers in the sample name stand for the replicate number. Where there are NAs, the samples could not be amplified and therefore were not sequenced. '# post QC' represents the number of sequences that passed all quality filtering steps (up to removing of chimeric sequences). These are the number of sequences that were clustered into operational taxonomic units (OTUs) and classified.

	16S DNA		16S RNA		18S DNA		18S RNA	
Sample	#raw reads	# post QC	#raw reads	# post QC	#raw reads	# post QC	#raw reads	# post QC
C/C/C-1	248518	90509	222101	16028	97653	14276	133940	23342
C/C/C-2	191756	13399	270165	23798	149043	20503	152807	27591
C/C/C-3	189894	13015	446062	29906	119383	15811	145249	25187
C/C/D-1	520693	30847	165622	11454	145012	20875	119994	24149
C/C/D-2	245401	17822	156498	10669	122341	16210	131773	23922
C/C/D-3	218072	16476	141912	10948	112876	19721	107141	22528
C/H/C-1	210697	17011	204257	14430	131341	17739	133217	20414

continued on next page

Table A.1 – continued from previous page

	16S DNA		16S RNA		18S DNA		18S RNA	
Sample	#raw reads	# post QC	#raw reads	# post QC	#raw reads	# post QC	#raw reads	# post QC
C/H/C-2	163515	14267	212801	14211	119073	16210	152351	24630
C/H/C-3	79248	7592	260295	20087	106760	15223	150640	24338
C/H/D-1	175426	14198	241674	16731	103261	16139	101972	16591
C/H/D-2	413066	28876	190448	13965	121614	17796	132483	22580
C/H/D-3	172605	13009	160087	10762	60449	5149	85001	9255
C/L/C-1	241096	16673	176618	12789	153023	20106	165366	25855
C/L/C-2	185943	15835	209573	15568	121708	16786	156369	23322
C/L/C-3	183097	14284	237362	17479	146655	21868	114581	27385
C/L/D-1	202500	15827	164691	11520	138192	17495	149954	22593
C/L/D-2	NA	NA	219998	15309	122680	19250	114581	22411
C/L/D-3	182580	14945	211172	14857	115407	19722	185710	32448
H/C/C-1	313786	21169	307016	20008	128894	22625	152199	29027
H/C/C-2	NA	NA	199268	14001	107441	14149	86397	17428
H/C/C-3	199099	14383	168712	11846	70001	10671	155164	30220
H/C/D-1	207944	16301	208583	14518	69085	9225	122721	24312
H/C/D-2	258960	17129	704946	37406	128598	20146	130910	27222
H/C/D-3	237541	15991	211458	14998	83812	13817	99348	19463

continued on next page

Table A.1 – continued from previous page

	16S DNA		16S RNA		18S DNA		18S RNA	
Sample	#raw reads	# post QC	#raw reads	# post QC	#raw reads	# post QC	#raw reads	# post QC
H/H/C-1	425437	29863	484397	30167	71982	9272	88843	15286
H/H/C-2	192541	15780	241812	17737	77503	9033	66773	11439
H/H/C-3	230175	18646	886514	46463	100444	16571	121506	24234
H/H/D-1	224483	16453	443784	25773	90822	11821	123197	17122
H/H/D-2	246396	19048	164841	12174	44594	6250	51798	7365
H/H/D-3	304469	21807	231730	16064	113373	16842	116339	19239
H/L/C-1	233686	20767	197940	14139	117693	18649	192869	32073
H/L/C-2	231462	20439	196295	15120	58661	6626	59296	6997
H/L/C-3	150501	12490	144955	11760	101103	14931	131782	22961
H/L/D-1	224537	25339	167889	12237	81471	11551	153959	25522
H/L/D-2	169493	15634	192195	14299	91970	14195	115644	21087
H/L/D-3	186020	14397	294763	21194	124176	17617	NA	NA
M/C/C-1	213881	15696	261099	17203	115758	17711	131567	24636
M/C/C-2	227949	15830	173847	12726	133855	19529	144215	26741
M/C/C-3	185394	17060	314541	22557	103935	15882	178025	33587
M/C/D-1	143934	10945	213668	16030	159092	21800	77392	15868
M/C/D-2	473256	29482	203891	14725	76146	11651	74700	12575

continued on next page

Table A.1 – continued from previous page

	16S DNA		16S RNA		18S DNA		18S RNA	
Sample	#raw reads	# post QC	#raw reads	# post QC	#raw reads	# post QC	#raw reads	# post QC
M/C/D-3	195945	14885	200166	14547	137522	21570	133341	24899
M/H/C-1	399899	28177	204606	14610	83627	9614	17932	2634
M/H/C-2	664100	40958	197574	15251	111468	16052	103893	17706
M/H/C-3	129125	11288	323486	24140	101823	14470	140748	22990
M/H/D-1	217877	16510	187736	13226	100222	14116	139279	21285
M/H/D-2	248521	18618	336665	21779	100874	15726	132991	23865
M/H/D-3	210598	16290	183129	13013	114549	18730	123434	23152
M/L/C-1	320408	19221	145159	10659	141181	17981	125475	20209
M/L/C-2	217017	17279	215927	15718	115449	16573	135878	19841
M/L/C-3	225871	16351	282096	20993	122694	15747	213133	33286
M/L/D-1	190136	14870	168531	12001	168446	22598	126866	21114
M/L/D-2	206942	15745	164872	11638	119895	15831	91710	15924
M/L/D-3	238990	19276	208120	15081	128443	18590	109639	20513
VH/C/C-1	307884	19987	332825	21102	90596	15246	75926	16694
VH/C/C-2	271417	20092	168520	12206	93050	15500	84722	15189
VH/C/C-3	152726	11229	263420	14819	150863	21418	125920	24487
VH/C/D-1	216497	15953	251871	17372	82976	12163	148829	23541

continued on next page

Table A.1 – continued from previous page

	16S DNA		16S RNA		18S DNA		18S RNA	
Sample	#raw reads	# post QC	#raw reads	# post QC	#raw reads	# post QC	#raw reads	# post QC
VH/C/D-2	278549	19090	233787	16516	113027	19495	144777	28460
VH/C/D-3	269779	18563	269329	18879	28642	4820	60186	13347
VH/H/C-1	205897	16382	232525	16852	117862	16789	NA	NA
VH/H/C-2	195902	14817	206740	12713	97325	13061	124468	18104
VH/H/C-3	175794	14202	153416	11024	89769	13210	128664	20025
VH/H/D-1	234788	18993	209989	14538	101632	12511	75518	9967
VH/H/D-2	210693	16563	147960	10011	108487	16340	117397	21666
VH/H/D-3	311165	20478	285219	18914	108812	18570	86212	17104
VH/L/C-1	354049	25203	282177	23070	86073	14368	158045	26277
VH/L/C-2	207872	15260	254687	16862	126950	17781	110043	19835
VH/L/C-3	162250	13081	213030	15851	120048	18220	155275	27324
VH/L/D-1	244930	19130	295777	19985	96872	15884	114570	18560
VH/L/D-2	281485	22133	245387	16934	130251	17269	114313	21275
VH/L/D-3	220448	16424	257095	18226	115976	18649	73472	14453

Table A.2: Operational taxonomic unit (OTU) information per sample. Sample names are according to Table 2.1. The numbers in the sample name stand for the replicate number. Where there are NAs, the samples could not be amplified and therefore were not sequenced.

Sample	16S DNA #OTUs	16S RNA #OTUs	18S DNA #OTUs	18S RNA #OTUs
C/C/C-1	5043	5344	3373	5105
C/C/C-2	4448	7884	4751	5845
C/C/C-3	3852	7430	3397	4297
C/C/D-1	7274	4296	4677	5640
C/C/D-2	5072	3733	3488	4329
C/C/D-3	4702	4301	4219	5047
C/H/C-1	3960	3800	3705	3973
C/H/C-2	3339	4068	3475	4690
C/H/C-3	2279	4431	3175	4236
C/H/D-1	4239	5259	3408	3824
C/H/D-2	5677	3765	3464	3861
C/H/D-3	3804	3252	988	1776
C/L/C-1	4096	3312	3831	4738
C/L/C-2	3993	4289	3344	3695
C/L/C-3	4162	4644	4633	4886
C/L/D-1	4137	3335	3400	4371
C/L/D-2	NA	4292	3982	4240
C/L/D-3	4672	5059	4363	6324
H/C/C-1	5727	6288	4977	5653
H/C/C-2	NA	4361	3399	4111
H/C/C-3	4373	4245	2635	5988
H/C/D-1	5022	4907	2383	5256
H/C/D-2	5324	10145	4802	5151
H/C/D-3	4339	4657	3165	4460
H/H/C-1	5878	6162	1988	2938
H/H/C-2	3791	4489	1891	2590
H/H/C-3	5030	9522	3918	4620
H/H/D-1	4332	5407	2568	3409
H/H/D-2	5003	3195	1359	1544
H/H/D-3	5240	4289	3512	3817
H/L/C-1	4829	3731	3912	5531

continued on next page

Table A.2 – continued from previous page

Sample	16S DNA #OTUs	16S RNA #OTUs	18S DNA #OTUs	18S RNA #OTUs
H/L/C-2	5355	4407	1474	1638
H/L/C-3	3405	3212	3142	4070
H/L/D-1	5913	3425	2538	4687
H/L/D-2	4206	4033	3086	3588
H/L/D-3	4153	5398	3498	NA
M/C/C-1	4366	5826	3983	5262
M/C/C-2	4274	4409	4260	5659
M/C/C-3	5281	6966	3115	6758
M/C/D-1	3625	5203	4589	3884
M/C/D-2	7112	5155	2864	2738
M/C/D-3	4499	4953	4604	5377
M/H/C-1	5515	3793	2001	651
M/H/C-2	6541	3663	3233	3577
M/H/C-3	3046	4926	2829	3572
M/H/D-1	4092	3428	3078	3800
M/H/D-2	4943	5398	3481	4139
M/H/D-3	4561	4101	4228	4749
M/L/C-1	4893	3159	3735	3880
M/L/C-2	4475	4425	3550	4038
M/L/C-3	4086	4595	3278	5603
M/L/D-1	4012	3867	4950	4640
M/L/D-2	4283	3464	3216	3170
M/L/D-3	3983	3687	3822	4145
VH/C/C-1	5670	7022	3865	4286
VH/C/C-2	5064	4167	3597	3665
VH/C/C-3	3691	4984	4822	4809
VH/C/D-1	4196	5060	2569	4419
VH/C/D-2	5619	5837	4664	5623
VH/C/D-3	5240	6155	1241	3683
VH/H/C-1	3921	4502	3587	NA
VH/H/C-2	3371	3198	2809	3111
VH/H/C-3	3789	3442	2979	3325
VH/H/D-1	4615	4135	2693	1971
VH/H/D-2	4099	2959	3614	4099

continued on next page

Table A.2 – continued from previous page

Sample	16S DNA #OTUs	16S RNA #OTUs	18S DNA #OTUs	18S RNA #OTUs
VH/H/D-3	5719	5893	4166	3878
VH/L/C-1	5480	5767	3399	4725
VH/L/C-2	4205	4991	4087	4574
VH/L/C-3	3878	4901	4162	4904
VH/L/D-1	4630	5004	3430	3709
VH/L/D-2	5886	4845	3804	3972
VH/L/D-3	4968	5967	4151	3378

Table A.3: R output of the *adonis* (permutational multivariate analysis of variance) results for all four datasets (16S DNA, 16S RNA, 18S DNA, and 18S RNA). Significant *p*-values are highlighted in bold. A significance level of α=0.05 was applied.

		Df	SumsOfSqs	MeanSqs	F.Model	R2	Pr(>F)
16S DNA	metals	3	0.1160	0.0387	1.7758	0.0621	**0.0004**
	nutrients	2	0.3418	0.1709	7.8483	0.1830	**0.0001**
	dosing	1	0.0253	0.0253	1.1623	0.0136	0.1770
	metals:nutrients	6	0.1472	0.0245	1.1265	0.0788	0.1185
	metals:dosing	3	0.0633	0.0211	0.9683	0.0339	0.5092
	nutrients:dosing	2	0.0425	0.0212	0.9755	0.0228	0.4647
	metals:nutrients:dosing	6	0.1297	0.0216	0.9929	0.0695	0.4712
	Residuals	46	1.0016	0.0218	0.5364		
	Total	69	1.8673	1			
16S RNA	metals	3	0.2734	0.0911	1.5048	0.0514	**0.0098**
	nutrients	2	1.0056	0.5028	8.3021	0.1890	**0.0001**
	dosing	1	0.0722	0.0722	1.1928	0.0136	0.1563
	metals:nutrients	6	0.4076	0.0679	1.1217	0.0766	0.1315
	metals:dosing	3	0.1692	0.0564	0.9313	0.0318	0.6233
	nutrients:dosing	2	0.1207	0.0603	0.9963	0.0227	0.3959
	metals:nutrients:dosing	6	0.3647	0.0608	1.0035	0.0685	0.4286

continued on next page

Table A.3 – continued from previous page

		Df	SumsOfSqs	MeanSqs	F.Model	R2	Pr(>F)
	Residuals	48	2.9072	0.0606	0.5464		
	Total	71	5.3207	1			
18S DNA	metals	3	0.1685	0.0562	1.2588	0.0472	**0.0252**
	nutrients	2	0.4705	0.2353	5.2708	0.1317	**0.0001**
	dosing	1	0.0536	0.0536	1.2001	0.0150	0.1210
	metals:nutrients	6	0.2712	0.0452	1.0127	0.0759	0.3880
	metals:dosing	3	0.1273	0.0424	0.9509	0.0356	0.6194
	nutrients:dosing	2	0.0826	0.0413	0.9256	0.0231	0.6767
	metals:nutrients:dosing	6	0.2560	0.0427	0.9561	0.0717	0.6761
	Residuals	48	2.1424	0.0446	0.5997		
	Total	71	3.5722	1			
18S RNA	metals	3	0.1615	0.0538	1.0344	0.0396	0.3254
	nutrients	2	0.6252	0.3126	6.0076	0.1535	**0.0001**
	dosing	1	0.0661	0.0661	1.2710	0.0162	0.1018
	metals:nutrients	6	0.2892	0.0482	0.9262	0.0710	0.7728
	metals:dosing	3	0.1368	0.0456	0.8767	0.0336	0.8474
	nutrients:dosing	2	0.0909	0.0455	0.8735	0.0223	0.7980

continued on next page

Table A.3 – continued from previous page

	Df	SumsOfSqs	MeanSqs	F.Model	R2	Pr(>F)
metals:nutrients:dosing	6	0.3108	0.0518	0.9954	0.0763	0.4692
Residuals	46	2.3935	0.0520	0.5875		
Total	69	4.0740	1			

B

Appendix - Chapter 3

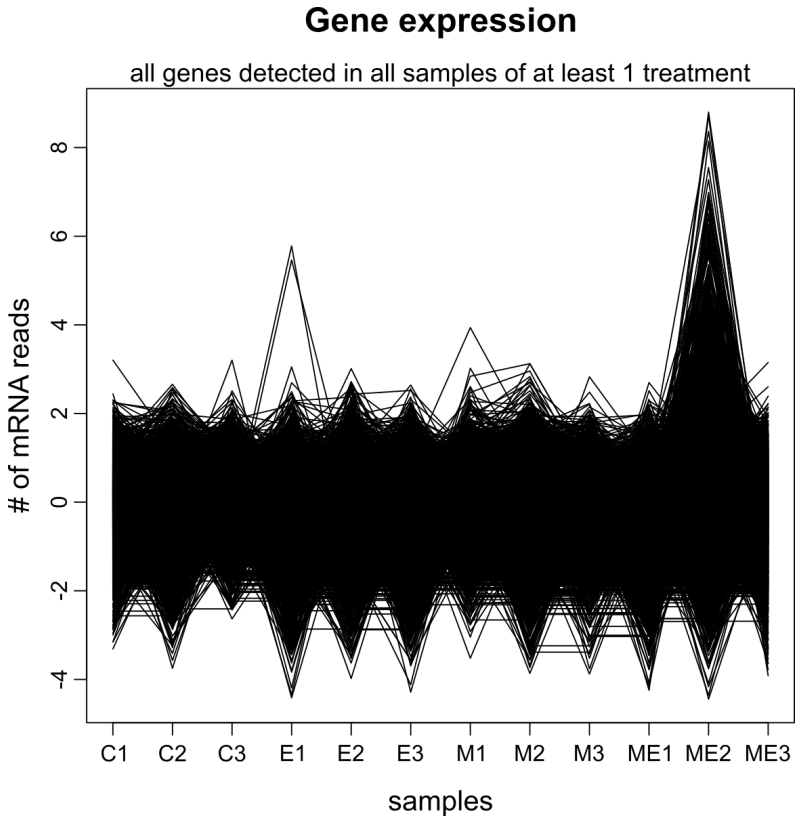

Figure B.1: Gene expression values for all genes included in the final dataset used for statistical analyses (detected in all samples of at least one treatment). Sample names are according to treatments: C for control, E for enriched, M for metals, and ME for metals/enriched. This plot identifies **sample ME2** as an outlier and justifies its exclusion from further analyses.

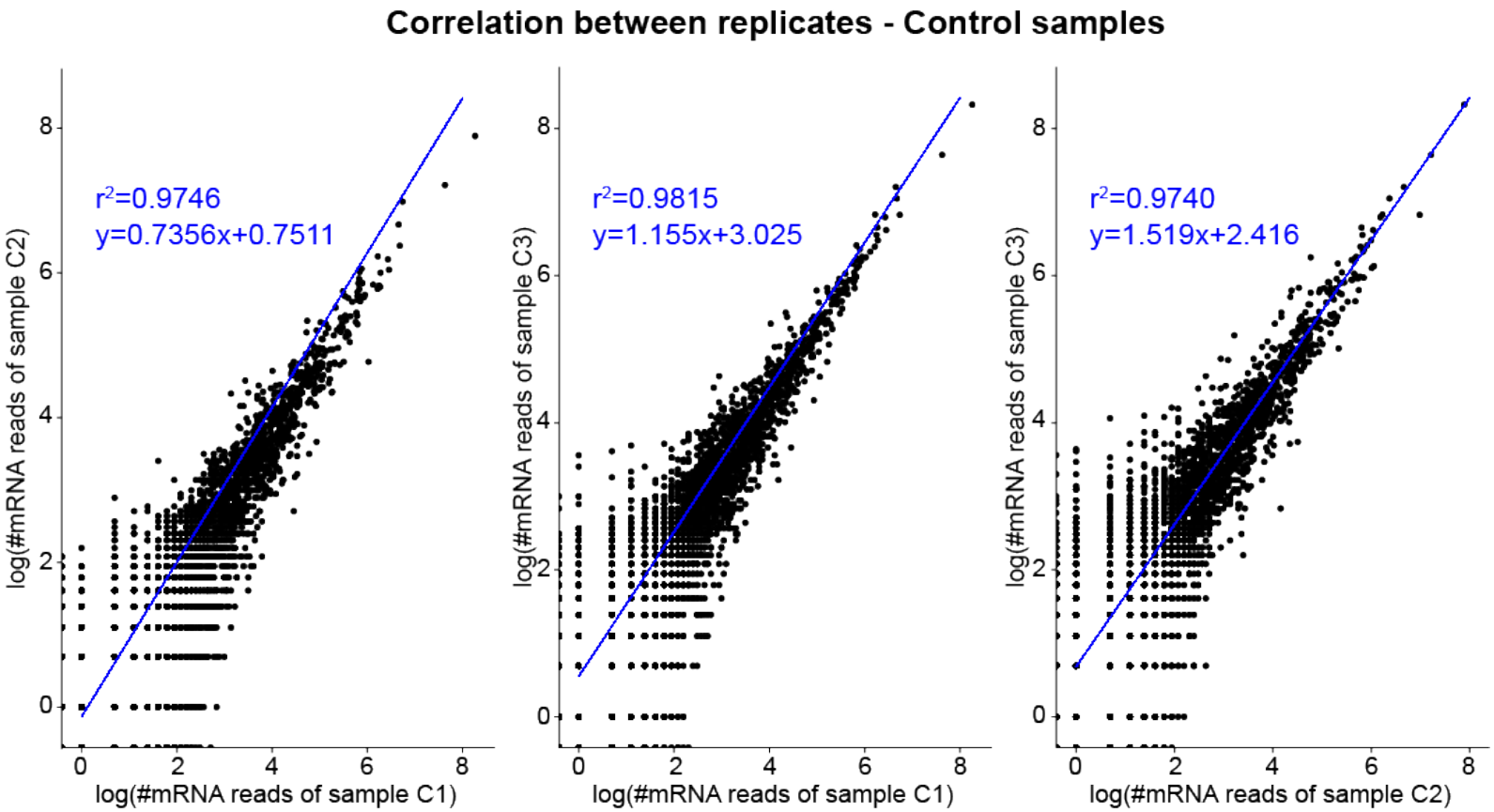

Figure B.2: Correlation plots between all replicates within the **control treatment**. Linear regression is plotted as a blue line. Correlation and linear regression formula are shown in blue.

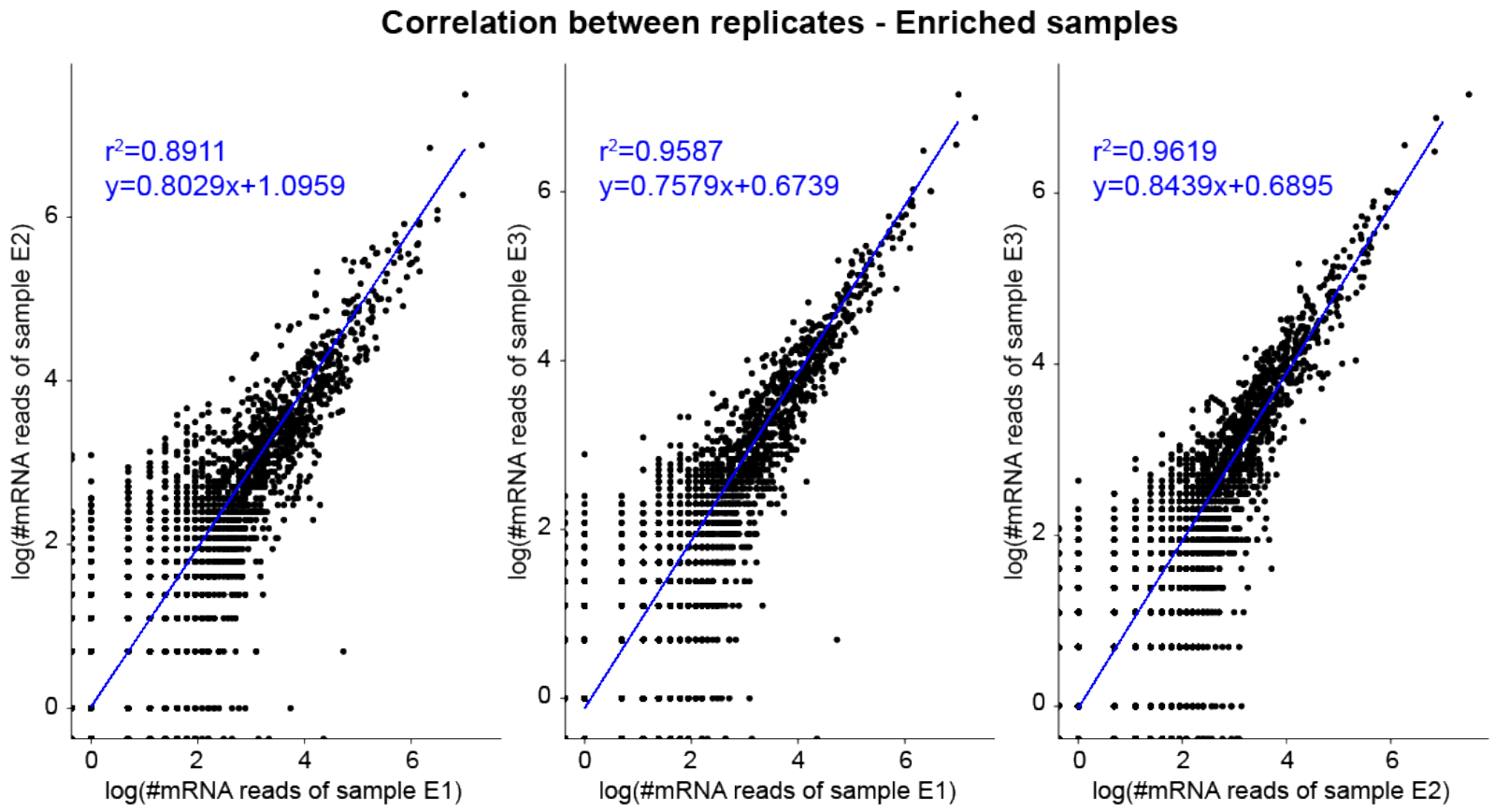

Figure B.3: Correlation plots between all replicates within the **enriched treatment**. Linear regression is plotted as a blue line. Correlation and linear regression formula are shown in blue.

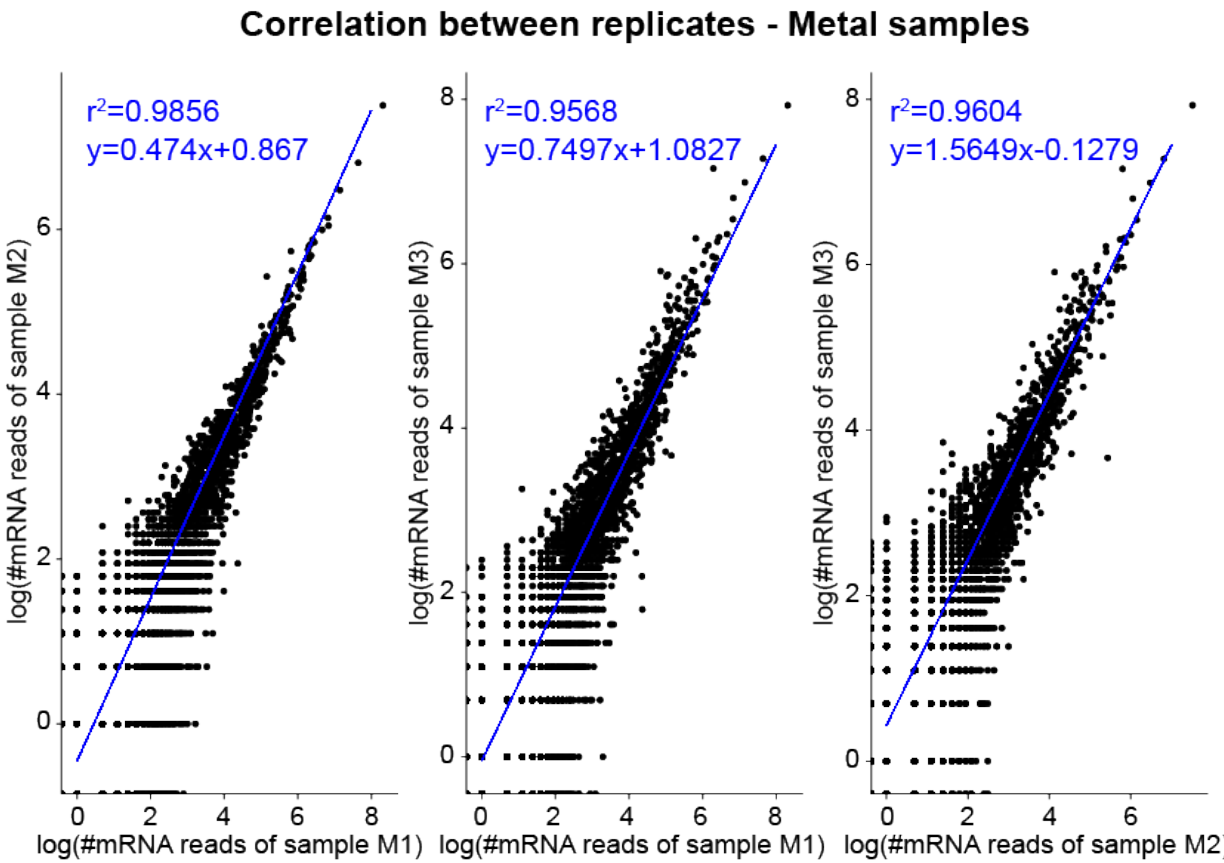

Figure B.4: Correlation plots between all replicates within the **metal treatment**. Linear regression is plotted as a blue line. Correlation and linear regression formula are shown in blue.

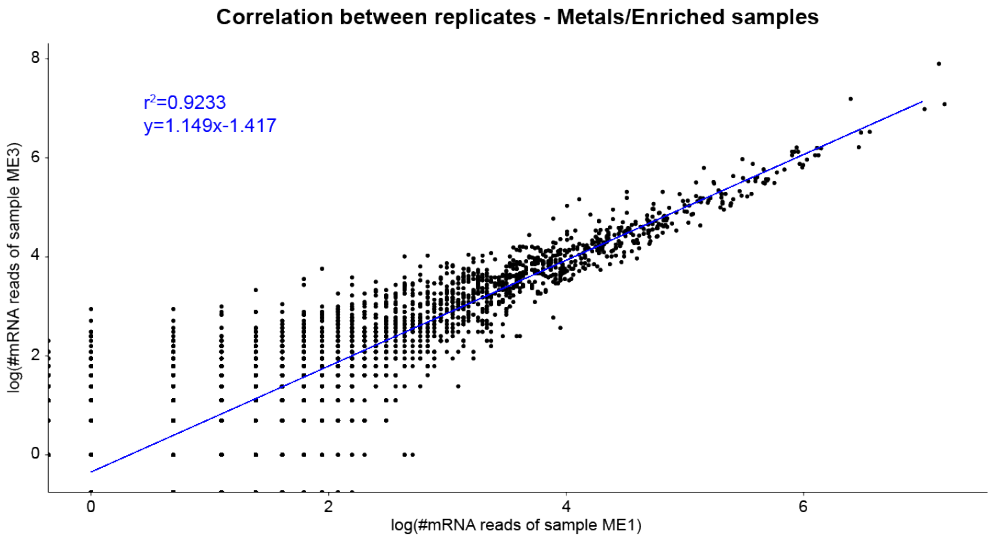

Figure B.5: Correlation plots between all replicates within the **metals/enriched treatment**. Linear regression is plotted as a blue line. Correlation and linear regression formula are shown in blue.

Table B.1: Sequencing information per sample. * highlights the sample which was identified as an outlier and removed from further analyses. C stands for control samples, E for organically enriched, M for high metal contaminated and ME for high metals and enriched samples. The numbers in the sample name stand for the replicate number.

Sample	#raw reads	#reads after trimming	#mRNA reads
C1	40,147,416	39,955,014	2,637,549
C2	38,317,630	38,127,864	2,181,852
C3	50,025,594	49,751,382	2,716,359
E1	39,002,492	38,821,548	1,513,501
E2	40,499,178	40,310,115	1,706,735
E3	34,668,978	34,499,412	1,536,940
M1	39,975,956	39,752,361	2,343,434
M2	36,962,844	36,773,304	1,997,633
M3	40,564,048	40,350,583	2,006,609
ME1	42,151,632	41,965,846	1,712,440
ME2*	41,253,546	41,047,248	2,569,894
ME3	40,773,954	40,598,662	1,482,383

Table B.2: Top 50 genes with highest gene expression across all samples. The gene KO, gene name, pathway KO, and pathway group are shown. Genes that belong to multiple pathways are listed once for every associated pathway.

gene KO ID	gene name	pathway name	pathway category
K02703	psbA	Photosynthesis	Energy Metabolism
K00394	aprA	Sulfur metabolism	Energy Metabolism
K04077	groEL	RNA degradation	Folding, Sorting and Degradation
K04043	dnaK	RNA degradation	Folding, Sorting and Degradation
K03046	rpoC	Purine metabolism	Nucleotide Metabolism
K03046	rpoC	Pyrimidine metabolism	Nucleotide Metabolism
K03046	rpoC	RNA polymerase	Transcription
K01130	aslA	Steroid hormone biosynthesis	Lipid Metabolism
K01130	aslA	Sphingolipid metabolism	Lipid Metabolism
K02406	fliC	Two-component system	Signal Transduction
K02406	fliC	Flagellar assembly	Cell Motility
K03043	rpoB	Purine metabolism	Nucleotide Metabolism
K03043	rpoB	Pyrimidine metabolism	Nucleotide Metabolism
K03043	rpoB	RNA polymerase	Transcription
K02945	RP-S1	Ribosome	Translation
K00088	guaB	Purine metabolism	Nucleotide Metabolism

continued on next page

Table B.2 – continued from previous page

gene KO	gene name	pathway name	pathway category
K00088	guaB	Drug metabolism - other enzymes	Xenobiotics Biodegradation and Metabolism
K02112	ATPF1B	Oxidative phosphorylation	Energy Metabolism
K02112	ATPF1B	Photosynthesis	Energy Metabolism
K02111	ATPF1A	Oxidative phosphorylation	Energy Metabolism
K02111	ATPF1A	Photosynthesis	Energy Metabolism
K01895	ACSS	Glycolysis / Gluconeogenesis	Carbohydrate Metabolism
K01895	ACSS	Pyruvate metabolism	Carbohydrate Metabolism
K01895	ACSS	Propanoate metabolism	Carbohydrate Metabolism
K01895	ACSS	Methane metabolism	Energy Metabolism
K01895	ACSS	Carbon fixation pathways in prokaryotes	Energy Metabolism
K03388	hdrA	Methane metabolism	Energy Metabolism
K03737	nifJ	Carbon fixation pathways in prokaryotes	Energy Metabolism
K03737	nifJ	Nitrogen metabolism	Energy Metabolism
K00286	proC	Arginine and proline metabolism	Amino Acid Metabolism
K01338	lon	Cell cycle - Caulobacter	Cell Growth and Death
K00958	met3	Purine metabolism	Nucleotide Metabolism
K00958	met3	Selenocompound metabolism	Metabolism of Other Amino Acids
K00958	met3	Sulfur metabolism	Energy Metabolism

continued on next page

Table B.2 – continued from previous page

gene KO	gene name	pathway name	pathway category
K01507	ppa	Oxidative phosphorylation	Energy Metabolism
K03738	aor	Glycolysis / Gluconeogenesis	Carbohydrate Metabolism
K03738	aor	Pentose phosphate pathway	Carbohydrate Metabolism
K01647	CS	Citrate cycle (TCA cycle)	Carbohydrate Metabolism
K01647	CS	Glyoxylate and dicarboxylate metabolism	Carbohydrate Metabolism
K00134	GAPDH	Glycolysis / Gluconeogenesis	Carbohydrate Metabolism
K00395	aprB	Sulfur metabolism	Energy Metabolism
K03782	katG	Phenylalanine metabolism	Amino Acid Metabolism
K03782	katG	Tryptophan metabolism	Amino Acid Metabolism
K03782	katG	Methane metabolism	Energy Metabolism
K03782	katG	Phenylpropanoid biosynthesis	Biosynthesis of Other Secondary Metabolites
K00962	pnp	Purine metabolism	Nucleotide Metabolism
K00962	pnp	Pyrimidine metabolism	Nucleotide Metabolism
K00962	pnp	RNA degradation	Folding, Sorting and Degradation
K05692	ACTB_G1	Phagosome	Transport and Catabolism
K05692	ACTB_G1	Focal adhesion	Cell Communication
K05692	ACTB_G1	Adherens junction	Cell Communication
K05692	ACTB_G1	Tight junction	Cell Communication

continued on next page

Table B.2 – continued from previous page

gene KO	gene name	pathway name	pathway category
K05692	ACTB_G1	Regulation of actin cytoskeleton	Cell Motility
K01999	livK	ABC transporters	Membrane Transport
K01006	ppdK	Pyruvate metabolism	Carbohydrate Metabolism
K01006	ppdK	Carbon fixation in photosynthetic organisms	Energy Metabolism
K01915	glnA	Alanine, aspartate and glutamate metabolism	Amino Acid Metabolism
K01915	glnA	Arginine and proline metabolism	Amino Acid Metabolism
K01915	glnA	Glyoxylate and dicarboxylate metabolism	Carbohydrate Metabolism
K01915	glnA	Nitrogen metabolism	Energy Metabolism
K01915	glnA	Two-component system	Signal Transduction
K01938	fhs	One carbon pool by folate	Metabolism of Cofactors and Vitamins
K01938	fhs	Carbon fixation pathways in prokaryotes	Energy Metabolism
K00123	E1.2.1.2A	Glyoxylate and dicarboxylate metabolism	Carbohydrate Metabolism
K00123	E1.2.1.2A	Methane metabolism	Energy Metabolism
K11181	dsrB	Nitrotoluene degradation	Xenobiotics Biodegradation and Metabolism
K00525	nrdE	Purine metabolism	Nucleotide Metabolism
K00525	nrdE	Pyrimidine metabolism	Nucleotide Metabolism
K01624	FBA	Glycolysis / Gluconeogenesis	Carbohydrate Metabolism
K01624	FBA	Pentose phosphate pathway	Carbohydrate Metabolism

continued on next page

Table B.2 – continued from previous page

gene KO	gene name	pathway name	pathway category
K01624	FBA	Fructose and mannose metabolism	Carbohydrate Metabolism
K01624	FBA	Methane metabolism	Energy Metabolism
K01624	FBA	Carbon fixation in photosynthetic organisms	Energy Metabolism
K02886	RP-L2	Ribosome	Translation
K00198	cooS	Nitrotoluene degradation	Xenobiotics Biodegradation and Metabolism
K00198	cooS	Methane metabolism	Energy Metabolism
K00058	serA	Glycine, serine and threonine metabolism	Amino Acid Metabolism
K00058	serA	Methane metabolism	Energy Metabolism
K00626	atoB	Fatty acid metabolism	Lipid Metabolism
K00626	atoB	Synthesis and degradation of ketone bodies	Lipid Metabolism
K00626	atoB	Valine, leucine and isoleucine degradation	Amino Acid Metabolism
K00626	atoB	Lysine degradation	Amino Acid Metabolism
K00626	atoB	Benzoate degradation	Xenobiotics Biodegradation and Metabolism
K00626	atoB	Tryptophan metabolism	Amino Acid Metabolism
K00626	atoB	Pyruvate metabolism	Carbohydrate Metabolism
K00626	atoB	Glyoxylate and dicarboxylate metabolism	Carbohydrate Metabolism
K00626	atoB	Propanoate metabolism	Carbohydrate Metabolism
K00626	atoB	Butanoate metabolism	Carbohydrate Metabolism

continued on next page

Table B.2 – continued from previous page

gene KO	gene name	pathway name	pathway category
K00626	atoB	Carbon fixation pathways in prokaryotes	Energy Metabolism
K00626	atoB	Terpenoid backbone biosynthesis	Metabolism of Terpenoids and Polyketides
K00626	atoB	Two-component system	Signal Transduction
K00404	ccoN	Oxidative phosphorylation	Energy Metabolism
K00404	ccoN	Two-component system	Signal Transduction
K01251	ahcY	Cysteine and methionine metabolism	Amino Acid Metabolism

Table B.3: Results from the Fisher's exact test and the subsequent Benjamini-Hochberg correction for multiple testing. This test reveals which pathways contain more differentially expressed (DE) genes than expected by chance, given the number of DE genes in the entire dataset. Significant *p*-values (at a level of α=0.05) are highlighted in bold.

pathway KO ID	pathway name	Fisher's p-value	p_{corr}
path:ko00010	Glycolysis / Gluconeogenesis	0.1370	0.9959
path:ko00020	Citrate cycle (TCA cycle)	**0.0109**	0.5924
path:ko00030	Pentose phosphate pathway	0.7519	0.9959
path:ko00040	Pentose and glucuronate interconversions	0.8610	0.9959
path:ko00051	Fructose and mannose metabolism	0.8917	0.9959
path:ko00052	Galactose metabolism	0.9198	0.9959
path:ko00053	Ascorbate and aldarate metabolism	0.9620	0.9959
path:ko00061	Fatty acid biosynthesis	0.9937	0.9959
path:ko00062	Fatty acid elongation	0.9311	0.9959
path:ko00071	Fatty acid metabolism	0.9165	0.9959
path:ko00072	Synthesis and degradation of ketone bodies	0.0769	0.9003
path:ko00100	Steroid biosynthesis	0.8318	0.9959
path:ko00120	Primary bile acid biosynthesis	0.2733	0.9959
path:ko00121	Secondary bile acid biosynthesis	0.2568	0.9959
path:ko00130	Ubiquinone and other terpenoid-quinone biosynthesis	0.4524	0.9959
path:ko00140	Steroid hormone biosynthesis	0.0659	0.8572

continued on next page

Table B.3 – continued from previous page

pathway KO ID	pathway name	Fisher's p-value	p_{corr}
path:ko00190	Oxidative phosphorylation	0.5051	0.9959
path:ko00195	Photosynthesis	0.4333	0.9959
path:ko00196	Photosynthesis - antenna proteins	0.5721	0.9959
path:ko00230	Purine metabolism	0.3255	0.9959
path:ko00240	Pyrimidine metabolism	0.7863	0.9959
path:ko00250	Alanine, aspartate and glutamate metabolism	0.9760	0.9959
path:ko00260	Glycine, serine and threonine metabolism	0.1370	0.9959
path:ko00270	Cysteine and methionine metabolism	0.5994	0.9959
path:ko00280	Valine, leucine and isoleucine degradation	0.5988	0.9959
path:ko00281	Geraniol degradation	0.6881	0.9959
path:ko00290	Valine, leucine and isoleucine biosynthesis	0.6712	0.9959
path:ko00300	Lysine biosynthesis	0.9664	0.9959
path:ko00310	Lysine degradation	0.8787	0.9959
path:ko00311	Penicillin and cephalosporin biosynthesis	0.4478	0.9959
path:ko00330	Arginine and proline metabolism	0.7010	0.9959
path:ko00340	Histidine metabolism	0.9830	0.9959
path:ko00350	Tyrosine metabolism	0.4001	0.9959
path:ko00351	DDT degradation	0.2568	0.9959

continued on next page

Table B.3 – continued from previous page

pathway KO ID	pathway name	Fisher's p-value	p_{corr}
path:ko00360	Phenylalanine metabolism	0.3315	0.9959
path:ko00361	Chlorocyclohexane and chlorobenzene degradation	0.5721	0.9959
path:ko00362	Benzoate degradation	0.8331	0.9959
path:ko00363	Bisphenol degradation	0.2578	0.9959
path:ko00364	Fluorobenzoate degradation	0.7735	0.9959
path:ko00380	Tryptophan metabolism	0.8089	0.9959
path:ko00400	Phenylalanine, tyrosine and tryptophan biosynthesis	0.9034	0.9959
path:ko00401	Novobiocin biosynthesis	0.9072	0.9959
path:ko00410	beta-Alanine metabolism	0.5621	0.9959
path:ko00430	Taurine and hypotaurine metabolism	0.5660	0.9959
path:ko00440	Phosphonate and phosphinate metabolism	0.4823	0.9959
path:ko00450	Selenocompound metabolism	0.6129	0.9959
path:ko00460	Cyanoamino acid metabolism	0.7714	0.9959
path:ko00472	D-Arginine and D-ornithine metabolism	0.2568	0.9959
path:ko00473	D-Alanine metabolism	0.5897	0.9959
path:ko00480	Glutathione metabolism	0.8276	0.9959
path:ko00500	Starch and sucrose metabolism	0.6721	0.9959
path:ko00510	N-Glycan biosynthesis	0.5897	0.9959

continued on next page

Table B.3 – continued from previous page

pathway KO ID	pathway name	Fisher's p-value	p_{corr}
path:ko00511	Other glycan degradation	0.9311	0.9959
path:ko00520	Amino sugar and nucleotide sugar metabolism	0.7847	0.9959
path:ko00521	Streptomycin biosynthesis	0.7161	0.9959
path:ko00523	Polyketide sugar unit biosynthesis	0.6952	0.9959
path:ko00531	Glycosaminoglycan degradation	0.5721	0.9959
path:ko00540	Lipopolysaccharide biosynthesis	0.9840	0.9959
path:ko00550	Peptidoglycan biosynthesis	0.7591	0.9959
path:ko00561	Glycerolipid metabolism	0.9167	0.9959
path:ko00562	Inositol phosphate metabolism	0.8846	0.9959
path:ko00564	Glycerophospholipid metabolism	0.6923	0.9959
path:ko00565	Ether lipid metabolism	0.1639	0.9959
path:ko00591	Linoleic acid metabolism	0.4478	0.9959
path:ko00600	Sphingolipid metabolism	0.8544	0.9959
path:ko00620	Pyruvate metabolism	0.6546	0.9959
path:ko00621	Dioxin degradation	0.4823	0.9959
path:ko00622	Xylene degradation	0.3385	0.9959
path:ko00623	Toluene degradation	0.3055	0.9959
path:ko00624	Polycyclic aromatic hydrocarbon degradation	0.2578	0.9959

continued on next page

Table B.3 – continued from previous page

pathway KO ID	pathway name	Fisher's p-value	p_{corr}
path:ko00625	Chloroalkane and chloroalkene degradation	0.3945	0.9959
path:ko00626	Naphthalene degradation	0.7714	0.9959
path:ko00627	Aminobenzoate degradation	0.4626	0.9959
path:ko00630	Glyoxylate and dicarboxylate metabolism	0.6612	0.9959
path:ko00633	Nitrotoluene degradation	**0**	**0.0027**
path:ko00640	Propanoate metabolism	0.0679	0.8572
path:ko00642	Ethylbenzene degradation	0.5897	0.9959
path:ko00643	Styrene degradation	0.7714	0.9959
path:ko00650	Butanoate metabolism	0.0608	0.8572
path:ko00660	C5-Branched dibasic acid metabolism	**0.0304**	0.8445
path:ko00670	One carbon pool by folate	0.3273	0.9959
path:ko00680	Methane metabolism	**0.0385**	0.8445
path:ko00710	Carbon fixation in photosynthetic organisms	0.9167	0.9959
path:ko00720	Carbon fixation pathways in prokaryotes	**0.0008**	0.0668
path:ko00730	Thiamine metabolism	0.8171	0.9959
path:ko00740	Riboflavin metabolism	0.4950	0.9959
path:ko00750	Vitamin B6 metabolism	0.7161	0.9959
path:ko00760	Nicotinate and nicotinamide metabolism	0.6599	0.9959

continued on next page

Table B.3 – continued from previous page

pathway KO ID	pathway name	Fisher's p-value	p_{corr}
path:ko00770	Pantothenate and CoA biosynthesis	0.8519	0.9959
path:ko00780	Biotin metabolism	0.3816	0.9959
path:ko00785	Lipoic acid metabolism	0.5897	0.9959
path:ko00790	Folate biosynthesis	0.9439	0.9959
path:ko00830	Retinol metabolism	0.2733	0.9959
path:ko00860	Porphyrin and chlorophyll metabolism	0.5649	0.9959
path:ko00900	Terpenoid backbone biosynthesis	0.8553	0.9959
path:ko00903	Limonene and pinene degradation	0.3724	0.9959
path:ko00910	Nitrogen metabolism	0.5185	0.9959
path:ko00920	Sulfur metabolism	0.7031	0.9959
path:ko00940	Phenylpropanoid biosynthesis	**0.0144**	0.5924
path:ko00945	Stilbenoid, diarylheptanoid and gingerol biosynthesis	0.2568	0.9959
path:ko00950	Isoquinoline alkaloid biosynthesis	0.9072	0.9959
path:ko00960	Tropane, piperidine and pyridine alkaloid biosynthesis	0.9620	0.9959
path:ko00970	Aminoacyl-tRNA biosynthesis	0.9959	0.9959
path:ko00980	Metabolism of xenobiotics by cytochrome P450	0.3816	0.9959
path:ko00982	Drug metabolism - cytochrome P450	0.1803	0.9959
path:ko00983	Drug metabolism - other enzymes	0.9885	0.9959

continued on next page

Table B.3 – continued from previous page

pathway KO ID	pathway name	Fisher's p-value	p_{corr}
path:ko01040	Biosynthesis of unsaturated fatty acids	0.9885	0.9959
path:ko01053	Biosynthesis of siderophore group nonribosomal peptides	0.5897	0.9959
path:ko02010	ABC transporters	0.9946	0.9959
path:ko02020	Two-component system	0.7192	0.9959
path:ko02030	Bacterial chemotaxis	0.9477	0.9959
path:ko02040	Flagellar assembly	0.9435	0.9959
path:ko02060	Phosphotransferase system (PTS)	0.8519	0.9959
path:ko03008	Ribosome biogenesis in eukaryotes	0.9284	0.9959
path:ko03010	Ribosome	0.8266	0.9959
path:ko03013	RNA transport	0.4231	0.9959
path:ko03015	mRNA surveillance pathway	0.5660	0.9959
path:ko03018	RNA degradation	0.4001	0.9959
path:ko03020	RNA polymerase	0.4524	0.9959
path:ko03022	Basal transcription factors	0.7735	0.9959
path:ko03030	DNA replication	0.0648	0.8572
path:ko03040	Spliceosome	0.8331	0.9959
path:ko03050	Proteasome	0.8089	0.9959
path:ko03060	Protein export	0.8276	0.9959

continued on next page

Table B.3 – continued from previous page

pathway KO ID	pathway name	Fisher's p-value	p_{corr}
path:ko03070	Bacterial secretion system	0.8610	0.9959
path:ko03410	Base excision repair	0.5624	0.9959
path:ko03420	Nucleotide excision repair	0.4524	0.9959
path:ko03430	Mismatch repair	0.6084	0.9959
path:ko03440	Homologous recombination	0.3273	0.9959
path:ko03450	Non-homologous end-joining	0.5897	0.9959
path:ko03460	Fanconi anemia pathway	0.0659	0.8572
path:ko04010	MAPK signalling pathway	0.1805	0.9959
path:ko04011	MAPK signalling pathway - yeast	**0.0412**	0.8445
path:ko04012	ErbB signalling pathway	0.1237	0.9959
path:ko04020	Calcium signalling pathway	0.5086	0.9959
path:ko04060	Cytokine-cytokine receptor interaction	0.1639	0.9959
path:ko04070	Phosphatidylinositol signalling system	0.4185	0.9959
path:ko04080	Neuroactive ligand-receptor interaction	0.5897	0.9959
path:ko04110	Cell cycle	0.6881	0.9959
path:ko04111	Cell cycle - yeast	0.9089	0.9959
path:ko04112	Cell cycle - Caulobacter	0.9658	0.9959
path:ko04113	Meiosis - yeast	0.6306	0.9959

continued on next page

Table B.3 – continued from previous page

pathway KO ID	pathway name	Fisher's p-value	p_{corr}
path:ko04114	Oocyte meiosis	0.9734	0.9959
path:ko04120	Ubiquitin mediated proteolysis	0.7825	0.9959
path:ko04122	Sulfur relay system	0.2786	0.9959
path:ko04130	SNARE interactions in vesicular transport	0.5897	0.9959
path:ko04140	Regulation of autophagy	0.2733	0.9959
path:ko04141	Protein processing in endoplasmic reticulum	0.9301	0.9959
path:ko04142	Lysosome	0.5633	0.9959
path:ko04144	Endocytosis	0.0336	0.8445
path:ko04145	Phagosome	0.7591	0.9959
path:ko04146	Peroxisome	0.3887	0.9959
path:ko04150	mTOR signalling pathway	0.9311	0.9959
path:ko04210	Apoptosis	0.6500	0.9959
path:ko04310	Wnt signalling pathway	0.7775	0.9959
path:ko04330	Notch signalling pathway	0.7735	0.9959
path:ko04370	VEGF signalling pathway	0.8171	0.9959
path:ko04510	Focal adhesion	0.6052	0.9959
path:ko04512	ECM-receptor interaction	0.7735	0.9959
path:ko04520	Adherens junction	0.9718	0.9959

continued on next page

Table B.3 – continued from previous page

pathway KO ID	pathway name	Fisher's p-value	p_{corr}
path:ko04530	Tight junction	0.9914	0.9959
path:ko04540	Gap junction	0.8171	0.9959
path:ko04630	Jak-STAT signalling pathway	0.5897	0.9959
path:ko04810	Regulation of actin cytoskeleton	0.5086	0.9959

C

Appendix - Chapter 4

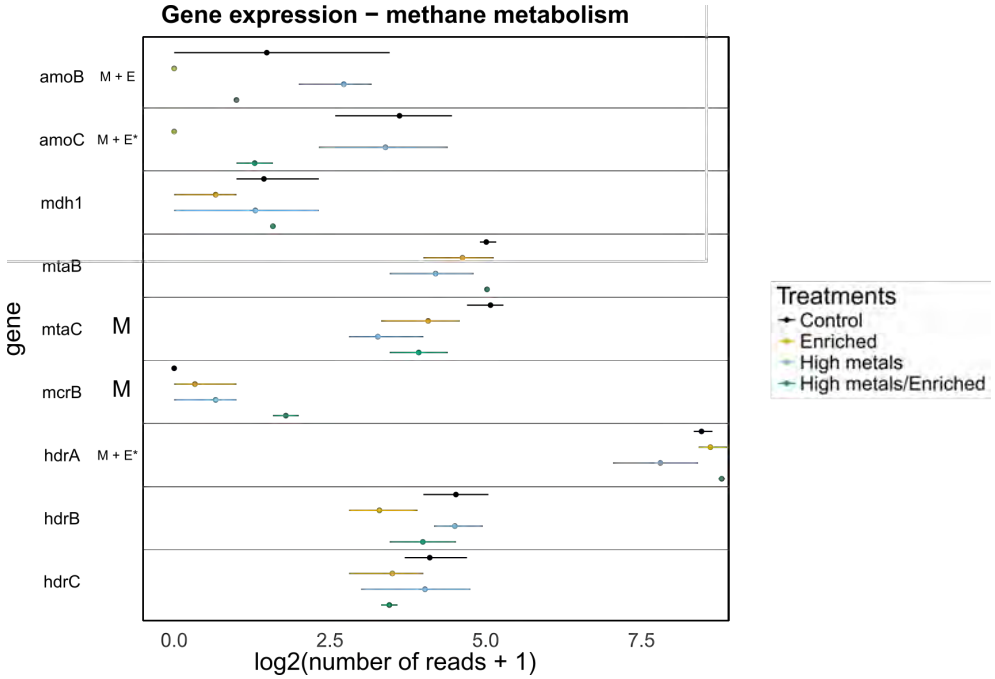

Figure C.1: Gene expression levels of all methane metabolism genes that were detected in our dataset. The letters next to the gene name indicate the treatment (M = High metals, E = Enrichment) that has significantly affected the expression of that gene, whereas M+E means that both metal contaminants and organic enrichment had a significant effect and MxE indicates that there was a significant interaction between the treatments. An asterisk (*) next to the treatment letter indicates that the *p*-value was still significant (at an α level of 0.1) after false discovery rate (FDR) correction.

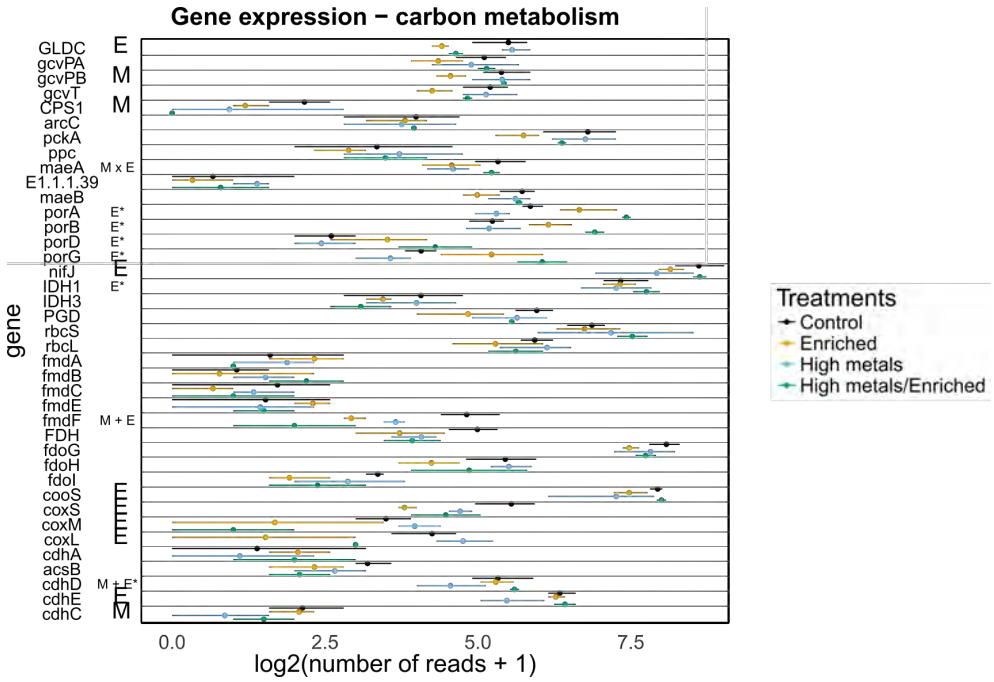

Figure C.2: Gene expression levels of all genes involved with CO and CO_2 production that were detected in our dataset. The letters next to the gene name indicate the treatment (M = High metals, E = Enrichment) that has significantly affected the expression of that gene, whereas M+E means that both metal contaminants and organic enrichment had a significant effect and MxE indicates that there was a significant interaction between the treatments. An asterisk (*) next to the treatment letter indicates that the *p*-value was still significant (at an α level of 0.1) after false discovery rate (FDR) correction.

Table C.1: ANOVA results and false discovery rate (FDR) corrected *p*-values (p_{adj}) for all treatments and genes from the (a) nitrogen, (b) sulphur, (c) methane and (d) carbon metabolisms. Significant values are highlighted in bold. Significance values are based on an α value of 0.05.

	Gene	Treatment	Df	Sum Sq	Mean Sq	F value	Pr(>F)	p_{adj}
(a)	nifD	metals	1	0.3670	0.3670	0.0930	0.7692	0.8876
		enriched	1	35.5090	35.5090	8.9939	**0.0200**	0.0691
		metals*enriched	1	0.2230	0.2230	0.0564	0.8191	0.9535
	nifH	metals	1	3.2484	3.2484	1.1254	0.3240	0.6234
		enriched	1	13.6609	13.6609	4.7326	0.0661	0.1699
		metals*enriched	1	0.3227	0.3227	0.1118	0.7479	0.9535
	nifK	metals	1	0.2460	0.2460	0.0395	0.8481	0.9250
		enriched	1	14.8770	14.8770	2.3890	0.1661	0.3398
		metals*enriched	1	0.3720	0.3717	0.0597	0.8140	0.9535
	CPS1	metals	1	9.8467	9.8467	9.0612	**0.0197**	0.3339
		enriched	1	1.5607	1.5607	1.4362	0.2698	0.4390
		metals*enriched	1	0.2322	0.2322	0.2137	0.6580	0.9535
	pmoB-amoB	metals	1	10.5681	10.5681	8.9496	**0.0202**	0.3339
		enriched	1	8.1213	8.1213	6.8776	**0.0343**	0.0995
		metals*enriched	1	0.0099	0.0099	0.0084	0.9296	0.9956
	pmoC-amoC	metals	1	4.4703	4.4703	6.3741	**0.0395**	0.3339

continued on next page

Table C.1 – continued from previous page

Gene	Treatment	Df	Sum Sq	Mean Sq	F value	Pr(>F)	p_{adj}
	enriched	1	28.3140	28.3140	40.3719	**0.0004**	**0.0058**
	metals*enriched	1	3.2278	3.2278	4.6025	0.0691	0.9147
hcp	metals	1	0.4338	0.4338	1.7739	0.2246	0.5708
	enriched	1	3.4288	3.4288	14.0228	**0.0072**	**0.0406**
	metals*enriched	1	0.1436	0.1436	0.5872	0.4685	0.9159
hao	metals	1	2.0892	2.0892	3.4307	0.1064	0.5132
	enriched	1	1.2827	1.2827	2.1063	0.1900	0.3565
	metals*enriched	1	0.5026	0.5026	0.8252	0.3939	0.9159
narG	metals	1	0.4434	0.4434	0.6563	0.4445	0.7019
	enriched	1	6.3127	6.3127	9.3444	**0.0184**	0.0691
	metals*enriched	1	0.0440	0.0440	0.0652	0.8058	0.9535
narH	metals	1	0.8108	0.8108	2.6252	0.1492	0.5708
	enriched	1	0.0476	0.0476	0.1540	0.7064	0.7754
	metals*enriched	1	0.0000	0.0000	0.0001	0.9940	0.9956
narI	metals	1	0.4590	0.4590	2.0455	0.1957	0.5708
	enriched	1	0.4865	0.4865	2.1681	0.1844	0.3565
	metals*enriched	1	0.6772	0.6772	3.0178	0.1259	0.9147
napA	metals	1	0.3542	0.3542	3.2582	0.1140	0.5132

continued on next page

Table C.1 – continued from previous page

Gene	Treatment	Df	Sum Sq	Mean Sq	F value	Pr(>F)	p_{adj}
	enriched	1	0.0301	0.0301	0.2765	0.6153	0.7286
	metals*enriched	1	0.0060	0.0060	0.0556	0.8204	0.9535
napB	metals	1	0.4743	0.4743	1.4393	0.2693	0.6059
	enriched	1	0.1693	0.1693	0.5137	0.4968	0.6463
	metals*enriched	1	0.5590	0.5590	1.6963	0.2340	0.9159
nasA	metals	1	1.9308	1.9308	1.1175	0.3256	0.6234
	enriched	1	2.6812	2.6812	1.5518	0.2529	0.4295
	metals*enriched	1	0.5814	0.5814	0.3365	0.5800	0.9159
ncd2	metals	1	1.2445	1.2445	7.5894	**0.0283**	0.3339
	enriched	1	1.2544	1.2544	7.6497	**0.0279**	0.0836
	metals*enriched	1	0.0001	0.0001	0.0003	0.9857	0.9956
nirA	metals	1	0.0314	0.0314	0.0198	0.8919	0.9250
	enriched	1	0.0216	0.0216	0.0136	0.9104	0.9311
	metals*enriched	1	1.0547	1.0547	0.6658	0.4414	0.9159
nirB	metals	1	0.0443	0.0443	0.0266	0.8751	0.9250
	enriched	1	1.6736	1.6736	1.0060	0.3493	0.5239
	metals*enriched	1	0.1367	0.1367	0.0822	0.7827	0.9535
nrfA	metals	1	0.6702	0.6702	4.1047	0.0824	0.4944

continued on next page

Table C.1 – continued from previous page

	Gene	Treatment	Df	Sum Sq	Mean Sq	F value	Pr(>F)	p_{adj}
		enriched	1	0.4707	0.4707	2.8827	0.1333	0.3000
		metals*enriched	1	0.5622	0.5622	3.4436	0.1059	0.9147
	nrfC	metals	1	0.2546	0.2546	3.2928	0.1125	0.5132
		enriched	1	4.0713	4.0713	52.6479	**0.0002**	**0.0038**
		metals*enriched	1	0.1947	0.1947	2.5179	0.1566	0.9147
	nirK	metals	1	0.0106	0.0106	0.0321	0.8628	0.9250
		enriched	1	6.4459	6.4459	19.5288	**0.0031**	**0.0199**
		metals*enriched	1	2.6731	2.6731	8.0984	**0.0249**	0.8793
	norB	metals	1	0.0646	0.0646	0.1619	0.6994	0.8487
		enriched	1	0.0443	0.0443	0.1110	0.7488	0.8119
		metals*enriched	1	0.5429	0.5429	1.3600	0.2817	0.9159
	norC	metals	1	0.0199	0.0199	0.0123	0.9149	0.9250
		enriched	1	1.1432	1.1432	0.7041	0.4291	0.5942
		metals*enriched	1	4.2577	4.2577	2.6224	0.1494	0.9147
	nosZ	metals	1	0.2364	0.2364	1.4419	0.2689	0.6059
		enriched	1	4.9792	4.9792	30.3692	**0.0009**	**0.0091**
		metals*enriched	1	0.0098	0.0098	0.0599	0.8136	0.9535
(b)	CYC	metals	1	0.0197	0.0197	0.0095	0.9250	0.9250

continued on next page

Table C.1 – continued from previous page

Gene	Treatment	Df	Sum Sq	Mean Sq	F value	Pr(>F)	p_{adj}
	enriched	1	0.4410	0.4410	0.2135	0.6581	0.7497
	metals*enriched	1	3.1828	3.1828	1.5406	0.2545	0.9159
cysD	metals	1	0.0230	0.0230	0.0586	0.8156	0.9250
	enriched	1	0.0863	0.0863	0.2197	0.6535	0.7497
	metals*enriched	1	0.6303	0.6303	1.6049	0.2457	0.9159
cysN	metals	1	0.4427	0.4427	1.3169	0.2889	0.6190
	enriched	1	0.3700	0.3700	1.1007	0.3290	0.5018
	metals*enriched	1	0.2326	0.2326	0.6919	0.4330	0.9159
sat	metals	1	0.1860	0.1860	1.0015	0.3503	0.6386
	enriched	1	1.9518	1.9518	10.5112	**0.0142**	0.0640
	metals*enriched	1	0.1011	0.1011	0.5443	0.4847	0.9159
PAPSS	metals	1	2.8246	2.8246	1.9570	0.2045	0.5708
	enriched	1	1.9959	1.9959	1.3828	0.2781	0.4390
	metals*enriched	1	1.0745	1.0745	0.7445	0.4168	0.9159
cysC	metals	1	0.5554	0.5554	2.3975	0.1655	0.5708
	enriched	1	0.2011	0.2011	0.8682	0.3825	0.5464
	metals*enriched	1	0.0230	0.0230	0.0992	0.7620	0.9535
cysNC	metals	1	2.0216	2.0216	5.1515	0.0575	0.3981

continued on next page

Table C.1 – continued from previous page

Gene	Treatment	Df	Sum Sq	Mean Sq	F value	Pr(>F)	p_{adj}
	enriched	1	0.3528	0.3528	0.8990	0.3746	0.5438
	metals*enriched	1	0.0017	0.0017	0.0044	0.9488	0.9956
BPNT1	metals	1	0.7920	0.7920	0.4274	0.5341	0.7396
	enriched	1	0.0143	0.0143	0.0077	0.9324	0.9429
	metals*enriched	1	0.0741	0.0741	0.0400	0.8472	0.9535
aprA	metals	1	0.5227	0.5227	1.6535	0.2394	0.5818
	enriched	1	3.1713	3.1713	10.0313	**0.0158**	0.0645
	metals*enriched	1	0.0309	0.0309	0.0978	0.7636	0.9535
aprB	metals	1	0.4526	0.4526	1.9197	0.2084	0.5708
	enriched	1	1.8721	1.8721	7.9406	**0.0259**	0.0824
	metals*enriched	1	0.0472	0.0472	0.2000	0.6683	0.9535
cysH	metals	1	1.3401	1.3401	1.1946	0.3106	0.6212
	enriched	1	0.4735	0.4735	0.4220	0.5367	0.6557
	metals*enriched	1	0.8194	0.8194	0.7304	0.4210	0.9159
ssuD	metals	1	0.4320	0.4320	0.6039	0.4626	0.7099
	enriched	1	4.0626	4.0626	5.6786	**0.0487**	0.1288
	metals*enriched	1	4.5892	4.5892	6.4146	**0.0391**	0.8793
E1.8.2.1	metals	1	7.8298	7.8298	21.2873	**0.0024**	0.2200

continued on next page

Table C.1 – continued from previous page

Gene	Treatment	Df	Sum Sq	Mean Sq	F value	Pr(>F)	p_{adj}
	enriched	1	4.3106	4.3106	11.7194	**0.0111**	0.0540
	metals*enriched	1	3.4485	3.4485	9.3755	**0.0183**	0.8793
SUOX	metals	1	0.5898	0.5898	0.4645	0.5175	0.7396
	enriched	1	4.9303	4.9303	3.8822	0.0895	0.2118
	metals*enriched	1	0.7132	0.7132	0.5616	0.4780	0.9159
TST	metals	1	0.5475	0.5475	0.4100	0.5424	0.7396
	enriched	1	0.2420	0.2420	0.1813	0.6831	0.7685
	metals*enriched	1	2.0097	2.0097	1.5050	0.2596	0.9159
dsrA	metals	1	0.0866	0.0866	0.7420	0.4176	0.6746
	enriched	1	3.3245	3.3245	28.4777	**0.0011**	**0.0091**
	metals*enriched	1	0.3433	0.3433	2.9406	0.1301	0.9147
dsrB	metals	1	0.0282	0.0282	0.1672	0.6949	0.8487
	enriched	1	3.2883	3.2883	19.4908	**0.0031**	**0.0199**
	metals*enriched	1	0.0810	0.0810	0.4804	0.5106	0.9159
cysI	metals	1	9.2576	9.2576	3.8576	0.0903	0.5078
	enriched	1	1.0374	1.0374	0.4323	0.5319	0.6557
	metals*enriched	1	0.0068	0.0068	0.0029	0.9589	0.9956
sir	metals	1	0.5915	0.5915	2.4968	0.1581	0.5708

continued on next page

Table C.1 – continued from previous page

	Gene	Treatment	Df	Sum Sq	Mean Sq	F value	Pr(>F)	p_{adj}
		enriched	1	16.0989	16.0989	67.9569	$\mathbf{7.5200 \cdot 10^{-5}}$	**0.0023**
		metals*enriched	1	0.1060	0.1060	0.4474	0.5250	0.9159
	asrC	metals	1	0.8372	0.8372	1.8026	0.2213	0.5708
		enriched	1	0.0159	0.0159	0.0342	0.8585	0.8985
		metals*enriched	1	0.0592	0.0592	0.1275	0.7315	0.9535
	phsA	metals	1	0.0497	0.0497	0.1429	0.7167	0.8487
		enriched	1	3.2273	3.2273	9.2707	**0.0187**	0.0691
		metals*enriched	1	0.0241	0.0241	0.0691	0.8002	0.9535
	phsC	metals	1	0.0811	0.0811	0.4167	0.5392	0.7396
		enriched	1	5.5397	5.5397	28.4678	**0.0011**	**0.0091**
		metals*enriched	1	0.2502	0.2502	1.2860	0.2941	0.9159
(c)	pmoB-amoB	metals	1	10.5681	10.5680	8.9496	**0.0202**	0.3339
		enriched	1	8.1213	8.1213	6.8776	**0.0343**	0.0995
		metals*enriched	1	0.0099	0.0099	0.0084	0.9300	0.9956
	pmoC-amoC	metals	1	4.4703	4.4703	6.3741	**0.0395**	0.3339
		enriched	1	28.3140	28.3140	40.3719	**0.0004**	**0.0058**
		metals*enriched	1	3.2278	3.2278	4.6025	0.0691	0.9147
	mdh1	metals	1	0.2101	0.2101	0.1705	0.6920	0.8487

continued on next page

Table C.1 – continued from previous page

Gene	Treatment	Df	Sum Sq	Mean Sq	F value	Pr(>F)	p_{adj}
	enriched	1	0.0065	0.0065	0.0053	0.9440	0.9440
	metals*enriched	1	1.5164	1.5164	1.2307	0.3039	0.9159
mtaB	metals	1	0.4145	0.4145	1.7427	0.2283	0.5708
	enriched	1	1.0281	1.0281	4.3225	0.0762	0.1903
	metals*enriched	1	0.2925	0.2925	1.2297	0.3041	0.9159
mtaC	metals	1	3.5048	3.5048	9.9168	**0.0162**	0.3339
	enriched	1	0.0991	0.0991	0.2803	0.6129	0.7286
	metals*enriched	1	0.8197	0.8197	2.3193	0.1716	0.9147
mcrB	metals	1	6.0844	6.0844	7.8687	**0.0263**	0.3339
	enriched	1	2.8683	2.8683	3.7095	0.0955	0.2203
	metals*enriched	1	0.3822	0.3822	0.4943	0.5047	0.9159
hdrA	metals	1	0.5227	0.5227	6.2259	**0.0413**	0.3339
	enriched	1	2.6791	2.6791	31.9113	**0.0008**	**0.0091**
	metals*enriched	1	0.0506	0.0506	0.6026	0.4630	0.9159
hdrB	metals	1	0.2516	0.2516	1.2250	0.3050	0.6212
	enriched	1	0.5710	0.5710	2.7800	0.1394	0.3060
	metals*enriched	1	0.0238	0.0238	0.1158	0.7436	0.9535
hdrC	metals	1	0.0282	0.0282	0.1231	0.7360	0.8603

continued on next page

Table C.1 – continued from previous page

	Gene	Treatment	Df	Sum Sq	Mean Sq	F value	Pr(>F)	p_{adj}
		enriched	1	0.0502	0.0502	0.2194	0.6537	0.7497
		metals*enriched	1	0.1582	0.1582	0.6908	0.4333	0.9159
(d)	GLDC	metals	1	0.0550	0.0550	0.8279	0.3931	0.6746
		enriched	1	0.8065	0.8065	12.1313	**0.0102**	0.0540
		metals*enriched	1	0.0959	0.0959	1.4425	0.2688	0.9159
	gcvPA	metals	1	0.0768	0.0768	0.5665	0.4762	0.7143
		enriched	1	0.0659	0.0659	0.4860	0.5082	0.6463
		metals*enriched	1	0.1431	0.1431	1.0551	0.3385	0.9159
	gcvPB	metals	1	0.3236	0.3236	15.0614	**0.0060**	0.2721
		enriched	1	0.0007	0.0007	0.0338	0.8593	0.8985
		metals*enriched	1	0.0666	0.0666	3.0973	0.1218	0.9147
	gcvT	metals	1	0.1003	0.1003	1.3265	0.2872	0.6190
		enriched	1	0.1065	0.1065	1.4080	0.2741	0.4390
		metals*enriched	1	0.0071	0.0071	0.0940	0.7681	0.9535
	CPS1	metals	1	9.8467	9.8467	9.0612	**0.0197**	0.3339
		enriched	1	1.5607	1.5607	1.4362	0.2698	0.4390
		metals*enriched	1	0.2322	0.2322	0.2137	0.6579	0.9535
	arcC	metals	1	0.0703	0.0703	0.2552	0.6289	0.8204

continued on next page

Table C.1 – continued from previous page

Gene	Treatment	Df	Sum Sq	Mean Sq	F value	Pr(>F)	p_{adj}
	enriched	1	0.5362	0.5362	1.9456	0.2057	0.3630
	metals*enriched	1	0.0141	0.0141	0.0511	0.8276	0.9535
pckA	metals	1	0.1499	0.1499	1.8999	0.2105	0.5708
	enriched	1	0.2098	0.2098	2.6590	0.1470	0.3150
	metals*enriched	1	0.0075	0.0075	0.0949	0.7670	0.9535
ppc	metals	1	0.4942	0.4941	0.7662	0.4104	0.6746
	enriched	1	0.0190	0.0190	0.0295	0.8685	0.8985
	metals*enriched	1	0.0505	0.0505	0.0783	0.7877	0.9535
maeA	metals	1	0.1073	0.1073	1.6056	0.2456	0.5818
	enriched	1	0.2839	0.2839	4.2486	0.0782	0.1903
	metals*enriched	1	0.4633	0.4633	6.9341	**0.0338**	0.8793
E1.1.1.39	metals	1	3.1870	3.1870	2.1482	0.1862	0.5708
	enriched	1	0.6184	0.6184	0.4168	0.5391	0.6557
	metals*enriched	1	0.5089	0.5089	0.3430	0.5765	0.9159
maeB	metals	1	0.0899	0.0899	2.3890	0.1661	0.5708
	enriched	1	0.0211	0.0211	0.5599	0.4787	0.6360
	metals*enriched	1	0.0387	0.0387	1.0287	0.3442	0.9159
porA	metals	1	0.1153	0.1153	0.9016	0.3740	0.6599

continued on next page

Table C.1 – continued from previous page

Gene	Treatment	Df	Sum Sq	Mean Sq	F value	Pr(>F)	p_{adj}
	enriched	1	9.3539	9.3539	73.1306	$\mathbf{5.9400 \cdot 10^{-5}}$	**0.0023**
	metals*enriched	1	0.3927	0.3927	3.0700	0.1232	0.9147
porB	metals	1	0.0173	0.0173	0.1499	0.7101	0.8487
	enriched	1	8.2245	8.2245	71.3823	$\mathbf{6.4200 \cdot 10^{-5}}$	**0.0023**
	metals*enriched	1	0.0426	0.0426	0.3697	0.5624	0.9159
porD	metals	1	0.0056	0.0056	0.0102	0.9223	0.9250
	enriched	1	8.2712	8.2712	15.0641	**0.0060**	**0.0363**
	metals*enriched	1	0.1126	0.1126	0.2051	0.6644	0.9535
porG	metals	1	0.0947	0.0947	0.3523	0.5715	0.7677
	enriched	1	13.0294	13.0290	48.4916	**0.0002**	**0.0039**
	metals*enriched	1	0.4145	0.4145	1.5426	0.2542	0.9159
nifJ	metals	1	0.2031	0.2031	2.4300	0.1630	0.5708
	enriched	1	0.7655	0.7655	9.1565	**0.0192**	0.0691
	metals*enriched	1	0.2416	0.2416	2.8897	0.1330	0.9147
IDH1	metals	1	0.0027	0.0027	0.0463	0.8358	0.9250
	enriched	1	1.2955	1.2955	22.6660	**0.0021**	0.0154
	metals*enriched	1	0.0020	0.0020	0.0353	0.8563	0.9535
IDH3	metals	1	0.1229	0.1229	0.2771	0.6149	0.8138

continued on next page

Table C.1 – continued from previous page

Gene	Treatment	Df	Sum Sq	Mean Sq	F value	Pr(>F)	p_{adj}
	enriched	1	0.2462	0.2462	0.5550	0.4806	0.6360
	metals*enriched	1	0.4523	0.4523	1.0196	0.3462	0.9159
PGD	metals	1	0.0325	0.0325	0.1543	0.7062	0.8487
	enriched	1	0.1016	0.1016	0.4820	0.5099	0.6463
	metals*enriched	1	0.1602	0.1602	0.7601	0.4122	0.9159
rbcS	metals	1	0.1304	0.1304	0.5959	0.4654	0.7099
	enriched	1	0.0342	0.0342	0.1564	0.7042	0.7754
	metals*enriched	1	0.1186	0.1186	0.5421	0.4855	0.9159
rbcL	metals	1	0.4624	0.4624	1.0834	0.3325	0.6235
	enriched	1	0.8634	0.8634	2.0232	0.1979	0.3565
	metals*enriched	1	0.0055	0.0055	0.0130	0.9125	0.9956
fmdA	metals	1	0.4533	0.4533	0.4438	0.5266	0.7396
	enriched	1	0.8622	0.8622	0.8440	0.3888	0.5468
	metals*enriched	1	3.8825	3.8825	3.8009	0.0922	0.9147
fmdB	metals	1	4.4829	4.4829	2.2754	0.1752	0.5708
	enriched	1	0.1027	0.1027	0.0521	0.8259	0.8849
	metals*enriched	1	0.7924	0.7924	0.4022	0.5461	0.9159
fmdC	metals	1	0.0535	0.0535	0.0265	0.8752	0.9250

continued on next page

Table C.1 – continued from previous page

Gene	Treatment	Df	Sum Sq	Mean Sq	F value	Pr(>F)	p_{adj}
	enriched	1	1.1598	1.1598	0.5752	0.4730	0.6360
	metals*enriched	1	0.0001	0.0001	0	0.9956	0.9956
fmdF	metals	1	2.5808	2.5808	5.9713	**0.0445**	0.3339
	enriched	1	5.0031	5.0031	11.5757	**0.0114**	0.0540
	metals*enriched	1	0.0738	0.0738	0.1707	0.6919	0.9535
fmdE	metals	1	1.2410	1.2410	0.7438	0.4170	0.6746
	enriched	1	3.4018	3.4018	2.0390	0.1964	0.3565
	metals*enriched	1	0.7274	0.7274	0.4360	0.5302	0.9159
FDH	metals	1	0.4992	0.4992	1.7658	0.2256	0.5708
	enriched	1	0.2714	0.2714	0.9599	0.3598	0.5309
	metals*enriched	1	0.2278	0.2278	0.8058	0.3992	0.9159
fdoG	metals	1	0.0204	0.0204	0.9817	0.3548	0.6386
	enriched	1	0.0310	0.0310	1.4940	0.2611	0.4352
	metals*enriched	1	0.0007	0.0007	0.0344	0.8582	0.9535
fdoH	metals	1	0.2605	0.2605	0.7346	0.4198	0.6746
	enriched	1	0.6616	0.6616	1.8662	0.2142	0.3707
	metals*enriched	1	0.0001	0.0001	0.0003	0.9856	0.9956
fdoI	metals	1	0.0048	0.0048	0.0116	0.9173	0.9250

continued on next page

Table C.1 – continued from previous page

Gene	Treatment	Df	Sum Sq	Mean Sq	F value	Pr(>F)	p_{adj}
	enriched	1	1.0706	1.0706	2.5755	0.1526	0.3193
	metals*enriched	1	0.1760	0.1760	0.4234	0.5360	0.9159
cooS	metals	1	0.1689	0.1689	1.2051	0.3086	0.6212
	enriched	1	0.8104	0.8104	5.7806	**0.0472**	0.1286
	metals*enriched	1	0.2737	0.2737	1.9525	0.2050	0.9159
coxS	metals	1	0.0575	0.0575	0.4432	0.5269	0.7396
	enriched	1	1.0163	1.0163	7.8354	**0.0266**	0.0824
	metals*enriched	1	0.6235	0.6235	4.8073	0.0644	0.9147
coxM	metals	1	0.0386	0.0386	0.0171	0.8998	0.9250
	enriched	1	14.7739	14.7739	6.5219	**0.0379**	0.1066
	metals*enriched	1	1.9686	1.9686	0.8691	0.3822	0.9159
coxL	metals	1	4.7503	4.7503	3.4552	0.1054	0.5132
	enriched	1	12.0840	12.0840	8.7896	**0.0210**	0.0699
	metals*enriched	1	0.5787	0.5787	0.4209	0.5371	0.9159
cdhA	metals	1	0.4341	0.4341	0.2071	0.6629	0.8487
	enriched	1	4.5260	4.5260	2.1590	0.1852	0.3565
	metals*enriched	1	0.0192	0.0192	0.0092	0.9264	0.9956
acsB	metals	1	0.4727	0.4727	1.8331	0.2178	0.5708

continued on next page

Table C.1 – continued from previous page

Gene	Treatment	Df	Sum Sq	Mean Sq	F value	Pr(>F)	p_{adj}
	enriched	1	0.2967	0.2967	1.1504	0.3190	0.4951
	metals*enriched	1	0.0224	0.0224	0.0867	0.7769	0.9535
cdhD	metals	1	0.5199	0.5199	6.5056	**0.0381**	0.3339
	enriched	1	2.2518	2.2518	28.1800	**0.0011**	**0.0091**
	metals*enriched	1	0.1842	0.1842	2.3046	0.1728	0.9147
cdhE	metals	1	0.8269	0.8269	4.1577	0.0808	0.4944
	enriched	1	1.9964	1.9964	10.0383	**0.0157**	0.0645
	metals*enriched	1	0.1358	0.1358	0.6831	0.4358	0.9159
cdhC	metals	1	4.7241	4.7241	6.1730	**0.0419**	0.3339
	enriched	1	1.5471	1.5471	2.0217	0.1981	0.3565
	metals*enriched	1	0.2603	0.2603	0.3402	0.5780	0.9159

Table C.2: Mass balance calculations. Benthic Community Respiration (BCR) represents the dissolved oxygen (DO) fluxes out of the sediment under dark conditions. C:N ratios are calculated as the mean total organic carbon (TOC) to total nitrogen (TN) ratio in non-enriched (C, M) and enriched (E, ME) treatments, respectively. Pot(N) represents the potential number of N molecules produced in a certain sample and is calculated as BCR/C:N, assuming a 1:1 conversion ratio of C and N. NH_3/NH_4^+ stands for ammonia/ammonium and NO_x stands for nitrogen oxides (nitrite (NO_2^-) and nitrate (NO_3^-)). DIN (Dissolved Inorganic Nitrogen) fluxes are defined as dark_NH_3/NH_4^+ + dark_NO_x. pot(N gas) represents the potential number of N gas molecules produced and is calculated as pot(N) – dark_DIN. The proportion of total N molecules theoretically produced in gaseous form, prop(N gas), is calculated as mean pot(N gas) / mean pot(N). † highlights the control sample which was excluded from the mass balance calculations due to greatly different flux values than other samples. These different values suggest that an error was committed during sampling or measurement of the gas content in the water sample. * highlights the sample which was identified as an outlier in the genetic data and therefore excluded from further analyses. C stands for control treatment, E stands for high organically enriched, M for high metal contamination and ME for high metal contamination with high organic enrichment.

sample	C:N	BCR	pot(N)	dark_NH_3/NH_4+	dark_NO_x	dark_DIN	pot(N gas)	mean pot(N)	mean pot(N gas)	prop(N gas)
C1	13.6	-3180	240	190	-20	170	70			
C2	13.6	-1840	140	100	-10	90	50			
C3†	13.6	-2620	190	130	70	200	-10			
M1	13.6	-3230	240	120	-10	110	130	180	45	0.25
M2	13.6	-2040	150	90	20	110	40			
M3	13.6	-1860	140	170	-20	150	-10			
E1	15.5	-2040	130	210	-30	180	-50			
E2	15.5	-2440	160	100	-30	70	90			
E3	15.5	-3170	200	100	-30	70	130			
ME1	15.5	-2240	140	140	-30	110	30	160	40	0.25
ME2*	15.5	-1920	120	150	-30	120	0			
ME3	15.5	-3030	200	180	-10	170	30			

Table C.3: Average of total measured metals and nutrients per treatment at the beginning (T0) and end (T1) of the field experiment. Metals and nutrients were measured in mg/kg sediment dry weight. TP stands for Total Phosphorous, TN for Total Nitrogen and TOC for Total Organic Carbon. C stands for control treatment, E stands for organically enriched, M for high metal contamination and ME for high metal contamination with organic enrichment.

		T0				T1			
		C	E	M	ME	C	E	M	ME
Metals	Al	2650	2600	4200	3700	2000	2750	3300	3600
	As	5.9	7.1	14.8	11.8	5.4	5.3	10.9	11.4
	Ba	2.5	6.6	10.4	13.2	6.7	7.3	11.4	12.8
	Cd	<1	<1	<1	<1	0.1	0.4	0.5	0.5
	Co	4.2	4.8	4.9	5.2	3.6	3.1	3.7	5.3
	Cr	10.5	11.3	28.0	24.1	10.0	14.3	23.2	25.4
	Cu	14.3	22.2	273.3	209.2	30.6	40.4	211.8	176.6
	Fe	10 000	9750	13 666.7	11 333.3	7750	13 000	11 050	13 600
	Mn	140.0	177.1	177.6	171.4	94.6	90.3	130.6	134.1
	Ni	4.4	4.7	6.5	5.4	4.1	5.6	6.2	6.4
	Pb	58.9	58.7	355.8	264.6	71.7	93.7	289.0	266.7
	S	2150	3100	2366.7	2566.7	1350	1900	1450	1600
	Sn	<2	<2	52.0	41.3	2.6	2.8	43.0	53.4
	V	19.3	19.2	34.1	27.9	17.5	27.9	30.4	35.0
	Zn	183.1	209.6	565.3	479.3	159.4	231.6	460.8	477.3
Nutrients	TP	385	995	560	1180	290	590	445	740
	TN	1100	2000	1150	2550	1005	1055	1250	1050
	TOC	14 000	16 500	18 500	26 000	14 000	15 000	17 000	21 500

Table C.4: Dissolved Oxygen (DO) and nutrient fluxes out of the sediment into the overlying water column. Benthic Community Respiration (BCR) represents the DO fluxes under dark conditions, while Net Primary Productivity (NPP) represents the DO fluxes under light conditions. Gross Primary Productivity (GPP) is calculated as NPP-BCR. Net nutrient fluxes are calculated as the mean of light and dark fluxes. NH_3/NH_4^+ stands for ammonia/ammonium, NO_x stands for nitrate (NO_3^-) and nitrite (NO_2^-), DON stands for Dissolved Organic Nitrogen and TDN for Total Dissolved Nitrogen (includes organic and inorganic N fluxes). * highlights the sample which was identified as an outlier in the genetic data and therefore excluded from further analyses. C stands for control samples, E for organically enriched, M for high metal contaminated and ME for high metals and enriched samples. The numbers stand for the replicate number.

	DO FLUXES			DARK FLUXES				LIGHT FLUXES				NET FLUXES			
Sample	NPP	BCR	GPP	NH_3/NH_4^+	NO_x	DON	TDN	NH_3/NH_4^+	NO_x	DON	TDN	NH_3/NH_4^+	NO_x	DON	TDN
C1	-3230	-3180	-50	190	-20	120	280	180	-10	90	270	180	-10	110	280
C2	-1860	-1840	-20	100	-10	60	150	100	-10	90	250	100	-10	70	200
C3	-2420	-2616	196	130	70	-40	160	130	10	60	200	130	40	10	180
E1	-2560	-2030	-530	210	-30	90	270	160	-20	40	170	180	-30	70	220
E2	-2620	-2440	-180	100	-30	60	120	70	-30	50	130	80	-30	50	130
E3	-2490	-3170	680	100	-30	40	110	50	-80	80	60	70	-50	60	80
M1	-2220	-3230	1010	120	-10	40	160	80	0	40	110	100	0	40	140
M2	-1660	-2040	380	90	20	80	180	60	20	60	190	70	20	70	190
M3	-1580	-1850	270	170	-20	130	280	120	-10	100	210	150	-20	110	240
ME1	-2240	-2230	-10	140	-30	80	200	150	-30	60	190	150	-30	70	190
ME2*	-1780	-1920	140	150	-30	40	160	60	-10	110	160	100	-20	70	160
ME3	-2210	-3030	820	180	-10	80	250	150	-20	170	410	160	-10	120	330

Table C.5: ANOVA results for flux data. DO stands for dissolved oxygen, NO_x for nitrogen oxides (nitrite and nitrate), NH_3/NH_4^+ for ammonia/ammonium, TDN for total dissolved nitrogen and DON for dissolved organic nitrogen. BCR stands for benthic community respiration (DO fluxes in the dark), NPP for net primary productivity (DO fluxes in light), NEM for net ecosystem metabolism (average of BCR and NPP) and GPP for gross primary productivity (NPP - BCR). Net flux for nutrients was calculated as the average of light and dark fluxes. Significant *p*-values are highlighted in bold.

	Flux type	Treatment	Df	Sum Sq	Mean Sq	F value	Pr(>F)
DO	BCR	metals	1	79197	79197	0.1898	0.6746
		enriched	1	530	530	0.0013	0.9724
		metals*enriched	1	236	236	0.0006	0.9816
	NPP	metals	1	1018016	1018016	6.1261	**0.0384**
		enriched	1	70059	70059	0.4216	0.5343
		metals*enriched	1	32146	32146	0.1934	0.6717
	NEM	metals	1	416274	416274	1.7021	0.2283
		enriched	1	20695	20695	0.0846	0.7785
		metals*enriched	1	9474	9474	0.0387	0.8489
	GPP	metals	1	529327	529327	2.804	0.1326
		enriched	1	58398	58398	0.3093	0.5933
		metals*enriched	1	26870	26870	0.1423	0.7158
NO_x	dark	metals	1	75.3	75.32	0.1027	0.7568
		enriched	1	2801.9	2801.86	3.8211	0.0864
		metals*enriched	1	372.7	372.66	0.5082	0.4962

continued on next page

Table C.5 – continued from previous page

	Flux type	Treatment	Df	Sum Sq	Mean Sq	F value	Pr(>F)
	light	metals	1	639.57	639.57	2.0773	0.1875
		enriched	1	2544.49	2544.49	8.2645	**0.0207**
		metals*enriched	1	223.05	223.05	0.7245	0.41942
	net	metals	1	68.98	68.98	0.1999	0.66664
		enriched	1	2671.64	2671.64	7.7425	**0.0238**
		metals*enriched	1	293.1	293.1	0.8494	0.3837
NH_3/NH_4^+	dark	metals	1	112.6	112.58	0.0553	0.82
		enriched	1	435	434.95	0.2137	0.6562
		metals*enriched	1	1021.3	1021.27	0.5019	0.4988
	light	metals	1	572.3	572.3	0.267	0.6193
		enriched	1	92.8	92.8	0.0433	0.8403
		metals*enriched	1	4829.3	4829.3	2.2534	0.1717
	net	metals	1	44.3	44.3	0.0229	0.8835
		enriched	1	31.5	31.47	0.0163	0.9017
		metals*enriched	1	2573	2573.04	1.33	0.2821
TDN	dark	metals	1	1438	1438.1	0.2878	0.6062
		enriched	1	1040	1040.2	0.2082	0.6603

continued on next page

Table C.5 – continued from previous page

	Flux type	Treatment	Df	Sum Sq	Mean Sq	F value	Pr(>F)
		metals*enriched	1	378	378.3	0.0757	0.7902
	light	metals	1	3141	3141.2	0.4772	0.5092
		enriched	1	701	700.8	0.1065	0.7526
		metals*enriched	1	30336	30335.6	4.6087	0.0641
	net	metals	1	2208	2207.5	0.4699	0.5124
		enriched	1	862	862.2	0.1835	0.6797
		metals*enriched	1	9372	9372.2	1.9951	0.1955
DON	dark	metals	1	1295.3	1295.32	0.5386	0.484
		enriched	1	0	0.03	0	0.9972
		metals*enriched	1	1012	1012.02	0.4208	0.5347
	light	metals	1	1322.5	1322.5	1.1791	0.3092
		enriched	1	597.2	597.2	0.5325	0.4864
		metals*enriched	1	3766.1	3766.1	3.3576	0.1043
	net	metals	1	1308.9	1308.9	1.1618	0.3125
		enriched	1	147.2	147.19	0.1306	0.7271
		metals*enriched	1	218.4	218.37	0.1938	0.6714

D

Appendix - Chapter 5

Table D.1: Linear model results for all genes significant for distance only (after exclusion of all interactions). The estimate is the estimated slope in the linear models. Positive and negative estimates symbolise up- and down-regulation adjacent to stormwater drains, respectively.

gene KO	gene name	p-value	estimate	SE
K00005	gldA	0.0348	−0.61	0.26
K00025	MDH1	0.0171	−0.92	0.34
K00027	maeA	0.0189	−0.47	0.18
K00029	maeB	0.0361	−0.34	0.15
K00100	E1.1.1.-	0.0404	0.38	0.17
K00108	CHDH	0.0208	−0.62	0.23
K00114	E1.1.2.8	0.0052	−1.02	0.31
K00117	gcd	0.0178	−0.69	0.25
K00119	E1.1.99.-	0.0490	−0.55	0.25
K00121	frmA	0.0003	−1.06	0.22
K00122	FDH	0.0212	−0.71	0.27
K00125	E1.2.1.2B2	0.0201	0.97	0.37
K00128	E1.2.1.3	0.0011	−0.55	0.13
K00140	mmsA	0.0002	−0.65	0.13
K00155	E1.2.1.-	0.0001	0.87	0.16
K00161	PDHA	0.0007	−0.50	0.12
K00162	PDHB	0.0146	−0.55	0.19
K00194	cdhD	0.0301	0.43	0.18
K00196	cooF	0.0295	−0.59	0.24
K00226	pyrD	0.0040	−0.31	0.08
K00234	SDHA	0.0157	−0.88	0.31
K00259	ald	0.0001	−0.62	0.12
K00260	gudB	0.0108	−0.73	0.25
K00265	gltB	0.0242	0.63	0.25
K00290	LYS1	0.0157	0.79	0.28

continued on next page

Table D.1 – continued from previous page

gene KO	gene name	p-value	estimate	SE
K00303	soxB	0.0091	−0.89	0.29
K00315	DMGDH	0.0248	−0.62	0.24
K00319	mtd	0.0328	−0.58	0.24
K00323	NNT	0.0005	−0.76	0.17
K00326	E1.6.2.2	0.0440	−0.51	0.23
K00327	E1.6.2.4	0.0007	−0.79	0.18
K00359	E1.6.-.-	0.0213	0.55	0.21
K00364	guaC	0.0253	−0.56	0.22
K00376	nosZ	0.0005	−1.25	0.27
K00401	mcrB	0.0110	−0.71	0.24
K00425	cydA	0.0129	0.70	0.24
K00434	E1.11.1.11	0.0259	−0.77	0.31
K00457	HPD	0.0419	−0.65	0.29
K00477	PHYH	0.0420	−0.39	0.17
K00496	E1.14.15.3	0.0092	−0.52	0.17
K00500	phhA	0.0096	−0.71	0.23
K00507	SCD	0.0278	−0.56	0.23
K00574	cfa	0.0289	0.54	0.22
K00602	purH	0.0364	0.37	0.16
K00606	panB	0.0468	0.35	0.16
K00611	OTC	0.0060	−0.64	0.20
K00665	FASN	0.0016	−1.07	0.27
K00666	K00666	0.0008	−0.54	0.12
K00671	NMT	0.0296	−0.57	0.23
K00677	lpxA	0.0431	0.41	0.18
K00691	mapA	0.0063	0.84	0.25
K00710	GALNT	0.0380	−0.71	0.31
K00794	ribH	0.0028	0.43	0.12
K00827	AGXT2	0.0149	−0.63	0.22
K00859	coaE	0.0430	0.53	0.23
K00864	glpK	0.0237	−0.70	0.27
K00889	PIP5K	0.0440	−0.54	0.24
K00910	ADRBK	0.0426	−0.46	0.20
K00926	arcC	0.0450	−0.42	0.19
K00928	lysC	0.0121	0.50	0.17

continued on next page

Table D.1 – continued from previous page

gene KO	gene name	p-value	estimate	SE
K00937	ppk	0.0304	−0.43	0.18
K00939	adk	0.0270	0.45	0.18
K00944	E2.7.4.10	0.0238	−0.81	0.32
K00946	thiL	0.0066	0.72	0.22
K00957	cysD	0.0227	−0.58	0.22
K01083	E3.1.3.8	0.0161	−0.95	0.34
K01092	suhB	0.0319	0.63	0.26
K01110	PTEN	0.0031	−0.86	0.24
K01115	PLD	0.0017	−0.68	0.17
K01130	aslA	0.0005	−0.60	0.13
K01183	E3.2.1.14	0.0001	−0.64	0.11
K01191	E3.2.1.24	0.0098	−0.86	0.28
K01193	sacA	0.0178	−0.79	0.29
K01236	E3.2.1.141	0.0295	0.61	0.25
K01273	DPEP1	0.0146	−0.69	0.25
K01277	DPP3	0.0011	0.90	0.21
K01279	TPP1	0	−1.03	0.17
K01280	TPP2	0.0453	−0.50	0.23
K01286	E3.4.16.4	0.0327	0.48	0.20
K01295	E3.4.17.11	0.0043	−0.81	0.24
K01379	CTSD	0.0367	−0.57	0.24
K01381	E3.4.23.25	0.0225	−0.55	0.21
K01419	clpQ	0.0364	0.48	0.20
K01426	amiE	0.0266	−0.36	0.14
K01434	E3.5.1.11	0.0320	−0.68	0.28
K01464	DPYS	0.0043	−0.71	0.21
K01537	E3.6.3.8	0.0079	−0.46	0.15
K01539	ATP1A	0.0017	−1.29	0.32
K01577	oxc	0.0361	−0.47	0.20
K01579	panD	0.0340	0.54	0.23
K01610	pckA	0.0056	−0.56	0.17
K01623	ALDO	0.0122	−0.90	0.31
K01627	kdsA	0.0096	0.50	0.17
K01630	garL	0.0150	−0.57	0.20
K01637	aceA	0.0343	−0.58	0.24

continued on next page

Table D.1 – continued from previous page

gene KO	gene name	p-value	estimate	SE
K01647	CS	0.0026	−0.63	0.17
K01649	leuA	0.0121	0.30	0.10
K01693	hisB	0.0212	0.47	0.18
K01696	trpB	0.0334	0.35	0.15
K01698	hemB	0.0150	0.55	0.19
K01699	pduC	0.0036	−0.76	0.21
K01736	aroC	0.0266	0.32	0.13
K01738	cysK	0.0451	−0.47	0.21
K01739	metB	0.0081	−0.42	0.13
K01749	hemC	0.0084	0.60	0.19
K01778	dapF	0.0069	0.74	0.23
K01779	E5.1.1.13	0.0374	−0.61	0.26
K01805	xylA	0.0457	−0.47	0.21
K01838	pgmB	0.0107	−0.56	0.19
K01847	MUT	0.0481	−0.40	0.18
K01868	TARS	0.0397	0.40	0.17
K01876	DARS	0.0249	0.34	0.13
K01879	glyS	0.0011	0.72	0.17
K01881	PARS	0.0348	0.42	0.18
K01895	ACSS	0.0201	−0.20	0.08
K01933	purM	0.0332	0.38	0.16
K01934	E6.3.3.2	0.0051	0.64	0.19
K01935	bioD	0.0302	0.41	0.17
K01940	argG	0.0085	0.39	0.13
K01941	E6.3.4.6	0.0326	−0.55	0.23
K01945	purD	0.0008	0.49	0.11
K01952	purL	0.0262	0.26	0.10
K01953	asnB	0.0053	0.48	0.14
K01955	carB	0.0027	0.27	0.07
K01969	E6.4.1.4B	0.0482	−0.50	0.23
K01993	ABC-2.TX	0.0224	0.61	0.24
K01995	livG	0.0042	−0.52	0.15
K01997	livH	0.0417	−0.38	0.17
K01999	livK	0.0124	−0.40	0.14
K02009	cbiN	0.0238	1.20	0.47

continued on next page

Table D.1 – continued from previous page

gene KO	gene name	p-value	estimate	SE
K02012	afuA	0.0129	−0.51	0.18
K02025	ABC.MS.P	0.0429	−0.68	0.30
K02026	ABC.MS.P1	0.0074	−0.72	0.22
K02027	ABC.MS.S	0.0242	−0.65	0.25
K02030	ABC.PA.S	0.0082	−0.44	0.14
K02031	ABC.PE.A	0.0063	−0.52	0.16
K02033	ABC.PE.P	0.0378	−0.43	0.18
K02034	ABC.PE.P1	0.0137	−0.61	0.21
K02054	ABC.SP.P1	0.0017	−0.79	0.20
K02055	ABC.SP.S	0.0057	−0.56	0.17
K02056	ABC.SS.A	0.0139	−0.63	0.22
K02057	ABC.SS.P	0.0209	−0.53	0.20
K02105	CTNNB1	0.0032	−1.01	0.28
K02210	MCM7	0.0057	−0.81	0.24
K02216	CHK1	0.0095	−0.48	0.16
K02274	coxA	0.0191	−0.80	0.29
K02401	flhB	0.0407	−0.53	0.23
K02426	sufE	0.0102	−0.58	0.19
K02428	rdgB	0.0010	0.72	0.17
K02440	GLPF	0.0175	−1.10	0.40
K02472	wecC	0.0109	0.85	0.29
K02510	hpaI	0.0065	−0.72	0.22
K02567	napA	0.0019	−0.97	0.25
K02573	napG	0.0285	−0.68	0.28
K02667	pilR	0.0082	0.49	0.16
K02775	PTS-Gat-EIIC	0.0032	−0.98	0.27
K02823	pyrDII	0.0359	0.57	0.25
K02868	RP-L11e	0.0153	−0.72	0.25
K02871	RP-L13	0.0278	0.43	0.17
K02873	RP-L13e	0.0127	−0.56	0.19
K02875	RP-L14e	0.0419	−0.62	0.28
K02878	RP-L16	0.0006	0.59	0.12
K02880	RP-L17e	0.0018	−1.04	0.26
K02881	RP-L18	0.0098	0.64	0.21
K02884	RP-L19	0.0111	0.54	0.18

continued on next page

Table D.1 – continued from previous page

gene KO	gene name	p-value	estimate	SE
K02888	RP-L21	0.0099	0.81	0.27
K02891	RP-L22e	0.0415	−0.43	0.19
K02893	RP-L23Ae	0.0106	−1.01	0.34
K02898	RP-L26e	0.0491	−0.39	0.18
K02907	RP-L30	0.0010	0.69	0.16
K02918	RP-L35e	0.0092	−0.96	0.31
K02920	RP-L36e	0.0147	−0.69	0.24
K02923	RP-L38e	0.0036	−0.73	0.20
K02927	RP-L40e	0.0072	−0.90	0.28
K02930	RP-L4e	0.0007	−0.97	0.22
K02935	RP-L7	0.0427	0.39	0.18
K02937	RP-L7e	0.0396	−0.69	0.30
K02941	RP-LP0	0.0295	−0.82	0.33
K02945	RP-S1	0.0099	0.35	0.12
K02950	RP-S12	0.0249	0.35	0.14
K02953	RP-S13e	0.0034	−0.82	0.23
K02954	RP-S14	0.0386	0.54	0.23
K02958	RP-S15e	0.0003	−1.28	0.25
K02959	RP-S16	0.0341	0.30	0.13
K02960	RP-S16e	0.0174	−0.97	0.36
K02961	RP-S17	0.0209	0.51	0.19
K02971	RP-S21e	0.0469	−0.63	0.28
K02974	RP-S24e	0.0261	−0.46	0.18
K02986	RP-S4	0.0018	0.49	0.12
K02987	RP-S4e	0.0035	−1.22	0.34
K02990	RP-S6	0.0375	0.62	0.27
K02992	RP-S7	0.0011	0.61	0.15
K02997	RP-S9e	0.0094	−0.88	0.28
K03002	RPA2	0.0009	−0.74	0.16
K03006	RPB1	0.0326	−0.64	0.27
K03007	RPB10	0.0432	−0.41	0.18
K03010	RPB2	0.0201	−0.57	0.21
K03028	PSMD2	0.0173	−0.73	0.26
K03032	PSMD1	0.0024	−0.74	0.19
K03033	PSMD3	0.0142	−0.71	0.25

continued on next page

Table D.1 – continued from previous page

gene KO	gene name	p-value	estimate	SE
K03047	rpoD	0.0095	0.66	0.22
K03086	rpoD	0.0244	0.30	0.12
K03106	SRP54	0.0320	0.30	0.12
K03110	ftsY	0.0271	0.36	0.15
K03118	tatC	0.0145	0.80	0.28
K03125	TAF1	0.0206	−0.53	0.20
K03178	UBE1	0.0243	−0.85	0.33
K03183	ubiE	0.0256	0.79	0.31
K03255	CLU1	0.0381	−0.62	0.27
K03267	ERF3	0.0160	−0.40	0.14
K03301	TC.AAA	0.0496	0.57	0.26
K03310	TC.AGCS	0.0033	−0.60	0.17
K03312	TC.ESS	0.0105	0.66	0.22
K03315	nhaC	0.0016	−0.69	0.17
K03319	TC.DASS	0.0456	−0.48	0.22
K03327	dinF	0.0091	0.65	0.21
K03379	E1.14.13.22	0.0098	−0.66	0.22
K03386	ahpC	0.0001	1.29	0.22
K03442	mscS	0.0104	0.55	0.18
K03520	coxL	0	−1.46	0.22
K03561	exbB	0.0098	0.41	0.14
K03564	DOT5	0.0028	0.47	0.13
K03583	recC	0.0301	0.54	0.22
K03608	minE	0.0312	0.45	0.19
K03609	minD	0.0218	0.56	0.21
K03621	plsX	0.0030	1.01	0.28
K03628	rho	0.0073	0.31	0.10
K03637	moaC	0.0078	0.33	0.11
K03641	tolB	0.0006	0.48	0.11
K03650	MSS1	0.0116	0.97	0.33
K03667	hslU	0.0061	0.48	0.15
K03684	rnd	0.0312	0.54	0.23
K03702	uvrB	0.0128	0.36	0.12
K03721	tyrR	0.0383	0.44	0.19
K03762	proP	0.0101	−0.52	0.17

continued on next page

Table D.1 – continued from previous page

gene KO	gene name	p-value	estimate	SE
K03781	katE	0.0005	0.86	0.18
K03799	htpX	0.0142	0.60	0.21
K03806	ampD	0.0440	−0.54	0.24
K03821	phbC	0.0003	−0.97	0.20
K03885	ndh	0.0392	−0.58	0.25
K03929	pnbA	0.0085	0.99	0.32
K03941	NDUFS8	0.0040	−0.71	0.20
K03955	NDUFAB1	0.0453	−0.44	0.20
K03969	pspA	0.0354	−0.44	0.18
K03979	obg	0.0376	0.49	0.21
K04047	dps	0.0239	0.51	0.20
K04078	HSPE1	0.0137	0.59	0.21
K04080	ibpA	0.0008	0.68	0.16
K04102	E4.1.1.55	0.0337	−0.57	0.24
K04112	badD	0.0007	−0.93	0.21
K04114	badF	0.0141	0.71	0.25
K04345	PKA	0.0418	−0.69	0.30
K04348	PPP3C	0.0260	−0.64	0.25
K04353	RAP1A	0.0249	−0.57	0.22
K04361	EGFR	0.0381	−0.66	0.28
K04392	RAC1	0.0095	−0.93	0.30
K04412	STK3	0.0326	−0.53	0.22
K04413	MINK	0.0141	−0.60	0.21
K04437	FLNA	0.0013	−1.38	0.34
K04445	MSK	0.0175	−0.61	0.22
K04468	NLK	0	−0.85	0.12
K04498	EP300	0.0110	−0.83	0.28
K04523	UBQLN	0.0229	−0.45	0.17
K04536	GNB1	0.0063	−0.84	0.25
K04550	LRP1	0.0024	−0.72	0.19
K04630	GNAI	0.0290	−0.62	0.25
K04632	GNAS	0.0137	−0.60	0.21
K04646	CLTC	0.0065	−0.98	0.30
K04651	hybF	0.0289	−0.79	0.32
K04656	hypF	0.0073	−0.58	0.18

continued on next page

Table D.1 – continued from previous page

gene KO	gene name	p-value	estimate	SE
K04688	RPS6KB	0.0284	−0.64	0.26
K04772	hhoA	0.0423	0.73	0.33
K04958	ITPR1	0.0064	−0.88	0.27
K04962	RYR2	0.0005	−1.60	0.34
K05290	PIGK	0.0181	−0.47	0.17
K05305	FUK	0.0096	−0.47	0.15
K05312	CHRNN	0	−1.16	0.10
K05351	E1.1.1.9	0.0197	−0.63	0.24
K05643	ABCA3	0.0327	−0.61	0.25
K05756	ARPC3	0.0082	−0.68	0.22
K05762	RDX	0.0424	−0.60	0.27
K05813	ugpB	0.0081	−0.81	0.26
K05849	SLC8A	0.0001	−1.17	0.20
K05850	ATP2B	0.0002	−1.48	0.29
K05853	ATP2A	0.0045	−1.37	0.40
K05857	PLCD	0.0023	−0.72	0.19
K05858	PLCB	0.0180	−0.53	0.20
K05879	dhaL	0.0304	−0.70	0.29
K05919	E1.15.1.2	0.0223	0.74	0.28
K06068	NPKC	0.0450	−0.40	0.18
K06071	PKN	0.0182	−0.57	0.21
K06114	SPTA	0.0067	−1.41	0.44
K06115	SPTB	0.0021	−1.55	0.40
K06178	rluB	0.0332	0.43	0.18
K06185	ABCF2	0.0244	−0.62	0.24
K06207	bipA	0.0500	0.59	0.27
K06215	pdxS	0.0384	0.28	0.12
K06233	LRP2	0.0061	−0.94	0.29
K06236	COL1AS	0.0178	−1.17	0.43
K06240	LAMA3_5	0.0178	−0.81	0.30
K06252	TN	0.0004	−0.99	0.21
K06269	PPP1C	0.0082	−1.09	0.35
K06271	TLN	0.0057	−0.85	0.25
K06282	E1.12.99.6S	0.0005	−0.69	0.15
K06445	fadE	0.0005	−0.65	0.14

continued on next page

Table D.1 – continued from previous page

gene KO	gene name	p-value	estimate	SE
K06525	ITGB4	0.0001	−0.97	0.17
K06639	CDC14	0.0479	−0.52	0.24
K06674	SMC2	0.0028	−0.83	0.23
K06839	SLIT2	0.0245	−0.55	0.22
K06902	UMF1	0.0278	0.68	0.27
K06910	K06910	0.0246	−0.92	0.36
K06943	NOG1	0.0114	−0.86	0.29
K07033	K07033	0.0002	1.07	0.21
K07043	K07043	0.0193	−0.65	0.24
K07080	K07080	0.0158	−0.35	0.13
K07090	K07090	0.0487	0.59	0.27
K07100	K07100	0.0434	−0.49	0.22
K07138	K07138	0.0491	−0.67	0.31
K07164	K07164	0.0449	0.56	0.25
K07203	FRAP	0.0231	−0.67	0.26
K07235	tusD	0.0127	1.22	0.42
K07278	ytfM	0.0015	0.66	0.17
K07299	SLC2A1	0.0112	−0.57	0.19
K07335	tmpC	0.0096	−0.76	0.25
K07341	doc	0.0209	−0.44	0.16
K07376	PRKG	0.0061	−0.73	0.22
K07402	xdhC	0.0452	−0.44	0.20
K07403	nfeD	0.0148	−0.64	0.23
K07445	K07445	0.0003	−0.79	0.16
K07507	mgtC	0.0075	0.51	0.16
K07516	fadN	0.0273	−0.27	0.11
K07538	had	0.0447	0.62	0.28
K07560	dtd	0.0421	−0.36	0.16
K07742	K07742	0.0401	−0.52	0.23
K07793	tctA	0.0168	−0.58	0.21
K07795	tctC	0.0274	−0.55	0.22
K08100	E1.3.3.5	0.0002	−1.06	0.21
K08253	E2.7.10.2	0.0307	0.50	0.21
K08352	phsA	0.0129	1.15	0.39
K08356	E1.20.9.1L	0.0012	−0.89	0.22

continued on next page

Table D.1 – continued from previous page

gene KO	gene name	p-value	estimate	SE
K08384	spoVD	0.0096	−0.46	0.15
K08585	CAPNN	0.0210	−0.61	0.23
K08653	MBTPS1	0.0197	−0.45	0.17
K08678	UXS1	0.0117	−0.51	0.17
K08746	SLC27A2	0.0432	−0.41	0.18
K08789	MAST	0.0490	−0.45	0.21
K08796	BRSK	0.0442	−0.40	0.18
K08826	HIPK	0.0019	−0.86	0.22
K08867	PRKWNK	0.0110	−0.69	0.23
K08958	CSNK1G	0.0016	−0.70	0.18
K09013	sufC	0.0260	0.53	0.21
K09125	K09125	0.0163	0.53	0.19
K09160	K09160	0.0482	0.44	0.20
K09267	SOX1S	0.0437	−0.41	0.18
K09457	queF	0.0105	0.61	0.20
K09478	ACADSB	0.0435	−0.52	0.23
K09490	HSPA5	0.0098	−0.82	0.27
K09495	TRIC5	0.0483	−0.52	0.24
K09496	CCT4	0.0150	−0.92	0.33
K09497	CCT5	0.0085	−0.86	0.27
K09498	CCT6	0.0032	−0.84	0.23
K09516	RETSAT	0.0420	−0.46	0.20
K09540	SEC63	0.0117	−0.69	0.24
K09580	PDIA1	0.0465	−0.81	0.37
K09582	PDIA4	0.0062	−0.65	0.20
K09702	K09702	0.0120	−0.52	0.18
K09767	K09767	0.0174	0.63	0.23
K09816	znuB	0.0127	0.67	0.23
K09888	zapA	0.0016	0.73	0.18
K09949	K09949	0.0471	0.59	0.27
K10024	aotQ	0.0139	−0.62	0.22
K10025	aotP	0.0465	−0.49	0.22
K10112	msmX	0.0222	−0.55	0.21
K10117	msmE	0.0049	−1.02	0.30
K10352	MYH	0.0067	−1.45	0.45

continued on next page

Table D.1 – continued from previous page

gene KO	gene name	p-value	estimate	SE
K10354	ACTA1	0.0235	−0.78	0.31
K10357	MYO5	0.0008	−1.00	0.22
K10359	MYO7	0.0038	−0.98	0.28
K10361	MYO15	0.0489	−0.53	0.24
K10389	TUBG	0.0018	−0.76	0.20
K10395	KIF4S	0.0240	−0.53	0.21
K10440	rbsC	0.0051	−0.64	0.19
K10441	rbsA	0.0099	−0.51	0.17
K10593	EDD1	0.0089	−0.68	0.22
K10601	SYVN1	0.0397	−0.56	0.24
K10691	ZUBR1	0.0027	−0.82	0.22
K10693	PAM	0.0113	−0.70	0.24
K10705	GAPDHS	0.0006	−1.10	0.25
K10747	LIG1	0.0483	−0.68	0.31
K10823	oppF	0.0428	−0.46	0.20
K10843	ERCC3	0.0181	0.34	0.13
K11070	potC	0.0391	−0.53	0.23
K11076	potG	0.0179	−0.57	0.21
K11088	SNRPD3	0	−1.03	0.14
K11098	SNRPF	0.0146	−0.68	0.24
K11173	ADHFE1	0.0381	−0.65	0.28
K11179	tusE	0.0018	0.60	0.15
K11180	dsrA	0.0088	0.89	0.29
K11181	dsrB	0.0175	0.72	0.26
K11188	PRDX6	0.0194	−1.12	0.42
K11212	cofD	0.0177	−0.61	0.22
K11253	H3	0.0052	−1.09	0.33
K11254	H4	0.0048	−1.08	0.32
K11263	bccA	0.0136	−0.69	0.24
K11290	I2PP2A	0.0001	−0.90	0.16
K11422	SETD1	0.0432	−0.41	0.18
K11481	AURKA	0.0458	−0.48	0.22
K11584	PPP2R5	0.0105	−0.79	0.26
K11593	ELF2C	0.0142	−0.83	0.29
K11600	RRP41	0.0485	0.58	0.27

continued on next page

Table D.1 – continued from previous page

gene KO	gene name	p-value	estimate	SE
K11645	K11645	0.0372	−0.45	0.19
K11647	SMARCA2_4	0.0182	−0.72	0.27
K11824	AP2A	0.0269	−0.56	0.23
K11895	vasB	0.0085	0.70	0.23
K11912	ppkA	0.0004	−1.02	0.22
K11997	TRIM2_3	0.0033	−0.90	0.25
K12184	VPS28	0.0015	−0.63	0.16
K12194	CHMP4	0.0138	−0.46	0.16
K12323	ANPRA	0.0406	−0.49	0.22
K12340	tolC	0.0104	−0.78	0.26
K12355	REF1	0.0097	−0.47	0.16
K12368	dppA	0.0049	−0.38	0.11
K12375	ARSI_J	0.0150	−0.50	0.18
K12483	EHD1	0.0307	−0.51	0.21
K12511	tadC	0.0344	−0.46	0.19
K12574	rnj	0.0102	0.35	0.12
K12604	CNOT1	0.0095	−0.84	0.28
K12619	XRN2	0.0202	−0.69	0.26
K12818	DHX8	0.0339	−0.67	0.28
K12820	DHX15	0.0427	−0.63	0.28
K12829	SF3B2	0.0179	−0.74	0.27
K12830	SF3B3	0.0394	−0.59	0.26
K12837	U2AF2	0.0197	−0.59	0.22
K12838	PUF60	0.0097	−0.47	0.16
K12845	SNU13	0.0466	−0.46	0.21
K12854	SNRNP200	0.0270	−0.70	0.28
K12856	PRPF8	0.0085	−0.87	0.28
K12858	DDX23	0.0441	−0.49	0.22
K12867	SYF1	0.0470	−0.74	0.34
K12868	SYF2	0.0437	−0.41	0.18
K12869	CRN	0.0445	−0.59	0.26
K12879	THOC2	0.0450	−0.40	0.18
K13044	HNRNPABD	0.0434	−0.46	0.21
K13182	DDX39	0.0472	−0.47	0.22
K13207	CELF	0.0016	−0.83	0.21

continued on next page

Table D.1 – continued from previous page

gene KO	gene name	p-value	estimate	SE
K13279	PRDX1	0.0371	−0.62	0.27
K13529	ada-alkA	0.0426	−0.46	0.20
K13652	K13652	0.0400	0.50	0.22
K13693	K13693	0.0492	−0.54	0.25
K13811	PAPSS	0.0105	−0.83	0.28
K13831	hps-phi	0.0099	0.56	0.18
K13922	pduP	0.0142	−0.67	0.24
K13988	NUDT9	0.0195	−0.45	0.17
K14006	SEC23	0.0191	−0.64	0.24
K14081	mtaC	0.0224	−0.66	0.25
K14084	mttC	0.0028	−0.71	0.19
K14152	HIS4	0.0095	−0.48	0.16
K14326	UPF1	0.0009	−1.04	0.24
K14327	UPF2	0.0443	−0.56	0.25
K14402	CPSF2	0.0176	−0.58	0.21
K14469	K14469	0.0114	−0.52	0.18
K14563	NOP1	0.0399	−0.81	0.35
K14640	PIT	0.0417	0.48	0.21
K14652	ribBA	0.0126	0.50	0.17
K14802	ATP8A	0.0098	−0.57	0.19
K14820	BRIX1	0.0124	−0.54	0.19
K14986	fixL	0.0011	−0.78	0.19
K15012	regA	0.0114	−0.52	0.18
K15022	fdhB	0.0081	0.95	0.30
K15029	EIF3L	0.0491	−0.57	0.26
K15030	EIF3M	0.0454	−0.39	0.18
K15034	yaeJ	0.0390	0.60	0.26
K15172	SPT5	0.0192	−0.60	0.23
K15223	SPP27	0.0014	−0.68	0.17
K15283	SLC35E1	0.0491	−0.53	0.24
K15292	STXBP1	0.0103	−0.69	0.23
K15423	PPP4C	0.0034	−0.76	0.21
K15498	PPP6C	0.0496	−0.61	0.28
K15509	hpsN	0.0200	−0.70	0.26
K15512	boxB	0.0048	−0.80	0.24

continued on next page

Table D.1 – continued from previous page

gene KO	gene name	p-value	estimate	SE
K15598	thiY	0.0490	−0.47	0.22
K15601	KDM3	0.0204	−0.53	0.20
K15620	GOLPH3	0.0121	−0.60	0.21
K15698	RNF121	0.0095	−0.49	0.16
K15778	pmm-pgm	0.0304	0.68	0.28
K15836	fhlA	0.0004	0.72	0.15
K15864	nirS	0	−1.34	0.20
K15893	HPR1	0.0075	−0.76	0.24
K15916	pgi-pmi	0.0327	0.48	0.20
K16178	NA	0.0097	−0.76	0.25
K16185	NA	0.0251	−0.59	0.23
K16213	NA	0.0110	−0.65	0.22
K16307	NA	0.0013	−0.76	0.19
K16681	NA	0.0048	−0.90	0.27
K16846	NA	0.0216	−0.61	0.23
K16850	NA	0.0038	0.72	0.20
K17081	NA	0.0038	−0.70	0.19
K17086	NA	0.0027	−0.77	0.21
K17204	NA	0.0168	−0.71	0.26
K17225	NA	0.0014	1.03	0.25
K17229	NA	0.0068	−1.22	0.38
K17230	NA	0	−0.80	0.13
K17263	NA	0.0263	−0.51	0.20
K17307	NA	0.0254	−0.56	0.22
K17320	NA	0.0441	−0.70	0.31
K17540	NA	0.0126	−1.44	0.50
K17732	NA	0	−0.99	0.14
K17734	NA	0.0299	−0.89	0.36
K17751	NA	0.0011	−1.83	0.44
K17760	NA	0.0394	−0.50	0.22
K17865	NA	0.0006	1.02	0.22
K17871	NA	0.0455	−0.40	0.18
K17898	NA	0.0351	−0.49	0.21
K17923	NA	0.0097	−0.47	0.16
K17943	NA	0.0029	−0.77	0.21

continued on next page

Table D.1 – continued from previous page

gene KO	gene name	p-value	estimate	SE
K18029	NA	0.0012	−0.72	0.17
K18139	NA	0.0301	0.46	0.19
K18277	NA	0.0496	−0.53	0.25
K18441	NA	0.0234	−0.48	0.19
K18585	NA	0.0183	−1.20	0.44
K18622	NA	0.0096	−0.47	0.16
K18669	NA	0.0246	−0.45	0.17
K18749	NA	0.0435	−0.46	0.20

Table D.2: All genes that were significant for distance only (after exclusion of all interactions) and had an estimate of >1 or <-1. The estimate is the estimated slope in the linear models. Estimates of >1 and <-1 symbolise an up- and down-regulation of the gene at the stormwater drain, respectively. Gene KEGG orthologous ID (KO), pathway KO and pathway name are shown for every gene.

gene KO	pathway KO	pathway name
estimate<-1		
K10352	path:ko04530	Tight junction
K02987	path:ko03010	Ribosome
K03520	path:ko00633	Nitrotoluene degradation
K03520	path:ko00680	Methane metabolism
K06269	path:ko03015	mRNA surveillance pathway
K06269	path:ko04113	Meiosis - yeast
K06269	path:ko04114	Oocyte meiosis
K06269	path:ko04510	Focal adhesion
K06269	path:ko04810	Regulation of actin cytoskeleton
K00376	path:ko00910	Nitrogen metabolism
K08100	path:ko00860	Porphyrin and chlorophyll metabolism
K02958	path:ko03010	Ribosome
K00121	path:ko00010	Glycolysis / Gluconeogenesis
K00121	path:ko00071	Fatty acid metabolism
K00121	path:ko00350	Tyrosine metabolism
K00121	path:ko00625	Chloroalkane and chloroalkene degradation
K00121	path:ko00626	Naphthalene degradation
K00121	path:ko00680	Methane metabolism

continued on next page

Table D.2 – continued from previous page

gene KO	pathway KO	pathway name
K00121	path:ko00830	Retinol metabolism
K00121	path:ko00980	Metabolism of xenobiotics by cytochrome P450
K00121	path:ko00982	Drug metabolism - cytochrome P450
K06236	path:ko04510	Focal adhesion
K06236	path:ko04512	ECM-receptor interaction
K10117	path:ko02010	ABC transporters
K05853	path:ko04020	Calcium signaling pathway
K14326	path:ko03013	RNA transport
K14326	path:ko03015	mRNA surveillance pathway
K05850	path:ko04020	Calcium signaling pathway
K00114	path:ko00010	Glycolysis / Gluconeogenesis
K00114	path:ko00625	Chloroalkane and chloroalkene degradation
K00114	path:ko00640	Propanoate metabolism
K15864	path:ko00910	Nitrogen metabolism
K02880	path:ko03010	Ribosome
K04962	path:ko04020	Calcium signaling pathway
K02893	path:ko03010	Ribosome
K01279	path:ko04142	Lysosome
K04437	path:ko04010	MAPK signaling pathway
K04437	path:ko04510	Focal adhesion
K00665	path:ko00061	Fatty acid biosynthesis
K11188	path:ko00360	Phenylalanine metabolism
K11188	path:ko00680	Methane metabolism
K11188	path:ko00940	Phenylpropanoid biosynthesis
K11912	path:ko03070	Bacterial secretion system
K02105	path:ko04310	Wnt signaling pathway
K02105	path:ko04510	Focal adhesion
K02105	path:ko04520	Adherens junction
K02105	path:ko04530	Tight junction
K05849	path:ko04020	Calcium signaling pathway
K11088	path:ko03040	Spliceosome
K10705	path:ko00010	Glycolysis / Gluconeogenesis
estimate>1		
K03621	path:ko00561	Glycerolipid metabolism

continued on next page

Table D.2 – continued from previous page

gene KO	pathway KO	pathway name
K03621	path:ko00564	Glycerophospholipid metabolism
K07235	path:ko04122	Sulfur relay system
K02009	path:ko02010	ABC transporters

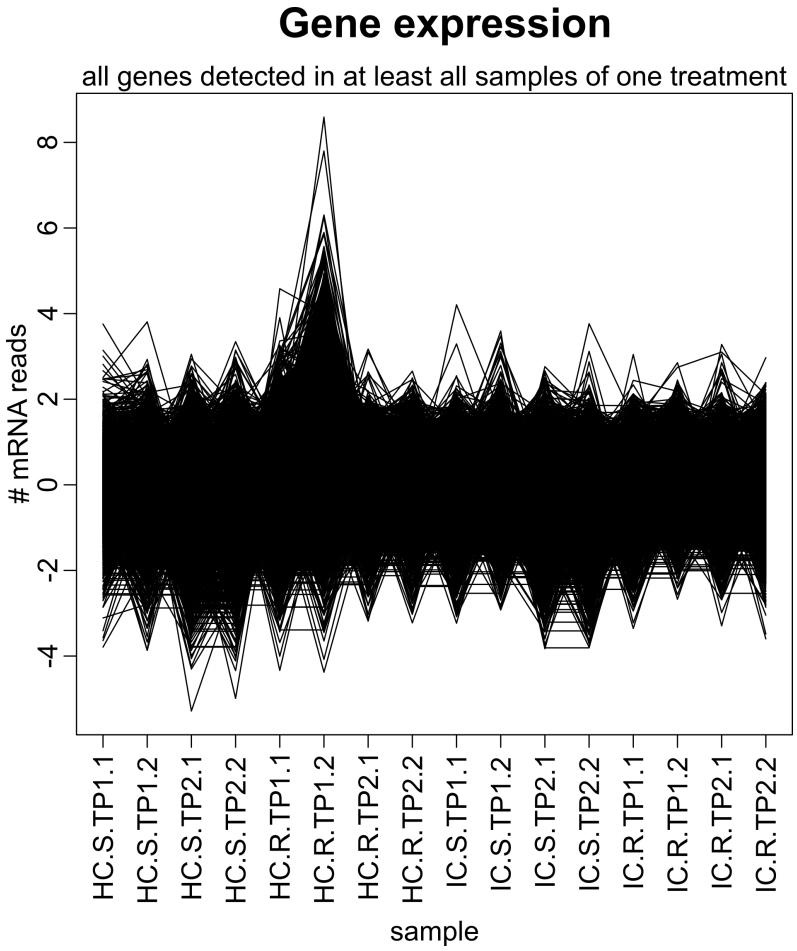

Figure D.1: Gene expression values for all genes included in the final dataset used for statistical analyses (detected in all samples of at least one treatment). This plot identifies sample HC.R.TP1.2 as an outlier based on generally higher reads (probably due to RNA degradation; RIN=5.9) and justifies its exclusion from further analyses. Samples are named according to their location (HC: Hen and Chicken Bay; IC: Iron Cove), distance from stormwater drains (S: adjacent to stormwater drain; R: reference site 1 km away), time point of sampling (TP1: February 2014; TP2: March 2014) and replicate number (1 and 2).

Table D.3: Temperature and salinity of the water at sampling sites. Samples are named according to their location (HC: Hen and Chicken Bay; IC: Iron Cove), distance from stormwater drains (S: adjacent to stormwater drain; R: reference site 1km away), time point of sampling (TP1: February 2014; TP2: March 2014) and replicate number (1 and 2).

Sample	Temperature	Salinity
HC.R.TP1.1	25.44	35.73
HC.R.TP1.2		
HC.R.TP2.1	24.3	32.36
HC.R.TP2.2		
IC.R.TP1.1	24.74	36.04
IC.R.TP1.2		
IC.R.TP2.1	25.59	34.96
IC.R.TP2.2		
HC.S.TP1.1	25.03	35.98
HC.S.TP1.2		
HC.S.TP2.1	25.26	33.22
HC.S.TP2.2		
IC.S.TP1.1	25.13	36.08
IC.S.TP1.2		
IC.S.TP2.1	25.89	34.68
IC.S.TP2.2		

References

Aelion, C. M. and Warttinger, U. (2010). Sulfide inhibition of nitrate removal in coastal sediments. *Estuaries and Coasts*, 33(3):798–803.

Ager, D., Evans, S., Li, H., Lilley, A. K., and van der Gast, C. J. (2010). Anthropogenic disturbance affects the structure of bacterial communities. *Environmental microbiology*, 12(3):670–678.

Aiken, G. R., Hsu-Kim, H., and Ryan, J. N. (2011). Influence of dissolved organic matter on the environmental fate of metals, nanoparticles, and colloids. *Environmental Science & Technology*, 45:3196–3201.

Allison, G. (2004). The influence of species diversity and stress intensity on community resistance and resilience. *Ecological Monographs*, 74(1):117–134.

Allison, S. D., Lu, Y., Weihe, C., Goulden, M. L., Martiny, A. C., Treseder, K. K., and Martiny, J. B. H. (2013). Microbial abundance and composition influence litter decomposition response to environmental change. *Ecology*, 94(3):714–725.

Allison, S. D. and Martiny, J. B. H. (2008). Resistance, resilience, and redundancy in microbial communities. *Proceedings of the National Academy of Sciences*, 105:11512–11519.

Altmann, D., Stief, P., Amann, R., Beer, D. D., and Schramm, A. (2003). In situ distribution and activity of nitrifying bacteria in freshwater sediment. *Environmental Microbiology*, 5(9):798–803.

Amaral-Zettler, L. A., McCliment, E. A., Ducklow, H. W., and Huse, S. M. (2009). A method for studying protistan diversity using massively parallel sequencing of V9 hypervariable regions of small-subunit ribosomal RNA genes. *PLoS ONE*, 4(7):e6372.

Anders, S. and Huber, W. (2010). Differential expression analysis for sequence count data. *Genome Biology*, 11:R106.

Antizar-Ladislao, B. (2010). Bioremediation: Working with bacteria. *Elements*, 6:389–394.

Arias-Estévez, M., López-Periago, E., Martínez-Carballo, E., Simal-Gándara, J., Mejuto, J. C., and García-Río, L. (2008). The mobility and degradation of pesticides in soils and the pollution of groundwater resources. *Agriculture, Ecosystems and Environment*, 123:247–260.

Arnold, C. L. and Gibbons, C. J. (1996). Impervious surface coverage: The emergence of a key environmental indicator. *Journal of the American Planning Association*, 62(2):243–258.

Arrigo, K. R. (2005). Marine microorganisms and global nutrient cycles. *Nature*, 437:349–355.

Asami, H., Aida, M., and Watanabe, K. (2005). Accelerated sulfur cycle in coastal marine sediment beneath areas of intensive shellfish aquaculture. *Applied and Environmental Microbiology*, 71(6):2925–2933.

Aylagas, E., Borja, Á., Irigoien, X., and Rodríguez-Ezpeleta, N. (2016). Benchmarking DNA metabarcoding for biodiversity-based monitoring and assessment. *Frontiers in Marine Science*, 3:Article 96.

Aylagas, E., Borja, Á., and Rodríguez-Ezpeleta, N. (2014). Environmental status assessment using DNA metabarcoding: Towards a genetics based marine biotic index (gAMBI). *PLoS ONE*, 9(3):e90529.

Azam, F. (1998). Microbial control of oceanic carbon flux: The plot thickens. *Science*, 280:694–696.

Azarbad, H., Niklińska, M., Van Gestel, C. A. M., Van Straalen, N. M., Röling, W. F. M., and Laskowski, R. (2013). Microbial community structure and functioning along metal pollution gradients. *Environmental Toxicology and Chemistry*, 32(9):1992–2002.

Babich, H. and Stotzky, G. (1985). Heavy metal toxicity to microbe-mediated ecologic processes: A review and potential application to regulatory policies. *Environmental Research*, 36:111–137.

Baird, D. J., Baker, C. J. O., Brua, R. B., Hajibabaei, M., McNicol, K., Pascoe, T. J., and de Zwart, D. (2011). Toward a knowledge infrastructure for traits-based ecological risk assessment. *Integrated Environmental Assessment and Management*, 7(2):209–215.

Baird, D. J. and Hajibabaei, M. (2012). Biomonitoring 2.0: A new paradigm in ecosystem assessment made possible by next-generation DNA sequencing. *Molecular Ecology*, 21:2039–2044.

Barbier, E. B., Hacker, S. D., Kennedy, C., Koch, E. W., Stier, A. C., and Silliman, B. R. (2011). The value of estuarine and coastal ecosystem services. *Ecological Monographs*, 81(2):169–193.

Barbour, M. T. and Paul, M. J. (2010). Adding value to water resource management through biological assessment of rivers. *Hydrobiologia*, 651:17–24.

Basak, P., Pramanik, A., Sengupta, S., Nag, S., Bhattacharyya, A., Roy, D., Pattanayak, R., Ghosh, A., Chattopadhyay, D., and Bhattacharyya, M. (2016). Bacterial diversity assessment of pristine mangrove microbial community from Dhulibhashani, Sundarbans using 16S rRNA gene tag sequencing. *Genomics Data*, 7:76–78.

Batley, G. E. and Simpson, S. L. (2009). Development of guidelines for ammonia in estuarine and marine water systems. *Marine Pollution Bulletin*, 58:1472–1476.

Bender, E. A., Case, T. J., and Gilpin, M. E. (1984). Perturbation experiments in community ecology: Theory and practice. *Ecology*, 65(1):1–13.

Benedetti, M. F., Van Riemsdijk, W. H., Koopal, L. K., Kinniburgh, D. G., Gooddy, D. C., and Milne, C. J. (1996). Metal ion binding by natural organic matter: From the model to the field. *Geochimica et Cosmochimica Acta*, 60(14):2503–2513.

Bengtsson-Palme, J., Alm Rosenblad, M., Molin, M., and Blomberg, A. (2014). Metagenomics reveals that detoxification systems are underrepresented in marine bacterial communities. *BMC genomics*, 15(749):1–17.

Berga, M., Székely, A. J., and Langenheder, S. (2012). Effects of disturbance intensity and frequency on bacterial community composition and function. *PLoS ONE*, 7(5).

Bergmann, G. T., Bates, S. T., Eilers, K. G., Lauber, C. L., Caporaso, J. G., Walters, W. A., Knight, R., and Fierer, N. (2011). The under-recognized dominance of Verrucomicrobia in soil bacterial communities. *Soil Biology and Biochemistry*, 43:1450–1455.

Bernard, R. J., Mortazavi, B., and Kleinhuizen, A. A. (2015). Dissimilatory nitrate reduction to ammonium (DNRA) seasonally dominates NO3- reduction pathways in an anthropogenically impacted sub-tropical coastal lagoon. *Biogeochemistry*, 125(1):47–64.

Birch, G. F., Eyre, B. D., and Taylor, S. E. (1999). The distribution of nutrients in bottom sediments of Port Jackson (Sydney Harbour), Australia. *Marine Pollution Bulletin*, 38(12):1247–1251.

Birch, G. F., Gunns, T. J., Chapman, D., and Harrison, D. (2016). Development of an estuarine assessment scheme for the management of a highly urbanised catchment/estuary system, Sydney estuary, Australia. *Environmental Monitoring and Assessment*, 188(294):1–14.

Birch, G. F., Lean, J., and Gunns, T. J. (2015). Historic change in catchment land use and metal loading to Sydney estuary, Australia (1788 - 2010). *Environmental Monitoring and Assessment*, 187(594):1–15.

Birch, G. F. and McCready, S. (2009). Catchment condition as a major control on the quality of receiving basin sediments (Sydney Harbour, Australia). *Science of the Total Environment*, 407:2820–2835.

Birch, G. F., McCready, S., Long, E. R., Taylor, S. E., and Spyrakis, G. (2008). Contaminant chemistry and toxicity of sediments in Sydney Harbour, Australia: Spatial extent and chemistry-toxicity relationships. *Marine Ecology Progress Series*, 363:71–87.

Birch, G. F. and Rochford, L. (2010). Stormwater metal loading to a well-mixed/stratified estuary (Sydney Estuary, Australia) and management implications. *Environmental Monitoring and Assessment*, 169:531–551.

Birch, G. F. and Taylor, S. E. (1999). Source of heavy metals in sediments of the Port Jackson estuary, Australia. *Science of the Total Environment*, 227:123–138.

Bissett, A., Brown, M. V., Siciliano, S. D., and Thrall, P. H. (2013). Microbial community responses to anthropogenically induced environmental change: Towards a systems approach. *Ecology Letters*, 16:128–139.

Bissett, A., Burke, C., Cook, P. L. M., and Bowman, J. P. (2007). Bacterial community shifts in organically perturbed sediments. *Environmental Microbiology*, 9(1):46–60.

Bogdan, J. J., Budd, J. W., Eadie, B. J., and Hornbuckle, K. C. (2002). The effect of a large resuspension event in Southern Lake Michigan on the short-term cycling of organic contaminants. *Journal of Great Lakes Research*, 28(3):338–351.

Bonada, N., Prat, N., Resh, V. H., and Statzner, B. (2006). Developments in aquatic insect biomonitoring: A comparative analysis of recent approaches. *Annual Review of Entomology*, 51:495–523.

Borja, Á. and Elliott, M. (2013). Marine monitoring during an economic crisis: The cure is worse than the disease. *Marine Pollution Bulletin*, 68:1–3.

Borja, Á., Muxika, I., and Rodríguez, J. G. (2009). Paradigmatic responses of marine benthic communities to different anthropogenic pressures, using M-AMBI, within the European Water Framework Directive. *Marine Ecology*, 30:214–227.

Bourlat, S. J., Borja, Á., Gilbert, J. A., Taylor, M. I., Davies, N., Weisberg, S. B., Griffith, J. F., Lettieri, T., Field, D., Benzie, J., Glöckner, F. O., Rodríguez-Ezpeleta, N., Faith, D. P., Bean, T. P., and Obst, M. (2013). Genomics in marine monitoring: New opportunities for assessing marine health status. *Marine Pollution Bulletin*, 74:19–31.

Bowen, J. L., Babbin, A. R., Kearns, P. J., and Ward, B. B. (2014). Connecting the dots: Linking nitrogen cycle gene expression to nitrogen fluxes in marine sediment mesocosms. *Frontiers in Microbiology*, 5:Article 429.

Brunet, R. C. and Garcia-Gil, L. J. (1996). Sulfide-induced dissimilatory nitrate reduction to ammonia in anaerobic freshwater sediments. *FEMS Microbiology Ecology*, 21:131–138.

Buchfink, B., Xie, C., and Huson, D. H. (2015). Fast and sensitive protein alignment using DIAMOND. *Nature Methods*, 12(1):59–60.

Bulow, S. E., Francis, C. A., Jackson, G. A., and Ward, B. B. (2008). Sediment denitrifier community composition and nirS gene expression investigated with functional gene microarrays. *Environmental Microbiology*, 10(11):3057–3069.

Bundschuh, M. and Mckie, B. G. (2015). An ecological and ecotoxicological perspective on fine particulate organic matter in streams. *Freshwater Biology*, optdoi:10.111.

Burgin, A. J. and Hamilton, S. K. (2007). Have we overemphasized the role of denitrification in aquatic ecosystems? A review of nitrate removal pathways. *Frontiers in Ecology and the Environment*, 5(2):89–96.

Burgin, A. J. and Hamilton, S. K. (2008). NO3–driven SO42- production in freshwater ecosystems: Implications for N and S cycling. *Ecosystems*, 11(6):908–922.

Burke, C., Steinberg, P. D., Rusch, D., Kjelleberg, S., and Thomas, T. (2011). Bacterial community assembly based on functional genes rather than

species. *Proceedings of the National Academy of Sciences*, 108(34):14288–14293.

Burton, G. A. and Johnston, E. L. (2010). Assessing contaminated sediments in the context of multiple stressors. *Environmental Toxicology and Chemistry*, 29(12):2625–2643.

Calmano, W., Hong, J., and Förstner, U. (1993). Binding and mobilization of heavy metals in contaminated sediments affected by pH and redox potential. *Water Science and Technology*, 28(8-9):223–236.

Campana, O., Taylor, A. M., Blasco, J., Maher, W. A., and Simpson, S. L. (2015). Importance of subcellular metal partitioning and kinetics to predicting sublethal effects of copper in two deposit-feeding organisms. *Environmental Science and Technology*, 49:1806–1814.

Capone, D. G. and Kiene, R. P. (1988). Comparison of microbial dynamics in marine and freshwater sediments: Contrasts in anaerobic carbon catabolism. *Limnology and Oceanography*, 33(4, part 2):725–749.

Caporaso, J. G., Lauber, C. L., Walters, W. A., Berg-Lyons, D., Huntley, J., Fierer, N., Owens, S. M., Betley, J., Fraser, L., Bauer, M., Gormley, N., Gilbert, J. A., Smith, G., and Knight, R. (2012). Ultra-high-throughput microbial community analysis on the Illumina HiSeq and MiSeq platforms. *The ISME Journal*, 6:1621–1624.

Caron, D. A. (2009). New accomplishments and approaches for assessing protistan diversity and ecology in natural ecosystems. *BioScience*, 59(4):287–299.

Carvalhais, L. C., Dennis, P. G., Tyson, G. W., and Schenk, P. M. (2012). Application of metatranscriptomics to soil environments. *Journal of Microbiological Methods*, 91:246–51.

Chapin, F. S., Zavaleta, E. S., Eviner, V. T., Naylor, R. L., Vitousek, P. M., Reynolds, H. L., Hooper, D. U., Lavorel, S., Sala, O. E., Hobbie, S. E., Mack, M. C., and Díaz, S. (2000). Consequences of changing biodiversity. *Nature*, 405:234–42.

Chapman, P. M., Wang, F., Janssen, C., Persoone, G., and Allen, H. E. (1998). Ecotoxicology of metals in aquatic sediments: Binding and release, bioavailability, risk assessment, and remediation. *Canadian Journal of Fisheries and Aquatic Sciences*, 55(10):2221–2243.

Chariton, A. A., Sun, M. Y., Gibson, J., Webb, J. A., Leung, K. M. Y., Hickey, C. W., and Hose, G. C. (2016). Emergent technologies and analytical approaches for understanding the effects of multiple stressors in aquatic environments. *Marine and Freshwater Research*, 67:414–428.

Christensen, M. R., Graham, M. D., Vinebrooke, R. D., Findlay, D. L., Paterson, M. J., and Turner, M. A. (2006). Multiple anthropogenic stressors cause ecological surprises in boreal lakes. *Global Change Biology*, 12:2316–2322.

Cohen, J. E. (2003). Human population: The next half century. *Science*, 302:1172–1175.

Cohn, S. A. and McGuire, J. R. (2000). Using diatom motility as an indicator of environmental stress: Effects of toxic sediment elutriates. *Diatom Research*, 15(1):19–29.

Collins, K. A., Lawrence, T. J., Stander, E. K., Jontos, R. J., Kaushal, S. S., Newcomer, T. A., Grimm, N. B., and Cole Ekberg, M. L. (2010). Opportunities and challenges for managing nitrogen in urban stormwater: A review and synthesis. *Ecological Engineering*, 36:1507–1519.

Condon, C. (2007). Maturation and degradation of RNA in bacteria. *Current Opinion in Microbiology*, 10:271–278.

Crain, C. M., Kroeker, K., and Halpern, B. S. (2008). Interactive and cumulative effects of multiple human stressors in marine systems. *Ecology Letters*, 11:1304–1315.

Creer, S., Deiner, K., Frey, S., Porazinska, D., Taberlet, P., Thomas, K., Potter, C., and Bik, H. (2016). The ecologist's field guide to sequence-based identification of biodiversity. *Methods in Ecology and Evolution*, opt-doi:10.111.

Dafforn, K. A., Baird, D. J., Chariton, A. A., Sun, M. Y., Brown, M. V., Simpson, S. L., Kelaher, B. P., and Johnston, E. L. (2014). Faster, higher and stronger? The pros and cons of molecular faunal data for assessing ecosystem condition. *Advances in Ecological Research*, 51:1–40.

Dafforn, K. A., Johnston, E. L., Ferguson, A. J. P., Humphrey, C. L., Monk, W., Nichols, S. J., Simpson, S. L., Tulbure, M. G., and Baird, D. J. (2016). Big data opportunities and challenges for assessing multiple stressors across scales in aquatic ecosystems. *Marine and Freshwater Research*, 67:393–413.

Dafforn, K. A., Kelaher, B. P., Simpson, S. L., Coleman, M. A., Hutchings, P. A., Clark, G. F., Knott, N. A., Doblin, M. A., and Johnston, E. L. (2013). Polychaete richness and abundance enhanced in anthropogenically modified estuaries despite high concentrations of toxic contaminants. *PLoS ONE*, 8(9):e77018.

Dafforn, K. A., Simpson, S. L., Kelaher, B. P., Clark, G. F., Komyakova, V., Wong, C. K. C., and Johnston, E. L. (2012). The challenge of choosing environmental indicators of anthropogenic impacts in estuaries. *Environmental Pollution*, 163:207–217.

Dai, L., Vorselen, D., Korolev, K. S., and Gore, J. (2012). Generic indicators for loss of resilience before a tipping point leading to population collapse. *Science*, 336:1175–1177.

Dalsgaard, T., Thamdrup, B., and Canfield, D. E. (2005). Anaerobic ammonium oxidation (anammox) in the marine environment. *Research in Microbiology*, 156:457–464.

Das, N. and Chandran, P. (2011). Microbial degradation of petroleum hydrocarbon contaminants: An overview. *Biotechnology Research International*, Article ID.

Davidson, E. A., Savage, K., Verchot, L. V., and Navarro, R. (2002). Minimising artifacts and biases in chamber-based measurements of soil respiration. *Agricultural and Forest Meterology*, 113:21–37.

Davis, B. S. and Birch, G. F. (2009). Catchment-wide assessment of the cost-effectiveness of stormwater remediation measures in urban areas. *Environmental Science and Policy*, 12:84–91.

Davis, W. R. (1993). The role of bioturbation in sediment resuspension and its interaction with physical shearing. *Journal of Experimental Marine Biology and Ecology*, 171:187–200.

de Juan, S., Hewitt, J., Thrush, S., and Freeman, D. (2014). Standardising the assessment of functional integrity in benthic ecosystems. *Journal of Sea Research*, 98:33–41.

del Giorgio, P. A. and Scarborough, G. (1995). Increase in the proportion of metabolically active bacteria along gradients of enrichment in freshwater and marine plankton: Implications for estimates of bacterial growth and production rates. *Journal of Plankton Research*, 17(10):1905–1924.

Dell'Anno, A., Mei, M. L., Ianni, C., and Danovaro, R. (2003). Impact of bioavailable heavy metals on bacterial activities in coastal marine sediments. *World Journal of Microbiology & Biotechnology*, 19:93–100.

Dequiedt, S., Saby, N. P. A., Lelievre, M., Jolivet, C., Thioulouse, J., Toutain, B., Arrouays, D., Bispo, A., Lemanceau, P., and Ranjard, L. (2011). Biogeographical patterns of soil molecular microbial biomass as influenced by soil characteristics and management. *Global Ecology and Biogeography*, 20:641–652.

Devol, A. H. (2003). Nitrogen cycle: Solution to a marine mystery. *Nature*, 422:575–576.

Devol, A. H. (2015). Denitrification, anammox, and N2 production in marine sediments. *Annual Review of Marine Science*, 7:403–423.

Díez, B., Nylander, J. A. A., Ininbergs, K., Dupont, C. L., Allen, A. E., Yooseph, S., Rusch, D. B., and Bergman, B. (2016). Metagenomic analysis of the Indian Ocean picocyanobacterial community: Structure, potential function and evolution. *PLoS ONE*, 11(5):e0155757.

Dong, Y., Rosenbaum, R. K., and Hauschild, M. Z. (2016). Assessment of metal toxicity in marine ecosystems: Comparative toxicity potentials for nine cationic metals in coastal seawater. *Environmental Science and Technology*, 50:269–278.

Ducklow, H. W. (2008). Microbial services: Challenges for microbial ecologists in a changing world. *Aquatic Microbial Ecology*, 53:13–19.

Edge, K. J., Dafforn, K. A., Simpson, S. L., Ringwood, A. H., and Johnston, E. L. (2015). Resuspended contaminated sediments cause sublethal stress to oysters: A biomarker differentiates total suspended solids and contaminant effects. *Environmental Toxicology and Chemistry*, 34(6):1345–1353.

Eggleton, J. and Thomas, K. V. (2004). A review of factors affecting the release and bioavailability of contaminants during sediment disturbance events. *Environment International*, 30:973–980.

Eloe-Fadrosh, E. A., Ivanova, N. N., Woyke, T., and Kyrpides, N. C. (2016). Metagenomics uncovers gaps in amplicon-based detection of microbial diversity. *Nature Microbiology*, (February):15032.

Engström, P., Dalsgaard, T., Hulth, S., and Aller, R. C. (2005). Anaerobic ammonium oxidation by nitrite (anammox): Implications for N2 production

in coastal marine sediments. *Geochimica et Cosmochimica Acta*, 69(8):2057–2065.

Eyre, B. D. and Ferguson, A. J. P. (2005). Benthic metabolism and nitrogen cycling in a subtropical east Australian estuary (Brunswick): Temporal variability and controlling factors. *Limnology and Oceanography*, 50(1):81–96.

Falkowski, P. G., Fenchel, T., and Delong, E. F. (2008). The microbial engines that drive Earth's biogeochemical cycles. *Science*, 320:1034–1039.

Fernández-Gómez, B., Richter, M., Schüler, M., Pinhassi, J., Acinas, S. G., González, J. M., and Pedrós-Alió, C. (2013). Ecology of marine Bacteroidetes: A comparative genomics approach. *The ISME Journal*, 7:1026–37.

Fialkowski, W. and Rainbow, P. S. (2006). The discriminatory power of two biomonitors of trace metal bioavailabilities in freshwater streams. *Water Research*, 40:1805–1810.

Field, C. B., Berhenfeld, M. J., Randerson, J. T., and Falkowski, P. G. (1998). Primary production of the biosphere: Integrating terrestrial and oceanic components. *Science*, 281:237–240.

Finlay, B. J. and Clarke, K. J. (1999). Ubiquitous dispersal of microbial species. *Nature*, 400:828.

Folt, C. L., Chen, Y. C., Moore, M. V., and Burnaford, J. (1999). Synergism and antagonism among multiple stressors. *Limnology and Oceanography*, 44(3):864–877.

Forster, P., Ramaswamy, V., Artaxo, P., Berntsen, T., Betts, R., Fahey, D. W., Haywood, J., Lean, J., Lowe, D. C., Myhre, G., Nganga, J., Prinn, R., Raga, G., Schulz, M., and Van Dorland, R. (2007). Changes in atmospheric constituents and in radiative forcing. In *Climate Change 2007: The Physical Science Basis. Contribution of Working Group I to the Fourth Assessment Report of the Intergovernmental Panel on Climate Change*.

Franzosa, E. A., Morgan, X. C., Segata, N., Waldron, L., Reyes, J., Earl, A. M., Giannoukos, G., Boylan, M. R., Ciulla, D., Gevers, D., Izard, J., Garrett, W. S., Chan, A. T., and Huttenhower, C. (2014). Relating the metatranscriptome and metagenome of the human gut. *Proceedings of the National Academy of Sciences*, 111(22):E2329–38.

Frias-Lopez, J., Shi, Y., Tyson, G. W., Coleman, M. L., Schuster, S. C., Chisholm, S. W., and DeLong, E. F. (2008). Microbial community gene expression in ocean surface waters. *Proceedings of the National Academy of Sciences*, 105(10):3805–3810.

Gabric, A. J., Qu, B., Rotstayn, L., and Shephard, J. M. (2013). Global simulations of the impact on contemporary climate of a perturbation to the sea-to-air flux of dimethylsulfide. *Australian Meteorological and Oceanographic Journal*, 63:365–376.

Gardner, W. S. and McCarthy, M. J. (2009). Nitrogen dynamics at the sediment-water interface in shallow, sub-tropical Florida Bay: Why denitrification efficiency may decrease with increased eutrophication. *Biogeochemistry*, 95:185–198.

Gibson, B. D., Ptacek, C. J., Blowes, D. W., and Daugherty, S. D. (2015). Sediment resuspension under variable geochemical conditions and implications for contaminant release. *Journal of Soils and Sediments*, 15(7):1644–1656.

Gifford, S. M., Sharma, S., Booth, M., and Moran, M. A. (2013). Expression patterns reveal niche diversification in a marine microbial assemblage. *The ISME Journal*, 7:281–298.

Gifford, S. M., Sharma, S., Rinta-Kanto, J. M., and Moran, M. A. (2011). Quantitative analysis of a deeply sequenced marine microbial metatranscriptome. *The ISME Journal*, 5:461–472.

Glibert, P. M., Hinkle, D. C., Sturgis, B., and Jesien, R. V. (2014). Eutrophication of a Maryland/Virginia coastal lagoon: A tipping point, ecosystem changes, and potential causes. *Estuaries and Coasts*, 37(Suppl 1):S128–S146.

Glibert, P. M., Wilkerson, F. P., Dugdale, R. C., Raven, J. A., Dupont, C. L., Leavitt, P. R., Parker, A. E., Burkholder, J. M., and Kana, T. M. (2016). Pluses and minuses of ammonium and nitrate uptake and assimilation by phytoplankton and implications for productivity and community composition, with emphasis on nitrogen-enriched conditions. *Limnology and Oceanography*, 61:165–197.

Göbel, P., Dierkes, C., and Coldewey, W. G. (2007). Storm water runoff concentration matrix for urban areas. *Journal of Contaminant Hydrology*, 91:26–42.

Graham, E. B., Knelman, J. E., Schindlbacher, A., Siciliano, S. D., Breulmann, M., Yannarell, A., Beman, J. M., Abell, G., Philippot, L., Prosser, J. I., Foulquier, A., Yuste, J. C., Glanville, H. C., Jones, D. L., Angel, R., Salminen, J., Newton, R. J., Bürgmann, H., Ingram, L. J., Hamer, U., Siljanen, H. M. P., Peltoniemi, K., Potthast, K., Bañeras, L., Hartmann, M., Banerjee, S., Yu, R. Q., Nogaro, G., Richter, A., Koranda, M., Castle, S. C., Goberna, M., Song, B., Chatterjee, A., Nunes, O. C., Lopes, A. R., Cao, Y., Kaisermann, A., Hallin, S., Strickland, M. S., Garcia-Pausas, J., Barba, J., Kang, H., Isobe, K., Papaspyrou, S., Pastorelli, R., Lagomarsino, A., Lindström, E. S., Basiliko, N., and Nemergut, D. R. (2016). Microbes as engines of ecosystem function: When does community structure enhance predictions of ecosystem processes? *Frontiers in Microbiology*, 7:Article 214.

Grattepanche, J. D., Santoferrara, L. F., McManus, G. B., and Katz, L. A. (2014). Diversity of diversity: Conceptual and methodological differences in biodiversity estimates of eukaryotic microbes as compared to bacteria. *Trends in Microbiology*, 22(8):432–437.

Gray, J. S., Wu, R. S., and Or, Y. Y. (2002). Effects of hypoxia and organic enrichment on the coastal marine environment. *Marine Ecology Progress Series*, 238:249–279.

Griffen, B. D., Belgrad, B. A., Cannizzo, Z. J., Knotts, E. R., and Hancock, E. R. (2016). Rethinking our approach to multiple stressor studies in marine environments. *Marine Ecology Progress Series*, 543:273–281.

Hajibabaei, M., Shokralla, S., Zhou, X., Singer, G. A. C., and Baird, D. J. (2011). Environmental barcoding: A next-generation sequencing approach for biomonitoring applications using river benthos. *PLoS ONE*, 6(4):e17497.

Hall, N. (2007). Advanced sequencing technologies and their wider impact in microbiology. *The Journal of Experimental Biology*, 209:1518–1525.

Halpern, B. S., Walbridge, S., Selkoe, K. A., Kappel, C. V., Micheli, F., D'Agrosa, C., Bruno, J. F., Casey, K. S., Ebert, C., Fox, H. E., Fujita, R., Heinemann, D., Lenihan, H. S., Madin, E. M., Perry, M. T., Selig, E. R., Spalding, M., Steneck, R., and Watson, R. (2008). A global map of human impact on marine ecosystems. *Science*, 319:948–953.

Halstead, N. T., Mcmahon, T. A., Johnson, S. A., Raffel, T. R., Romansic, J. M., Crumrine, P. W., and Rohr, J. R. (2014). Community ecology theory

predicts the effects of agrochemical mixtures on aquatic biodiversity and ecosystem properties. *Ecology Letters*, 17:932–941.

Hansen, M. H., Ingvorsen, K., and Jorgensen, B. B. (1978). Mechanisms of hydrogen sulfide release from coastal marine sediments to the atmosphere. *Limnology and Oceanography*, 23(1):68–76.

Harter, J., Krause, H. M., Schuettler, S., Ruser, R., Fromme, M., Scholten, T., Kappler, A., and Behrens, S. (2014). Linking N2O emissions from biochar-amended soil to the structure and function of the N-cycling microbial community. *The ISME Journal*, 8:660–674.

He, Z. and Morrison, R. J. (2001). Changes in the marine environment of Port Kembla Harbour, NSW, Australia, 1975-1995: A review. *Marine Pollution Bulletin*, 42(3):193–201.

Helbling, D. E., Ackermann, M., Fenner, K., Kohler, H.-P. E., and Johnson, D. R. (2012). The activity level of a microbial community function can be predicted from its metatranscriptome. *The ISME Journal*, 6:902–904.

Hemme, C. L., Tu, Q., Shi, Z., Qin, Y., Gao, W., Deng, Y., Van Nostrand, J. D., Wu, L., He, Z., Chain, P. S. G., Tringe, S. G., Fields, M. W., Rubin, E. M., Tiedje, J. M., Hazen, T. C., Arkin, A. P., and Zhou, J. (2015). Comparative metagenomics reveals impact of contaminants on groundwater microbiomes. *Frontiers in Microbiology*, 6:Article 1205.

Hering, D., Borja, Á., Carstensen, J., Carvalho, L., Elliott, M., Feld, C. K., Heiskanen, A. S., Johnson, R. K., Moe, J., Pont, D., Solheim, A. L., and van de Bund, W. (2010). The European Water Framework Directive at the age of 10: A critical review of the achievements with recommendations for the future. *Science of the Total Environment*, 408:4007–4019.

Hill, A. J., Teraoka, H., Heideman, W., and Peterson, R. E. (2005). Zebrafish as a model vertebrate for investigating chemical toxicity. *Toxicological Sciences*, 86(1):6–19.

Hillebrand, H., Bennet, D. M., and Cadotte, M. W. (2008). Consequences of dominance: A review of evenness effects on local and regional ecosystem processes. *Ecology*, 89(6):1510–1520.

Hilton, J. a., Satinsky, B. M., Doherty, M., Zielinski, B., and Zehr, J. P. (2015). Metatranscriptomics of N2-fixing cyanobacteria in the Amazon River plume. *The ISME Journal*, 9:1557–1569.

Hitt, N. P. and Angermeier, P. L. (2006). Effects of adjacent streams on local fish assemblage structure in western Virginia: Implications for biomonitoring. *Landscape Influences on Stream Habitats and Biological Assemblages*, 48(August):75–86.

Hook, S. E., Osborn, H. L., Golding, L. A., Spadaro, D. A., and Simpson, S. L. (2014). Dissolved and particulate copper exposure induces differing gene expression profiles and mechanisms of toxicity in the deposit feeding amphipod Melita plumulosa. *Environmental Science and Technology*, 48:3504–3512.

Hopkins, G. W. and Freckleton, R. P. (2002). Declines in the numbers of amateur and professional taxonomists: Implications for conservation. *Animal Conservation*, 5:245–249.

Horvath, S. and Dong, J. (2008). Geometric interpretation of gene coexpression network analysis. *PLoS Computational Biology*, 4(8):e1000117.

Howarth, R., Chan, F., Conley, D. J., Garnier, J., Doney, S. C., Marino, R., and Billen, G. (2011). Coupled biogeochemical cycles: Eutrophication and hypoxia in temperate estuaries and coastal marine ecosystems. *Frontiers in Ecology and the Environment*, 9(1):18–26.

Hügler, M. and Sievert, S. M. (2011). Beyond the Calvin Cycle: Autotrophic carbon fixation in the ocean. *Annual Review of Marine Science*, 3:261–289.

Hultman, J., Waldrop, M. P., Mackelprang, R., David, M. M., McFarland, J., Blazewicz, S. J., Harden, J., Turetsky, M. R., McGuire, A. D., Shah, M. B., VerBerkmoes, N. C., Lee, L. H., Mavrommatis, K., and Jansson, J. K. (2015). Multi-omics of permafrost, active layer and thermokarst bog soil microbiomes. *Nature*, 521:208–212.

Huson, D. H., Mitra, S., Ruscheweyh, H. J., Weber, N., and Schuster, S. C. (2011). Integrative analysis of environmental sequences using MEGAN4. *Genome Research*, 21:1552–1560.

Ininbergs, K., Bergman, B., Larsson, J., and Ekman, M. (2015). Microbial metagenomics in the Baltic Sea: Recent advancements and prospects for environmental monitoring. *AMBIO*, 44(Suppl 3):S439–S450.

Irvine, I. and Birch, G. F. (1998). Distribution of heavy metals in surficial sediments of Port Jackson, Sydney, New South Wales. *Australian Journal of Earth Sciences*, 45(2):297–304.

Ishii, S., Suzuki, S., Norden-Krichmar, T. M., Tenney, A., Chain, P. S. G., Scholz, M. B., Nealson, K. H., and Bretschger, O. (2013). A novel metatranscriptomic approach to identify gene expression dynamics during extracellular electron transfer. *Nature Communications*, 4:1601.

Jeffries, T. C., Ostrowski, M., Williams, R. B., Xie, C., Jensen, R. M., Grzymski, J. J., Senstius, S. J., Givskov, M., Hoeke, R., Philip, G. K., Neches, R. Y., Drautz-Moses, D. I., Chénard, C., Paulsen, I. T., and Lauro, F. M. (2015). Spatially extensive microbial biogeography of the Indian Ocean provides insights into the unique community structure of a pristine coral atoll. *Scientific Reports*, 5:15383.

Ji, Y., Ashton, L., Pedley, S. M., Edwards, D. P., Tang, Y., Nakamura, A., Kitching, R., Dolman, P. M., Woodcock, P., Edwards, F. A., Larsen, T. H., Hsu, W. W., Benedick, S., Hamer, K. C., Wilcove, D. S., Bruce, C., Wang, X., Levi, T., Lott, M., Emerson, B. C., and Yu, D. W. (2013). Reliable, verifiable and efficient monitoring of biodiversity via metabarcoding. *Ecology Letters*, 16:1245–1257.

Jiang, Y., Kirkman, H., and Hua, A. (2001). Megacity development: Managing impacts on marine environments. *Ocean and Coastal Management*, 44:293–318.

Johnson, D. R., Helbling, D. E., Men, Y., and Fenner, K. (2015). Can metaopics help to establish causality between contaminant biotransformations and genes or gene products? *Environmental Science: Water Research & Technology*, 1:272–278.

Johnston, E. L., Hedge, L. H., and Mayer-Pinto, M. (2015a). The urgent global need to understand port and harbour systems. *Marine and Freshwater Research*, 66:i–ii.

Johnston, E. L. and Keough, M. J. (2002). Direct and indirect effects of repeated pollution events on marine hard-substrate assemblages. *Ecological Applications*, 12(4):1212–1228.

Johnston, E. L., Keough, M. J., and Qian, P. Y. (2002). Maintenance of species dominance through pulse disturbances to a sessile marine invertebrate assemblage in Port Shelter, Hong Kong. *Marine Ecology Progress Series*, 226:103–114.

Johnston, E. L., Mayer-Pinto, M., and Crowe, T. P. (2015b). Chemical contaminant effects on marine ecosystem functioning. *Journal of Applied Ecology*, 52:140–149.

Johnston, E. L. and Roberts, D. A. (2009). Contaminants reduce the richness and evenness of marine communities: A review and meta-analysis. *Environmental Pollution*, 157:1745–1752.

Jones, C. M., Stres, B., Rosenquist, M., and Hallin, S. (2008). Phylogenetic analysis of nitrite, nitric oxide, and nitrous oxide respiratory enzymes reveal a complex evolutionary history for denitrification. *Molecular Biology and Evolution*, 25(9):1955–1966.

Jones, R. T., Robeson, M. S., Lauber, C. L., Hamady, M., Knight, R., and Fierer, N. (2009). A comprehensive survey of soil acidobacterial diversity using pyrosequencing and clone library analyses. *The ISME Journal*, 3:442–453.

Joye, S. B. and Hollibaugh, J. T. (1995). Influence of sulfide inhibition of nitrification on nitrogen regeneration in sediments. *Science*, 270(5236):623–625.

Kandeler, F., Kampichler, C., and Horak, O. (1996). Influence of heavy metals on the functional diversity of soil microbial communities. *Biology and Fertility of Soils*, 23:299–306.

Kearns, P. J., Angell, J. H., Feinman, S. G., and Bowen, J. L. (2015). Long-term nutrient addition differentially alters community composition and diversity of genes that control nitrous oxide flux from salt marsh sediments. *Estuarine, Coastal and Shelf Science*, 154:39–47.

Kelaher, B. P., Bishop, M. J., Potts, J., Scanes, P., and Skilbeck, G. (2013). Detrital diversity influences estuarine ecosystem performance. *Global Change Biology*, 19:1909–1918.

Kellermann, C., Selesi, D., Lee, N., Hügler, M., Esperschütz, J., Hartmann, A., and Griebler, C. (2012). Microbial CO2 fixation potential in a tar-oil-contaminated porous aquifer. *FEMS Microbiology Ecology*, 81:172–187.

Kennish, M. J. (2002). Environmental threats and environmental future of estuaries. *Environmental Conservation*, 29(01):78–107.

Khan, M. S., Haas, F. H., Samami, A. A., Gholami, A. M., Bauer, A., Fellenberg, K., Reichelt, M., Hänsch, R., Mendel, R. R., Meyer, A. J., Wirtz, M., and Hell, R. (2010). Sulfite reductase defines a newly discovered bottleneck for assimilatory sulfate reduction and is essential for growth and development in Arabidopsis thaliana. *The Plant Cell*, 22:1216–1231.

Knott, N. A., Aulbury, J. P., Brown, T. H., and Johnston, E. L. (2009). Contemporary ecological threats from historical pollution sources: Impacts of large-scale resuspension of contaminated sediments on sessile invertebrate recruitment. *Journal of Applied Ecology*, 46:770–781.

Kohlmann, Y., Pohlmann, A., Schwartz, E., Zühlke, D., Otto, A., Albrecht, D., Grimmler, C., Ehrenreich, A., Voigt, B., Becher, D., Hecker, M., Friedrich, B., and Cramm, R. (2014). Coping with anoxia: A comprehensive proteomic and transcriptomic survey of denitrification. *Journal of Proteome Research*, 13:4325–4338.

Kopylova, E., Noe, L., and Touzet, H. (2012). SortMeRNA: Fast and accurate filtering of ribosomal RNAs in metatranscriptomic data. *Bioinformatics*, 28(24):3211–3217.

Kozich, J. J., Westcott, S. L., Baxter, N. T., Highlander, S. K., and Schloss, P. D. (2013). Development of a dual-index sequencing strategy and curation pipeline for analyzing amplicon sequence data on the MiSeq Illumina sequencing platform. *Applied and Environmental Microbiology*, 79(17):5112–5120.

Kraft, B., Tegetmeyer, H. E., Sharma, R., Klotz, M. G., Ferdelman, T. G., Hettich, R. L., Geelhoed, J. S., and Strous, M. (2014). The environmental controls that govern the end product of bacterial nitrate respiration. *Science*, 345(6197):676–679.

Kump, L. R., Pavlov, A., and Arthur, M. A. (2005). Massive release of hydrogen sulfide to the surface ocean and atmosphere during intervals of oceanic anoxia. *Geology*, 33(5):397–400.

Lacroute, F., Pierard, A., Grenson, M., and Wiame, J. M. (1965). The biosynthesis of carbamoyl phosphate in Saccharomyces cerevisiae. *Journal of General Microbiology*, 40:127–142.

Laetz, C. A., Hecht, S. A., Incardona, J. P., Collier, T. K., and Scholz, N. L. (2015). *Ecotoxicological risk of mixtures*. Elsevier Inc., San Diego, CA, USA.

Lane, D. J. (1991). 16S/23S rRNA Sequencing. In Stackebrandt, E. and Goodfellow, M., editors, *Nucleic acid techniques in bacterial systematics*, chapter 6, pages 115–175. John Wiley & Sons, New York, NY.

Latimer, J. S., Davis, W. R., and Keith, D. J. (1999). Mobilization of PAHs and PCBs from in-place contaminated marine sediments during simulated resuspension events. *Estuarine, Coastal and Shelf Science*, 49:577–595.

Lauffenburger, D., Aris, R., and Keller, K. (1982). Effects of cell motility and chemotaxis on microbial population growth. *Biophysical Journal*, 40:209–219.

Law, C. S. and Owens, N. J. P. (1990). Significant flux of atmospheric nitrous oxide from the northwest Indian Ocean. *Nature*, 346:826–828.

Lawes, J. C., Clark, G. F., and Johnston, E. L. (2016a). Contaminant cocktails: Interactive effects of fertiliser and copper paint on marine invertebrate recruitment and mortality. *Marine Pollution Bulletin*, 102:148–159.

Lawes, J. C., Neilan, B. A., Brown, M. V., Clark, G. F., and Johnston, E. L. (2016b). Elevated nutrients change bacterial community composition and connectivity: High throughput sequencing of young marine biofilms. *Biofouling*, 32(1):57–69.

Leifer, I. and Patro, R. K. (2002). The bubble mechanism for methane transport from the shallow sea bed to the surface: A review and sensitivity study. *Continental Shelf Research*, 22:2409–2428.

Lejzerowicz, F., Esling, P., Pillet, L. L., Wilding, T. a., Black, K. D., and Pawlowski, J. (2015). High-throughput sequencing and morphology perform equally well for benthic monitoring of marine ecosystems. *Scientific Reports*, 5:13932.

Lintern, A., Deletic, A., Leahy, P., and McCarthy, D. (2015). Digging up the dirty past: Evidence for stormwater's contribution to pollution of an urban floodplain lake. *Marine and Freshwater Research*, 66:596–608.

Logares, R., Audic, S., Bass, D., Bittner, L., Boutte, C., Christen, R., Claverie, J. M., Decelle, J., Dolan, J. R., Dunthorn, M., Edvardsen, B., Gobet, A., Kooistra, W. H. C. F., Mahé, F., Not, F., Ogata, H., Pawlowski, J., Pernice, M. C., Romac, S., Shalchian-Tabrizi, K., Simon, N., Stoeck, T., Santini, S., Siano, R., Wincker, P., Zingone, A., Richards, T. A., De Vargas, C., and Massana, R. (2014). Patterns of rare and abundant marine microbial eukaryotes. *Current Biology*, 24:813–821.

Long, E. R., Ingersoll, C. G., and MacDonald, D. D. (2006). Calculation and uses of mean sediment quality guideline quotients: A critical review. *Environmental Science and Technology*, 40(6):1726–1736.

Louati, H., Ben Saïd, O., Soltani, A., Got, P., Mahmoudi, E., Cravo-Laureau, C., Duran, R., Aissa, P., and Pringault, O. (2013). The roles of biologi-

cal interactions and pollutant contamination in shaping microbial benthic community structure. *Chemosphere*, 93:2535–2546.

Lücker, S., Nowka, B., Rattei, T., Spieck, E., and Daims, H. (2013). The genome of Nitrospina gracilis illuminates the metabolism and evolution of the major marine nitrite oxidizer. *Frontiers in Microbiology*, 4:Article 27.

Luo, W., D'Angelo, E. M., and Coyne, M. S. (2008). Organic carbon effects on aerobic polychlorinated biphenyl removal and bacterial community composition in soils and sediments. *Chemosphere*, 70:364–373.

Lürling, M. and Scheffer, M. (2007). Info-disruption: Pollution and the transfer of chemical information between organisms. *Trends in Ecology and Evolution*, 22(7):374–379.

Lyons, K. G. and Schwartz, M. W. (2001). Rare species loss alters ecosystem function - invasion resistance. *Ecology Letters*, 4:358–365.

Magurran, A. E., Baillie, S. R., Buckland, S. T., Dick, J. M., Elston, D. A., Scott, E. M., Smith, R. I., Somerfield, P. J., and Watt, A. D. (2010). Long-term datasets in biodiversity research and monitoring: Assessing change in ecological communities through time. *Trends in Ecology and Evolution*, 25(10):574–582.

Martin, M. (2011). Cutadapt removes adapter sequences from high-throughput sequencing reads. *EMBnet Journal*, 17(1):10–12.

Mascher, T., Helmann, J. D., and Unden, G. (2006). Stimulus perception in bacterial signal-transducing histidine kinases. *Microbiology and Molecular Biology Reviews*, 70(4):910–938.

Mason, O. U., Scott, N. M., Gonzalez, A., Robbins-Pianka, A., Bælum, J., Kimbrel, J., Bouskill, N. J., Prestat, E., Borglin, S., Joyner, D. C., Fortney, J. L., Jurelevicius, D., Stringfellow, W. T., Alvarez-Cohen, L., Hazen, T. C., Knight, R., Gilbert, J. A., and Jansson, J. K. (2014). Metagenomics reveals sediment microbial community response to Deepwater Horizon oil spill. *The ISME Journal*, 8:1464–1475.

Mayer-Pinto, M., Johnston, E. L., Hutchings, P. A., Marzinelli, E. M., Ahyong, S. T., Birch, G. F., Booth, D. J., Creese, R. G., Doblin, M. A., Figueira, W., Gribben, P. E., Pritchard, T., Roughan, M., Steinberg, P. D., and Hedge, L. H. (2015). Sydney Harbour: A review of anthropogenic impacts on the biodiversity and ecosystem function of one of the world's largest natural harbours. *Marine and Freshwater Research*, 66:1088–1105.

McGrath, K. C., Thomas-Hall, S. R., Cheng, C. T., Leo, L., Alexa, A., Schmidt, S., and Schenk, P. M. (2008). Isolation and analysis of mRNA from environmental microbial communities. *Journal of Microbiological Methods*, 75:172–176.

McIntyre, A. M. and Guéguen, C. (2013). Binding interactions of algal-derived dissolved organic matter with metal ions. *Chemosphere*, 90:620–626.

Meyer-Reil, L.-A. and Köster, M. (2000). Eutrophication of marine waters: Effects on benthic microbial communities. *Marine Pollution Bulletin*, 41(1-6):255–263.

Middelburg, J. J. and Levin, L. A. (2009). Coastal hypoxia and sediment biogeochemistry. *Biogeosciences*, 6:1273–1293.

Miller, D. N., Bryant, J. E., Madsen, E. L., and Ghiorse, W. C. (1999). Evaluation and optimization of DNA extraction and purification procedures for soil and sediment samples. *Applied and Environmental Microbiology*, 65(11):4715–4724.

Mitchell, R. J., Lee, S. K., Kim, T., and Ghim, C. M. (2011). Microbial linguistics: Perspectives and applications of microbial cell-to-cell communication. *BMB Reports*, 44(1):1–10.

Morales, S. E., Cosart, T., and Holben, W. E. (2010). Bacterial gene abundances as indicators of greenhouse gas emission in soils. *The ISME Journal*, 4:799–808.

Moran, M. A. (2009). Metatranscriptomics: Eavesdropping on complex microbial communities. *Microbe*, 4(7):329–335.

Moran, M. A., Satinsky, B. M., Gifford, S. M., Luo, H., Rivers, A., Chan, L.-K., Meng, J., Durham, B. P., Shen, C., Varaljay, V. A., Smith, C. B., Yager, P. L., and Hopkinson, B. M. (2013). Sizing up metatranscriptomics. *The ISME Journal*, 7:237–243.

Muir, P., Li, S., Lou, S., Wang, D., Spakowicz, D. J., Salichos, L., Zhang, J., Weinstock, G. M., Isaacs, F., Rozowsky, J., and Gerstein, M. (2016). The real cost of sequencing: Scaling computation to keep pace with data generation. *Genome Biology*, 17(53):1–9.

Murray, R. H., Erler, D. V., and Eyre, B. D. (2015). Nitrous oxide fluxes in estuarine environments: Response to global change. *Global Change Biology*, 21(9):3219–3245.

Nakamura, Y., Yamamoto, N., Kino, Y., Yamamoto, N., Kamei, S., Mori, H., Kurokawa, K., and Nakashima, N. (2016). Establishment of a multi-species biofilm model and metatranscriptomic analysis of biofilm and planktonic cell communities. *Applied Microbiology and Biotechnology*, 100:7263–7279.

Nicholson, F. A., Smith, S. R., Alloway, B. J., Carlton-Smith, C., and Chambers, B. J. (2003). An inventory of heavy metals inputs to agricultural soils in England and Wales. *Science of the Total Environment*, 311:205–219.

Nielsen, K. M., Johnsen, P. J., Bensasson, D., and Daffonchio, D. (2007). Release and persistence of extracellular DNA in the environment. *Environmental Biosafety Research*, 6:37–53.

Nixon, S. W., Oviatt, C. A., Frithsen, J., and Sullivan, B. (1986). Nutrients and the productivity of estuarine and coastal marine ecosystems. *Journal of the Limnological Society of Southern Africa*, 12(1/2):43–71.

Nizzoli, D., Welsh, D. T., Fano, E. A., and Viaroli, P. (2006). Impact of clam and mussel farming on benthic metabolism and nitrogen cycling, with emphasis on nitrate reduction pathways. *Marine Ecology Progress Series*, 315:151–165.

Nogales, B., Lanfranconi, M. P., Piña-Villalonga, J. M., and Bosch, R. (2011). Anthropogenic perturbations in marine microbial communities. *FEMS Microbiology Reviews*, 35:275–298.

Oksanen, J., Blanchet, F. G., Kindt, R., Minchin, P. R., Hara, R. B. O., Simpson, G. L., Solymos, P., Stevens, M. H. H., and Wagner, H. (2016). Package 'vegan'.

Pearson, T. H. and Rosenberg, R. (1978). Macrobenthic succession in relation to organic enrichment and pollution of the marine environment. *Oceanography and Marine Biology Annual Review*, 16:229–311.

Penn, K., Wang, J., Fernando, S. C., and Thompson, J. R. (2014). Secondary metabolite gene expression and interplay of bacterial functions in a tropical freshwater cyanobacterial bloom. *The ISME Journal*, 8:1866–1878.

Philippot, L., Andert, J., Jones, C. M., Bru, D., and Hallin, S. (2011). Importance of denitrifiers lacking the genes encoding the nitrous oxide reductase for N2O emissions from soil. *Global Change Biology*, 17:1497–1504.

Pik, A. J., Oliver, I., and Beattie, A. J. (1999). Taxonomic sufficiency in ecological studies of terrestrial invertebrates. *Austral Journal of Ecology*, 24:555–562.

Piotrowska-Seget, Z., Cycoń, M., and Kozdrój, J. (2005). Metal-tolerant bacteria occurring in heavily polluted soil and mine spoil. *Applied Soil Ecology*, 28:237–246.

Poissant, L. and Casimir, A. (1998). Water-air and soil-air exchange rate of total gaseous mercury measured at background sites. *Atmospheric Environment*, 32(5):883–893.

Proia, L., Morin, S., Peipoch, M., Romaní, A. M., and Sabater, S. (2011). Resistance and recovery of river biofilms receiving short pulses of Triclosan and Diuron. *Science of the Total Environment*, 409:3129–3137.

Prosser, J. I. (2010). Replicate or lie. *Environmental Microbiology*, 12(7):1806–1810.

Proulx, S. R., Promislow, D. E. L., and Phillips, P. C. (2005). Network thinking in ecology and evolution. *Trends in Ecology and Evolution*, 20(6):345–353.

Pruitt, K. D. (2004). NCBI Reference Sequence (RefSeq): A curated non-redundant sequence database of genomes, transcripts and proteins. *Nucleic Acids Research*, 33:D501–D504.

Puckett, L. J. (1995). Identifying the major sources of nutrient water pollution. *Environmental Science & Technology*, 29(9):408A–414A.

Qu, J., Zhang, Q., Zhang, N., Shen, L., and Liu, P. (2015). Microbial community diversity in water and sediment of an eutrophic lake during harmful algal bloom using MiSeq Illumina technology. In *International Conference on Advances in Environmental Research*, volume 87, pages 67–72.

Rachlin, J. W., Jensen, T. E., Baxter, M., and Jani, V. (1982). Utilization of morphometric analysis in evaluating response of Plectonema boryanum (Cyanophyceae) to exposure to eight heavy metals. *Archives of Environmental Contamination and Toxicology*, 11:323–333.

Rainbow, P. S. (1995). Biomonitoring of heavy metal availability in the marine environment. *Marine Pollution Bulletin*, 31(4-12):183–192.

Rainbow, P. S. (2002). Trace metal concentrations in aquatic invertebrates: Why and so what? *Environmental Pollution*, 120:497–507.

Rainbow, P. S. and Phillips, D. J. H. (1993). Cosmopolitan biomonitors of trace metals. *Marine Pollution Bulletin*, 26(11):593–601.

Ravishankara, A. R., Daniel, J. S., and Portmann, R. W. (2009). Nitrous oxide (N2O): The dominant ozone-depleting substance emitted in the 21st century. *Science*, 326:123–125.

Reavie, E. D., Jicha, T. M., Angradi, T. R., Bolgrien, D. W., and Hill, B. H. (2010). Algal assemblages for large river monitoring: Comparison among biovolume, absolute and relative abundance metrics. *Ecological Indicators*, 10:167–177.

Reed, H. E. and Martiny, J. B. H. (2012). Microbial composition affects the functioning of estuarine sediments. *The ISME Journal*, 7:868–879.

Reese, A. T., Savage, A., Youngsteadt, E., McGuire, K. L., Koling, A., Watkins, O., Frank, S. D., and Dunn, R. R. (2016). Urban stress is associated with variation in microbial species composition - but not richness - in Manhattan. *The ISME Journal*, 10:751–760.

Reichenbach, H. (2006). The order Cytophagales. In Dworkin, M., Falkow, S., Rosenberg, E., Schleifer, K.-H., and Stackebrandt, E., editors, *The Prokaryotes*, chapter 6.7, pages 549–590. Springer, New York, USA, 3rd edition.

Ren, Y., Niu, J., Huang, W., Peng, D., Xiao, Y., Zhang, X., Liang, Y., Liu, X., and Yin, H. (2016). Comparison of microbial taxonomic and functional shift pattern along contamination gradient. *BMC Microbiology*, 16(110):1–9.

Reuter, J. H. and Perdue, E. M. (1977). Importance of heavy metal-organic matter interactions in natural waters. *Geochimica et Cosmochimica Acta*, 41:325–334.

Roberts, D. A. (2012). Causes and ecological effects of resuspended contaminated sediments (RCS) in marine environments. *Environment International*, 40:230–243.

Roig, N., Sierra, J., Nadal, M., Moreno-Garrido, I., Nieto, E., Hampel, M., Gallego, E. P., Schuhmacher, M., and Blasco, J. (2015). Assessment of sediment ecotoxicological status as a complementary tool for the evaluation of surface water quality: The Ebro river basin case study. *Science of the Total Environment*, 503-504:269–278.

Ross-Gillespie, A. and Kümmerli, R. (2014). Collective decision-making in microbes. *Frontiers in Microbiology*, 5:Article 54.

Ruiz, G., Jeison, D., and Chamy, R. (2003). Nitrification with high nitrite accumulation for the treatment of wastewater with high ammonia concentration. *Water Research*, 48:1371–1377.

Sanz-Lázaro, C., Valdemarsen, T., and Holmer, M. (2015). Effects of temperature and organic pollution on nutrient cycling in marine sediments. *Biogeosciences*, 12:4565–4575.

Schimel, J. P., Balser, T. C., and Wallenstein, M. (2007). Microbial stress-response physiology and its implications for ecosystem function. *Ecology*, 88(6):1386–1394.

Schimel, J. P. and Gulledge, J. (1998). Microbial community structure and global trace gases. *Global Change Biology*, 4:745–758.

Schloss, P. D., Westcott, S. L., Ryabin, T., Hall, J. R., Hartmann, M., Hollister, E. B., Lesniewski, R. a., Oakley, B. B., Parks, D. H., Robinson, C. J., Sahl, J. W., Stres, B., Thallinger, G. G., Van Horn, D. J., and Weber, C. F. (2009). Introducing mothur: Open-source, platform-independent, community-supported software for describing and comparing microbial communities. *Applied and Environmental Microbiology*, 75(23):7537–7541.

Schreiber, F., Wunderlin, P., Udert, K. M., and Wells, G. F. (2012). Nitric oxide and nitrous oxide turnover in natural and engineered microbial communities: Biological pathways, chemical reactions, and novel technologies. *Frontiers in Microbiology*, 3:Article 372.

Scott, N. M., Hess, M., Bouskill, N. J., Mason, O. U., Jansson, J. K., and Gilbert, J. A. (2014). The microbial nitrogen cycling potential is impacted by polyaromatic hydrocarbon pollution of marine sediments. *Frontiers in Microbiology*, 5:Article 108.

Seitzinger, S. P. and Kroeze, C. (1998). Global distribution of nitrous oxide production and N inputs in freshwater and coastal marine ecosystems. *Global Biogeochemical Cycles*, 12(1):93–113.

Shank, E. A. and Kolter, R. (2009). New developments in microbial interspecies signaling. *Current Opinion in Microbiology*, 12:205–214.

Shcherbak, I., Millar, N., and Robertson, G. P. (2014). Global metaanalysis of the nonlinear response of soil nitrous oxide (N2O) emissions to fertilizer nitrogen. *Proceedings of the National Academy of Sciences*, 111(25):9199–9204.

Shedd, T. R., Van der Schalie, W. H., Widder, M. W., Burton, D. T., and Burrows, E. P. (2001). Long-term operation of an automated fish biomonitoring system for continuous effluent acute toxicity surveillance. *Bulletin of Environmental Contamination and Toxicology*, 66(3):392–399.

Simpson, S. L. and Batley, G. E. (2016). *Sediment quality assessment: A practical guide*. CSIRO Publishing, Victoria, Australia.

Simpson, S. L., Batley, G. E., and Chariton, A. A. (2013). Revision of the ANZECC / ARMCANZ sediment quality guidelines. Technical Report CSIRO Land and Water Science Report 08/07, CSIRO Land and Water.

Simpson, S. L. and Spadaro, D. A. (2011). Performance and sensitivity of rapid sublethal sediment toxicity tests with the amphipod Melita plumulosa and copepod Nitocra spinipes. *Environmental Toxicology and Chemistry*, 30(10):2326–2334.

Sims, A., Zhang, Y., Gajaraj, S., Brown, P. B., and Hu, Z. (2013). Toward the development of microbial indicators for wetland assessment. *Water Research*, 47:1711–1725.

Sims, D., Sudbery, I., Ilott, N. E., Heger, A., and Ponting, C. P. (2014). Sequencing depth and coverage: Key considerations in genomic analyses. *Nature Reviews Genetics*, 15:121–132.

Singh, B. K., Bardgett, R. D., Smith, P., and Reay, D. S. (2010). Microorganisms and climate change: terrestrial feedbacks and mitigation options. *Nature Reviews Microbiology*, 8:779–790.

Small, C. and Nicholls, R. (2003). A global analysis of human settlement in coastal zones. *Journal of Coastal Research*, 19(3):584–599.

Smayda, T. J. (1997). Harmful algal blooms: Their ecophysiology and general relevance to phytoplankton blooms in the sea. *Limnology and Oceanography*, 42(5, part 2):1137–1153.

Smith, V. H., Tilman, G. D., and Nekola, J. C. (1999). Eutrophication: Impacts of excess nutrient on freshwater, marine and terrestrial ecosystems. *Environmental Pollution*, 100:179–196.

Smolders, A. J. P., Lamers, L. P. M., Lucassen, E. C. H. E. T., Van Der Velde, G., and Roelofs, J. G. M. (2006). Internal eutrophication: How it works and what to do about it - a review. *Chemistry and Ecology*, 22(2):93–111.

Srivastava, D. S. and Vellend, M. (2005). Biodiversity-ecosystem function research: Is it relevant to conservation? *Annual Review of Ecology, Evolution and Systematics*, 36:267–294.

Stachowicz, J. J. (2001). Mutualism, facilitation, and the structure of ecological communities. *BioScience*, 51(3):235–246.

Stevenson, R. J., Pan, Y., Manoylov, K. M., Parker, C. a., Larsen, D. P., and Herlihy, A. T. (2008). Development of diatom indicators of ecological conditions for streams of the Western US. *Journal of the North American Benthological Society*, 27(4):1000–1016.

Stewart, F. J., Ulloa, O., and Delong, E. F. (2012). Microbial metatranscriptomics in a permanent marine oxygen minimum zone. *Environmental Microbiology*, 14(1):23–40.

Strickland, M. S., Lauber, C. L., Fierer, N., and Bradford, M. A. (2009). Testing the functional significance of microbial community composition. *Ecology*, 90(2):441–451.

Strom, D., Simpson, S. L., Batley, G. E., and Jolley, D. F. (2011). The influence of sediment particle size and organic carbon on toxicity of copper to benthic invertebrates in oxic/suboxic surface sediments. *Environmental Toxicology and Chemistry*, 30(7):1599–1610.

Sun, M. Y. (2016). *Impacts of anthropogenic modification on the taxonomic and functional structure of estuarine sediment communities*. PhD thesis, University of New South Wales.

Sun, M. Y., Dafforn, K. A., Brown, M. V., and Johnston, E. L. (2012). Bacterial communities are sensitive indicators of contaminant stress. *Marine Pollution Bulletin*, 64:1029–1038.

Sundbäck, K. and Granéli, W. (1988). Influence of microphytobenthos on the nutrient flux between sediment and water: A laboratory study. *Marine Ecology Progress Series*, 43:63–69.

Sutherland, M. D., Dafforn, K. A., Scanes, P., Potts, J., Simpson, S. L., Sim, V. X. Y., and Johnston, E. L. (2016). Links between contaminant hotspots in low flow estuarine systems and altered sediment biogeochemical processes. *Estuarine, Coastal and Shelf Science*.

Tan, B., Ng, C., Nshimyimana, J. P., Loh, L. L., Gin, K. Y. H., and Thompson, J. R. (2015). Next-generation sequencing (NGS) for assessment of microbial water quality: Current progress, challenges, and future opportunities. *Frontiers in Microbiology*, 6:Article 1027.

Taniguchi, Y., Choi, P. J., Li, G.-w., Chen, H., Babu, M., Hearn, J., Emili, A., and Xie, X. S. (2010). Quantifying E. coli proteome and transcriptome with single-molecule sensitivity in single cells. *Science*, 329:533–539.

Tarazona, S., García-Alcalde, F., Dopazo, J., Ferrer, A., and Conesa, A. (2011). Differential expression in RNA-seq: A matter of depth. *Genome Research*, 21:2213–2223.

Taylor, N. S., Kirwan, J. A., Yan, N. D., Viant, M. R., Gunn, J. M., and McGeer, J. C. (2016). Metabolomics confirms that dissolved organic carbon mitigates copper toxicity. *Environmental Toxicology and Chemistry*, 35(3):635–644.

Terlizzi, A., Bevilacqua, S., Fraschetti, S., and Boero, F. (2003). Taxonomic sufficiency and the increasing insufficiency of taxonomic expertise. *Marine Pollution Bulletin*, 46:556–561.

Thamdrup, B. and Dalsgaard, T. (2002). Production of N2 through anaerobic ammonium oxidation coupled to nitrate reduction in marine sediments. *Applied and Environmental Microbiology*, 68(3):1312–1318.

Thomas, F., Hehemann, J. H., Rebuffet, E., Czjzek, M., and Michel, G. (2011). Environmental and gut Bacteroidetes: The food connection. *Frontiers in Microbiology*, 2:Article 93.

Thomsen, P. F. and Willerslev, E. (2015). Environmental DNA - An emerging tool in conservation for monitoring past and present biodiversity. *Biological Conservation*, 183:4–18.

Thureborn, P., Franzetti, A., Lundin, D., and Sjöling, S. (2016). Reconstructing ecosystem functions of the active microbial community of the Baltic Sea oxygen depleted sediments. *PeerJ*, 4:e1593.

Tobor-Kaplon, M. A., Bloem, J., Römkens, P. F. A. M., and De Ruiter, P. C. (2005). Functional stability of microbial communities in contamined soils. *Oikos*, 111:119–129.

Torres, E., Cid, A., Herrero, C., and Abalde, J. (2000). Effect of cadmium on growth, ATP content, carbon fixation and ultrastructure in the marine diatom Phaeodactylum tricornutum Bohlin. *Water, Air and Soil Pollution*, 117:1–14.

Trenberth, K. E. (1998). Atmospheric moisture residence times and cycling: Implications for rainfall rates and climate change. *Climatic Change*, 39:667–694.

Tsementzi, D., Poretsky, R., Rodriguez-R, L. M., Luo, C., and Konstantinidis, K. T. (2014). Evaluation of metatranscriptomic protocols and application to

the study of freshwater microbial communities. *Environmental Microbiology Reports*, 6(6):640–655.

Turner, S., Pryer, K. M., Miao, V. P., and Palmer, J. D. (1999). Investigating deep phylogenetic relationships among cyanobacteria and plastids by small subunit rRNA sequence analysis. *The Journal of Eukaryotic Microbiology*, 46(4):327–338.

Turner, T. R., Ramakrishnan, K., Walshaw, J., Heavens, D., Alston, M., Swarbreck, D., Osbourn, A., Grant, A., and Poole, P. S. (2013). Comparative metatranscriptomics reveals kingdom level changes in the rhizosphere microbiome of plants. *The ISME Journal*, 7:2248–2258.

Urich, T., Lanzén, A., Qi, J., Huson, D. H., Schleper, C., and Schuster, S. C. (2008). Simultaneous assessment of soil microbial community structure and function through analysis of the meta-transcriptome. *PLoS ONE*, 3(6):e2527.

Urich, T., Lanzén, A., Stokke, R., Pedersen, R. B., Bayer, C., Thorseth, I. H., Schleper, C., Steen, I. H., and Øvreas, L. (2014). Microbial community structure and functioning in marine sediments associated with diffuse hydrothermal venting assessed by integrated meta-omics. *Environmental Microbiology*, 16(9):2699–2710.

Van den Brink, P. J., Baird, D. J., Baveco, H. J. M., and Focks, A. (2013). The use of traits-based approaches and eco(toxico)logical models to advance the ecological risk assessment framework for chemicals. *Integrated Environmental Assessment and Management*, 9(3):e47–57.

van der Linden, P., Borja, Á., Rodríquez, J. G., Muxika, I., Galparsoro, I., Patrício, J., Veríssimo, H., and Marques, J. C. (2016). Spatial and temporal response of multiple trait-based indices to natural- and anthropogenic seafloor disturbance (effluents). *Ecological Indicators*, 69:617–628.

Van Der Zaan, B., Smidt, H., De Vos, W. M., Rijnaarts, H., and Gerritse, J. (2010). Stability of the total and functional microbial communities in river sediment mesocosms exposed to anthropogenic disturbances. *FEMS Microbiology Ecology*, 74:72–82.

Van Ryssen, R., Leermakers, M., and Baeyens, W. (1999). The mobilisation potential of trace metals in aquatic sediments as a tool for sediment quality classiffication. *Environmental Science & Policy*, 2:75–86.

Vidali, M. (2011). Bioremediation - An overview. *Pure and Applied Chemistry*, 73(7):1163–1172.

Vinebrooke, R. D., Cottingham, K. L., Norberg, J., Scheffer, M., Dodson, S. I., Maberly, S. C., and Sommer, U. (2004). Impacts of multiple stressors on biodiversity and ecosystem functioning: The role of species co-tolerance. *Oikos*, 104:451–457.

Vitousek, P. M., Mooney, H. A., Lubchenco, J., and Melillo, J. M. (1997). Human domination of Earth' s ecosystems. *Science*, 277:494–499.

Vye, S. R., Emmerson, M. C., Arenas, F., Dick, J. T. A., and O'Connor, N. E. (2015). Stressor intensity determines antagonistic interactions between species invasion and multiple stressor effects on ecosystem functioning. *Oikos*, 124:1005–1012.

Wagner, M. and Horn, M. (2006). The Planctomycetes, Verrucomicrobia, Chlamydiae and sister phyla comprise a superphylum with biotechnological and medical relevance. *Current Opinion in Biotechnology*, 17:241–249.

Wahl, M. C., Will, C. L., and Lührmann, R. (2009). The spliceosome: Design principles of a dynamic RNP machine. *Cell*, 136:701–718.

Wang, D., Tan, Y., Yu, Z., Li, Y., Chang, S., Deng, H., Hu, B., and Chen, Z. (2015). Nitrous oxide production in river sediment of highly urbanized area and the effects of water quality. *Wetlands*, 35:1213–1223.

Watnick, P. and Kolter, R. (2000). Biofilm, city of microbes. *Journal of Bacteriology*, 182(10):2675–2679.

Watts, S. F. (2000). The mass budgets of carbonyl sulfide, dimethyl sulfide, carbon disulfide and hydrogen sulfide. *Atmospheric Environment*, 34:761–779.

Westerhoff, H. V., Brooks, A. N., Simeonidis, E., García-Contreras, R., He, F., Boogerd, F. C., Jackson, V. J., Goncharuk, V., and Kolodkin, A. (2014). Macromolecular networks and intelligence in microorganisms. *Frontiers in Microbiology*, 5:Article 379.

Wiatrowski, H. A. and Barkay, T. (2005). Monitoring of microbial metal transformations in the environment. *Current Opinion in Biotechnology*, 16:261–268.

Wickham, H. (2009). *ggplot2: Elegant graphics for data analysis*. Springer, New York, NY.

Williams, P. (2007). Quorum sensing, communication and cross-kingdom signalling in the bacterial world. *Microbiology*, 153:3923–3938.

Winter, J. G. and Duthie, H. C. (2000). Stream epilithic, epipelic and epiphytic diatoms: Habitat fidelity and use in biomonitoring. *Aquatic Ecology*, 34(4):345–353.

Xu, M., Zhang, Q., Xia, C., Zhong, Y., Sun, G., Guo, J., Yuan, T., Zhou, J., and He, Z. (2014). Elevated nitrate enriches microbial functional genes for potential bioremediation of complexly contaminated sediments. *The ISME Journal*, 8:1932–1944.

Yang, W., Traut, B., and Silver, W. L. (2015). Microbially mediated nitrogen retention and loss in a salt marsh soil. *Ecosphere*, 6(1):1–15.

Zhang, H. K., Lu, H., Wang, J., Liu, G. F., Zhou, J. T., and Xu, M. Y. (2013). Global transcriptome analysis of Escherichia coli exposed to immobilized anthraquinone-2-sulfonate and azo dye under anaerobic conditions. *Applied Microbiology and Biotechnology*, 97:6895–6905.

Zhang, X. J., Chen, C., Ding, J. Q., Hou, A., Li, Y., Niu, Z. B., Su, X. Y., Xu, Y. J., and Laws, E. A. (2010). The 2007 water crisis in Wuxi, China: Analysis of the origin. *Journal of Hazardous Materials*, 182:130–135.

Zhao, B. and Su, Y. (2014). Process effect of microalgal-carbon dioxide fixation and biomass production: A review. *Renewable and Sustainable Energy Reviews*, 31:121–132.

Zhao, Y., Tang, H., and Ye, Y. (2012). RAPSearch2: A fast and memory-efficient protein similarity search tool for next-generation sequencing data. *Bioinformatics*, 28(1):125–126.

Zhou, J., He, Z., Yang, Y., Deng, Y., Tringe, S. G., and Alvarez-Cohen, L. (2015). High-throughput metagenomic technologies for complex microbial community analysis: Open and closed formats. *mBio*, 6(1):e02288–14.

Žifčáková, L., Větrovský, T., Howe, A., and Baldrian, P. (2016). Microbial activity in forest soil reflects the changes in ecosystem properties between summer and winter. *Environmental Microbiology*, 18(1):288–301.

Zimmerman, N., Izard, J., Klatt, C., Zhou, J., and Aronson, E. (2014). The unseen world: Environmental microbial sequencing and identification methods for ecologists. *Frontiers in Ecology and the Environment*, 12(4):224–231.

Zoumis, T., Schmidt, A., Grigorova, L., and Calmano, W. (2001). Contaminants in sediments: Remobilisation and demobilisation. *Science of the Total Environment*, 266:195–202.

Zumft, W. G. (1997). Cell biology and molecular basis of denitrification. *Microbiology and Molecular Biology Reviews*, 61(4):533–616.

Simone C. Birrer

21.11.1987, Swiss citizenship

60 Carrington Road
Randwick NSW 2031
+61 481 342 727
simone.birrer@gmail.com

Education

2013-present **PhD candidate**, *UNSW*, Sydney, Australia.

2009-2011 **Master of Science ETH in Biology**, *ETH*, Zürich, Switzerland.
Specialisation in *Ecology and Evolution*. Master thesis at the Leibniz Institute of Marine Sciences, IFM-GEOMAR, Kiel, Germany. *GPA: 5.5/6*

2006-2009 **Bachelor of Science ETH in Biology**, *ETH*, Zürich, Switzerland. *GPA: 4.79/6*.

Professional Experience

June 2014-present **Health and safety manager**, *Applied Marine and Estuarine Ecology Lab*, UNSW, Sydney, Australia.

Sep. 2014-July 2016 **Postgraduate representative**, *Workplace Health and Safety Committee*, School of Biological, Earth and Environmental Sciences, UNSW, Sydney, Australia.

Feb 2016 **Invited panellist**, *Expert Panel on Environmental Risk Assessment*, NSW Office of Environment and Heritage, Sydney, Australia.

Nov. 2015-present **President**, *Sydney Society for Conservation Biology*, Sydney, Australia.
I have been volunteering my time to help fundraise, launch projects and do outreach for Sydney SCB, which was recently founded in 2013. Together with a great team, we have launched several conservation themed outreach projects and have made it our main goal to create networking opportunities for conservation professionals, volunteers and interested members of the public.

Feb. 2014-Nov. 2015 **Vice president**, *Sydney Society for Conservation Biology*, Sydney, Australia.

Jun. 2012-2013 **Biologist and marketing staff**, *ecaVert Sàrl*, Bussigny, Switzerland.
At this two-man start-up I worked as a biologist and in the marketing section. ecaVert Sàrl has specialized in selling and continuously improving the Vertical-Green Biobed^{TM}(VG Biobed^{TM}) system, which was built to filter pesticides and other contaminants from the waters on farms and in public parks, and thus to avoid a pollution of the rivers and lakes in Switzerland. In particular, I was responsible for the marketing in the German part of Switzerland and also built up a new website.

Research Experience

Mar. 2013-Aug. 2016 **PhD thesis: "Microbes, contaminants, and molecular biomonitoring: Structural and functional sediment community responses to multiple stressors."**, *Applied Marine and Estuarine Ecology Lab*, UNSW, Sydney, Australia.

Oct. 2010-Oct. 2011 **Master thesis: "How salinity affects the pipefish-*Vibrio* interaction"**, *Research Unit Evolutionary Ecology of Marine Fishes*, IFM-GEOMAR, Kiel, Germany.

Mar. 2010-Jun. 2010 **Semester thesis: "Comparison of the PO and ProPO activity between two *Gammarus spp.* (Crustacea, Amphipoda)"**, *Department for Aquatic Ecology*, Eawag Zürich, Switzerland.

Oct. 2009-Jan. 2010 **Semester thesis: "What is the function of non-linear phenomena in meerkat (*Suricata suricatta*) vocalisations?"**, *Department for Behavioural Studies*, University of Zürich, Switzerland.

Teaching Experience

July 2016 **Symposium organiser: "Land-based threats to coastal ecosystems."**, *Society for Conservation Biology 4th Oceania Congress*, Brisbane, QLD, Australia.

Feb. 2014-July 2016 **Casual teacher**, *UNSW Foundation Studies*, Sydney, NSW, Australia.
Foundation Studies is a program for international students who want to study at an Australian university. This course prior to university studies ensures they have reached the Australian level and provides them with an opportunity to achieve the necessary grades to get into specific courses. I have taught tutorials, marked exams, and demonstrated for biology practicals.

Publications

2012 **Simone C. Birrer, Thorsten B.H. Reusch and Olivia Roth**, *Salinity change impairs pipefish immune defence*, Fish & Shellfish Immunology **33**:1238-1248, doi: 10.1016/j.fsi.2012.08.028.

Grants and Awards

Nov. 2015 **Ecological Society of Australia Student Research Award**, *ESA*.

July 2015 **CAPIM award for the Best Oral Presentation on Marine Contamination**, *AMSA Conference 2015*.

Feb. 2015 **Greater Sydney Local Land Services Mini-Grant**, *Main author on grant for Conservation Café project by the Sydney Society for Conservation Biology*.

Aug. 2013 **E&ERC Postgraduate Research Start-Up Grant**.

March 2013 **University International Postgraduate Award**, *3.5-year PhD scholarship*, UNSW, Sydney, Australia.

Conference Presentations

July 2016 **Investigating functional responses of an estuarine sediment community to land-based contaminants using metatranscriptomics**, *Society for Conservation Biology 4th Oceania Congress*, Brisbane, QLD, Australia, *oral presentation*.

Sept. 2015 **Functional responses of an estuarine sediment community to pulse disturbances using metatranscriptomics**, *55th Conference of Estuarine Coastal Sciences Association*, London, UK, *oral presentation*.

Sept. 2015 **Functional responses of an estuarine sediment community to pulse disturbances using metatranscriptomics**, *Aquatic Biodiversity & Ecosystems Conference*, Liverpool, UK, *oral presentation*.

July 2015 **Heavy metals and organic enrichment affect greenhouse gas production pathways in sediment microbial communities**, *Australian Marine Sciences Association Conference 2015*, Geelong, VIC, Australia, *oral presentation*.

Nov. 2014 **Meta-omics elucidate sediment community and functional responses to field manipulated stressors**, *SETAC North America 35th Annual Meeting*, Vancouver, BC, Canada, *oral presentation*.

Nov. 2014 **Amplicon sequencing disentangles the effect of field manipulated press and pulse disturbances on sediment community responses**, *SETAC North America 35th Annual Meeting*, Vancouver, BC, Canada, *poster*.

Sept. 2014 **Meta-omics elucidate sediment community and functional responses to field manipulated stressors**, *SETAC Asia/Pacific 2014 Conference*, Adelaide, VIC, Australia, *oral presentation*.

Aug. 2014 **Meta-omics elucidate sediment community and functional responses to field manipulated stressors**, *15th International Symposium on Microbial Ecology*, Seoul, South Korea, *poster*.

July 2014 **Next-generation sequencing as a tool to elucidate structural and functional responses of a sediment community to field manipulated stressors**, *Society for Conservation Biology 2014 Conference*, Suva, Fiji, *oral presentation*.

Key Skills

Immune Assays	Immune activity measurements: cell count, cell-cycle stage determination, PO activity measurements, respiration burst assay, and plasma inhibition zone
Genetics	Cloning, Primer design, Quantitative real-time RT-PCR, Meta-omics
Laboratory	PC1 and PC2 laboratory experience
IT	MS Office, R, ImageJ, BioEdit, The Observer XT, Wordpress, HPC

Languages

German	Mother tongue	
English	Very good spoken and written	*Cambridge Certificate of Advanced English [12/2006] & TOEFL 118/200 points [05/2012]*
French	Very good spoken and written	
Portuguese	Very good spoken and written	*Six years of education in Portuguese at the School of Nations in Brasília, Brasil [1991-1997]*
Swedish	Very good spoken and written	*Four years of education in Swedish at the Deutsche Schule in Stockholm, Sweden [1997-2001]*
Spanish	Basic knowledge	